The Role of Histone Deacetylases in Cartilage Gene Regulation and Chondroprotection

Kirsty Leesa Culley

Thesis submitted for the degree of Doctor of Philosophy.

University of East Anglia
School of Biological Sciences
Norwich, United Kingdom

July 2010

Abstract

The expression of cartilage-degrading metalloproteinases (MMPs or ADAMTSs) is regulated in part via changes in acetylation mediated by histone acetyltransferases and histone deacetylases (HDACs). Classical HDACs can be divided into class I (HDAC1, 2, 3 and 8), class II (HDAC4, 5, 6, 7, 9 and 10) and Class IV (HDAC11). Broad spectrum HDAC inhibitors (HDACi) block cytokine-induction of key proteases in SW1353 chondrosarcoma cells and primary human articular chondrocytes (HACs), resulting in chondroprotection. This study aimed to elucidate the role of HDACs in chondroprotection using selective chemical HDACi and siRNA technology.

Trichostatin A (TSA) (broad spectrum) and valproic acid (VPA) (class I selective at <1mM) repressed all cytokine-induced metalloproteinase genes in SW1353 cells, and *MMP13* expression in HACs. MS-275 (class I selective) failed to repress cytokine-induced *MMP1* and *MMP13* expression in SW1353 cells, but repressed *MMP13* expression in HACs. Tubacin (HDAC6 specific) decreased cytokine-induced *MMP1* and *MMP13* in SW1353 cells. All inhibitors prevented cytokine-induced degradation of bovine nasal cartilage, where MS-275 was also able to repress cytokine-induced MMP expression, including *MMP1* and *MMP13*.

A profile of HDAC expression showed that the majority have reduced expression in OA cartilage compared to normal. TSA increased HDAC3 expression and decreased HDAC7 expression in SW1353 cells, suggesting that HDACi may both inhibit HDAC catalytic activity, and regulate HDAC expression.

Knockdown of individual HDACs in SW1353 cells using siRNA showed that inhibition of all HDACs, except HDAC1, caused a repression of basal and IL-1α-induced *MMP13* expression, with HDAC1 knockdown potentiating IL-1α-induced *MMP13* expression. In HACs, HDAC3 or HDAC8 knockdown resulted in reduced basal and IL-1α-induced *MMP13* expression, HDAC1 or HDAC11 knockdown potentiated both of these and HDAC5 or HDAC6 knockdown potentiated only IL-1α-induced *MMP13* expression. Problems with non-targeting control siRNAs made interpretation of experiments difficult.

HDACs therefore play a key role in metalloproteinase expression, with inhibition of class I HDACs, or separately HDAC6, capable of altering metalloproteinase expression to confer chondroprotection.

Contents

List of Figures

List of Tables

List of Appendices

Acknowledgements

Firstly I would like to thank my supervisor Prof. Ian Clark. Thank you for all your time, support and encouragement throughout my PhD. It has been a huge privilege to be part of the Clark laboratory, and thank you for letting me be part of it. I would also like to thank my industrial supervisor Dr. Steve Fenwick for all his advice and support throughout my PhD.

Thank you to the wonderful and incredibly talented Clark laboratory, members past and present, for all your help, advice, support and laughs throughout my PhD. I will miss working with you all immensely. A special thank you to Dr. Ursula Rodgers, Dr. Tracey Swingler and Dr. Rose Davidson who have put up with me for my entire three years in the laboratory. I have learnt so much from you all and don't think I could ever thank you enough for all your help, patience and friendship.

I would also like to thank Ellie Jones for never failing to make me smile, even when things were not quite going according to plan. Thanks to Dr. Gavin Jones for being great to work with and for answering my constant string of questions. Thank you to Dr. Sarah Snelling for all her help with accessing journals and in the laboratory. I would also like to thank Alba Warn and Jasmine Waters for being fantastic to work with and for fixing all the things I have broken over the last three years. Thank you to Dr. Caroline Pennington for knowing everything there is to know about gene expression profiling, and for being so willing to share your expertise.

Many thanks to my advisor Dr. Ernst Pöschl for his continued help and guidance throughout my project.

I would also like to thank Dr. David Young for his invaluable counsel throughout my project. Collaborations with the Young laboratory enabled the completion of the TLDA profile of HDAC expression in OA cartilage, and to learn new laboratory techniques which I have implemented throughout my project.

Thank you to my partner Lex for his continued support, love and understanding. I hope now our worldwide adventures together can really begin.

My deepest appreciation goes to my parents for their constant love, friendship and encouragement to pursue my goals. I would also like to thank the rest of my family and friends who have also been incredibly supportive.

Finally I would like to thank the BBSRC and Smith and Nephew who funded this project, and the John and Pamela Salter Trust who enabled me to buy the siRNAs used in this project. Also thank you to the UEA for hosting my project.

Chapter I: General Introduction

Chapter I

Introduction

1.1 The Structure and Tissues of Synovial Joints

The most common joint of the human skeleton is the synovial joint. The bones of the synovial joint (see Fig. 1.0) are capped with a thin layer of hyaline cartilage, known as articular cartilage, which provides a smooth surface for joint movement. The joint is enclosed within a fibrous capsule which holds it together. The fibrous capsule is lined with a synovial membrane, the resident cells of which secrete synovial fluid into the joint cavity to lubricate and reduce friction upon movement. The bones of the joint are further held together by ligaments made of dense connective tissue.

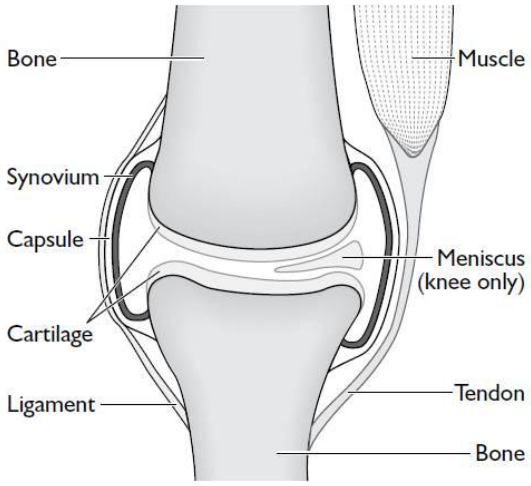

Figure 1.0. The structure of the synovial joint

(*Taken from the osteoarthritis information booklet from Arthritis Research UK- http://www.arthritisresearchuk.org*).

1.1.1 Articular Cartilage

Articular cartilage is a specialised avascular tissue which provides a low friction surface for movement and distributes load equally throughout the joint. The cartilage matrix is produced and maintained by a sparse population of specialised cells called chondrocytes, which are embedded within the matrix itself. Articular cartilage is composed of two main extracellular matrix (ECM) components, type II collagen and aggrecan. Type II collagen forms a highly organised fibrous scaffold which interacts with other cartilage specific collagens, including collagen types IX and XI, and other matrix components, providing cartilage with tensile strength. Large proteoglycan aggregates, mainly composed of hyaluronan and aggrecan, are embedded within and interact with the collagen scaffold. The proteoglycan aggregates have an intense negative charge that attracts water molecules into the tissue, causing the aggregates to swell against the collagen network and giving cartilage the ability to resist compression. The hydration of aggrecan also allows nutrient and solute transport from the synovial fluid into the cartilage tissue, thus maintaining the metabolic activity of resident chondrocytes (Dudhia, 2005). Overall articular cartilage is composed of approximately 70% water, 25% ECM protein and 5% chondrocytes (Kumar et al, 2001). Other smaller leucine-rich proteoglycans, including decorin, biglycan, fibromodulin and lumican, help maintain the cartilage structure through interaction with the collagen scaffold (Goldring, 2000). It is postulated that PRELP (proline/arginine-rich end leucine-rich repeat protein) and chondroadherin receptors provide interaction between the cartilage matrix and chondrocytes by binding cell membrane proteins, such as syndecan and $\alpha 2\beta 1$ integrin (Goldring, 2000).

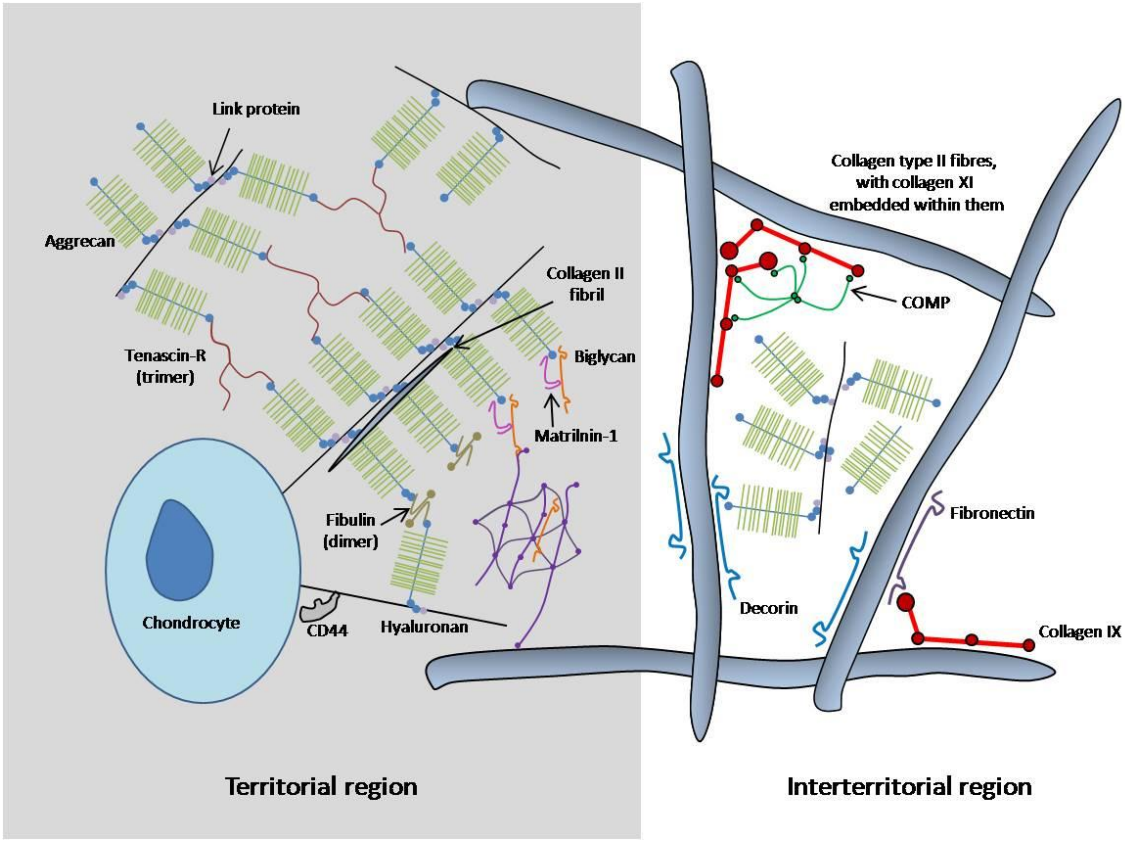

Figure 1.1. The structure of articular cartilage.

Cartilage consists of a territorial (peri-cellular) region and interterritorial region. The territorial region is rich in collagen type VI. Aggrecan can associate with proteins, such as fibulin and tenascin-R. Large aggregates of hyaluronan and aggrecan are trapped between the collagen type II network in the interterritorial region. The collagen network is further strengthened by collagen binding proteins, including decorin, fibromodulin and collagen type IX. (Adapted from (Dudhia, 2005)).

Mature human articular cartilage is composed of four major layers: the superficial, middle (transitional), deeper and calcified zones. Each zone can be distinguished by differences in chondrocyte morphology and content of glycosaminoglycans, collagen, water and minerals. The integrity of the superficial layer is essential for weight distribution throughout the joint (Kumar et al, 2001), with any change in structure or morphology potentially leading to cartilage breakdown and disease onset. The superficial layer is divided into the 'outermost' and 'deepest' layer. The outermost layer (facing the joint space) is acellular and contains types I, II and III collagen fibres that orientate parallel to the articular surface, and a low amount of proteoglycan (Clouet et al, 2009). The deepest superficial layer also contains types I, II and III collagen fibres (Clouet et al, 2009; Kuettner, 1992), but also contains chondrocytes. The tissue's main mechanical properties can be attributed to the zonal organisation of deeper cartilage

layers (Kumar et al, 2001). The middle and deeper zone matrices contain high proteoglycan content and the prominent collagen fibres increase in diameter, acquiring a more perpendicular orientation in respect to the articular surface (Schumacher et al, 1994). The cartilage in contact with the subchondral bone is known as the calcified zone, containing a limited number of hypertrophic chondrocytes that synthesise type X collagen. Calcification takes place on collagen fibres, which anchors cartilage to the subchondral bone (Clouet et al, 2009). The role of each cartilage ECM component is complex, but primarily they interact to enable interaction and communication between the chondrocytes and surrounding ECM to provide the correct structural properties of cartilage.

Chondrocytes within the adult cartilage are organised in well-defined vertical columns and horizontal strata (Hunziker et al, 2007) and are often surrounded by a peri-cellular matrix. The peri-cellular matrix is rich in hyaluronan, proteoglycans and aggregates of type VI collagen. The chondrocyte and its peri-cellular matrix are collectively known as a chondron. The depth-related differences in biochemical composition and macromolecule organisation of cartilage arise from the metabolic specialisation of the resident chondrocytes in each layer (Schumacher et al, 1994). The deepest superficial layer is the most cellular region of the tissue, containing ellipsoidal chondrocytes (Clouet et al, 2009; Schumacher et al, 1994). The orientation of chondrocytes within this layer is debated, but a recent study found grouped cell patterns that were orientated parallel to the articular surface (Rolauffs et al, 2008). The resident chondrocytes of the middle zone are rounded rather than ellipsoidal, and those of the deep zone are larger, elongated and arranged in vertical columns (Schumacher et al, 1994).

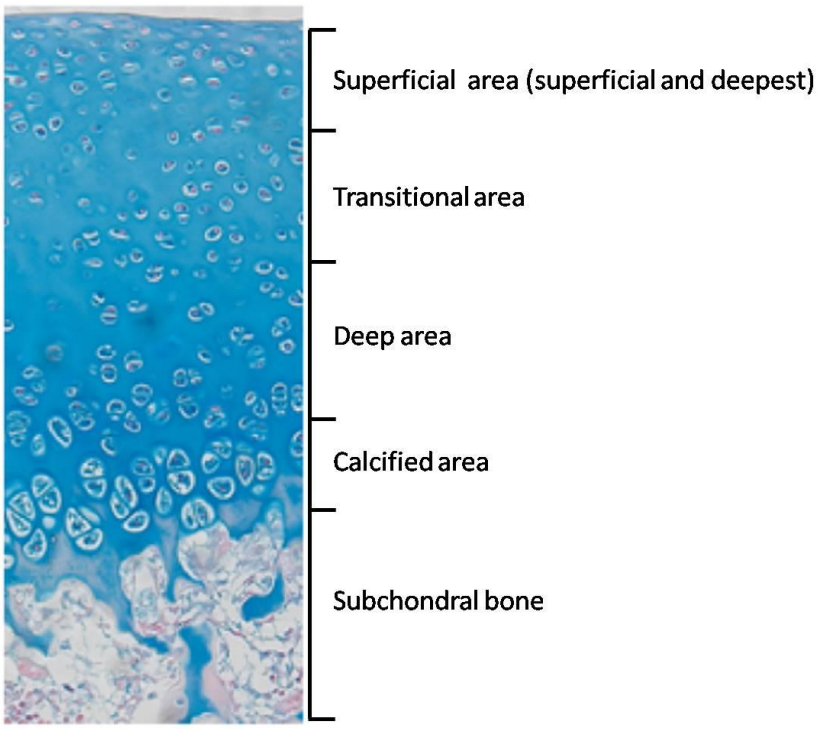

Figure 1.2. The histological organisation of articular cartilage.

Mature human articular cartilage is composed of four major layers: the superficial, middle (transitional), deeper and calcified zones. Each zone can be distinguished by differences in chondrocyte morphology and content of glycosaminoglycans, collagen, water and minerals. The chondrocytes are organised anisotropically into distinct vertical columns and horizontal strata within the cartilage deep zone. (Adapted from (Clouet et al, 2009)).

1.1.2 Chondrocytes

Chondrocytes are the single cellular component of adult hyaline cartilage and responsible for the maintenance of cartilage structure and function (Archer et al, 1982; Goldring, 2000; Goldring & Goldring, 2007). The cells are derived from differentiated mesenchymal cells during the process of chondrogenesis. This is an essential part of skeletal development, allowing the formation of cartilage intermediate templates for future limb development (Goldring et al, 2006). Following the aggregation and differentiation of chondroprogenitor mesenchymal cells, the chondrocytes undergo proliferation, terminal differentiation, hypertrophy, ending with apoptosis or autophagy (Goldring & Goldring, 2007). The process of chondrogenesis is followed by endochondral ossification, during which the hypertrophic chondrocyte matrix is invaded by vascular elements, allowing entry of skeletal cells from the osteoblast lineage for bone development.

Chondrocytes of adult cartilage are fully differentiated and survive under relatively hypoxic conditions in the absence of a vascular supply. The cells have low metabolic activity and possess little regenerative ability (Goldring & Goldring, 2007). In the absence of disease, chondrocytes maintain low replacement of cartilage matrix proteins; cartilage collagen has a half life of >100 years (Verzijl et al, 2000) and glycosaminoglycan constituents an estimated half-life of 3-24 years (Maroudas et al, 1998). Cartilage matrix homeostasis is maintained by the chondrocyte through a synchronised balance between anabolism and catabolism.

The chondrocytes of the cartilage superficial zone are particularly important due to their synthesis and secretion of lubricin into the joint space, thus contributing to joint lubrication. Chondrocytes of the superficial zone are predominately the first to respond to mediators within the synovial fluid and changes in mechanical stimuli (Rolauffs et al, 2008; Schumacher et al, 1994).

Chondrocytes express cell membrane receptors that bind components of ECM, enabling them to recognise and respond to biomechanical stimuli within the joint (Millward-Sadler & Salter, 2004). For example, chondrocytes respond to dynamic compression by increasing matrix synthesis and decrease synthesis in response to joint injury (Sauerland et al, 2003). Chondrocytes also respond to joint injury by increasing their expression of inflammatory mediators, cartilage degrading proteases and stress response factors

(Sauerland et al, 2003). There are many potential cell membrane mechanoreceptors, including stretch activated ion channels, hyaluronan receptor CD44, anchorin II (a collagen type II receptor) and integrin receptors.

1.1.3 Collagen

Collagen is the main protein responsible for the structural integrity of vertebrates and many multicellular organisms, with collagen fibrils providing the major biomechanical scaffold for cell attachment and macromolecule anchorage (Kadler et al, 1996). Suprafibrillar collagen architecture is tissue dependent and defines and maintains the structure of many tissues such as the skin, tendon, bone and cartilage (Hulmes, 2002; Kadler et al, 1996).

Fibrillar collagen type II is one of the main ECM components of articular cartilage. All fibrillar collagens begin synthesis in the endoplasmic reticulum (ER) from three constituent polypeptide α-chains, forming a unique triple helical structure known as pro-collagen (Lamande & Bateman, 1999). The pro-collagen molecules are then secreted from the ER and transported to the cis-Golgi, followed by transportation from the Golgi apparatus to the plasma membrane for secretion into the ECM (Canty & Kadler, 2005; Hulmes, 2002).

The three α-chains that form the pro-collagen molecule can be identical, such as collagen type II which contains three α1(II) chains, or differ such as collagen type I which contains two α1(I) chains and one α2(I) chain. To allow formation of the pro-collagen triple helix each α-chain consists of the repeating structure Gly-Xaa-Yaa, where Xaa and Yaa residues are commonly proline or hydroxyproline. The single hydrogen side chain of glycine allows tight interaction between α-chains (Kadler et al, 1996).

Each pro-collagen molecule consists of an uninterrupted triple helix flanked by short extrahelical telopeptides at the N- and C-terminus. The telopeptides, known as pro-domains, do not have the Gly-Xaa-Yaa repeat sequence or form part of the triple helical structure (Hulmes, 2002). However, both pro-domains are essential for pro- and mature-collagen formation. Initial interaction between the α-chains occurs at the C-propeptide and ensures constituent chains are correctly aligned prior to triple helical nucleation, which occurs in a zip-like manner, from the C- to N-terminus (Engel & Prockop, 1991).

The highly conserved 245 amino acid sequence of the C-propeptide also contains a 15 residue discontinuous variable sequence which determines α-chain stoichiometry (Lees et al, 1997).

During and following secretion from the cell into the ECM the pro-collagens are proteolytically processed at the N- and C-telopeptides by specific N- and C-terminus metalloproteinases, producing mature-collagen molecules that spontaneously assemble into fibrils (Fukui et al, 2002). N-terminus proteases include ADAMTS2, ADAMTS3 and ADAMTS14, a family of proteases discussed further in section 1.3.3 (Colige et al, 1997; Colige et al, 2002; Fernandes et al, 2001). C-terminus proteases include bone morphogenic protein-1 (BMP-1) and mammalian Tolloid-like (mTLL)-1 and -2 (two genetically distinct BMP-1-related proteases) (Li et al, 1996; Pischon et al, 2004; Uzel et al, 2001). The C-propeptide is responsible for solubility post ER secretion, thus its main extracellular function is to prevent fibril formation. The N-propeptide, which has greater variability than the C-propeptide, influences fibril shape and diameter. Finally, following spontaneous assembly fibrils are stabilised by covalent cross-linking initiated by oxidative de-amination of specific lysine and hydroxylysine residues, within collagen, by lysyl oxidase (Kadler et al, 1996; Siegel et al, 1970).

In addition to this, long collagen fibrils can be traced from locations deep within the cell, where they may coexist with numerous shorter fibrils, through a distinctive fibripositor (fibril-depositor) structure (Canty & Kadler, 2005; Canty et al, 2004). In embryonic tendon this structure is located at the side of the cell, aligns along the long axis of the tendon and protrudes into the spaces between cells to extracellular collagen fibril bundles (Canty & Kadler, 2005; Canty et al, 2004). It is now postulated that collagen fibrillogenesis is initiated during transport from the Golgi apparatus to the plasma membrane, in transport carriers known as the Golgi-to-PM transport compartments (GPCs). These carriers are thought to fuse with the plasma membrane to form new fibripositors, or fuse with the base of existing fibripositors, which then direct collagen deposition. Fibripositors have also been shown to facilitate collagen fibril growth, which may occur at the base of the fibril in the fibripositor through the addition of individual collagen molecules (Holmes et al, 1998), or by end-to-end fusion with nascent short fibrils (Canty & Kadler, 2005; Kadler et al, 2000).

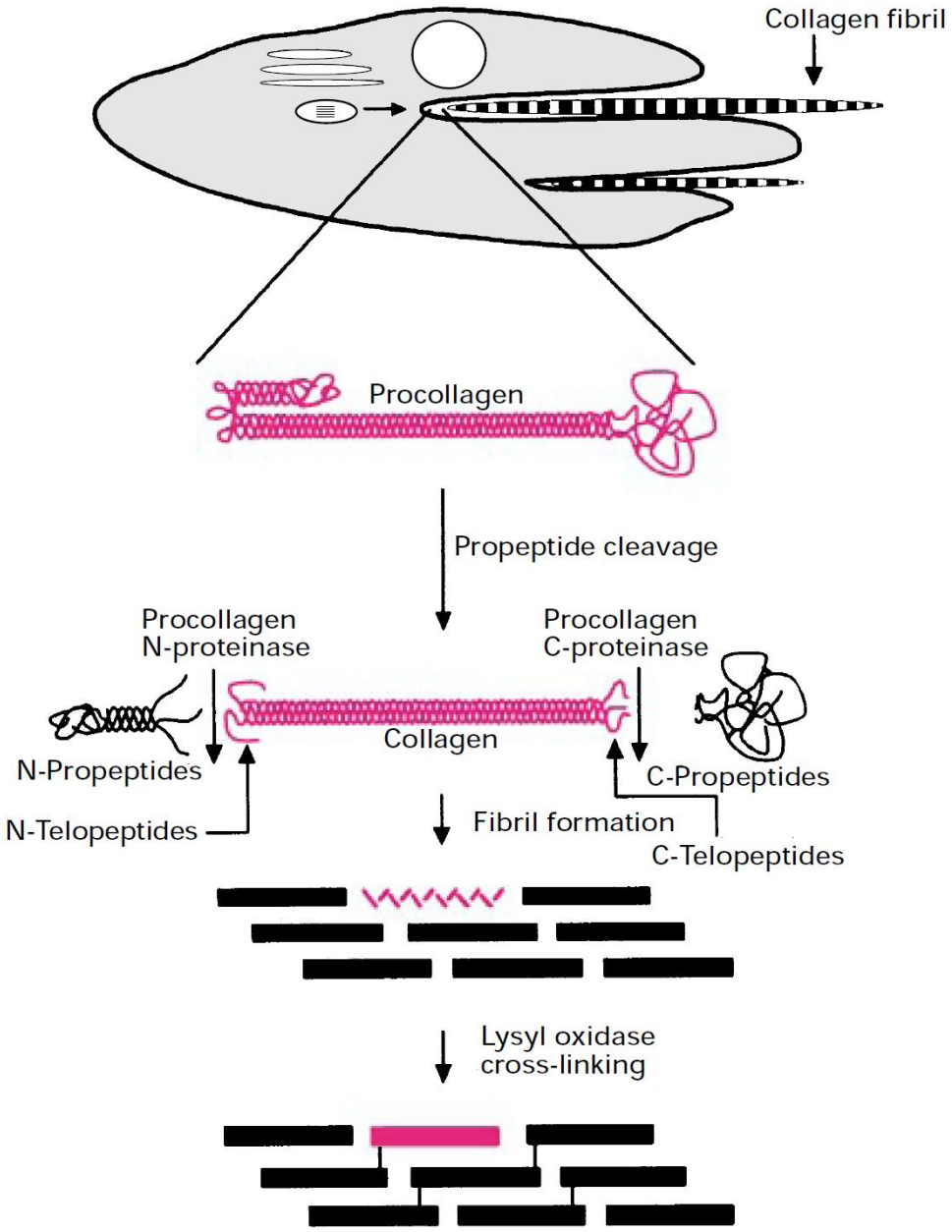

Figure 1.3. The formation of collagen fibrils.

Pro-collagen consists of a 300nm long triple helical domain (comprised of three α-chains) flanked by a trimeric globular C-peptide domain and a trimeric N-propeptide domain. Pro-collagen is secreted from cells and converted into collagen by removal of the N- and C-propeptides by pro-collagen metalloproteinases. This produces mature collagen that spontaneously self-assembles into cross-striated fibrils. (Taken from (Kadler et al, 1996)).

1.1.4 Aggrecan and Hyaluronan

Proteoglycan aggregates are mainly composed of aggrecan molecules non-covalently bound to a central hyaluronan molecule (Hardingham & Muir, 1974). Hyaluronan molecules are intensely negatively charged and composed of alternating polymers of glucuronic acid and N-acetylglucosamine joined together by ß1-3 linkage. Hyaluronan extensively expands in solution, forming a net of extended random coiled molecules. The molecule can be found intra-cellularly, but is predominantly found within the cartilaginous ECM in large aggregates with aggrecan. Up to a hundred aggrecan monomers can bind to a single hyaluronan molecule, with the interaction stabilised via a link protein (Morgelin et al, 1988) (Figure 1.4).

Aggrecan is composed of a long core protein consisting of functional domains (see Figure 1.4). At the N-terminus are two globular domains, G1 and G2, separated by a 150 residue interglobular domain (IGD) (Roughley, 2001). The G2 domain is followed by a long central glycosaminoglycan (GAG) attachment region, where keratan sulphate and chondroitin sulphate covalently bind. A final globular domain, G3, is found at the C-terminus. The G1 domain, along with link protein, is responsible for aggrecan-hyaluronan interaction (Roughley, 2001). The function of the other globular domains is unclear (Roughley, 2001). The GAG attachment region is separated into three domains responsible for the binding of keratan sulphate (KS domain) and chondroitin sulphate (CS1 and CS2 domains) (Roughley, 2001).

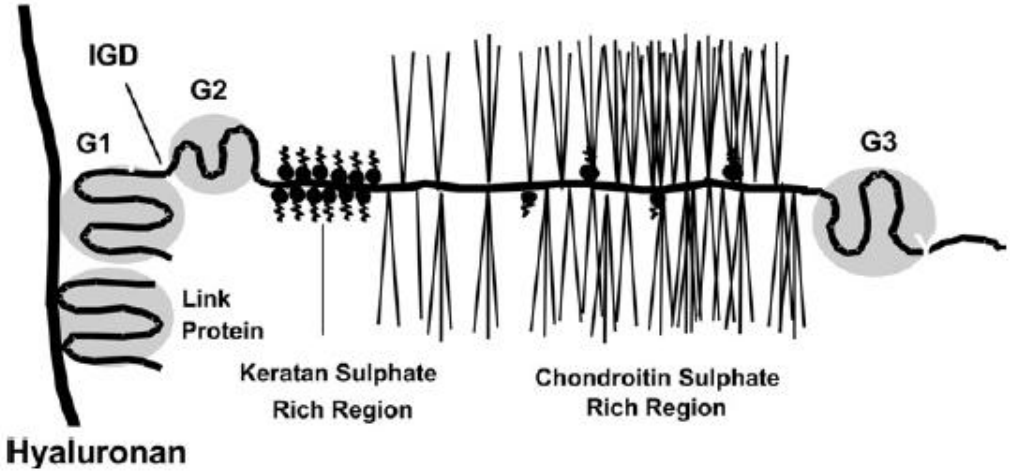

Figure 1.4. The structure of aggrecan

The structure of aggrecan consists of three globular domains (G1, G2 and G3) and a glycosaminoglycan (GAG) attachment region. The GAG attachment region is separated into three domains responsible for keratan sulphate (KS domain) and chondroitin sulphate (CS1 and C2) binding. (Taken from (Porter et al, 2005)).

The functional properties of proteoglycan aggregates are dependent on the amount and structure of aggrecan, the size of hyaluronan, and the proportion of link protein (Roughley et al, 2003). Aggrecan structure is dependent on many factors such as age, species and anatomical site (Glant et al, 1986). Structural variations in aggrecan can occur during synthesis and by proteolytic processing once within the ECM. Aggrecan has 5 proteolytic cleavage sites for resident articular cartilage proteases. The first is located in the IGD between G1 and G2, and the remaining four in the CS2 domain (Loulakis et al, 1992; Roughley et al, 2003; Sandy et al, 1991). Proteolytic cleavage and loss of aggrecan from articular cartilage characterises many joint pathologies, such as osteoarthritis, and is predominantly driven by ADAMTS enzymes (Little et al, 2007).

1.1.5 Synovium and Synovial Fluid

The synovium is a soft connective tissue which lines the inner surface of the joint capsule. It is divided into two layers, the subintima and intima. Normal synovial intima consists of two cell populations, the macrophage-like synoviocytes (type A) and the fibroblast-like synoviocytes (type B) (Henderson et al, 1988). The synovial intima cells are responsible for the production of synovial fluid components, absorption from the joint cavity, and blood/synovial fluid exchange. The main function of the synovial fluid is to act as a lubricant to the joint, with its viscosity and lubricating properties attributed to its hyaluronan and lubricin content. A normal joint should only contain a microscopic film of synovial fluid, allowing hydrodynamic lubrication and nutrition of cartilage.

1.2 Osteoarthritis

1.2.1 Osteoarthritis Pathology

Osteoarthritis (OA) is a multifactorial, degenerative, progressive joint disease, characterised by degeneration of articular cartilage, synovitis and changes in the peri-articular and subchondral bone (Goldring & Goldring, 2007). It is currently the leading cause of pain and disability in the aging population (>60 years of age) (Franses et al, 2009).

OA is commonly characterised by cartilage degradation, with almost complete cartilage loss observed in the final stages of the disease. Early OA is associated with sub-clinical lesion development in the cartilage articular surface, causing it to gradually roughen and thin (see Figure 1.5b). Lesion progression leads to almost complete cartilage degradation and exposure of the subchondral bone beneath (see Figure 1.5c). In severe cases the sufferer is left with major joint deformity and loss of normal joint function.

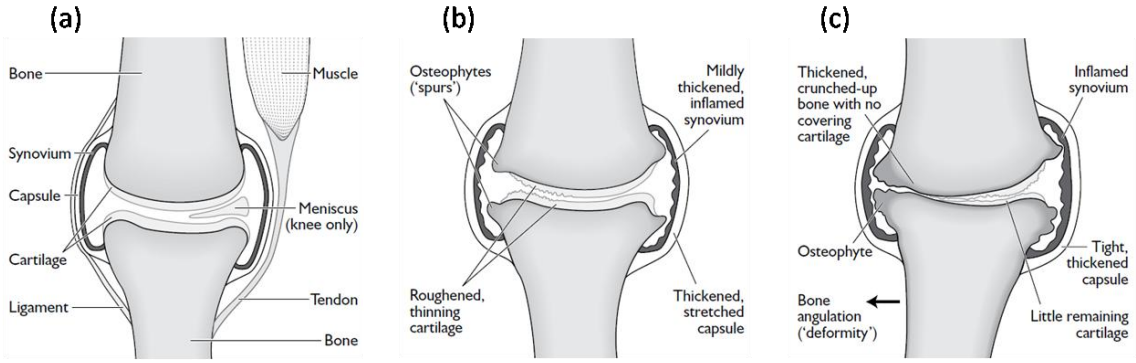

Figure 1.5. Schematic representation of OA progressive joint destruction.

(a) The normal joint: the subchondral bone is covered by smooth articular cartilage **(b)** Early osteoarthritic joint: thinning of the articular cartilage is coupled with thickening of the subchondral bone and osteophyte growth at the joint margins. Joint space narrowing and mild synovium inflammation is also evident. **(c)** Severe osteoarthritic joint: there is little remaining cartilage and the exposed subchondral bone is flattened and deformed. Large osteophytes have formed and inflammation of the synovium is still apparent. (*Adapted from the osteoarthritis information booklet from Arthritis Research UK- http://www.arthritisresearchuk.org*).

Angiogenic vascular invasion of cartilage, originating from the subchondral bone, has been detected in the OA joint (Suri et al, 2007). Angiogenic invasion results in cartilage calcification, causing reduced cartilage thickness and innervation. The innervation of cartilage provides a possible source of OA pain (Franses et al, 2009). Increased expression of the pro-angiogenic factor VEGF (vascular endothelial growth factor) by OA chondrocytes has been shown, and it is suggested that the failure of deep zone chondrocytes to express anti-angiogenic protease inhibitors may permit vascular invasion from the subchondral bone (Franses et al, 2009).

The subchondral bone within the OA joint has increased thickness and often develops bony outgrowths at joint margins, known as osteophytes. The exposure of bone at the articular surface is thought to allow 'leakage' of synovial fluid towards the medullar spaces, affecting the bone-marrow mesenchymal stem cells (MSCs), and thereby contributing to the formation of osteophytes and cartilage nodules (Clouet et al, 2009). The excessive remodelling of bone is itself linked to increased cytokine production and cartilage loss (Sakao et al, 2009). The deterioration of the subchondral bone is postulated to be largely responsible for joint pain, but this claim is yet to be substantiated.

Supporting connective tissues are also affected in OA, with articular muscles surrounding the joint often becoming weaker, thin and wasted, whilst surrounding joint ligaments become thicker and contracted. These changes can result in bones being pushed out of their normal position, resulting in biomechanical changes within the joint. However, it is unclear if changes to the supporting tissues are the cause or an effect of OA.

The OA synovium undergoes hypertrophy and hyperplasia due to an increased number of lining cells and infiltration of the sublining tissue with activated B-cells and T-lymphocytes (Pelletier et al, 2001). Despite synovial inflammation, OA is not classified as an inflammatory disease due to an absence of neutrophils in the synovial fluid and a lack of systemic inflammation (Goldring & Goldring, 2007). However, clinical presentation of the OA joint includes stiffness, effusions and swelling which indicates that the synovium does have a low-grade contribution to the disease (Krasnokutsky et al, 2007). Areas of synovial inflammation are commonly localised to areas of pathologically damaged cartilage and bone (Krasnokutsky et al, 2007), thus

inflammation tends to occur in patches rather than inflammation of the entire synovium. It has been demonstrated that synovitis leads to an over-expression of pro-inflammatory cytokines, such as interleukin-1β (IL-1β), tumour necrosis factor-α (TNF-α) and -β, leading to protease expression and subsequent cartilage destruction (Benito et al, 2005). One suggestion is that synovial inflammation is a secondary phenomenon related to the release of cartilage breakdown products into the synovial fluid (Pelletier et al, 2001).

The adult chondrocyte plays a critical role in OA pathogenesis by responding to adverse environmental stimuli. It does this by promoting cartilage degradation and down-regulating matrix synthesis and repair through the release of cytokines and growth factors (Goldring & Goldring, 2007). This is partially mediated via chondrocyte cell membrane receptors binding components of the ECM. These receptors include integrins which activate upon binding to ECM components, such as fibronectin (FN) and type II collagen fragments, causing chondrocyte production of inflammatory cytokines, chemokines and matrix degrading proteases (Pulai et al, 2002). Chondrocyte production of IL-1 and TNFα is thought to be the primary mediator of the increased expression of cartilage catabolic enzymes detected in the OA joint (Clouet et al, 2009). Interestingly, in early OA increased chondrocyte matrix synthesis is detected. This is thought to be an attempt by the chondrocytes to counterbalance the increased catabolism within the joint. Increased cartilage metabolism in response to cartilage damage is demonstrated in early cartilage studies, but increased metabolism rapidly decreases (Meachim, 1963). Chondrocyte death is also increased in OA, with both apoptotic and non-apoptotic signals detected (Almonte-Becerril et al, 2010).

In conclusion, the current view is that an increased expression of catabolic enzymes from the articular chondrocytes is responsible for ECM degradation and the subsequent changes within the OA joint. The expression of these enzymes is induced via the secretion of pro-inflammatory cytokines from OA chondrocytes and activated synoviocytes. The catabolic enzymes are predominantly from the metalloproteinase family, including the MMPs (matrix metalloproteinases) and ADAMTSs (a disintegrin and metalloproteinase with thrombospondin motifs). The increased catabolism is coupled with reduced expression of TIMPs (Tissue Inhibitors of Metalloproteinases), the endogenous inhibitors of MMPs and anabolic growth factors, which are discussed in more detail in section 1.3.5 and 1.3.6 (Figure 1.6) (Davidson et al, 2006; Kevorkian et al, 2004; Murphy et al, 2002).

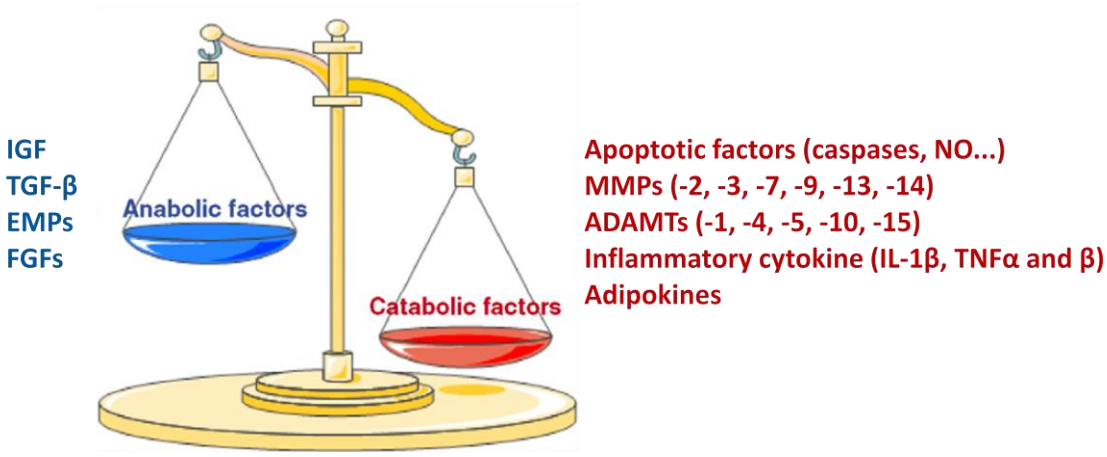

Figure 1.6. The imbalance between anabolic and catabolic factors in the physiopathology of osteoarthritis.

The imbalance between catabolic and anabolic factors contributes to the alteration of the biomechanical properties of articular cartilage, leading to the destruction of its ECM. (IGF: insulin-like growth factors, TGF-β: transforming growth factor-β, BMPs: bone morphogenetic proteins, FGFs: fibroblast growth factors, NO: nitric oxide, MMPs: matrix metalloproteinases, ADAMTS: a disintegrin and metalloproteinase with thrombospondin repeats, IL-1β: interleukin-1β, TNF: tumour necrosis factor). (Taken from (Clouet et al, 2009))

Thus OA is a multi-faceted disease affecting all major components of the joint. However, the interaction between the joint components and where pathology begins still remains unclear.

1.2.2 Osteoarthritis Epidemiology

OA is the leading cause of physical disability and impaired quality of life in industrialised nations, affecting over 50 million people worldwide (Dai & Ikegawa, 2010). The study of OA epidemiology is difficult due to complex disease pathology, the inability to detect the point of OA onset and the inability to grade disease severity (Pollard et al, 2008). OA is diagnosed primarily through radiography, with magnetic resonance imaging (MRI) and arthroscopy used more rarely. The severity of joint damage is then graded, commonly using the Kellgren and Lawrence system (Kellgren & Lawrence, 1957), from 0 to 4 depending on sequential appearance of osteophytes, joint space loss, sclerosis and cysts (Arden & Nevitt, 2006). Several joints might be affected by OA, but the sites most commonly affected are the knees, hips, fingers and the lumbar and cervical spine (Clouet et al, 2009). Age is a key risk factor associated with OA development, affecting 9.6% of men and 18% of women over the age of 60 years worldwide. Thus population aging is predicted to worsen the socio-economic impact of OA (Bitton, 2009). (For epidemiology review refer to Ref: (Arden & Nevitt, 2006))

1.2.3 Osteoarthritis Aetiology

The risk factors associated with OA include; age, previous joint injury, joint instability and/or malalignment, genetic inheritability, female gender, intra-articular crystal deposition, muscle weakness, peripheral neuropathy and obesity (Goldring & Goldring, 2007; Valdes et al, 2007). Thus identifying the reason or reasons responsible for the onset of OA in any given individual is complex due the various factors affecting the joint.

Age is a primary risk factor for OA onset, with disease development commonly seen between the ages of 40 and 60 years. It is thought OA affects people later in life due to the contributing factors of weakening muscles, weight gain and the bodies lessening ability to heal itself. Age-related changes in the composition and structure of the cartilage ECM also contribute to OA onset, often causing softening of the articular surface and decreased tensile strength of the matrix (Goldring & Goldring, 2007). However, despite the clear association between increased age and OA onset it is also important to remember that erosive lesions can be found in young cartilage and that not everyone over the age of 40 develops OA. Therefore aging alone is unlikely to be the causative factor.

A number of twin-pair, sibling risk and segregation epidemiology studies have been completed for OA, and have indicated that genetic contribution plays a major role in OA predisposition and onset (Chitnavis et al, 1997; Dai & Ikegawa, 2010; Doherty, 2000; MacGregor et al, 2000; Spector & MacGregor, 2004). The data produced from these studies and genome linkage maps have enabled inheritance patterns and the location of potentially causative mutations to be identified. The identification of OA susceptibility genes would lead to a better fundamental understanding of the disease, but the data produced across past studies is not always consistent (Valdes et al, 2007). To date, several groups have reported the identification of OA susceptibility genes through candidate gene association studies (Dai & Ikegawa, 2010). One such example is a single nucleotide polymorphism (SNP) identified in the GDF5 gene (growth differentiation factor 5) known as rs143383, which has been found to associate with knee OA in a large-scale meta-analysis study and smaller scale genetic studies (Chapman et al, 2008; Evangelou et al, 2009). The identification of this polymorphism is important as GDF5 has a known role in the development and maintenance of bone and cartilage (Francis-West et al, 1999), with mutations in this gene linked to several disorders of skeletal development, such as chondrodysplasia (Evangelou et al, 2009; Miyamoto et al, 2007). Thus, its function in OA aetiology appears highly plausible (Chapman et al, 2008; Evangelou et al, 2009). However, SNPs identified in small cohorts, such as the identification of the FRZB T/G haplotype which was associated with susceptibility to OA in the hip and knee (Valdes et al, 2007), are not always replicated in large cohort analysis (Evangelou et al, 2009). This emphasises the difficulty in identifying OA susceptibility genes. Other genetic mutations yet to be identified are postulated to affect chondrocyte differentiation and function, cartilage matrix formation and skeletal development. These all potentially affect joint structure and function, leading to OA onset. Therefore, further genetic association studies on OA susceptibility are necessary to capture the complete picture of the genetic aspect of OA (Dai & Ikegawa, 2010).

OA is more common in women, especially in the hip and knee, and is often more severe. It is thought that estrogen loss after menopause may accompany OA onset. The evidence currently available on the effect estrogen has on cartilage is conflicting. However, studies researching prevalence and incidence of OA in post-menopausal women with or without hormone replacement strongly indicates estrogen has a chondroprotective effect (Richette et al, 2003). The literature also indicates that animal

models undergoing ovariectomy and subsequent estrogen reduction often exhibit signs of cartilage damage (Sniekers et al, 2008). Chondrocytes have been shown to express estrogen alpha and beta receptors, suggesting that cartilage is sensitive to the hormone (Richmond et al, 2000). It is also postulated that estrogen may decrease the acceleration of subchondral bone remodelling in postmenopausal women (Felson et al, 1993). Furthermore, synoviocytes have also been shown to express an estrogen receptor, which makes synoviocytes another possible target for estrogen's effects on the joint (Ushiyama et al, 1995).

Traumatic joint injury and joint misalignment are linked to OA onset. *In vitro* experiments suggest that injurious static compression of cartilage results in reduced proteoglycan, damage to the collagen network and reduction in chondrocyte matrix protein production (Goldring & Goldring, 2007; Guilak et al, 2004). These all result in the loss of cartilage matrix integrity, possibly leading to the development of OA.

Obesity is also a key factor associated with OA onset, which will only be exacerbated with the currently growing obesity epidemic (Cicuttini et al, 1996; Oliveria et al, 1999). Increased body weight leads to increased load bearing for all joints, which contributes to cartilage wear, lesion formation and OA progression (Messier et al, 2005). Adipokines produced by white adipose tissue, including leptin, adiponectin and restin, have been detected in the synovial fluid of OA joints (Presle et al, 2006). Adipokines are known regulators of inflammation and immune response, so their presence in OA synovial fluid indicates that fat actively contributes to inflammation and cartilage destruction. Obesity and OA correlates strongly in the knee joint (Felson et al, 1988). Obesity also increases the likelihood of OA development in non-weight-bearing joints, supporting the role of adipokines and other systemic factors in obesity-associated OA development (Presle et al, 2006).

1.2.4 Osteoarthritis Therapy

Currently there are no efficacious therapies for OA, with available treatments only partially addressing the clinical issue. Therapies are divided into pharmacological and non-pharmalogical treatments. The first pharmacological step after diagnosis is pain management using painkillers ranging from mild, such as paracetamol, to strong, including non-steroidal anti-inflammatory drugs (NSAIDs), cyclooxygenase-2 (Cox-2) inhibitors, glucocorticoids and opioids. However, these treatments can have severe side

effects, exhibiting gastrointestinal, renal and cardiovascular toxicity. Glucocorticoid injections directly into the joint can reduce pain for several weeks and is particularly effective in knee and finger joints. These injections are limited to every 3-4 months due to metabolic events. Slow-acting treatments aim to slow OA progression and reduce pain include dietary supplements glucosamine and chondroitin sulphate, co-enzyme S-adenosyl methionine and hyaluronan joint injection. The dietary supplements have been shown to possibly stimulate matrix synthesis (Clouet et al, 2009; Derfoul et al, 2007), but there are no current data to support pain relief and their use remains controversial. S-adenosyl methionine treatment has been shown to increase GAG synthesis, accompanied by significant pain relief and improvement of joint function (Najm et al, 2004). Injections of hyaluronan solutions, naturally found in the synovium, into the knee can be given over a period of 3-5 weeks to reduce pain. Hyaluronan is thought to provide a protective coating over the articular surface and to act as a shock absorber for the joint, but there is contention over the effectiveness of this treatment (Bannuru et al, 2009). Hyaluronan has also been found to bind and activate Toll-like receptor-4 (Termeer et al, 2002). Toll-like receptors are known to play a role in inflammatory arthritis, thus hyaluronan could mediate its effects though this pathway (Brentano et al, 2005). Non-pharmalogical treatments are also encouraged. These include: weight loss, physical therapy, aerobics, muscle strengthening, walking aids, thermal treatment and acupuncture (Clouet et al, 2009). Patients that cannot achieve adequate pain relief from these methods are then considered for total joint replacement. Joint replacement is the only method available to truly ‘cure’ OA, which is accompanied by its own complications.

Future treatments under investigation include novel analgesic and anti-inflammatory treatments COX/LOX inhibitors (cyclooxygenase/lipooxygenase) and CINODs (Cyclooxygenase-inhibiting nitric oxide donors), which have exhibited minimal side effects in phase III trials. Disease modifying osteoarthritis drugs (DMOADs), which aim to slow cartilage degradation by targeting specific catabolic enzymes or cytokine activated signalling cascades, are also in development. However, clinical trials have indicated adverse side effects (Hellio Le Graverand-Gastineau, 2009). New surgical techniques are continuously being developed. These include stem cell, cartilage grafting, cell-based implantation and tissue-scaffold engineering procedures. These all have displayed variable success. (For full review Ref: (Clouet et al, 2009)).

1.3 Metalloproteinases

Chondrocytes and synoviocytes are thought to maintain the homeostasis of anabolic and catabolic processes within the joint through the secretion of regulatory mediators. Both cell types are major sources of cytokines and growth factors that can promote or inhibit the expression of proteolytic enzymes. The regulation of MMP and ADAMTS expression is a key mechanism in this process. The MMP and ADAMTS enzymes are members of the metalloendopeptidase family and between them can degrade all components of the ECM matrix. The metzincin metalloproteinase superfamily consists of four subfamilies, adamalysins, matrixins, astacins and serralysins. The matrixins are referred to as MMPs and the adamalysins are referred to as the ADAMs (a disintegrin and metalloproteinase) and ADAMTSs (a disintegrin and metalloproteinase domain with thrombospondin motifs). Metzincin metalloproteinases are named due to the conserved methionine residue found downstream of the catalytic zinc binding site that confers a right-handed 'Met-turn motif'. Although many classes of proteases have increased expression in OA, it is widely accepted that the MMPs and ADAMTSs are the primary mediators of joint destruction (Murphy et al, 2002).

1.3.1 Matrix Metalloproteinases

There are 23 secreted and cell-surface MMP enzymes in humans (Kevorkian et al, 2004). They are neutral endopeptidases which are synthesised as pro-enzymes or zymogens. MMPs were initially classified into five main groups regarding their primary structure, substrate specificity and cellular location; the collagenases (MMP-1, -8 and -13): gelatinases (MMP-2 and -9): stromelysins (MMP-3, -10 and -11): matrilysins (MMP-7 and -26) and membrane-type-MMPs (MMP-14, -15, -16, -17, -24 and -25). However, later identified MMPs did not fit this nomenclature, so currently MMPs are numbered 1 to 28 (not including MMP-4, MMP-5 and MMP-6). The MMP family has a wide range of substrates including other proteases, protease inhibitors, latent growth factors, chemotactic molecules, growth factor binding proteins, cell surface receptors and cell-cell/cell-matrix adhesion molecules (Table 1.0).

Table 1.0

MMP	Enzyme	Known substrates
MMP-1	Interstitial collagenase (Collagenase-1)	Collagens I, II, III, VII, VIII and X, gelatin, aggrecan, versican, proteoglycan link protein, casein, α1-proteinase inhibitor, α2-M, pregnancy zone protein, ovostatin, nidogen, MBP, proTNF, L-selectin, proMMP-2, proMMP-9
MMP-2	Gelatinase-1	Collagens I, IV, V, VII, X, XI and XIV, gelatin, elastin, fibronectin, aggrecan, versican, proteoglycan link protein, MBP, proTNF, α1-proteinase inhibitor, proMMP-9, proMMP-13
MMP-3	Stromelysin-1	Collagens III, IV, IX and X, gelatin, aggrecan, versican, perlecan, nidogen, proteoglycan link protein, fibronectin, laminin, elastin, casein, fibrinogen, antithrombin-III, α2M, ovostatin, α1-proteinase inhibitor, MBP, proTNF, proMMP-1, proMMP-7, proMMP-8, proMMP-9, proMMP-13
MMP-7	Matrilysin-1 (PUMP-1)	Collagens IV and X, gelatin, aggrecan, proteoglycan link protein, fibronectin, laminin, entactin, elastin, casein, transferrin, MBP, α1-proteinase inhibitor, proTNF, proMMP-1, proMMP-2, proMMP-9
MMP-8	Neutrophil collagenase (collagenase-2)	Collagens I, II, III, V, VII, VIII and X, gelatin, aggrecan, α1-proteinase inhibitor, α2-antiplasmin, fibronectin, laminin
MMP-9	Gelatinase B	Collagens IV, V, VII, X and XIV, gelatin, elastin, aggrecan, versican, proteoglycan link protein, fibronectin, nidogen, α1-proteinase inhibitor, MBP, proTNF
MMP-10	Stromelysin-2	Collagens III, IV and V, gelatin, casein, aggrecan, elastin, proteoglycan link protein, fibronectin, proMMP-1, proMMP-8
MMP-11	Stromelysin-3	α1-proteinase inhibitor, fibrin, gelatin
MMP-12	Macrophage metalloelastase	Collagen IV, gelatin, elastin, α1-proteinase inhibitor, fibronectin, vitronectin, laminin, proTNF, MBP
MMP-13	Collagenase-3	Collagens I, II, III and IV, gelatin, plasminogen activator inhibitor 2, aggrecan, perlecan, tenascin
MMP-14	MT1-MMP	Collagens I, II and III, gelatin, casein, elastin, fibronectin, laminin B chain, vitronectin, aggrecan, dermatan sulfate proteoglycan, MMP-2, MMP-13, proTNF
MMP-15	MT2-MMP	proMMP-2, gelatin, fibronectin, tenascin, nidogen, laminin
MMP-16	MT3-MMP	proMMP-2
MMP-17	MT4-MMP	
MMP-18	Xenopus collagenase	Collagen I

MMP-19	RASI-1	Collagen IV, gelatin, laminin, nidogen, tenascin, fibronectin, aggrecan, COMP
MMP-20	Enamelysin	Amelogenin
MMP-21	XMMP (xenopus) MMP-21 (human)	
MMP-22	CMMP (chicken)	Casein, gelatin
MMP-23	CA-MMP	
MMP-24	MT5-MMP	proMMP-2, proMMP-9, gelatin
MMP-25	MT6-MMP, leukolysin	Collagen IV, gelatin, fibronectin, fibrin
MMP-26	Matrilysin-2 endometase	Collagen IV, fibronectin, fibrinogen, gelatin, α1-proteinase inhibitor, proMMP-9
MMP-27	MMP-27 (human)	
MMP-28	Epilysin	Casein

Table 1.0. Matrix metalloproteinases and their substrates.

(CA, cysteine array; α2-M, α2-macroglobulin; COMP, cartilage oligomeric matrix protein; MBP, myelin basic protein; TNF, tumour necrosis factor).
(Adapted from (Murphy et al, 2002; Raffetto & Khalil, 2008)).

1.3.2 Matrix Metalloproteinase Structure

The basic metalloproteinase structure consists of a signal peptide for secretion, a pro-peptide for maintaining latency, a catalytic domain with conserved Zn^{2+} binding sequence, and a COOH-terminal domain with hemopexin domain (Cauwe et al, 2007). The MMPs are characterised by their conserved zinc binding motif **H**EXX**H**XXGXX**H** (X represents any amino acid) within the catalytic domain, and a conserved methionine which forms part of the 'Met-turn' structure (Nagase & Woessner, 1999). The histidines are responsible for the binding of the catalytic Zn^{2+} ion, which is essential for catalytic activity. The catalytic domain is approximately 170 amino acids and formed from a five stranded β-sheet, three α-helices, and bridging loops (Bode et al, 1993). MMPs are secreted in a latent form due to the presence of a pro-domain that must be cleaved before activation. The pro-domain maintains latency via a conserved PRCG(V/N)PD sequence, whose cysteine group interacts with the catalytic Zn^{2+} ion rendering the pro-MMP inactive. The removal of the pro-domain causes a conformational change in the MMP allowing the Zn^{2+} ion to bind water for the hydrolysis of peptide bonds, and for the enzyme to bind with its substrate. This mechanism is known as the 'cysteine switch mechanism' (Van Wart & Birkedal-Hansen, 1990). Cleavage of the pro-domain can be mediated by MMPs themselves, other proteases or chemical induction. However, MMP-11, -14, -15, -16, -17, -21, -23, -24, -25 and -28 have a peptide insert containing a furin recognition sequence, meaning these enzymes maybe activated in the golgi apparatus by furin cleavage before secretion (Berg & Miossec, 2004), although furin-like enzymes may also activate these enzymes extracellularly. The hemopexin domain, found in the stromelysins and collagenases, contributes to substrate specificity (at least for collagenases) and interacts with endogenous inhibitors (Piccard et al, 2007). The domain itself is approximately 210 amino acids and is composed of four anti-parallel β-strands and a α-helix. Its presence is essential for cleavage of the collagen triple-helix (Bode, 1995) and for MT1-MMP activation of pro-MMP2. The function of the proline-rich linker region is unknown. The membrane-bound MMPs (MT-MMPs) are linked to the cell surface through a COOH-terminal transmembrane domain (MT1, MT2, MT3, and MT5-MMP) or a glycosylphosphatidylinositol (GPI) anchor (MT4 and MT6-MMP) (Nagase & Woessner, 1999).

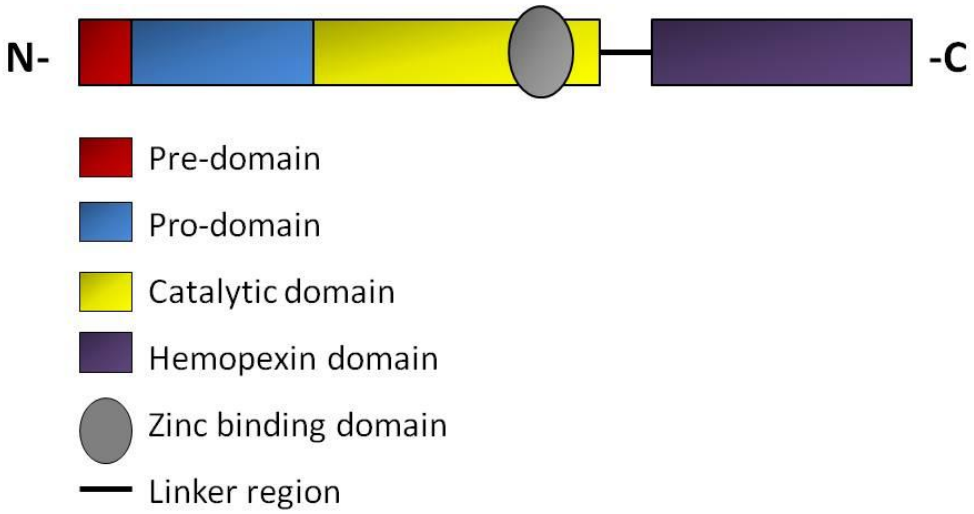

Figure1.7. Common domain structure of matrix metalloproteinases

The collagenases are the main focus of this study, due to the collagen loss observed during OA progression. The classical collagenases (MMP-1, -8 and -13) all cleave collagen α-chains at the same loci, producing a ¼ and ¾ fragment. MMP-2 and MMP-14 can also cleave collagen at this position, but with less efficiency.

MMP-1 and MMP-13 are synthesised by macrophages, fibroblasts and chondrocytes. MMP-8 is primarily synthesised by neutrophils but also by chondrocytes. The enzymes differ in their specific activity to collagen types, with MMP-13 having the highest specific activity for collagen type II (Knauper et al, 1996a). All collagenases are present in diseased cartilage, but MMP-8 expression is only detected at low levels (Berg & Miossec, 2004).

1.3.3 ADAMTSs

There are 19 known human ADAMTSs (a disintegrin and metalloproteinase with thrombospondin motifs) which are numbered 1 to 20 (there is no ADAMTS-11) (Porter et al, 2005). The ADAMTS enzymes are extracellular and can bind to the ECM. The function of only a few of these enzymes has been identified, but many are involved in the cleavage of the pro-collagen N-terminus and the matrix proteoglycans aggrecan, versican and brevican (Table 1.1). ADAMTS-1, -4, -5, -8 and -15 have been shown to cleave aggrecan with varying efficiency, and are therefore termed the aggrecanases. ADAMTS-2, -3 and -14 have been shown to cleave collagen N-propeptides during fibril assembly, and are termed N-propeptidases.

ADAMTS	Alternative names	Known substrates
ADAMTS-1	METH-1 Aggrecanase-3	Aggrecan Versican V1
ADAMTS-2	PCINP	Pro-collagen I, II and III N-propeptide
ADAMTS-3	KIAA0366	Pro-collagen II N-pro-peptide
ADAMTS-4	Aggrecanase-1 KIA0688	Aggrecan, brevican, versican V1, fibromodulin, decorin, carboxymethylated transferring
ADAMTS-5	Aggrecanase-2 ADAMTS11	Aggrecan, Brevican
ADAMTS-6		
ADAMTS-7	ADAMTS-7B	COMP, α2-M
ADAMTS-8	METH-2	Aggrecan
ADAMTS-9	KIAA1312	Aggrecan, versican
ADAMTS-10		
ADAMTS-12		COMP, Aggrecan, α2-M
ADAMTS-13	vWFCP	Von Willebrand factor
ADAMTS-14		Pro-collagen I N-propeptide
ADAMTS-15		Aggrecan
ADAMTS-16		α2-M
ADAMTS-17		
ADAMTS-18		
ADAMTS-19		Aggrecan
ADAMTS-20		Aggrecan

Table 1.1. Human ADAMTS names and known substrates.

(PCINP, pro-collagen I N-proteinase; COMP, cartilage oligomeric matrix protein; a2-M, alpha 2-macroglobulin; vWFCP, von Willebrand factor-cleaving protease). (Adapted from (Porter et al, 2005)).

1.3.4 ADAMTS Structure

The basic ADAMTS structure from N-terminus to C-terminus consists of a signal peptide, pro-domain, metalloproteinase catalytic domain, disintegrin-like domain, a central thrombospondin type-1 like motif, a cysteine-rich domain, a spacer region and finally a C-terminal containing variable numbers of thrombospondin repeats (Porter et al, 2005). The pro-domain is thought to retain enzyme latency, but it is also potentially important for correct protein folding and secretion (Cao et al, 2000; Porter et al, 2005). The metalloproteinase catalytic domain contains a reprolysin-type zinc-binding motif and a methionine residue or 'Met-turn' downstream of the third zinc binding histidine (Porter et al, 2005) (Figure 1.8). The C-terminal domain has a variable number of thrombospondin motifs and additional modules, which are enzyme-dependent; ADAMTS-7 and ADAMTS-12, mucin domain: ADAMTS-20 and the long isoform of ADAMTS-9, GON domain: ADAMTS-13, CUB domain: ADAMTS-2, -3, -10, -12, -14, -17 and -19, PLAC domain.

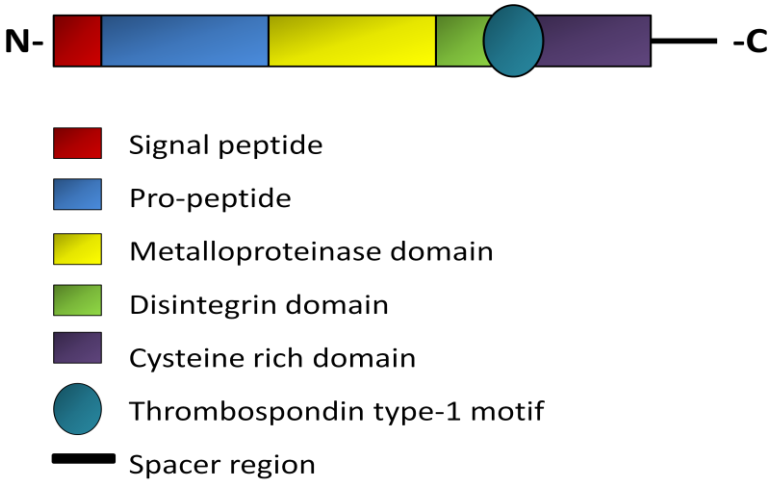

Figure 1.8. Common domain structure of ADAMTSs

The loss of aggrecan from cartilage is an early event in OA that is driven primarily by aggrecanases that cleave at a number of sites in the aggrecan core. The cleavage site within the interglobular domain (IGD), between the N-terminal G1 and G2 globular domains, is the predominantly cleaved site within diseased tissue. Cleavage of the IGD results in the loss of the entire glycosaminoglycan-containing region and subsequent loss of aggrecan function (Rogerson et al, 2008). ADAMTS-4 and ADAMTS-5 are the

most efficient of all the aggrecanases, suggesting an important role in OA pathology. Importantly, ADAMTS-5 null mice are protected against aggrecan loss and cartilage destruction in both inflammatory and osteoarthritis models (Glasson et al, 2005; Stanton et al, 2005). Surprisingly murine deletion of ADAMTS-4 does not confer the same protection as that seen in the ADAMTS-5 null mouse, suggesting ADAMTS-5 is the primary aggrecanase of murine cartilage (Glasson et al, 2004). Consistent with this, the aggrecanolytic activity of ADAMTS-5 was much greater than ADAMTS-4 in both the IGD and the CS-2 regions of aggrecan (Gendron et al, 2007). However, the main aggrecanase in human cartilage is still unknown.

1.3.5 TIMPs

A family of four MMP inhibitors known as the TIMPs (tissue inhibitors of metalloproteinases) have been described. They are endogenous inhibitors of metalloproteinases, binding to active MMPs in a 1:1 ratio, and potential inhibitors of the ADAMTSs. TIMPs are composed of a 125 amino acid N-terminal domain and a 65 amino acid C-terminal domain, each of which is stabilised by three disulphide bonds.

Due to their substantial role in controlling degradation of the connective tissue (via protease inhibition) the expression of TIMPs is carefully regulated during tissue remodelling and physiological conditions. The current view is that TIMP activity is a key factor in regulating cartilage homeostasis, with excess MMP activity and reduced TIMP expression causing pathological cartilage destruction.

The ability of TIMPs 1-4 to inhibit active MMPs is largely promiscuous, though a number of functional differences have been identified (Brew et al, 2000). For example, both TIMP-2 and TIMP-3, unlike TIMP-1, are effective inhibitors of the membrane-type MMPs (MT-MMPs), while TIMP-3, but not TIMP-1, -2 or -4, is a good inhibitor of tumour necrosis factor-κ converting enzyme (TACE) (ADAM-17) (Amour et al, 1998; Brew et al, 2000; Zucker et al, 1998). TIMP-3 is known as the most potent inhibitor of the ADAMTS family, inhibiting ADAMTS-4 and ADAMTS-5 at subnanomolar K_i (Kashiwagi et al, 2001). TIMP-4 is predominantly found in the heart but also found in the joint, implicating it in cartilage homeostasis (Greene et al, 1996). However, TIMP-4 has been found to be a poor inhibitor of ADAMTS-4 and ADAMTS-5 (Kashiwagi et al, 2001). TIMP-1 was used to affinity purify ADAMTS-4, suggesting it may inhibit this enzyme, but not very efficiently (Tortorella et al, 1999).

The functional interaction between TIMP and metalloproteinases has been established by crystallographic structures. Crystallographic structures that are available include the TIMP-1/MMP-3 complex, the TIMP-2/MT1-MMP complex and for uncomplexed TIMP-2 (Brew et al, 2000; Fernandez-Catalan et al, 1998; Gomis-Ruth et al, 1997; Tuuttila et al, 1998).

1.3.6 Metalloproteinases and Osteoarthritis

MMPs and ADAMTS enzymes have been shown to participate in a wide range of cellular processes, including cell adhesion and migration, ectodomain shedding, proteolysis, development, ovulation and angiogenesis. However, it is their important role in a number of pathologies, including arthritides, atherosclerosis, asthma and cancer progression, which has made them a major focus of scientific research and potential therapeutic targets.

There have been three comprehensive screens of *MMP*, *ADAMTS* and *TIMP* expression in osteoarthritis (Davidson et al, 2006; Kevorkian et al, 2004; Swingler et al, 2009), with other arthritide gene expression studies primarily focusing on rheumatoid arthritis (RA). The first study, completed by Kevorkian *et al*. (2004) screened the expression of all known metalloproteinases in OA femoral head cartilage versus normal femoral head cartilage. The second study, completed by Davidson *et al*. (2006) screened for gene expression in OA versus normal femoral head cartilage and synovium. The third study completed by Swingler *et al.* (2009) completed an expression profile for all known proteases within the human genome, known collectively as the 'degradome', in OA versus normal femoral head cartilage. In all studies OA cartilage was classed as late stage OA. All studies indicated aberrant gene expression for MMPs and ADAMTSs in OA cartilage, with many genes consistent between the studies. *MMP13* was one of the genes with the most significantly increased expression in all three studies (in cartilage and synovium), supporting the theory that MMP-13 is the key collagenase in OA. To further support this *MMP1* was decreased in OA cartilage, indicating that it does not play a significant role in late stage OA cartilage degradation in the hip (Davidson et al, 2006; Kevorkian et al, 2004). *ADAMTS4* and *ADAMTS5* had decreased expression in both OA cartilage and synovium (Davidson et al, 2006; Kevorkian et al, 2004). Proteolytically driven aggrecan loss occurs early in OA, indicating that increased aggrecanase mRNA expression would be seen in early OA cartilage samples rather than

the late OA samples used in these studies. Although, the decreased expression of *ADAMTS4* and *ADAMTS5* could also indicate that ADAMTS expression is regulated at levels other than at the mRNA level. The screens conducted by Davidson *et al*. (2006) and Kevorkian *et al*. (2004) also identified aberrant expression of TIMPs in OA cartilage. Importantly, a decrease in *TIMP1* and *TIMP4* was observed in OA cartilage, supporting the theory of an imbalance between protease and TIMP expression within the OA joint. Interestingly, *ADAMTS16* and *MMP28* were two of the genes with the most significantly increased expression in OA cartilage (Davidson et al, 2006; Kevorkian et al, 2004). The substrates and the functions of both genes remain unknown, but the data suggests a potential role in OA pathology.

It is clear that metalloproteinase gene regulation and expression is abnormal in OA cartilage and synovium. This suggests that the regulation of metalloproteinase expression is a potential therapeutic target in the treatment of OA. (For complete screen analysis please refer to (Davidson et al, 2006; Kevorkian et al, 2004; Swingler et al, 2009)

1.3.7 Cytokines and Osteoarthritis

Studies exploring the role of cytokines in arthritis have mainly focused on RA due to the characteristically high levels of cytokines expressed by the chronically inflamed synovium. However, cytokines have an important role in inflammation and cartilage degradation seen in both RA and OA.

IL-1 and TNFα are two of the most frequently studied and abundant cytokines found in the OA joint, which are primarily produced by chondrocytes and the macrophage- and fibroblast-like cells of the synovium (Bondeson et al, 2006; Goldring, 2000). The network of pro- and anti-inflammatory cytokines is complicated, but pharmacological neutralisation of IL-1 and TNFα, both *in vitro* and *in vivo*, has defined a significant role for both cytokines in arthritis onset and progression. It is generally accepted that IL-1 is the pivotal cytokine in OA (Goldring, 1999). Other cytokines released during the inflammatory process in the OA joint may be regulatory (IL-6, IL-8) or inhibitory (IL-4, IL-10, IL-13, IFN-gamma) (Goldring, 1999).

Both IL-1 and TNF mediate similar responses within the joint and have been shown to act synergistically. IL-1 and TNFα cause inflammation by inducing the expression of

cyclooxygenase type 2 (COX-2), phospholipase A and nitric oxide synthase (iNOS), resulting in the synthesis of inflammatory mediators prostaglandin E_2, platelet activating factor, leukotrienes and nitric oxide (NO) (Berg & Miossec, 2004). They have also been shown to increase the expression of intercellular adhesion molecule-1 (ICAM-1) and vascular-cell adhesion molecule-1 (VCAM-1) on mesenchymal and vascular cells, enhancing invasion of inflammatory and immune-competent cells into the joint space.

Mouse models over-expressing TNFα develop destructive arthritis, including synovial inflammation, cartilage damage and bone destruction (Keffer et al, 1991). The neutralisation of TNFα by anti-TNFα drugs, such as infliximab (Remicade®, Centocor Ortho Biotech Inc), etanercept (Enbrel®, Amgen/Wyeth), and adalimumab (Humira®, Abbott Laboratories), has proved successful in reducing the progression and symptoms of RA. These drugs have now been a favourable course of RA treatment for over a decade (Moreland, 2009). Pilot clinical trials for OA anti-TNF treatment have proved effective, but research is ongoing (Magnano et al, 2007). Inflammatory mouse models over-expressing TNFα and lacking IL-1 expression, exhibit joint inflammation but are protected from cartilage degradation and bone damage, indicating the importance of IL-1 in arthritis (Zwerina et al, 2007).

IL-1 has been shown to promote the synthesis of metalloproteases, inhibit growth factor induction of ECM protein synthesis, and to stimulate the synthesis of other pro-inflammatory cytokines such as TNF-alpha and IL-6 (Dayer & Bresnihan, 2002). *In vitro* and *in vivo* studies have demonstrated that IL-1 inhibition by IL-1 receptor antagonists (IL-1Ra) can reduce the severity of cartilage destruction (Caron et al, 1996; Fernandes et al, 1999; Pelletier et al, 1996). However, IL-1Ra clinical trials in humans are still rare. (For full review refer to (Calich et al, 2010)). The induction of metalloproteinases by IL-1 is further enhanced by the addition of the cytokine oncostatin M (OSM) (Barksby et al, 2006). The synergistic induction of metalloproteinases by I/O (a combination of IL-1α and oncostatin M) has been explored in both cell and bovine cartilage assays, determining that this induction can cause almost complete human and bovine cartilage resorption *in vitro* (Milner et al, 2006; Morgan et al, 2006).

These data show that cytokines play a central role in OA onset and progression, mediating the induction of inflammation and metalloproteinases expression.

1.4 Epigenetics and Transcription

1.4.1 Chromatin Structure

Eukaryotic DNA is compacted into the nucleus in the form of tightly condensed chromatin. Chromatin consists of repeating nucleosome units, consisting of 146 DNA nucleotide base pairs wrapped around a core histone octamer (Luger et al, 1997). The histone octamer contains two copies of H2A, H2B, H3 and H4 proteins, which are positively charged due to their lysine rich amino-terminal side chains. Negatively charged DNA tightly associates with positively charged histones. The degree of interaction between histones and DNA is a primary factor involved in determining chromatin conformation and transcriptional status. In general, transcriptionally active regions of chromatin are associated with a relaxed euchromatin conformation, mediated by hypomethylation of DNA and acetylation of histones. Conversely, transcriptionally silent regions of chromatin are associated with a compact heterochromatin confirmation, caused by hypermethylated DNA associated with deacetylated histones. Heritable changes in gene transcription mediated by acetylation and methylation of chromatin are referred to as 'epigenetic' modifications. Epigenetic processes will be discussed here due to their potential role in the aberrant gene expression observed within the OA joint.

1.4.2 Epigenetic Chromatin Modifications

Epigenetic processes are heritable changes in gene expression without change to the nucleotide sequence. While the genetic code is identical for every somatic cell in the body, epigenetic changes are generally confined to specific cells/tissues or even cells within a tissue (Roach & Aigner, 2007). Such processes include DNA methylation, histone modification and microRNA binding. Currently the two most widely studied epigenetic processes are DNA methylation and histone acetylation. The interaction between these processes can initiate and sustain gene expression and repression, integrating both genetic background and environmental factors for cell adaptation and survival (Karouzakis et al, 2009). However, disruption in these processes can lead to inappropriate gene expression and silencing causing the onset of 'epigenetic disease', such as cancer and potentially arthritis.

DNA methylation is thought to be a major mechanism by which cells maintain stable chromatin configuration that represses transcription, with methylation patterns inherited

during adult cell mitosis (Roach & Aigner, 2007). Methyl groups are added to cytosine (C) nucleotides, particularly those that are 5' to guanine (G) nucleotides (Roach & Aigner, 2007). These are classed as CpG sites (where p represents the phosphate that links the two nucleotides). This process is mediated by DNA methyltransferases (Dnmts), which catalyse the transfer of a methyl group from S-adenosyl-methionine (SAM) to the cytosine nucleotide. DNA methylation is also essential for normal cellular functions such as female X chromosome inactivation, imprinting of specific genes and cell-type specific gene expression through permanent silencing of all genes that are not expressed in a particular somatic cell (Roach & Aigner, 2007). DNA methylation inhibits gene transcription by preventing access of transcription factors and machinery to DNA binding motifs. Methyl-CpG-binding domain proteins (MBD1, MeCP2, MBD3 and MBD4) are important in implementing DNA methylation and further regulate chromatin structure through interaction with histone deacetylases (HDACs) (Dobosy & Selker, 2001).

The chromatin structure can be modulated by acetylation and deacetylation of lysine residues on core histone N-terminal tails (Grunstein, 1997). Acetylation occurs at the ε-amino groups of the highly conserved lysine residues. This is mediated by histone acetyltransferases (HATs) and results in the neutralisation of histone positive charge. Neutralisation of histone charge reduces histone-DNA interaction, resulting in a 'loose' euchromatin conformation that permits access of transcription factors and transcriptional machinery to binding motifs (de Ruijter et al, 2003). The sites of histone acetylation include at least four highly conserved lysines in histone H4 (K5, K8, K12 and K16), five in histone H3 (K9, K14, K18, K23 and K27), as well as less conserved sites in histones H2A and H2B (Kurdistani et al, 2004). The removal of acetyl groups is mediated by histone deacetylases (HDACs), which re-establishes the histone positive charge and tight DNA-histone interaction. Histone acetylation can be a dynamic process, but the rate of acetylation/deacetylation varies throughout the genome (Davie & Spencer, 1999).

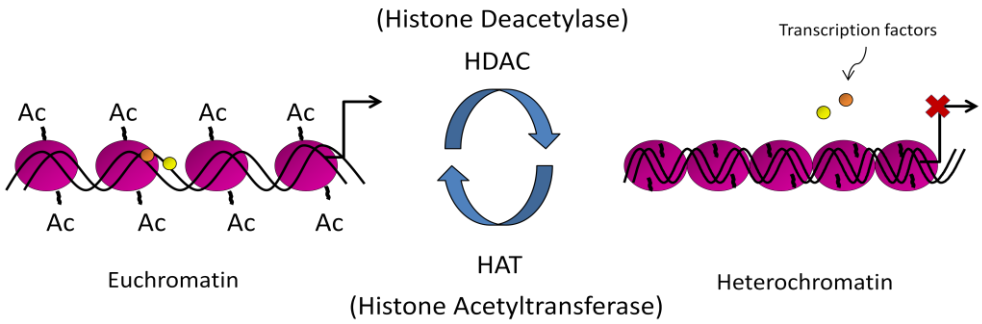

Figure 1.9. Schematic of histone acetyltransferase and histone deacetylase action.

Histone acetyltransferases (HATs) acetylate histone N-terminal tail lysine residues, neutralising histone positive charge and subsequently reducing histone-DNA interaction. This results in a loose DNA conformation, known as euchromatin, which exposes transcriptional machinery binding sites, allowing transcription to occur. Histone deacetylase enzymes (HDACs) remove acetyl groups from histone N-terminal tails, re-establishing histone-DNA interaction and a heterochromatin confirmation which is transcriptionally silent.

Core histones are susceptible to other post-translational modifications, including phosphorylation, methylation, ubiquitination, glycosylation, and ADP-ribosylation (Davie & Spencer, 1999). All of these modifications occur at the histone N-terminal tails, apart from ubiquitination.

1.4.3 Epigenetics and Disease

The role of epigenetics in disease onset has been the subject of much research due to aberrant gene expression and silencing observed in diseases such as cancer and arthritis. Epigenetic reviews primarily focus on cancer, while arthritis reviews tend to discuss the epigenetic changes within the synovial fibroblasts of the RA joint.

In addition to the genetic mutations observed in cancer, there are distinct epigenetic modifications. For example, despite a global decrease in DNA methylation, hypermethylation at the promoters of tumour suppressor genes is observed in almost all cancers (Kristensen et al, 2009). It has been shown that cancer cells have 20-60% less methylated CpG sites than non-transformed cells (Esteller, 2007). Global hypomethylation is thought to contribute to cancer onset and progression through several processes, such as loss of genetic imprinting, re-activation of transposons and the activation of normally methylated oncogenes (Cruickshanks & Tufarelli, 2009; Li et al, 2009; Nakayama et al, 1998). Hypermethylation of CpG regions within the promoters of tumour suppressor genes is known to suppress their expression, resulting in cancer development. An example of this is the hypermethylation of *BRCA1* in breast cancer (Dobrovic & Simpfendorfer, 1997). Over-expression of HDACs has also been observed in many cancers, resulting in the repression of important growth suppressor genes and promotion of cancer cell proliferation (Abbas & Gupta, 2008). This includes the over-expression of HDAC1 in prostate cancer, and HDAC2 in gastric cancers (Halkidou et al, 2004; Song et al, 2005).

A number of studies have looked at synovial fibroblasts from the RA joint (RASF cells). RASFs are aggressive, invasive and display apoptotic resistance, thus exhibiting a phenotype similar to transformed cells (Strietholt et al, 2008). Epigenetic processes are thought to contribute to this change in phenotype. For example, increased methylation of CpG regions within the promoter of death receptor 3 (DR3), which confers apoptotic resistance, has been reported in these cells (Takami et al, 2006).

Increased methylation is also predicted to play a role in OA. It is postulated that the aberrant expression of cartilage catabolic genes by OA chondrocytes is due to the loss of methyl-mediated silencing (Cheung et al, 2009; Roach et al, 2005). Data from Roach *et al*. (2005) demonstrating reduced methylation both globally and at the promoters of MMP-3, -9, -13 and ADAMTS-4 of OA chondrocytes support this theory (Cheung et al,

2009; Roach et al, 2005). They have also demonstrated that long term exposure of human chondrocytes to inflammatory cytokines can modulate the methylation status of key CpG sites, resulting in the long term expression of IL-1β (Hashimoto et al, 2009). (For full review of methylation in OA refer to (Roach & Aigner, 2007)). HDAC expression is also reportedly altered in OA chondrocytes, with a significantly increased expression of HDAC7 and decreased HDAC4 and HDAC10 detected in OA cartilage from the knee (Higashiyama et al, 2009).

The epigenetic changes that take place during the onset and progression of these diseases are potentially reversible, and have led to the development of a number of pharmaceuticals classed as 'epi-drugs'. These primarily consist of DNA methyltransferase inhibitors and histone deacetylase inhibitors (HDACi), which have both proven successful in the treatment of cancer. The data discussed suggests that HDAC inhibitors may be efficacious in the prevention of cartilage degeneration and hence this study will focus on the potential use of HDAC inhibitors as chondroprotective agents in the treatment of OA.

1.4.4 Histone Deacetylases Structure and Localisation

There are two distinct histone deacetylase families, the SIR2 (silent information regulators) family and the classical HDAC family. The SIR2 family contains the NAD^+ dependent HDACs found in yeast (Marmorstein, 2001), but will not be reviewed here. The classical HDAC family consists of eleven members, classified 1 to 11, which can be further divided into four sub-classes (class I, IIa IIb and IV) depending on phylogeny (Figure 1.10). The class I family (HDAC1, 2, 3 and 8) are closely related to yeast transcriptional regulator RPD3 (de Ruijter et al, 2003). The class IIa (HDAC4, 5, 7 and 9) and class IIb HDACs (HDAC6 and 10) share homology with yeast histone deacetylase HDA1 (Bjerling et al, 2002). Class IV consists of only HDAC11, which contains all the necessary features to be designated an HDAC, but shares too little sequence similarity with other HDACs to be placed in either class I or II (Gao et al, 2002). HDACs commonly function as transcriptional repressors in large, multi-subunit protein complexes (Alland et al, 1997; Nagy et al, 1997).

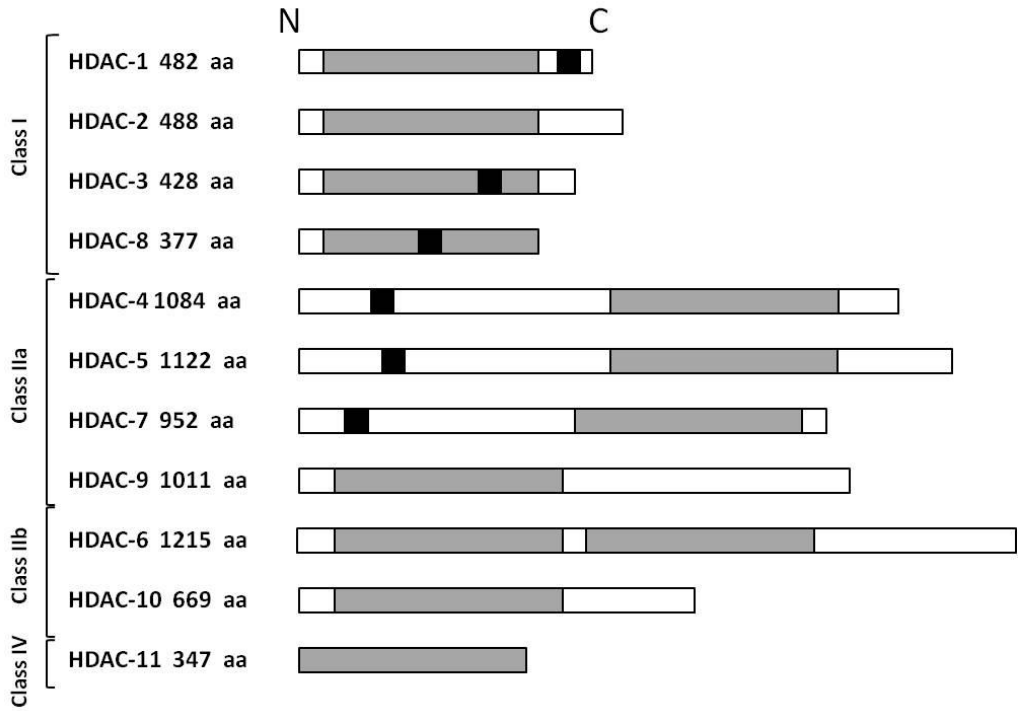

Figure 1.10. The classical histone deacetylase family.

The catalytic domain is depicted in grey and the nuclear localisation signal in black. (Adapted from (Balasubramanian et al, 2009)).

The class I HDACs are widely expressed in tissues and most cell types, and are primarily localised in the nucleus. The catalytic activity of class I enzymes requires a complex of other co-repressing proteins. Both HDAC1 and HDAC2 are exclusively nuclear as they lack a nuclear export signal. HDAC1 and HDAC2, which share approximately 84% homology, exist together in at least three distinct multiprotein complexes called the Sin3, the NuRD/NRD/Mi2 and the CoREST complexes (Humphrey et al, 2001; Laherty et al, 1997; Tong et al, 1998). Due to the high homology between HDAC1 and HDAC2, and co-residence within repressor complexes, it is difficult to determine the individual function of each of the proteins (Yang et al, 2002). HDAC3 requires the co-repressors silencing mediator of retinoid and thyroid hormone receptor (SMRT) and N-CoR for activity (Fischle et al, 2002; Yang et al, 2002). HDAC3 contains both a NLS and NES, suggesting it can localise in both the nucleus and cytoplasm. However, HDAC3 is predominantly reported in the nucleus, and this may be due to its presence in the SMRT/N-CoR complex, and its recruitment to DNA-bound class IIa HDACs (Fischle et al, 2002). HDAC8 is classed as a class I HDAC, but phylogenetic analysis indicates that it is closer to the class I-class II border.

HDAC8 varies from other class I HDACs due to negative regulation of its catalytic activity by phosphorylation on Ser39, and its predominant residence in the cytoplasm (Lee et al, 2004; Waltregny et al, 2004).

The expression pattern of class II HDACs is much more restricted, displaying limited tissue distribution (Acharya et al, 2005) and indicating that the class II family may have a role in cellular differentiation and developmental processes (de Ruijter et al, 2003). Class IIa members are expressed strongly in the heart, muscle and brain (Gregoretti et al, 2004; Verdin et al, 2003). These HDACs have been found to interact with SMRT/N-CoR and Bcl-6-interacting co-repressor (B-CoR), allowing them to interact with HDAC3, which they require for catalytic activity (Fischle et al, 2002; Verdin et al, 2003). The N-terminal domain of Class IIa HDACs contain two conserved cam-dependent protein kinase (CaMK) phosphorylation sites, which upon signal-dependent phosphorylation allows binding of 14-3-3 chaperone proteins and export of the HDACs from the nucleus into the cytoplasm (McKinsey et al, 2000; Zhang et al, 2002). Class IIb show specific expression patterns, with HDAC6 showing the highest expression in the testis and HDAC10 the highest expression in the liver, spleen and kidney (Kao et al, 2002; Zhang et al, 2008). HDAC6 and HDAC10 are unusual in that they contain two catalytic domains, both of which are required for HDAC6 catalytic activity (Carey & La Thangue, 2006).

Class IV HDAC11 expression is tissue-specific with high expression observed in the brain, heart, skeletal muscle and kidney. HDAC11 does not appear to reside in any known HDAC co-repressor complexes (Gao et al, 2002).

The structure of the HDAC active site consists of a tubular pocket containing a zinc binding site and two Asp-His charge relay systems. The removal of an acetyl group is mediated by the charge relay systems, but it can only work when specific cofactors are present, along with a zinc ion in the catalytic site (de Ruijter et al, 2003; Finnin et al, 1999; Marmorstein, 2001).

1.4.5 Histone Deacetylase Function

Other than histones HDACs have many cellular protein substrates, including alpha-tubulin, Ku-70, Bcl-6 and transcription factors, p53, STAT1, E2F1, GATA-1 and NF-kB (Balasubramanian et al, 2009). The broad range of substrates gives HDACs

numerous biological and developmental functions, many of which are yet to be characterised. Both siRNA (small interfering RNA) and knockout mouse models have been essential for understanding the biological function of individual isoforms. For example it has been reported that siRNA mediated knockdown of HDAC7 results in decreased levels of *MMP13* RNA (Higashiyama et al, 2009), supporting their previously reported regulatory role in metalloproteinase expression (Young et al, 2005). Null mouse models have also been central in deciphering the individual functions of HDACs in development as well as in adulthood.

However, both siRNA and mouse knockout studies must be interpreted with care as these experiments result in the complete loss of protein, thus abolishing not only enzymatic activity but also protein-protein interactions that may play a critical role in numerous cellular functions.

1.4.6 Histone Deacetylase Null Mouse Models: A Brief Review

1.4.6.1 Class I HDAC Murine Models

HDAC1

Homozygosity for the HDAC1-null allele results in embryonic lethality, caused by increased expression of cyclin-dependent kinase inhibitors p21 and p27, and subsequent inhibition of cell proliferation at gastrulation (Lagger et al, 2002; Montgomery et al, 2007). Mice generated with a HDAC1 cardiomyocyte-specific deletion (HDAC1cko) are phenotypically normal, exhibiting expected levels of cardiac hypertrophy when exposed to known inducers of hypertrophy. This indicates that HDAC1 does not play a regulatory role in preventing or inducing cardiac hypertrophy. HDAC1 tissue-specific deletion in the neural crest, skeletal muscle and secondary heart field produces viable mutants, which is attributed to HDAC1 redundancy with HDAC2 in later development.

HDAC2

There is disagreement regarding the function of HDAC2 *in vivo*. The first HDAC2$^{-/-}$ mouse was generated using a gene-trap embryonic stem cell line (Trivedi et al, 2007), causing complete deletion of the carboxy-terminal domain and part deletion of the catalytic domain. The mice exhibited partial penetrant embryonic lethality, but those that survived appeared normal and viable. Interestingly, in this model deletion of HDAC2 conferred resistance to induced cardiac hypertrophy. This was attributed to the

removal of the HDAC2-mediated repression of Inpp5f (phosphatidylinositol-3,4,5-triphosphate (PIP3) phosphatase), which was found to be up-regulated in HDAC2$^{-/-}$ mice. Induction of Inpp5f results in decreased levels of active phospho-Akt and phospho-GSK3β of the PI3K-Akt-GSK3β pathway, a pathway known to be activated by hypertrophic stimuli.

A second HDAC2 null mouse generated by homologous recombination, deleting a portion of the oligomerisation domain and residues of the catalytic domain, displayed a lethal phenotype 24 hours post-birth (Montgomery et al, 2007). Analysis of HDAC2$^{-/-}$ neonates detected morphologically abnormal hearts with obliteration of the right ventricular lumen and thickening of the interventricular septum. Specific HDAC2 deletion in cardiomyocytes (HDAC2cko) was completed by the same research group and generated a phenotypically normal mouse which exhibited normal hypertrophic response to known hypertrophic inducers. This indicates HDAC2 does not play a regulatory role in preventing or inducing cardiac hypertrophy. Other cell specific HDAC2 deletion was unable to phenocopy, suggesting that the HDAC2 null cardiac phenotype was caused by multiple cardio-cell types, not just cardiomyocytes. Therefore, the HDAC2 mouse models generated by Montgomery *et al*. (2007) indicate that HDAC2 is essential for normal cardiac growth and morphogenesis, with its deletion leading to cardiac defects superficially similar to many known congenital heart abnormalities.

Different murine genetic backgrounds could account for the conflicting phenotypes. Alternatively, Montgomery *et al*. (2007) suggests that the gene trap insertion, used by Trivedi *et al*. (2007) only ablated the C-terminus of HDAC2, which has uncertain function, thus not creating a true null mutant. It has recently been shown that deletion of the C-terminus does not affect the catalytic activity of HDAC2, but does reduce target gene specificity (Hong et al, 2009).

HDAC1 and HDAC2

Specific deletion of both HDAC1 and HDAC2 in cardiomyocytes results in cardiac arrhythmia, severe ventricular dilation and postnatal lethality (Montgomery et al, 2007). Analysis revealed increased apoptosis and fetal gene expression within mutant hearts, indicative of cardiac stress. Microarray of mutant heart transcripts indicated up-regulation of specific L-type and T-type calcium channel subunits. It was postulated that

induction of T-type and L-type calcium channels causes cardiomyocyte calcium influx and increases skeletal muscle-specific TnI (troponin I) expression, attributing to abnormal cardiac contraction and sudden death. Specific cardiomyocyte deletion of HDAC1 or HDAC2 had no effect on cardiac development or function, suggesting that HDAC1 and HDAC2 act redundantly to regulate cardiac gene expression.

Montgomery and colleagues also explored the molecular mechanism by which neural progenitor cells commit to a specified lineage of the central nervous system, through the specific deletion of HDAC1 and HDAC2 in neuronal precursors within the mouse (Montgomery et al, 2009). Mice lacking HDAC1 or HDAC2 in neuronal precursors exhibited no overt histo-architectural phenotype, whereas deletion of both HDAC1 and HDAC2 in developing neurons resulted in hippocampal abnormalities, absence of cerebellar foliation, disorganisation of cortical neurons, and lethality by P7. These abnormalities were attributed to a failure of neuronal precursors to differentiate into mature neurons and to excessive cell death. This demonstrated that HDAC1 and HDAC2 redundantly control neuronal development and are required for neuronal specification.

HDAC3

Homozygosity for HDAC3 null allele results in embryonic lethality due to defects in gastrulation (Knutson et al, 2008; Montgomery et al, 2008). The genes responsible for this are unknown, but loss of HDAC3 has been linked to defective double-stranded DNA repair (Bhaskara et al, 2008). To circumvent embryonic lethality, specific deletion of HDAC3 was completed in the heart and the liver (Knutson et al, 2008; Montgomery et al, 2008), with both conditional deletions resulting in metabolic dysfunction associated with changes in peroxisome proliferator-activated receptor (PPAR) signalling.

Specific deletion of HDAC3 in the murine liver induced liver hypertrophy attributed to reduced glucose and increased lipid storage (Knutson et al, 2008). Microarray analysis of mutant liver transcripts detected increased expression of PPARγ and aberrant expression of PPARγ target genes. PPARγ mediates metabolic homeostasis through transcriptional repression of target genes via the recruitment of the HDAC3/NCoR repressor-complex. This model indicates that HDAC3 mediated repression of PPARγ

target genes is essential for the regulation of glucose and lipid metabolism within the liver.

Specific cardiac deletion of HDAC3 (HDAC3cko) within the murine heart led to cardiac abnormalities mimicking the metabolic derangements observed in diabetic cardiomyopathies, including cardiac hypertrophy, increased fatty acid oxidation, up-regulation of cardiomyocyte lipid storage and decreased glucose metabolism (Montgomery et al, 2008). The severe cardiac phenotype was attributed to rampant PPARα activation, which requires the HDAC3/NCoR/SMRT repressor complex to mediate target gene repression. HDAC3 deletion also resulted in severe interstitial fibrosis, although the molecular events involved are still unknown.

HDAC8

The deletion of HDAC8 in mice results in a highly specific deficiency of cranial neural crest cells (NCCs), the loss of specific cranial skeletal elements, and consequent biomechanical instability of the skull, which results in perinatal death due to brain trauma (Haberland et al, 2009). Immediately after birth, HDAC8-deficient mice showed deficiencies in movement, signs of hypoxia and usually died within 4 to 6 hours after birth. The examination of the major organ systems did not reveal an obvious phenotype in the heart, lung, liver, kidney, intestine, and bladder of the mutant mice. However, haemorrhages in the brain, and in some severe cases herniation of brain and other soft tissue through the top of the skull, were observed in the null mice. Analysis of the mutant skulls revealed a distinct ossification defect with a wide foramen frontale and defects in the interparietal bone. No defects were observed in the rest of the mutant skeleton. Specific HDAC8 deletion in osteoblasts and chondrocytes did not replicate the skull phenotype observed with global deletion. However, specific deletion of HDAC8 in neural crest-derived tissue largely phenocopied the global deletion, with ossification defects observed in both the frontal and interparietal bones. No other defects in other neural crest-derived tissues were observed. Specific deletion of HDAC1 or HDAC2 in neural crest-derived tissue exhibited no skeletal phenotype. Microarray analysis comparing the transcripts from wildtype NCCs to those containing the HDAC8 deletion (derived from the frontal skull of mouse models) revealed the increased expression of 17 homeobox genes, including the genes encoding Hox transcription factors Lhx1 and Otx2. Hox transcription factors Lhx1 and Otx2 are known to be crucially important for the normal development of the frontal skull, and their specific over-expression in NCCs

caused a severe cranial phenotype resembling the HDAC8-null phenotype. Haberland and colleagues concluded that HDAC8 exerts transcriptional repression of certain homeobox genes within NCCs to control the formation of specific cranial skeletal elements. Therefore the loss of HDAC8 mediated repression presumably leads to mis-patterning of the skull elements, resulting in the lethal null-phenotype.

1.4.6.2 Class IIa Murine Models

All class IIa HDACs have been deleted in mouse models. Each HDAC has been shown to play a role in tissue-specific gene expression. However, all knockout model phenotypes seem to reflect class IIa repression of the myocyte enhancer factor 2 (MEF2) transcription factor.

HDAC4

HDAC4 deletion results in postnatal lethality at P10, with mutants distinguishable from their wildtype littermates at birth by their 'dome-shaped' heads, misshapen spines and runted phenotype (Vega et al, 2004). Histological analysis revealed growth retardation and death of HDAC4 null mice was due to inappropriate and premature ossification of all cartilaginous skeletal elements by the process of endochondral ossification. In particular, aberrant ossification of the chondralcostal regions, vertebrae and sternum led to impaired mobility and eventual suffocation, whilst premature mineralisation at skull synchondroses inhibited longitudinal skull growth resulting in 'dome-shaped' heads. The $HDAC4^{-/-}$ phenotype mirrors that of mice with constitutive expression of transcription factors Runx2 (runt-related transcription factor 2) or MEF2, which both have vital roles in the control of chondrocyte hypertrophy and bone formation (Arnold et al, 2007; Karsenty & Wagner, 2002; Takeda et al, 2001; Ueta et al, 2001). HDAC4 was shown to directly bind to Runx2 preventing it from activating target genes (Vega et al, 2004). HDAC4 is also known to directly repress MEF2 and the onset of endochondrial ossification (Miska et al, 1999). Vega *et al*. (2004) concluded that the absence of HDAC4 resulted in unrestrained transcriptional activation of these factors, leading to excessive bone formation.

No other class IIa HDACs were detected during bone development, and triple knockout of HDAC4/5/9 does not enhance the HDAC4 knockout phenotype. This suggests HDAC4 specifically regulates chondrocyte hypertrophy.

HDAC5 and HDAC9

HDAC5 and HDAC9 null mice both exhibited a histologically and pathologically normal phenotype at birth (Chang et al, 2004; Zhang et al, 2002). However, at 8 months of age mutants developed cardiac hypertrophy. Cardiac stress signals commonly activate both kinases and calcium/calmodulin-dependent phosphatase calcineurin. Activated kinases phosphorylate the amino-terminal extensions of class II HDACs, causing their dissociation from MEF2 and export from the nucleus. MEF2 is highly expressed in cardiomyocytes and known to activate foetal cardiac gene expression and cardiac hypertrophy in response to stress signals.

HDAC5 and HDAC9 null mice exhibited increased sensitivity to stress-induced cardiac hypertrophy, consistent with the theory that class IIa HDACs suppress pathological cardiac growth through interaction with MEF2. A double knockout mouse for HDAC5 and HDAC9 (generated by Chang *et al*. (2004)) was under represented at P7 and showed severe growth retardation. Histology and gross organ examination of double knockout mice revealed mutant hearts were larger than WT and expressed stress-induced hypertrophic genes. This suggests that double knockout causes stress-induced developmental cardiac augmentation, or that age-induced hypertrophy observed in the single knockouts is accelerated in the double knockout. Therefore, HDAC5 and HDAC9 act as suppressors of cardiac hypertrophy through interaction with MEF2, with stress stimuli resulting in their phosphorylation and export from the nucleus.

HDAC7

The HDAC7$^{-/-}$ mouse resulted in embryonic lethality after E11 (Chang et al, 2006). Mutants were indistinguishable for wildtype at E10.75, but by E11 widespread vasculature rupture, pericardial diffusion and enlarged dorsal aortae resulted in death. Electron microscopy determined fewer gap junctions between mutant endothelial cells (ECs) than wildtype, with mutant ECs producing long processes that failed to attach. Microscopy also revealed reduced endothelial recruitment of smooth muscle cells. The loss of gap junctions between endothelial cells and the subsequent loss of vascular integrity was attributed to a 6.5-fold increase in *MMP10* expression and an 8.6-fold decrease in *TIMP-1* expression. Further experiments in human umbilical vein endothelial cells (HUVECs) found HDAC7 inhibits MEF2 induction of *MMP10,* with CHIP analysis confirming MEF2, HDAC7 and CBP/p300 binding of the proximal

promoter of *MMP10*. Therefore, loss of HDAC7 induces *MMP10* expression, causing cleavage of endothelial cell-cell contacts and loss of vascular integrity.

HDAC7 was also specifically deleted in endothelial cells and cardiomyocytes. Deletion of HDAC7 in endothelial cells resulted in embryonic lethality at E.11.5 with circulatory abnormalities the same as those observed in the HDAC7 null mouse. Specific HDAC7 deletion within cardiomyocytes produced viable mice. Thus HDAC7 is postulated to be specifically required for endothelial cell-cell adhesion and maintenance of vascular integrity.

1.4.6.3 Class IIb HDAC Murine Models

HDAC6

The HDAC6 null mice were viable and showed increased tubulin acetylation in most tissues (Zhang et al, 2008). HDAC6 had previously been shown to interact and deacetylate lysine 40 of α-tubulin both *in vitro* and *in vivo* (Zhang et al, 2003). HDAC6 is known to interact with transcription factors Runx2/Cbfa1 to mediate transcriptional repression of $p21^{cip/waf1}$ promoter in differentiating osteoblasts. Overall skeletal development in the mutant was the same as WT, but a slightly increased density was detected in the cancellous bone of the tibial metaphysis, suggesting a minor role for HDAC6 in bone biology. The role of other HDACs in tubulin deacetylation was explored in mouse embryonic fibroblasts, but this was shown to be a HDAC6 specific role. Therefore, HDAC6 is not essential for normal development or physiological function in the murine model.

A HDAC knockout mouse has not been developed for HDAC10 or class IV HDAC11.

1.4.7 HDAC Inhibitors – 'Epi-Drugs'

HDAC inhibitors have been shown to induce differentiation, apoptosis, cell-cycle arrest, inhibition of DNA repair, up-regulation of tumour suppressors, down-regulation of growth factors, oxidative stress and autophagy of transformed cells at concentrations at which normal cells are relatively resistant (Balasubramanian et al, 2009; Kristensen et al, 2009; Ungerstedt et al, 2005). These effects are partially mediated by altering the acetylation status of chromatin and other non-histone proteins. However, the exact molecular basis of response to HDAC inhibitors is still not fully understood. There is currently a variety of proposed mechanisms, but the response to HDAC inhibitors seems

to be dependent on cell type, the specific compound and experimental conditions (Balasubramanian et al, 2009).

Currently vorinostat is the only HDAC inhibitor approved by the FDA (US Food and Drug Administration) for cancer treatment. However, a range of HDAC inhibitors are currently under clinical trial, some of which are stated in Table 1.2.

Name	Chemical nature	Clinical Status
Sodium phenylbutyrate	Short-chain fatty acid	Phases I, II
Valproic acid	Short-chain fatty acid	Phases I, II
OSU-HDAC42	Short-chain fatty acid	Not yet in clinical trial
Panobinostat	Hydroxamic acid	Phases I, II, III
Belinostat	Hydroxamic acid	Phases I, II
Romidepsin	Cyclic peptide	Phases I, II
Entinostat	Benzamide	Phases I, II
MGCD-0103	Benzamide	Phases I, II

Table 1.2. HDAC inhibitors in clinical trials for cancer treatment

HDAC inhibitors currently under development for cancer treatment and their clinical trial status. (Adapted from (Kristensen et al, 2009))

Inflammatory arthritis models, which mirror the events that take place in RA, have shown HDAC inhibitors can reduce joint damage *in vivo*. Chung *et al*. (2003) demonstrated that topical treatment of HDAC inhibitors trichostatin A (TSA) and phenylbutyrate can successfully inhibit joint swelling, synovial inflammation and subsequent cartilage and bone destruction in an adjuvant-induced arthritis rat model. The reduction in joint damage was associated with induction of cell-cycle regulators and reduced expression of TNFα (Chung et al, 2003). Consistent with this, a later study conducted by Keiichiro *et al*. (2004) demonstrated that a single intravenous injection of FK228 (Romidepsin), a class I 'selective' inhibitor can successfully inhibit joint swelling, synovial inflammation and subsequent cartilage and bone destruction in a murine autoantibody-mediated arthritis model (Keiichiro et al, 2004). The reduction in joint damage was accompanied by cell-cycle arrest of RASFs via induction of cell-cycle regulators $p16^{INK4a}$ and $p21^{WAF/Cip1}$, which showed increased promoter acetylation. Reduced joint damage in auto-antibody mediated arthritis models has also been shown

with inhibitors MS-275 and VPA (Lin et al, 2007; Saouaf et al, 2009). However, most importantly to this study intra-articular injection of TSA has also been shown to reduce cartilage damage and suppress increased *MMP1*, *MMP3*, *MMP13* and IL-1 expression (within cartilage) in an OA rabbit model (Chen et al, 2010). Bovine nasal cartilage assays have also shown that cytokine-driven cartilage degradation can be blocked with the addition of TSA and sodium butyrate (NaBy) (Young et al, 2005), accompanied by a reduction of collagenases in the explant-conditioned medium. Further investigation in cell culture models demonstrated that both TSA and NaBy significantly reduced cytokine-induced metalloproteinase expression (Young et al, 2005). Conceptually HDAC inhibitors increase the acetylation status of chromatin and other non histone proteins, resulting in increased gene transcription. However, microarray analysis has found that only 2-9% of the genome is regulated by HDAC inhibitors, with an equal number of genes suppressed as activated (Glaser et al, 2003; LaBonte et al, 2009). It is also surprising that such a small fraction of genome expression is affected by HDAC inhibitor treatment, due to the large range of HDAC substrates.

Therefore, the inhibition of HDACs provides a potential therapeutic route for future OA therapeutics. However, most of the currently available HDAC inhibitors are termed 'pan' inhibitors as they target nearly all isoforms of the classical HDAC family. Inhibitor administration can result in large global changes of cellular pathways that perturb normal cellular functions, potentially inducing severe side effects, including nausea, fatigue, vomiting, cardiac abnormalities and many more (Duvic et al, 2009; Shah et al, 2006). The toxicity profiles of these drugs are not outside that of other cancer therapeutics, but would not be used in the treatment of OA. The development of specific HDAC inhibitors to reduce their current side effects is essential and ongoing.

1.4.7.1 Histone Deacetylase Inhibitor Structure and Function

The structure and source of HDAC inhibitors varies greatly, but most can be grouped into seven major structural groups including; carboxylates, short-chain fatty acids, small-molecule hydroxamates, electrophilic ketones (epoxides), cyclic peptides, benzamides and other hybrid compounds (Acharya et al, 2005; Drummond et al, 2005). Most inhibitors have been designed to contain three basic structural components: a metal binding moiety, carbon linker and capping group (Bieliauskas et al, 2007). The capping group is thought to bind amino acids near the entrance of the HDAC active site,

enabling the inhibitor metal moiety to chelate with the HDAC metal ion required for catalytic activity. The linker region is thought to position the previous two domains to allow high affinity reactions with the classical HDACs (Bieliauskas et al, 2007).

Hydroxamate inhibitors, such as trichostatin A, contain a hydroxamate moiety which binds and chelates the catalytic zinc ion. The hydroxamate moiety is very efficient at chelating the zinc ion, but it does not generate sufficient secondary contacts to distinguish between the catalytic pockets of the different HDAC isoforms (Balasubramanian et al, 2009).

However, other structural HDAC inhibitors are slightly more specific and can preferentially bind to a specific class of classical HDACs, helping reduce side effects. Valproic acid (VPA), for example, was a well-known and tolerated epileptic anticonvulsant drug before its HDAC inhibitor properties were discovered (Bialer & Yagen, 2007; Gottlicher et al, 2001; Nissinen & Pitkanen, 2007; Phiel et al, 2001). Valproic acid causes relatively mild side effects in comparison to the side effects of hydroxamate TSA (Nau et al, 1991), and this may be attributed to its preferential inhibition of co-repressor associated HDACs, especially HDAC1 and HDAC2. It has been demonstrated that VPA inhibits class I HDACs at low concentrations (~ 0.7-1mM) and class II HDACs at higher concentrations (>1mM) (Gurvich et al, 2004). It has been shown that 0.3-1mM VPA detected in patient serum, during epilepsy therapy of a daily dose of 20-30mg/kg, achieves potent HDAC inhibition (Gottlicher et al, 2001). The HDAC inhibitory mode of action is thought to be independent of VPAs anticonvulsant properties and achieved through direct binding of the HDAC catalytic centre, preventing substrate binding (Gottlicher et al, 2001). MS-275 is another ‘selective’ HDAC inhibitor, which reportedly inhibits class I HDACs HDAC1, HDAC2 and HDAC3 (Hu et al, 2003; Inoue et al, 2006).

Developing selective HDAC inhibitors is a difficult process due to the homology between catalytic sites and the difficulty in isolating purified active proteins for both activity assays and x-ray structure analysis (Balasubramanian et al, 2009). However, the crystal structures that have been determined, such as that of HDAC8, do reveal unique structures which could be utilised in the development of specific HDAC inhibitors (Vannini et al, 2004). Tubacin, a HDAC6 specific inhibitor, is one of the only specific

HDAC inhibitors and the best characterised in terms of *in vitro* cancer assays (Hideshima et al, 2005).

1.5 Scope of Thesis

Pro-inflammatory cytokine IL-1α is known to induce the expression of many metalloproteinase genes in primary chondrocyte and chondrocyte cell lines, which is further potentiated when IL-1 is combined with cytokine OSM (Barksby et al, 2006; Koshy et al, 2002). Young *et al.* (2005) previously demonstrated that broad spectrum HDAC inhibitors TSA and NaBy can repress cytokine-induced metalloproteinase expression at the mRNA and protein level, both in the SW1353 cell line and primary chondrocytes. The study also demonstrated that cytokine-induced cartilage resorption, of bovine nasal cartilage explants, is prevented by TSA and NaBy treatment. It was postulated that this chondroprotective effect was due to transcriptional repression of cytokine-induced metalloproteinase expression by non-histone related pathways (Young et al, 2005). Milner *et al*. (2006) previously profiled metalloproteinase expression in the 14 day bovine nasal cartilage assay. The study revealed the induction of many metalloproteinase genes in IL-1α and OSM treated cartilage explants, and demonstrated that activation of pro-MMPs is a key regulatory control point in collagenolysis and cartilage degradation.

The chondroprotective property of HDAC inhibitors has also been demonstrated in animal models of both inflammatory arthritis and osteoarthritis, where HDAC inhibitor treatment resulted in reduced joint damage. The reduced joint damage mediated by TSA, VPA or MS-275 treatment in inflammatory animal models was associated with reduced cytokine expression and increased expression of cell cycle regulators $p16^{INK4a}$ and $p21^{WAF/Cip1}$ (Chung et al, 2003; Keiichiro et al, 2004; Lin et al, 2007). The recently published OA rabbit model demonstrated that intra-articular injection of TSA reduced cartilage damage and suppressed increased *MMP1*, *MMP3*, *MMP13* and IL-1 expression observed in the OA rabbit controls (Chen et al, 2010).

The molecular pathways by which HDAC inhibitors mediate repression of cytokine-induced metalloproteinase expression remain unknown. However, the chondroprotective affects of these inhibitors indicate that HDACs play important roles in the regulation of metalloproteinase expression and that these compounds could have a potential use in the treatment of OA. Compounds TSA and NaBy inhibit all members of the classical HDAC family, with the exception of HDAC6 for NaBy, with administration resulting in large global changes of cellular pathways that potentially induce severe side effects. The non-selective inhibition by these compounds makes it

unclear as to which HDACs may have been repressed in order to confer the chondroprotective effect observed in the study completed by Young *et al*. (2005). To elucidate which HDACs play a role in metalloproteinase gene regulation, this thesis will examine the differential effects of HDAC inhibitors with reportedly specific inhibitory profiles on metalloproteinase expression and cartilage degradation. The role of classical HDACs in the regulation of metalloproteinase expression will also be assessed by individual siRNA (small interfering RNA) knockdown of classical HDACs, followed by the detection of HDAC and *MMP13* expression by quantitative real-time PCR (qRT-PCR), in the SW1353 cell line and primary OA chondrocytes. If the HDACs involved in the regulation of metalloproteinase expression can be determined the specific inhibition of these enzymes could provide possible therapeutic targets for the treatment of OA.

Chapter II: Materials and Methods

Chapter II

Materials and Methods

2.1 Materials

2.1.1 Cell Lines

2.1.1.1 SW1353

The SW1353 human chondrosarcoma cell line was initiated by A. Leibovitz at the Scott and White Clinic, Texas in 1977 from a primary grade II chondrosarcoma of the right humerus, obtained from a 72-year-old female Caucasian. The cell line (product code: HTB-94) was purchased from the American Type Culture Collection (ATCC) (for further details visit www.atcc.org).

2.1.1.2 Primary Articular Chondrocytes

Primary human articular chondrocytes (HACs) were isolated from patients who underwent joint replacement surgery of the knee for osteoarthritis (all samples were collected with Ethical Committee approval and all patients provided informed consent). Articular cartilage was enzymatically digested overnight in digestion medium (D-MEM GlutaMax™ (Gibco Paisley, UK), 1mg/ml collagenase (Sigma-Aldrich, Dorset, UK), 0.4% hepes (Sigma-Aldrich, Dorset, UK), 100IU/ml penicillin and 100µg/ml streptomycin (Gibco)) at 37°C, with gentle rocking. The digestion mixture was strained through a 70µm cell strainer (BD Falcon) and washed twice. Cells were plated at 4x104 cells/cm^2 and grown to 80% confluence. All HACs were used at passage 1. Primary OA chondrocytes were a kind gift from Dr. Rose Davidson (University of East Anglia, UK).

2.1.2 Cell Culture Reagents

Dulbecco's Modified Eagle Medium (D-MEM) low glucose, Hanks' Balanced Salt Solution (HBSS), penicillin-streptomycin, and trypsin-EDTA (0.25% EDTA) were purchased from Invitrogen (GIBCO Paisley, UK). All filter cap culture flasks and sterile plates were

purchased from NUNC of Thermo Fisher Scientific (Waltham, USA). Heat inactivated fetal calf serum was purchased from BioSera (East Sussex, UK).

2.1.3 Cytokines

Recombinant human interleukin-1α (IL-1α) and recombinant human oncostatin M (OSM) were purchased from R&D Systems (Abingdon, UK), reconstituted in phosphate-buffered saline solution (PBS) containing 0.1% bovine serum albumin and stored at -80°C (as recommended by supplier).

2.1.4 HDAC Inhibitors

MS-275 was purchased from Alexis Biochemicals (Lausanne, Switzerland). Trichostatin A and valproic acid were purchased from Calbiochem (Merck Biosciences Nottingham, UK). Tubacin and niltubacin were kindly provided by Ralph Mazitschek and James Bradnerand (Harvard Medical School, USA). MS-275, TSA and tubacin/niltubacin were reconstituted in sterile DMSO, and VPA in sterile dH_2O, according to manufacturers' recommended concentrations and stored at -20°C.

2.1.5 Immunoblotting

All antibodies were rabbit polyclonal, unless otherwise stated. Anti-histone 3 (#9715), anti-acetyl-histone H3 (Lys9) (#9671), anti-histone 4 (#2592), anti-acetyl-histone H4 (Lys8) (#2594), anti-histone deacetylase 1 (#2062) and anti-histone deacetylase 2 (#2540) were purchased from Cell Signaling Technology (Beverly MA, USA). Mouse monoclonal anti-α-tubulin (#ab11304) and anti-acetylated α-tubulin (#ab24610) were purchased from Abcam plc (Cambridgeshire, UK). Horseradish peroxidase-conjugated anti-rabbit (PO448) and anti-mouse (PO260) secondary antibodies were purchased from Dako UK Ltd (Cambridgeshire, UK).

Tris Base Ultra Pure, Sodium dodecyl sulphate (SDS), N,N,N,N'-Tetramethylethylenediamine (TEMED), 30% acrylamide/bis acrylamide solution 37:5:1, extra thick filter paper, protein standard Precision Protein Plus^{TM}, gel rigs, electrophoresis tanks and a Trans-Blot SD Semi-dry electrophoretic transfer cell were all purchased from

Bio-Rad Laboratories (Hemel Hempstead, UK). Ammonium persulphate (APS), polyoxyethylenesorbitan monolaurate (Tween-20), Ponceau S solution, bovine serum albumin (BSA) and Kodak BioMax maximum sensitivity film were purchased from Sigma Aldrich (Dorset, UK). Immobilon-P polyvinylidene difluoride (PVDF) membrane was purchased from Millipore (Watford, UK). Protein standard Magic Marker™ was purchased from Invitrogen (Paisley, UK). Marvel non-fat dry milk powder was purchased from Premier Foods (St. Albans, UK). LumiGLO® chemiluminescent reagents were purchased from Cell Signaling Technology (Beverly MA, USA).

2.1.6 Bovine Nasal Cartilage Assay

D-MEM High Glucose, Dulbecco's phosphate buffered saline (PBS), nystatin and L-glutamine were purchased from Invitrogen (GIBCO Paisley, UK). Gentamicin was purchased from Fisher Scientific (Waltham, USA).

2.1.7 1,9-Dimethyl-Methylene Blue (DMB) and Hydroxyproline (DAB) Assays

1,9-dimethyl-methylene blue**,** chondroitin 4-sulphate sodium salt from bovine trachea, 4-(dimethyl-amino) benzaldehyde, chloramine T-hydrate and trans-4-hydroxy-L-proline were purchased from Sigma Aldrich (Dorset, UK). 70% perchloric acid was purchased from Fisher Scientific (Waltham, USA).

2.1.8 *SMART*pool Short Interfering RNAs (siRNAs)

Pre-designed siGENOME *SMART*pool siRNAs were purchased for all human classical HDACs from Thermo Scientific Dharmacon (Chicago, USA) (For catalogue numbers and target sequences refer to appendix III). All siRNAs were reconstituted to 20µM with 1x Dharmacon siRNA Buffer, aliquotted and stored at -80°C (according to manufacturer's instructions).

2.2 Methods

2.2.1 Cell Culture

Cells were cultured in D-MEM low glucose, containing 10% heat-inactivated fetal bovine serum, 100IU/ml penicillin and 100µg/ml streptomycin, in vented flasks. Cells were incubated at 37°C in a humidified atmosphere of 5% CO_2. Cells were grown until confluent, detached with trypsin-EDTA and then passaged. For long term storage, cells were detached with trypsin-EDTA, pelleted by centrifugation at 130g for 5 minutes and resuspended in cryo-preservation medium (90% FCS with 10% DMSO) before slow freezing (at approximately 1°C per minute) in liquid nitrogen.

2.2.2 HDAC Inhibitor Assays

SW1353 cells were plated in 6-well plates ($1.5x10^5$ cells/well) for dose response experiments with TSA, VPA and MS-275, or in 96-well plates ($6.5x10^3$ cells/well) for the dose response assay with tubacin. Primary articular chondrocytes were plated in 96-well plates ($6.5x10^3$ cells/well) for dose response experiments with TSA, VPA and MS-275. All cells were initially plated in serum-containing medium. Once cells had adhered, medium was removed and cells washed twice with HBSS to remove traces of serum and replaced with serum-free medium. Cells were serum-starved for 24hrs before the addition of treatments. Cells were treated with IL-1α (5ng/ml) alone or in combination with OSM (10ng/ml). HDAC inhibitor treatments included TSA (5ng/ml, 25ng/ml, 50ng/ml and 100ng/ml), VPA (0.5mM, 1mM, 5mM and 10mM), MS-275 (1µM, 2µM, 5µM and 10µM) or tubacin (1µM, 2.5µM, 5µM, 10µM and 20µM). All treatments were completed in triplicate. Supernatants were removed 6 hours post stimulation and cells washed twice with ice-cold PBS. 6-well plate assays were harvested into 500µl/well TRIzol® reagent and stored at -80°C until RNA extraction. 96-well plate assays were harvested into Cells-to-cDNA lysis buffer (30µl) (refer to section 2.2.14).

2.2.3 RNA Extraction from Cells

RNA was purified from 500µl TRIzol® whole cell lysates by adding 100µl chloroform followed by a 15 second vortex. The solution was incubated at room temperature for 2 minutes before centrifugation at 12000g for 10 minutes, at 4°C. The aqueous phase was recovered and 250µl of iso-propanol added. The resulting mixture was vortexed and incubated for 10 minutes at room temperature. The mixture was centrifuged at 12000g for 10 minutes, at 4°C and the supernatant discarded. The remaining pellet was washed with 1ml 75% ethanol solution followed by centrifugation at 12000g for 30 minutes, at 4°C. The pellet was re-suspended in 20µl RNase-free water (analytical reagent grade) (Fisher Scientific, Waltham USA). RNA was stored at -80°C until DNase I treatment (refer to section 2.2.4).

2.2.4 DNase I Treatment

RNA samples were DNase I treated (recombinant RNase-free) (Roche Diagnostics Ltd, West Sussex, UK) to remove any genomic DNA contaminants before reverse transcription. RNA, 1µl DNase I and 2µl 10x DNase I buffer were combined in a final volume of 20µl (according to manufacturer's instructions). Samples were incubated at 37˚C for 15 minutes followed by an inactivation step of 75˚C for 10 minutes. Samples were purified using the organic extraction method (refer to 2.2.5).

2.2.5 Organic Extraction of Nucleic Acid

RNA samples, post DNase I treatment, were combined with 1x volume phenol:chloroform:isoamyl alcohol (25:24:1) (Sigma Aldrich, Dorset, UK) then vortexed for 15 seconds. Samples were centrifuged at 9500g for 10 minutes at 4˚C and the aqueous phase recovered. The aqueous phase was combined with 3x volume 100% ethanol and 0.1x volume 3M sodium acetate (pH 4.8) then incubated at -80˚C for 1 hour. Samples were centrifuged at 9500g for 30 minutes at 4˚C and the supernatant removed. The remaining RNA pellet was washed with 1ml 75% ethanol then centrifuged at 9500g for 30 minutes at 4˚C. The supernatant was removed and the RNA pellet air dried. The pellet was re-suspended in 20µl RNase-free water and stored at -80˚C until RNA quantification using the NanoDrop® spectrophotometer (NanoDrop Technologies, Wilmington, Delaware, USA).

2.2.6 Reverse Transcriptase cDNA Synthesis

For cDNA synthesis, 2µg random hexamers ($pd(N)_6$) (GE Healthcare, Little Chalfont, UK) were added to 1µg of RNA, in a final volume of 11µl, and heated to 70˚C for 10 minutes (all heating steps in protocol were performed in MJ Research PTC-200 Peltier Thermal Cycler PCR machine). A mastermix of 4µl 5x First Strand Buffer (Invitrogen, Paisley, UK), 2µl 0.1M DTT (Invitrogen), 1µl 100mM dNTP Mix (Bioline, London, UK), 1µl RNasin® Ribonuclease Inhibitor (40U/µl) (Promega, Southampton, UK) and 1µl SuperScript™ Reverse Transcriptase (200U/µl) (Invitrogen) was added per sample, followed by heating steps of 42˚C for 1 hour and 70˚C for 10 minutes. The cDNA was stored at -20°C.

2.2.7 Immunoblotting

Buffers

- **Final sample buffer (FSB)** (6x FSB: 7ml 4x stacking gel buffer, 3ml glycerol, 1g SDS. 1x FSB: 333ul 6x FSB + 1667µl deionised water.)
- **Resolving buffer** (4x buffer: 91g Tris base dissolved in 300ml deionised water, made to pH8.8 with hydrochloric acid. Made to final 500ml volume with deionised water. 2g SDS added and dissolved.)
- **Stacking buffer** (4x buffer: 6.05g Tris base dissolved in 40ml deionised water, made to pH6.8 with hydrochloric acid. Made to final 100ml volume with deionised water. 0.4g SDS added and dissolved.)
- **Running buffer** (10x buffer: 30.2g Tris base, 144g glycine, 10g SDS made to 1L with deionised water.)
- **Transfer buffer** (10x buffer: 30.3g Tris base, 141g glycine made to 1L with deionised water. 1x buffer: 100ml 10x buffer made to 1L with deionised water.)
- **Tris buffered saline (TBS)** (10x TBS: 24.2g Tris base, 80g NaCl dissolved in 900ml deionised water and made to pH7.6 with hydrochloric acid. Made to final volume of 1L with deionised water.)
- **Blocking buffer** (TBS containing 5% (w/v) Marvel non-fat dry milk powder and 0.1% (v/v) Tween-20.)

- **Primary antibody buffer** (20ml TBS containing 5% (w/v) bovine serum albumin and 0.1% (v/v) Tween-20.)

Method

SW1353 cells were plated in 6-well plates ($1.5x10^5$ cells/well) and serum-starved (as described in section 2.2.2) for HDACi dose response immunoblots, or in 12-well plates ($6.5x\ 10^4$ cells/well) to assess protein knockdown after siRNA treatment (as described in section 2.2.13.2). SW1353 cells were harvested, by scraping, into final sample buffer (1xFSB), 100µl/per well of a 6-well plate or 50ul/per well of 12-well plate. Whole cell lysates were stored overnight at -20°C. Samples were sonicated using an Ultra Sonic Processor (model # GE50, Jencons Scientific LTD, Leicestershire, UK) and protein quantified using a BCA protein quantification kit (Pierce Proteomics, Thermo Fisher Scientific, Northumberland, UK) following manufacturer's instructions. Samples were diluted to contain 20µg (samples from 6-well plates) or 15µg (samples from 12-well plates) protein in a 30µl volume with deionised water, followed by addition of 20ng/µl bromophenol blue and 1.2µl 1M Dithiothreitol (DTT). Samples were electrophoresed on appropriate 15%, 10% or 7.5% polyacrylamide gels depending on the size of the protein of interest. Resolving gels were made as stated in Table 2.0.

	Percentage SDS-polyacrylamide gel		
	7.5%	**10%**	**15%**
30% Acrylamide	3.75ml	5ml	7.5ml
4x Resolving buffer	3.75ml	3.75ml	3.75ml
ddH_2O	7.5ml	6.25ml	3.75ml
10% APS	50µl	50µl	50µl
TEMED	10µl	10µl	10µl

Table 2.0. The reagents required for 4x mini resolving gels.

Resolving gels were cast and topped with iso-propanol until set. Once set, iso-propanol was removed and stacking gels (1 gel: 0.71ml 4x stacking buffer, 0.41ml 30% acrylamide/bis acrylamide solution 37:5:1, 1.91ml deionised water, 16µl 10% ammonium persulfate (APS) and 3.2µl TEMED) were cast on top of the set resolving gels and a comb inserted.

Samples were heated for 5 minutes at 95°C before electrophoresis by SDS-PAGE. Protein markers Magic Marker™ and Protein Precision Plus™ were electrophoresed in neighbouring lanes to samples. Samples were electrophoresed at 150V until standards had separated sufficiently.

PVDF Immobilon P membrane was primed in 100% methanol and thick filter paper soaked in transfer buffer. Proteins were transferred from the gel to PVDF membrane using a Trans-Blot SD Semi-dry Electrophoretic transfer cell at 25V for 40 minutes for two 1mm mini-gels.

Membranes were washed briefly in TBS followed by Ponceau S dye staining, used for reversible protein staining on PVDF membranes, to check for equal protein loading. Membranes were then washed three times with TBS-T (TBS with 0.1% (v/v) Tween-20) for 5 minutes. Membranes were incubated in blocking buffer for 1 hour, gently rocking at room temperature, then washed three times with TBS-T for 5 minutes. Primary antibodies were diluted in primary antibody buffer (according to manufacturers' suggestions) and incubated with membranes with gentle rocking (incubation time and temperature according to manufacturers' suggestions). Membranes were then washed in TBS-T three times for 5 minutes. Horseradish peroxidase-conjugated secondary antibodies were diluted in blocking buffer according to manufacturers' instructions and incubated with membranes, whilst gently rocking, for 1hour at room temperature. Membranes were washed three times with TBS-T for 5 minutes. Proteins were visualised with LumiGLO and signal detected by exposure to Kodak BioMax maximum sensitivity film.

2.2.8 Bovine Nasal Cartilage (BNC) Assay

Bovine cartilage explants were stimulated with I/O (IL-1α combined with OSM) (to stimulate cartilage degradation) with or without a HDAC inhibitor. Collagen and

glycosaminoglycan (GAG) release from the explants into the media was assayed as a measurement of cartilage degradation. Collagen release was assayed using the hydroxyproline (DAB) assay (refer to section 2.2.11) and GAG release measured using the 1,9-dimethyl-methylene blue (DMB) assay (refer to section 2.2.10). Cartilage explants remaining at the end of the assay were papain digested (refer to section 2.2.9) then assayed for GAG and collagen content. The percentage of collagen and glycosaminoglycan release from explants was then calculated.

2.2.8.1 Small Scale BNC Assay

Bovine nasal septa was dissected, scraped clean and washed in PBS containing 200U/ml penicillin, 0.2U/ml streptomycin and 100U/ml nystatin. The cartilage was sliced into ~2mm thick sections then punched into ~2 mm diameter by 2mm thick discs. Three cartilage discs per well were added to 24-well plates, plus 1ml of serum-free DMEM containing 2mM L-glutamine, 100U/ml penicillin, 0.1U/ml streptomycin, 50U/ml nystatin and 0.04mg/ml gentamicin. Cartilage discs were incubated at 37˚C in a 5% CO_2/humidified atmosphere for 24 hours to allow equilibration of explants. Media was removed after equilibration and replaced with 600µl DMEM containing cytokines and/or HDAC inhibitor, with each treatment completed in quadruplicate. Treatments included I/O (IL-1 0.5ng/ml, OSM 5ng/ml), trichostatin A (50ng/ml and 250ng/ml), VPA (0.5mM, 1mM, 5mM and 10mM) MS-275 (1µM, 2µM, 5µM and 10µM) or tubacin/niltubacin (10µM). Supernates from BNC assays completed with TSA, VPA and MS-275 were harvested at day 7, treatments replaced and explants incubated until day 14. Supernates from the BNC assay completed with tubacin/niltubacin were harvested and treatments replaced at days 3 and 7, then incubated until day 14. At day 14, any remaining cartilage and media was harvested. Supernates were stored at -20°C until assayed for GAG and collagen content. Remaining cartilage explants were papain digested then stored at -20°C until assayed for GAG and collagen content.

Lactate dehydrogenase (LDH) was also detected in harvested supernates as a measure of cytokine and HDAC inhibitor toxicity. This was completed with a Cyto Tox 96 Non-Radioactive Cytotoxicity Assay kit from Promega (Southampton, UK), following manufacturer's instructions.

2.2.8.2 Bovine Nasal Cartilage Assay Profile

For the BNC profile, three bovine nasal septa were dissected and scraped clean in PBS with antibiotics (as in section 2.2.8.1). The septa were sliced into strips and cut into ~2 mm diameter by 2mm thick cubes. The cubes from all noses were combined and mixed equally. Approximately 0.7g of cartilage cubes and 4ml serum-free DMEM (containing L-glutamine and antibiotics as in section 2.2.8.1) were added per well of a 12-well plate. The cartilage cubes were then incubated at 37˚C in 5% CO_2/humidified atmosphere for 24 hours to allow equilibration of explants. Media was removed after equilibration and replaced with 4ml DMEM containing I/O (IL-1 0.5ng/ml and OSM 5ng/ml) and/or MS-275 (5µM), with each treatment completed in quadruplicate. The cartilage explants were incubated for 14 days with treatments being replaced at days 3 and 7. Supernatants and cartilage were collected at days 0, 1, 3, 8, 10 and 14. Supernatants were stored at -20°C for collagen and proteoglycan assays. Harvested cartilage was washed once with PBS, covered in RNA*later* (Ambion, Warrington, UK) and stored at 4°C for 24 hours (to allow the RNA*later* to penetrate the sample). Samples were then stored at -80°C until RNA extraction (refer to section 2.2.12).

2.2.9 Papain-Digest of Cartilage Explants

Buffers

- **Phosphate buffer** (137ml 0.1M NaH_2PO_4 + 63ml 0.1M $NaHPO_4$ (pH 6.5))
- **Papain solution** (0.25g (12U/mg) papain + 10ml phosphate buffer)
- **Cysteine-HCl solution** (0.039g cysteine-HCl + 5ml phosphate buffer)
- **EDTA solution** (0.095g EDTA + 5ml phosphate buffer)

Method

To digest explants harvested at day 14, 350µl phosphate buffer, 100µl papain (from *Carica* papaya, Sigma Aldrich) solution, 50µl cysteine-HCl (Sigma Aldrich) solution and 50µl EDTA were added per well. The plates were then sealed and explants heated to 65˚C overnight to allow cartilage digestion. After digestion, samples were transferred to Eppendorf tubes and 450µl phosphate buffer was added to make a final volume of 1ml. Papain-digests were assayed to determine collagen and glycosaminoglycan content of explants at the assay endpoint (refer to section 2.2.10 and 2.2.11).

2.2.10 1,9-Dimethyl-Methylene Blue (DMB/Glycosaminoglycan) Assay

Glycosaminoglycan (GAG) content of BNC assay supernatants and papain-digested cartilage samples was quantified using the DMB assay.

Reagent

- **DMB solution** (3.04g glycine, 2.37g NaCl, 95ml 0.1M HCl, made to final volume of 1L with deionised water. 16mg DMB added and dissolved (absorbance of 0.3a.u at 530nm.)

Method

A standard curve of 0-40μg/ml chondroitin sulphate (from bovine trachea, Sigma Aldrich, Dorset, UK) (at 5μg/ml increments), was made in PBS buffer (the same as that used in section 2.2.9) and plated into a 96-well plate with supernatant or papain-digested samples (40μl/well). 250μl DMB solution was added per well and the plate was read immediately at 530nm on a Wallac Envision 2103 multi-label plate reader (PerkinElmer, Waltham, USA). The GAG content was quantified using the standard curve and following equation:

$$x = \frac{y-c}{m}$$

(Where *y* is absorbance, *c* is the intercept, *m* is the gradient, and *x* the concentration)
The final number was then multiplied by the volume of the medium the cartilage explants were stimulated in during the assay.

2.2.11 Hydroxyproline (DAB) Assay

200μl of supernatants or papain digests were combined with 200μl concentrated HCl (Sigma Aldrich. Dorset, UK) and heated to 105°C overnight (to hydrolyse protein and release hydroxyproline). Samples were dried at 60°C for 3 hours using the Savant Speed Vac Concentrator (SPD131DDA) and Universal Vacuum System (Thermo Electron Corporation, Waltham, USA). Finally, samples were re-suspended in 200μl deionised water and mixed thoroughly.

For the assay three stock solutions were made:
Solution A: 20g DAB (4-(dimethyl-amino) benzaldehyde) + 30ml 70% perchloric acid
Solution B: 0.14g chloramine T + 2ml dH_2O
Solution C: 2ml sodium acetate + 37.5g tri sodium citrate

Stock solutions were used to make two working solutions:
Solution 1 (*Chloramine-T solution*): 2ml solution B + 8ml solution C
Solution 2 (*DAB solution*): 10ml solution A + 30ml propan-2-ol

A standard curve containing 0-30μg/ml hydroxyproline (trans-4-hydroxy-L-proline) (at 5μg/ml increments) was made with deionised water and plated into a 96-well plate with re-suspended samples (40μl/well). 25μl/well of Solution 1 (Chloramine T solution) was added to samples and incubated at room temperature for 4 minutes. 150μl/well of solution 2 (DAB solution) was then added, and the plate sealed and incubated at 65°C for 35 minutes. The plate was allowed to cool before being read at 560nm on a NorthStar Scientific ELX800 plate reader (BioTek, Bedfordshire, UK). The final concentration of hydroxyproline in samples was determined using the equation in section 2.2.10.

2.2.12 RNA Extraction from Cartilage

Cartilage was defrosted, RNA*later* removed and the tissue ground under liquid nitrogen using the 6750 Freezer Mill (Spex Certiprep) (10 minute pre-cool, 5 cycles of 2 minute grind, 2 minute cool, at 10 Hz). TRIzol® reagent (1ml/0.2g cartilage) was added immediately to ground cartilage, mixed thoroughly and incubated at room temperature for 5 minutes. The mixture was centrifuged at 9500g for 10 minutes at 4°C to pellet the ground cartilage. Supernatants were collected and 300μl chloroform added per 500μl of sample. Samples were vortexed for 15 seconds followed by incubation at room temperature for 10 minutes. Samples were centrifuged at 9500g for 15 minutes at 4°C, and the aqueous layer recovered into RNase free tubes. Aqueous layers were combined with 0.5x volume 100% ethanol and mixed. The samples were added to RNeasy plus mini kit columns (Qiagen, West Sussex, UK. cat no: 74134), centrifuged at 9500g for 15 seconds and the flow-through discarded. 700μl RW1 buffer (Qiagen) was added to the columns then centrifuged at 9500g for 15 seconds and flow-through discarded. Columns were placed in new RNase-free collection tubes and 500μl RPE (Qiagen) added, followed by centrifugation at 9500g for 15 seconds and flow-through discarded. 500μl RPE was added to columns followed by centrifugation at 9500g for 2 minutes. Columns were then placed in RNase-free collection tubes and 30μl of RNase-free water added. Columns were then left to stand for 2 minutes

(to increase maximum RNA yield) then centrifuged at 9500g for 2 minutes. RNA was then stored at -80°C until quantification.

2.2.13 *SMART*pool Short Interfering RNAs *(siRNAs)*

*SMART*pool siRNAs combine four duplexes against different regions of the target gene, which potentially minimises off-target effects due to the reduced concentration of each single siRNA.

2.2.13.1 SMARTpool Short Interfering RNAs (siRNAs) Messenger RNA Knockdown

Cells (SW1353 and primary chondrocytes) were plated within 96-well plates ($6.5x10^3$ cells/well) for siRNA mRNA knockdown analysis, with experiments carried out 24hrs later. SMARTpool siRNA stocks were diluted to 2μM in 1x Dharmacon siRNA Buffer (Dharmacon, Chicago, USA). Transfections were carried out according to manufacturer's instructions. For each transfection two tubes were prepared as described in Table 2.1.

100nM transfection/well	
Tube 1	**Tube 2**
5μl siRNA (2μM) 5μl DMEM medium (serum and antibiotic-free)	0.2μl Dharmafect reagent 9.8μl DMEM medium (serum and antibiotic-free)

Table 2.1. Transfection reagents required for 100nM siRNA transfection per well of a 96-well plate.

Different amounts of siRNA were added to tube 1 to change the final siRNA concentration and 1x Dharmacon siRNA buffer used to maintain the same final volume. Tubes 1 and 2 were incubated at room temperature for 5 minutes then combined and incubated at room temperature for 20 minutes to allow liposome formation. The final volume was made to 100μl with DMEM containing 10% heat-inactivated FCS, 100IU/ml penicillin, and 100μg/ml streptomycin. Medium was aspirated from wells and replaced with 100μl transfection mixture. All treatments were completed in triplicate and cells incubated for

desired time. After incubation supernatants were removed and cells washed twice with ice-cold PBS. Cells were harvested into 30µl Cells-to-cDNA II cell lysis buffer (Ambion, Huntingdon, UK) followed by reverse transcription using the cells-to-cDNA II method (refer to section 2.2.14).

2.2.13.2 SMARTpool Short Interfering RNAs (siRNAs) Protein Knockdown

For *SMART*pool siRNA protein knockdown analysis, cells were plated in 12-well plates ($6.5x\ 10^4$ cells/well) and reagents scaled up by a factor of 10. To detect siRNA-mediated protein knockdown, cells were incubated for 48 hours post transfection, then harvested into 50µl 1x final sample buffer (FSB: refer to section 2.2.7). Samples were stored at -20°C until the protein content was quantified via BCA assay and immunoblotted with HDAC specific antibodies (refer to sections 2.1.5 and 2.2.7).

2.2.13.3 SMARTpool Short Interfering RNAs (siRNAs) Knockdown with Cytokines

SW1353 cells were plated and transfected with 25nM siRNA for all classical HDACs as in section 2.2.13.1. Cells were incubated with siRNA for 24 hours. The media was then removed and replaced with serum, antibiotic-free DMEM, and cells serum-starved overnight. Cells were stimulated with cytokine IL-1α (5ng/ml) in the presence or absence of 50ng/ml TSA. Media was removed 6 hours post stimulation and cells washed twice with ice-cold PBS. Cells were then harvested into 30µl Cells-to-cDNA II cell lysis buffer and reverse transcribed as in section 2.2.14.

2.2.14 Ambion Cells-to-cDNA II RNA Isolation from 96-Well Plate Monolayer

Reagent

Cells-to-cDNA II cell lysis buffer (Ambion, Huntingdon, UK) lyses cells and inactivates RNases, providing a cell lysate which can immediately be reverse transcribed without the need for RNA isolation.

Method

Lysates (from cells lysed into Cells-to-cDNA II lysis buffer) were transferred to ice-cold AB gene® PCR plates (Thermo Scientific ABgene, Surrey, UK). The lysates were heated to 75°C in a Verti 96-well Thermal Cycler for 15 minutes (Applied Biosystems, Warrington, UK) to inactivate RNases (after this step, lysates can be stored at -80°C until reverse transcription). For genomic DNA digestion, 1µl DNase I (RNase-free) (Ambion, Huntingdon, UK) (2U/µl) and 3µl DNase I 10x buffer (Ambion) were added per well and the plate heated to 37°C for 15 minutes, followed by an inactivation step 75°C for 5 minutes.

For reverse transcription 8µl of the DNase-treated samples were taken and placed into a new ice-cold PCR plate. Following this, 3µl of 10mM dNTP Mix (Bioline, London, UK) and 0.2µg random primers (Invitrogen, Paisley, UK) were added per well and samples heated to 70˚C for 5 minutes. Samples were chilled on ice then a master mix of 0.5µl M-MLV Reverse transcriptase (Invitrogen) (200U/µl), 4µl 5x First Strand Buffer (Invitrogen), 2µl 0.1M DTT (Invitrogen), 1µl RNasin® Ribonuclease Inhibitor (Promega, Southampton, UK) (40U/µl) and 1µl RNase-free water was added per well. Samples were then heated to 37˚C for 50 minutes, followed by a step of 75˚C for 15 minutes. 30µl of RNase-free water was then added per sample. For quantitative real-time PCR (qRT-PCR) analysis of the gene of interest, 5µl of sample was used. For analysis of 'house-keeping' gene 18S, samples were diluted 1:10 and 5µl used for qRT-PCR. Quantitative real-time PCR of samples was carried out as in sections 2.2.15.1 and 2.2.15.2

2.2.15 Real-Time Quantitative RT-PCR

2.2.15.1 Standard Probe-Based Real-Time qRT-PCR

The probe-based quantitative real-time PCR (qRT-PCR) method was used to detect the expression of human metalloproteinases and their inhibitors in the SW1353 cell line and primary chondrocytes. The primers and fluorescent probes for human MMPs and ADAMTS genes were designed using Primer Express 1.0 software (Applied Biosystems) and synthesised by PE Biosystems. To control against amplification of genomic DNA, primers and probes were designed to be close to intron/exon boundaries, with the probe spanning two neighbouring exons where possible. Primers and probe sequences are as described in Nuttall *et al*. (2003) and Porter *et al*. (2005) (See Appendix II for complete list) (Nuttall et al, 2003). Gene specificity of primers and probes was validated through BLAST (Basic Local Alignment Search Tool).

Reagents

MicroAmp optical 96-well plates, 2x Taqman® Universal PCR Master Mix and optical adhesive covers were all purchased from Applied Biosystems (Warrington, UK).

Method

Fluorescence-based relative quantification of genes was conducted on the ABI Prism 7500 sequence-detection system (Applied Biosystems, Warrington, UK), according to manufacturer's instructions. PCR reactions contained 1ng of reverse transcribed RNA for 'housekeeping' gene 18S analysis, and 5ng for the gene of interest when the RNA quantity was known. For Cells-to-cDNA II transcribed samples, 5µl of sample was used for gene of interest detection, or diluted 1:10 and 5µl used for the detection of 18S (refer to section 2.2.14).

The 18S rRNA gene was used as an endogenous control to normalize the total amount of cDNA found in each sample. The threshold cycle (C_T) is the cycle number at which the signal is detectable above baseline. The median C_T level of 18S was calculated and samples giving a C_T reading of 1.5 C_T greater or less than the median were excluded from analysis. This was done to ensure the quality of the final data.

To determine the relative cDNA input of each sample, standard curves for each gene were prepared using cDNA from one sample (known to express the gene of interest) and making 2-fold serial dilutions. 18S cDNA standards were serially diluted to 4, 2, 1, 0.5, 0.25, 0.125ng/10µl. Gene of interest standards were serially diluted to 20, 10, 5, 2.5, 1.25, 0.625/10µl. Relative input amounts of cDNA were then calculated from C_T using the standard curves.

The PCR reaction mix contained Taqman Universal 2x mastermix, final concentration 100nM of forward and reverse primer and 200nM of fluorescent probe (in a final volume of 25µl). PCR cycles: 2 minutes at 50°C, 10 minutes at 95°C, followed by 40 cycles for 15 seconds at 95°C and 1 minute at 60°C. Reactions were carried out in MicroAmp optical 96-well plates and sealed with optical adhesive covers.

2.2.15.2 Universal Probe Library Real-Time qRT-PCR

The Universal Probe Library (UPL) (Roche Diagnostics Ltd, West Sussex, UK) enables extensive transcript coverage due to the short 8-9 nucleotide-long probes. Each probe has a fluorescein (FAM™) label at the 5' end and a dark quencher dye at the 3' end. For specificity and melting temperature (Tm) required for hybridising probes, locked nucleic acids are incorporated into their sequence.

The UPL was used for detection of all classical HDACs within the SW1353 cell line and primary chondrocytes. The transcript DNA accession numbers for all classical HDACs were obtained from the GenBank National Centre of Biotechnology Information (NCBI) and entered into the Assay Design Centre, Roche Applied Science. The Assay Design Centre identifies a list of optimal primer/probe sets that can be used for the detection of the gene of interest. This was completed for all classical HDACs and primers purchased from Sigma Aldrich. (For primer sequences and UPL probe numbers refer to Appendix II).

The PCR reaction mix contained Taqman 2x mastermix, 100nM of forward and reverse primer and 200nM of fluorescent probe (in a final volume of 25µl). PCR cycles the same as section 2.2.15.1.

2.2.15.3 SYBR® Green Real-Time qRT-PCR

The SYBR Green dye fluoresces when bound to double stranded-DNA, enabling the measurement of double stranded-DNA amplification during PCR. The combination of dye with specific primers generates single gene-specific amplicons, thus allowing relative quantification of the original cDNA template.

SYBR® Green real-time qRT-PCR was used to detect bovine metalloproteinase and inhibitor gene expression. The design of the metalloproteinase and inhibitor primer sets was as described in Milner *et al*. (2006) (for full primer sequences refer to appendix II). Briefly, SYBR Green primers were designed using DNAstar (DNASTAR, Inc., Madison, WI, USA) and designed to cross intron/exon boundaries where possible. BLAST searches for all primer sequences were conducted to ensure gene specificity. All primers were purchased from Sigma-Aldrich DNA-Oligo design.

Method

SYBR® green reactions contained 5ng of cDNA for the detection of the gene of interest. The PCR reaction mix contained 50% SYBR® Green PCR Master Mix (Applied Biosystems) and 100nM of forward and reverse primer (in a final volume of 25µl). PCR cycles: 2 minutes at 50°C, 10 minutes at 95°C, 40 cycles for 15 seconds at 95°C, 1 minute at 60°C and a dissociation step. The dissociation step produces a melting curve for the PCR amplification product and ensures there is only amplification of the target gene. Reactions were carried out in MicroAmp optical 96-well plates sealed with optical adhesive covers (Applied Biosystems, Warrington, UK).

2.2.16 Data Analysis

2.2.16.1 Relative Gene Quantification: Standard Curve Method

The standard curve method of relative quantification uses standards of known amounts of positive control cDNA (as described in section 2.12.1). For relative quantification (RQ) for the target gene the following equation was used:

$$RQ = (C_T\text{-}intercept)/slope$$

The RQ was then transformed to inverse $\log_{10}$. All genes of interest were normalized to the relative gene expression of 18S.

2.2.16.2 Relative Gene Quantification: Comparative C_T Method

The 2-($C_T$gene-C_T18S) (2-ΔC_T) method was used as an approximate measure of target gene expression in the BNC assay screen, HDAC inhibitor dose responses (completed in chondrocytes) and for all siRNA knockdown assay experiments. The amount of target was normalised to 18S 'house-keeping' gene as an endogenous control. This method allowed comparison of expression levels between genes as it has been shown to correlate well between copy number and cycle threshold (C_T) values (as assessed by using *in vitro*-transcribed RNA to produce a standard curve) (Kevorkian et al, 2004; Milner et al, 2006). This method assumes that all primers and probe sets are working at the same efficiency.

2.2.17 Statistical Analysis

All values are given as mean values of replicates with error bars representing the standard error of the mean. Student's t-test (unpaired), completed using GraphPad Prism 4.00 (GraphPad software, San Diego, USA) was used to detect significant differences between independent sample groups, unless otherwise stated. Levels of statistical significance are depicted as * $p \leq 0.05$, ** $p \leq 0.01$ and *** $p \leq 0.001$.

Chapter III: The role of histone deacetylase inhibitors in metalloproteinase gene regulation and chondroprotection

Chapter III

The role of histone deacetylase inhibitors in metalloproteinase gene regulation and chondroprotection

3.1 Introduction

Cartilage destruction in osteoarthritis is thought to be mediated by the action of proteinases from the matrix metalloproteinase (MMP) and 'a disintegrin and metalloproteinase domain with thrombospondin motifs' (ADAMTS) families. OA chondrocytes are postulated to be one of the major sources of metalloproteinase expression within the OA joint (Goldring, 2000). Metalloproteinase expression is primarily regulated at the transcriptional level, which is partially mediated through changes in protein acetylation catalysed by enzymes from the histone acetyltransferase (HATs) and histone deacetylase (HDACs) families.

Previous work published by our laboratory has shown that broad spectrum HDAC inhibitors TSA and NaBy can repress cytokine-induced metalloproteinase expression at the mRNA and protein level, both in the SW1353 cell line and primary chondrocytes (Young et al, 2005). These compounds were also found to inhibit cytokine-induced cartilage resorption in the bovine nasal cartilage (BNC) assay, thought to be a result of the transcriptional repression of cytokine-induced metalloproteinase expression by non-histone related pathways (Young et al, 2005). The expression of metalloproteinases and their inhibitors has previously been profiled during the 14 day BNC assay, identifying a number of cytokine-induced metalloproteinase genes, such as the collagenases *MMP1* and *MMP13* and the aggrecanases *ADAMTS4* and *ADAMTS5* (Milner et al, 2006). Importantly the activation of pro-collagenases was also found to be a key regulatory step in collagenolysis (Milner et al, 2006).

The chondroprotective property of HDAC inhibitors has also been supported by the reduced joint damage observed in inflammatory, and most recently, osteoarthritic animal models as a result of HDAC inhibitor treatment *in vivo*. The reduced joint damage in inflammatory animal models, mediated by inhibitors such as TSA and MS-275, was associated with reduced cytokine expression and increased expression of cell cycle regulators $p16^{INK4a}$ and $p21^{WAF/Cip1}$ (Chung et al, 2003; Keiichiro et al, 2004; Lin

et al, 2007). The recently published OA rabbit model demonstrated that intra-articular injection of TSA reduced cartilage damage and suppressed increased *MMP1*, *MMP3*, *MMP13* and IL-1 expression detected in the OA rabbit controls (Chen et al, 2010).

The molecular pathways by which HDAC inhibitors mediate repression of cytokine-induced metalloproteinase expression remain unknown. Compounds TSA and NaBy reportedly inhibit all members of the classical HDAC family, with the exception of HDAC6 for NaBy, making it unclear which HDACs are involved in the regulation of metalloproteinase expression. In order to elucidate which HDACs need to be inhibited to repress metalloproteinase expression three reportedly selective inhibitors were chosen for use in cell monolayer and BNC assays. The inhibitors chosen were valproic acid (VPA), MS-275 and tubacin, which belong to different structural classes and have different inhibitory profiles. Short-chain fatty acid VPA reportedly inhibits class I HDACs at low concentrations (~0.7-1mM) and class II HDACs at higher concentrations (>1mM), preferentially targeting co-repressor-associated HDAC1 and HDAC2 (Gottlicher et al, 2001; Gurvich et al, 2004). Benzamide MS-275 is known to be class I selective, inhibiting the action of HDAC1, HDAC2 and HDAC3, but not HDAC8 (Hess-Stumpp et al, 2007; Hu et al, 2003; Inoue et al, 2006; Vannini et al, 2004). Tubacin is a recently developed inhibitor shown specifically to inhibit HDAC6, thus preventing α-tubulin acetylation in mammalian cells (Haggarty et al, 2003). The effect of these compounds on cytokine-induced metalloproteinase expression was assessed in the SW1353 cell line, OA primary articular chondrocytes and the BNC assay, alongside the previously studied inhibitor TSA.

Aims

- Establish the effect of HDAC inhibitors TSA, VPA and MS-275 on core histone and α-tubulin acetylation levels.

- Determine the effect of TSA, VPA and MS-275 on basal and cytokine-induced metalloproteinase expression in the SW1353 chondrosarcoma cell model, and confirm these effects in primary articular chondrocytes.

- Determine if TSA, VPA and MS-275 can prevent cytokine-induced cartilage degradation in the BNC assay.

- Profile the expression of OA-associated metalloproteinases and *TIMP1* during the BNC assay, and establish if MS-275 can modulate this expression.

- Determine the effect of tubacin on the level of α-tubulin acetylation and cytokine-induced metalloproteinase expression in the SW1353 cell line.

- Establish if tubacin can prevent cytokine-induced cartilage degradation in the BNC assay.

3.2 Results

3.2.1 The induction of core histone and α-tubulin acetylation in SW1353 cells

Human SW1353 chondrosarcoma cells were cultured and plated as described in section 2.2.7. SW1353 cells were incubated with increasing concentrations of TSA (5ng/ml, 25ng/ml, 50ng/ml and 100ng/ml), VPA (0.5mM, 1mM, 5mM and 10mM) and MS-275 (1μM, 2μM, 5μM and 10μM) for 6 hours. The effect of HDAC inhibitors on the cellular level of core histone and α-tubulin acetylation was assessed by immunoblotting, as described in section 2.2.7. Predominantly, HDAC inhibitors induce histone acetylation through the inhibition of HDACs. However, HDAC6 deletion in embryonic stem cells and the null mouse model has been shown to have no significant effect on histone 3 and histone 4 acetylation, leading to the identification of α-tubulin as its primary physiological substrate (Zhang et al, 2008; Zhang et al, 2003). Therefore, inhibition of HDAC6 catalytic activity can be detected by an increase in the cellular level of acetylated α-tubulin.

In this study, all inhibitors increased cellular histone 3 and histone 4 acetylation in a concentration-dependent manner, compared to total histone 3 and histone 4 levels (Figure 3.1 a and b). This indicates that all three compounds inhibit HDACs involved in histone deacetylation. TSA was shown to increase α-tubulin acetylation in a concentration-dependent manner compared to total α-tubulin (Figure 3.1c), indicating that TSA inhibits HDAC6 catalytic activity and supports its status as a ‘pan’ inhibitor. VPA had no effect on the level of acetylated α-tubulin, suggesting that it does not inhibit HDAC6 activity at these concentrations. MS-275 had no effect on the level of acetylated α-tubulin, supporting its status as a class I selective inhibitor.

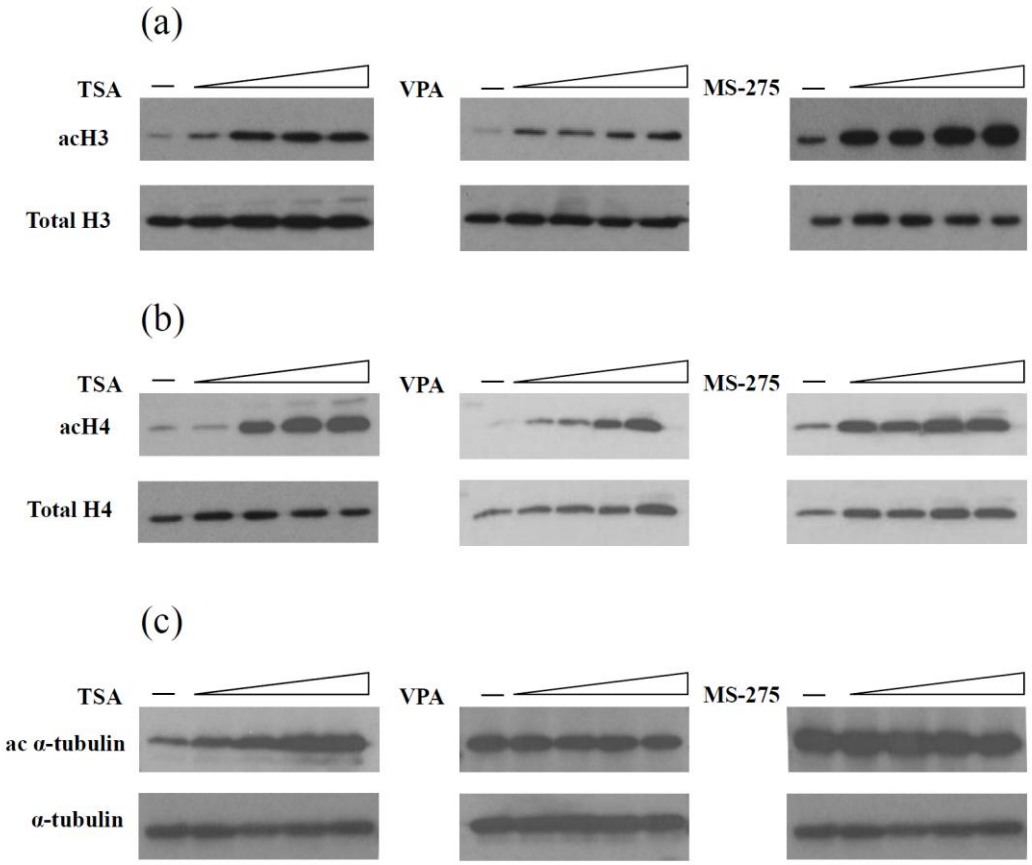

Figure 3.1. The effect of HDAC inhibitors on core histone and α-tubulin acetylation in the SW1353 cell line

SW1353 cells were incubated with increasing concentrations of TSA, VPA and MS-275 for 6 hours. Total protein was extracted, resolved by SDS-PAGE and acetylation levels of histone 3, histone 4 and α-tubulin assessed by immunoblotting with specific antibodies. The levels of histone and α-tubulin acetylation were compared to total levels. **(a)** Histone 3 acetylation in response to TSA (5ng/ml, 25ng/ml, 50ng/ml and 100ng/ml), VPA (0.5mM, 1mM, 5mM and 10mM) and MS-275 (1μM, 2μM, 5μM and 10μM). **(b)** Histone 4 acetylation in response to TSA, VPA and MS-275. **(c)** α-tubulin acetylation in response to TSA, VPA and MS-275. (acH3, acetylated histone 3: acH4, acetylated histone 4: ac α-tubulin, acetylated α-tubulin).

3.2.2 The effect of HDAC inhibitors on metalloproteinase expression in SW1353 cells

The pro-inflammatory cytokine IL-1α is known to induce the expression of many metalloproteinase genes in primary and chondrocyte cell lines. This induction is further potentiated when IL-1 is combined with the growth factor OSM (Barksby et al, 2006; Koshy et al, 2002). Previously published data demonstrated that the broad spectrum inhibitors TSA and NaBy can decrease cytokine-induced metalloproteinase expression in the SW1353 cell line (Young et al, 2005). To determine whether TSA-mediated metalloproteinase repression could be repeated with the more selective inhibitors VPA and MS-275, SW1353 cells were incubated with IL-1α alone and in combination with OSM (I/O) in the presence or absence of increasing concentrations of TSA, VPA and MS-275 (as described in section 2.2.2). The expression of *MMP1*, *MMP2*, *MMP3*, *MMP9*, *MMP10*, *MMP13*, *MMP28*, *ADAMTS4* and *ADAMTS5* were then measured by quantitative real-time PCR (qRT-PCR).

Of the genes detected, *MMP1*, *MMP3*, *MMP10* and *MMP13* were robustly induced by IL-1α, with the responses further potentiated in combination with OSM. Cytokine-induced *MMP9* expression was variable, showing induced expression in some assays and not others (Appendix I: Figure 1b, Figure 2b and Figure 3b). *ADAMTS4* and *ADAMTS5* were expressed at low levels in the SW1353 cell line, and exhibited variable response to cytokine treatment (Appendix I: Figure 1e and f, Figure 2e and f and Figure 3e and f).

TSA and VPA significantly decreased cytokine-induced *MMP1* and *MMP13* expression. TSA reduced both IL-1α- and I/O-induced *MMP1* and *MMP13* expression in a concentration-dependent manner (Figure 3.2a and c). VPA decreased I/O-induced *MMP1* and *MMP13* expression in a concentration-dependent manner. However, repression of IL-1α-induced *MMP1* and *MMP13* expression was not concentration-dependent, due to a reproducibly greater repression of both collagenases at 0.5mM VPA compared to 1mM (Figure 3.3a and c). This may be related to the concentration-dependent class switch of inhibition from class I to both class I and class II HDACs reported for VPA (Gurvich et al, 2004). The greatest level of VPA-mediated metalloproteinase repression was achieved at 5mM and 10mM. At these high concentrations it would be expected that the catalytic activity of both class I and class II HDACs would be inhibited by VPA. This suggests that to achieve maximum repression of cytokine-induced metalloproteinase expression with this compound, it is necessary to

inhibit members of both classes of HDAC. In contrast, despite a statistically significant repression of IL-1α-induced *MMP1* and *MMP13* expression achieved with 1μM MS-275, the class I specific inhibitor did not convincingly decrease cytokine-induced collagenase expression (Figure 3.4a and c). This indicated that class I HDACs may not play an important role in the regulation of collagenase expression in these cells.

Despite the differences observed between TSA, VPA and MS-275 regarding the repression of cytokine-induced *MMP1* and *MMP13* expression, all three inhibitors displayed the same pattern of concentration-dependent repression of cytokine-induced *MMP3* expression (Figure 3.2b, 3.3b and 3.4b). However, the repression of induced *MMP3* expression by MS-275 was not as efficient as that achieved with TSA and VPA. Interestingly, TSA and VPA also significantly decreased cytokine-induced *MMP10* (stromelysin-2) (Appendix I: Figure 1c and 2c), but MS-275 had no repressive effect (Appendix I: Figure 3c).

MMP2 expression was not induced in response to cytokines, which is consistent with Young *et al*. (2005). However, the current study detected decreased basal *MMP2* expression in response to TSA, VPA and MS-275 treatment (Appendix I: Figure 1a, 2a and 3a), which was not observed in response to TSA and NaBy treatment by Young *et al*. (2005). This current study also found that *MMP28* expression was not induced by cytokines, but detected increased basal expression in response to all three inhibitors (Appendix I: Figure 1d, 2d and 3d). The induction of *MMP28* expression by HDAC inhibitors is consistent with previous reports (Swingler et al, 2010; Young et al, 2005).

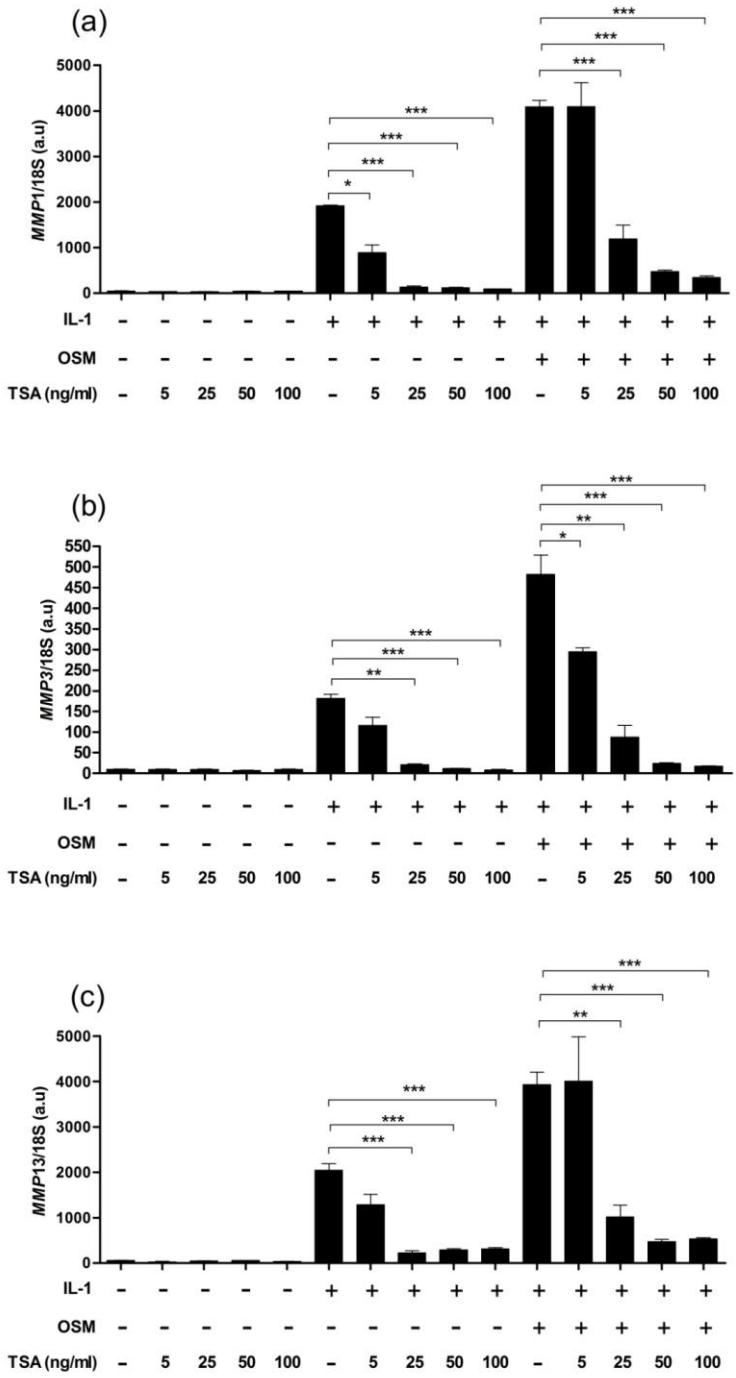

Figure 3.2. The effect of trichostatin A on cytokine-induced *MMP* expression in SW1353 cells

SW1353 cells were incubated with increasing concentrations of TSA (5ng/ml, 25ng/ml, 50ng/ml and 100ng/ml) in combination with IL-1α (5ng/ml) or I/O (combination of IL-1α and OSM (10ng/ml)) for 6 hours. Total RNA was extracted with Trizol, reverse transcribed to cDNA, and *MMP* levels detected by real-time qRT-PCR **(a)** *MMP1* expression in response to cytokine and TSA treatment. **(b)** *MMP3* expression in response to cytokine and TSA treatment. **(c)** *MMP13* expression in response to cytokine and TSA treatment. Assays were completed at least twice, using triplicate samples. Data presented is representative of one assay; means ± standard errors are represented. **P*<0.05, ***P*<0.01, ****P*<0.001. (a.u: arbitrary units).

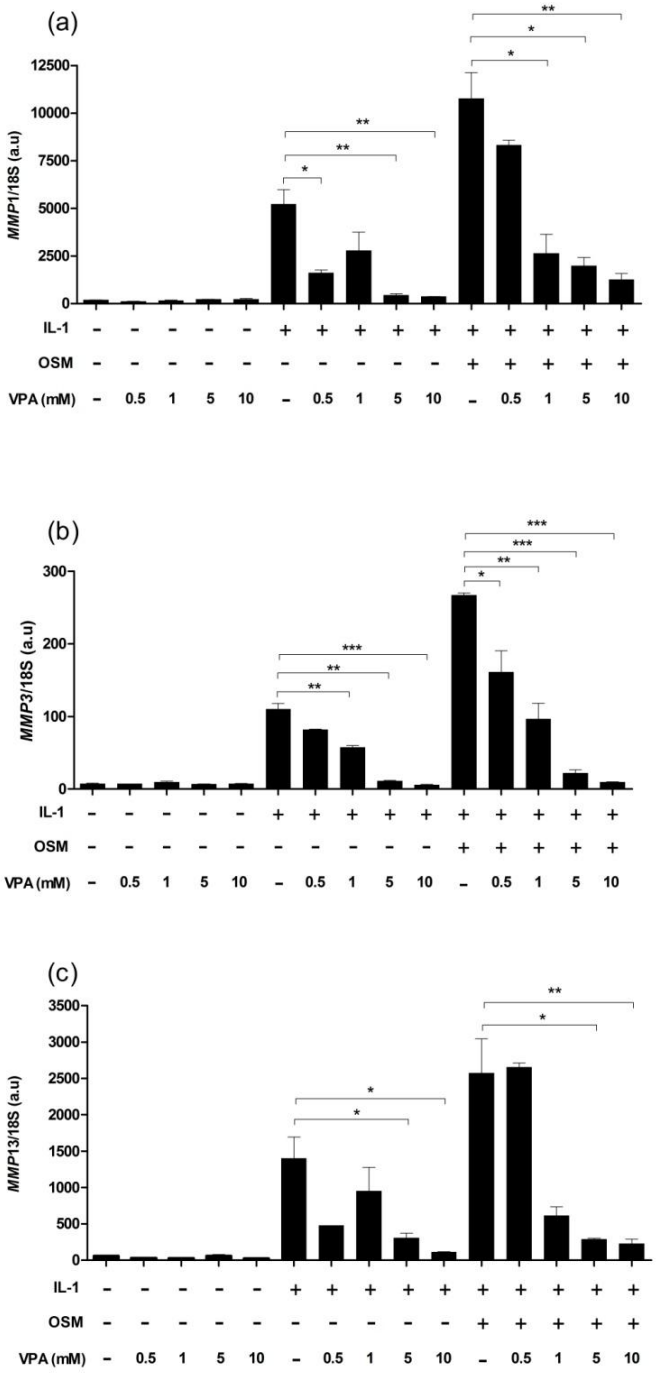

Figure 3.3. The effect of valproic acid on cytokine-induced *MMP* expression in SW1353 cells

SW1353 cells were incubated with increasing concentrations of VPA (0.5mM, 1mM, 5mM and 10mM) in combination with IL-1α (5ng/ml) or I/O (combination of IL-1α and OSM (10ng/ml)) for 6 hours. Total RNA was extracted with Trizol, reverse transcribed to cDNA, and *MMP* levels detected by real-time qRT-PCR **(a)** *MMP1* expression in response to cytokine and VPA treatment. **(b)** *MMP3* expression in response to cytokine and VPA treatment. **(c)** *MMP13* expression in response to cytokine and VPA treatment. Assays were completed at least twice, using triplicate samples. Data presented is representative of one assay; means ± standard errors are represented. **P*<0.05, ***P*<0.01, ****P*<0.001. (a.u: arbitrary units).

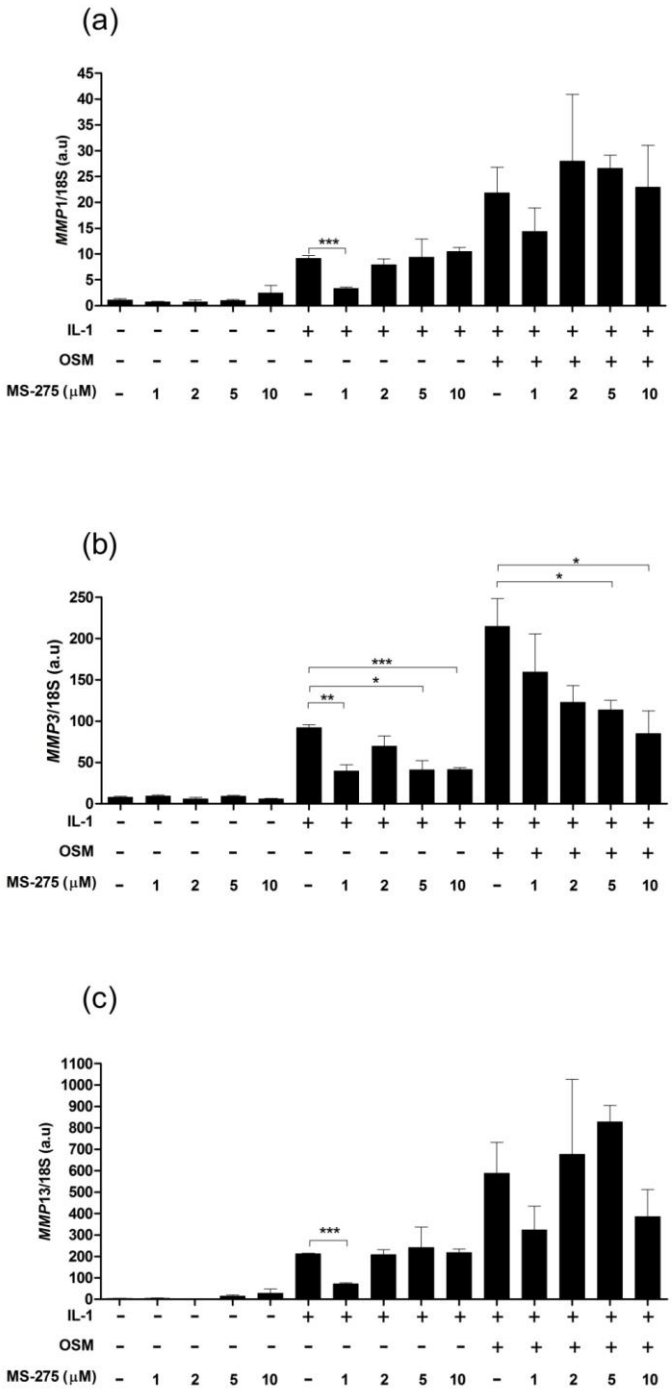

Figure 3.4. The effect of MS-275 on cytokine-induced *MMP* expression in SW1353 cells

SW1353 cells were incubated with increasing concentrations of MS-275 (1μM, 2μM, 5μM and 10μM) in combination with IL-1α (5ng/ml) or I/O (combination of IL-1α and OSM (10ng/ml)) for 6 hours. Total RNA was extracted with Trizol, reverse transcribed to cDNA, and *MMP* levels detected by real-time qRT-PCR **(a)** *MMP1* expression in response to cytokine and MS-275 treatment. **(b)** *MMP3* expression in response to cytokine and MS-275 treatment. **(c)** *MMP13* expression in response to cytokine and MS-275 treatment. Assays were completed at least twice, using triplicate samples. Data presented is representative of one assay; means ± standard errors are represented. **P*<0.05, ***P*<0.01, ****P*<0.001. (a.u: arbitrary units).

3.2.3 The effect of HDAC inhibitors on MMP13 expression in primary articular chondrocytes

Primary articular chondrocytes were treated with cytokines IL-1α and OSM either in the presence or absence of increasing concentrations of TSA, VPA and MS-275 (as described in section 2.2.2). This was to determine if HDAC inhibitors exhibited the same pattern of repression of cytokine-induced *MMP13* expression in primary cells as in the SW1353 cell line. The expression of *MMP13* was determined by qRT-PCR.

Cytokine treatment significantly induced *MMP13* expression in primary articular chondrocytes. All three HDAC inhibitors significantly repressed cytokine-induced *MMP13* expression, despite MS-275 previously exhibiting no repression in the SW1353 cell line (Figure 3.5c). This indicated that class I HDAC regulation of *MMP13* expression may be different in the transformed SW1353 cell line than in primary chondrocytes, with class I inhibition alone enough to repress cytokine-induced *MMP13* expression in primary cells. Interestingly, the repression of cytokine-induced *MMP13* expression by TSA was not as efficient in primary chondrocytes as in SW1353 cells, with significant repression only seen with 100ng/ml (Figure 3.5a). In contrast the repression of *MMP13* expression by VPA was more efficient in primary chondrocytes than in SW1353 cells, with massive repression achieved with just 0.5mM VPA (Figure 3.5b). VPA at 0.5mM is thought to only inhibit class I HDACs, which again indicates that class I HDAC inhibition alone is capable of repressing cytokine-induced *MMP13* expression in primary articular chondrocytes.

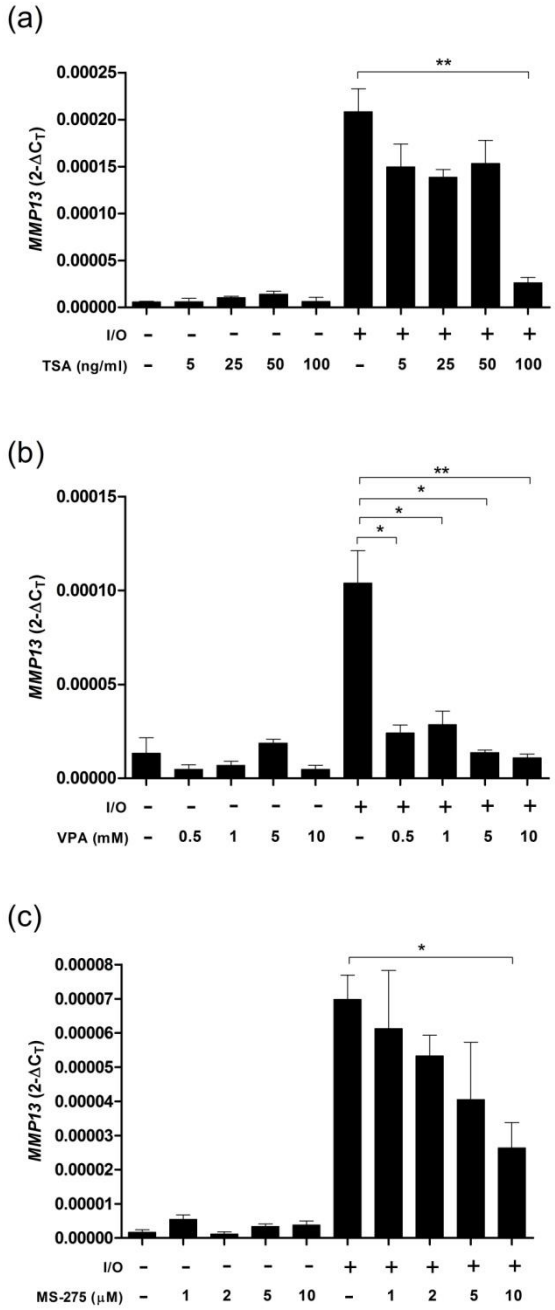

Figure 3.5. HDAC inhibitors down-regulate cytokine-induced *MMP13* expression in primary articular chondrocytes

Primary articular chondrocytes were incubated with increasing concentrations of TSA (5ng/ml, 25ng/ml, 50ng/ml and 100ng/ml), VPA (0.5mM, 1mM, 5mM and 10mM) or MS-275 (1μM, 2μM, 5μM and 10μM) in combination with I/O (combination of IL-1α (5ng/ml) and OSM (10ng/ml)) for 6 hours. Total RNA was extracted with Cells-to-cDNA lysis buffer, reverse transcribed to cDNA, and *MMP13* expression detected by real-time qRT-PCR **(a)** *MMP13* expression in response to cytokine and TSA treatment. **(b)** *MMP13* expression in response to cytokine and VPA treatment. **(c)** *MMP13* expression in response to cytokine and MS-275 treatment. Assays were completed once, using triplicate samples; means ± standard errors are represented. **P*<0.05, ***P*<0.01, ****P*<0.001.

3.2.4 The effect of HDAC inhibitors on cytokine-induced cartilage degradation

The combination of IL-1α and OSM has previously been shown to potently induce cartilage degradation both *in vitro* and *in* vivo (Cawston et al, 1998; Morgan et al, 2006; Rowan et al, 2003). *In vitro* cartilage degradation is commonly measured as proteoglycan and collagen release from cartilage explants. Previously published data demonstrated that broad spectrum HDAC inhibitors TSA and NaBy can block both collagen and proteoglycan proteolysis in the BNC assay (Young et al, 2005). This chondroprotective effect was thought to be mediated by the repression of cytokine-induced metalloproteinase expression, which was observed in monolayer SW1353 and primary chondrocyte assays (Young et al, 2005).

To determine if this could be repeated with TSA and the more selective inhibitors VPA and MS-275, bovine nasal cartilage chips were treated with IL-1α and OSM in the presence or absence of increasing concentrations of TSA (50ng/ml and 250ng/ml), VPA (0.5mM, 1mM, 5mM and 10mM) and MS-275 (1μM, 2μM, 5μM and 10μM) (as described in 2.2.8.1). The level of proteoglycan and collagen release was defined as the percentage loss from the total content of cartilage explants at the start of the assay. Proteoglycan release is shown as at day 7 and collagen release as at day 14, reflecting the time points at which proteoglycan and collagen were maximally released.

Proteoglycan and collagen proteolysis were significantly induced by IL-1α and OSM, causing release of approximately 80-100% of the total cartilage content of both ECM components. TSA and MS-275 significantly decreased cytokine-induced proteoglycan and collagen release in a concentration-dependent manner (Figure 3.6a, b, e and f). The significant reduction of proteoglycan and collagen release by MS-275 treatment indicates that inhibition of class I HDACs (HDAC1, 2 and 3) alone is capable of conferring a chondroprotective affect. VPA significantly reduced cytokine-induced proteoglycan and collagen release, but not in a strictly concentration-dependent manner (Figure 3.6c). Interestingly, I/O-induced collagen release was reduced to a greater level by 0.5mM VPA than 1mM VPA, reflecting the greater repression of induced collagenase expression by 0.5mM VPA in the SW1353 cell monolayer assays. Proteoglycan release demonstrated less sensitivity to HDAC inhibitors than collagen release in the BNC assays, which may be attributed to the rapid kinetics of proteoglycan release.

Lactate dehydrogenase (LDH) release was detected in harvested supernates as a measure of both cytokine and HDAC inhibitor toxicity. LDH release was slightly higher in cytokine-treated samples as previously reported, but was not significant when compared to non-treated controls. HDAC inhibitors did not increase LDH release above cytokine-induced levels at any concentration, and exhibited no concentration-dependent effect on LDH release (data not shown). This indicates that TSA, VPA and MS-275 were not toxic in the assay.

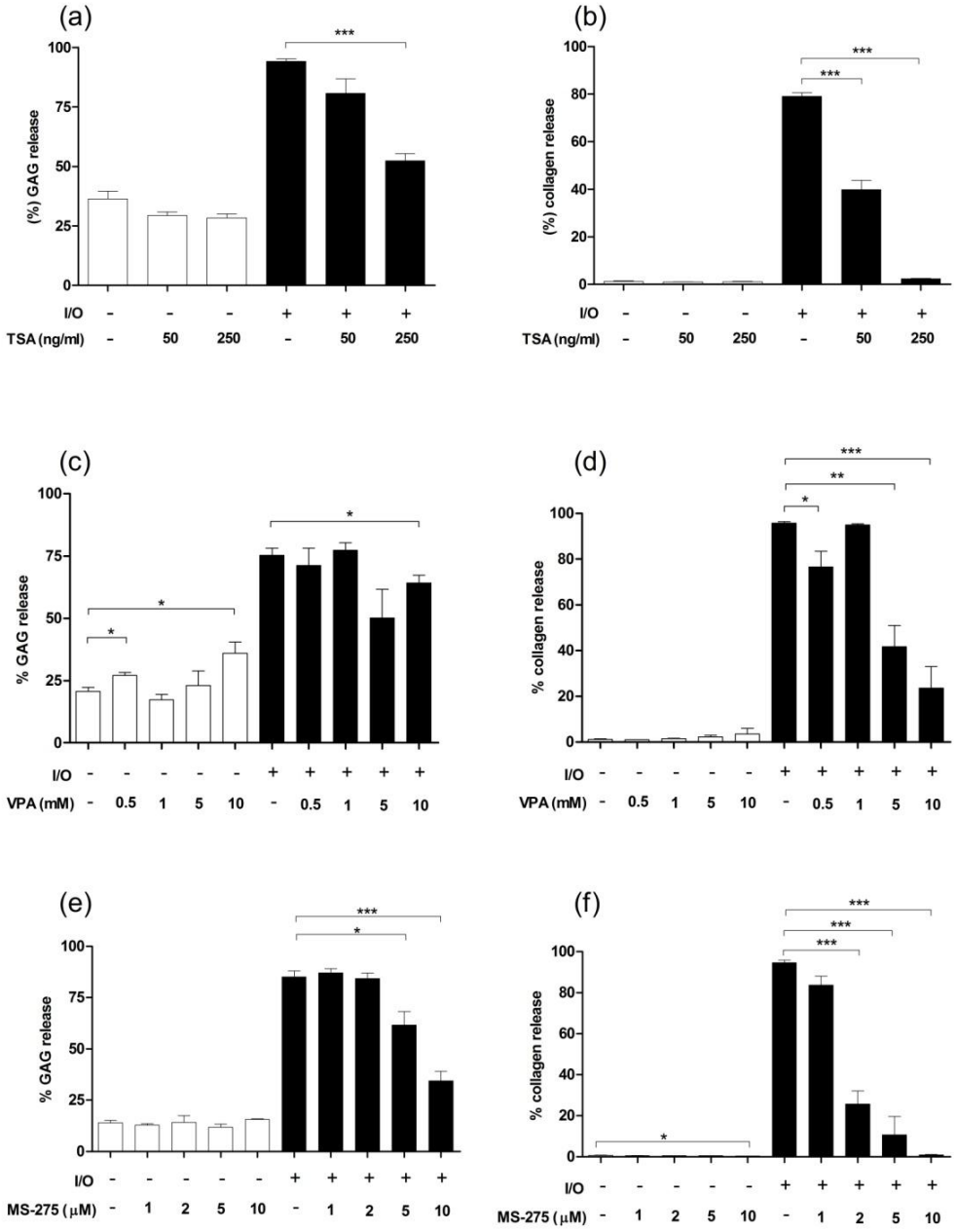

Figure 3.6. HDAC inhibitors prevent cytokine-induced cartilage degradation

Bovine nasal cartilage discs were cultured in the presence or absence of I/O (a combination of IL-1α (0.5ng/ml) and OSM (5ng/ml)) ± a histone deacetylase inhibitor. Cartilage was incubated until day 7, supernates harvested and reagents replaced until day 14. Glycosaminoglycan (GAG) release is shown as at day 7 and was assayed using the dimethylmethylene blue method. Collagen release is shown as at day 14 and was measured using a hydroxyproline assay. **(a)** GAG release in response to I/O and TSA (50ng/ml and 250ng/ml) treatment. **(b)** Collagen release in response to I/O and TSA treatment. **(c)** GAG release in response to I/O and VPA (0.5mM, 1mM, 5mM and 10mM) treatment. **(d)** Collagen release in response to I/O and VPA treatment. **(e)** GAG release in response to I/O and MS-275 (1μM, 2μM, 5μM and 10μM) treatment. **(f)** Collagen release in response to I/O and MS-275 treatment. Assays were performed using quadruplicate samples; means ± standard error are represented. **P*<0.05, ***P*<0.01, ****P*<0.001. GAG and collagen release are depicted as percentage release from total in tissue.

3.2.5 Profile of OA-associated metalloproteinases and TIMP1 in resorbing bovine cartilage

Metalloproteinase expression has previously been profiled during the 14 day BNC assay (Milner et al, 2006). The Milner study revealed the induction of many metalloproteinase genes in I/O-treated cartilage explants, such as *MMP1*, *MMP3*, *MMP13*, *ADAMTS4* and *ADAMTS5*. Milner *et al*. (2006) also demonstrated that activation of pro-MMPs is a key regulatory control point in collagenolysis and cartilage degradation. In order to determine if HDAC inhibitors mediate chondroprotection by the inhibition of cytokine-induced metalloproteinase expression, as postulated by Young *et al* (2005), this profile was repeated with the addition of MS-275. This also enabled us to confirm whether MS-275 could repress cytokine-induced *MMP1* and *MMP13* expression in primary bovine chondrocytes, in order to clarify if the lack of repression observed in SW1353 cells was due to altered HDAC regulation of these genes within the cell line compared to primary cells. Bovine nasal cartilage explants were incubated with IL-1α and OSM in the presence or absence of 5μM MS-275 for 14 days, with treatments replaced at day 3 and 7. Supernates and explants were harvested at day 0, 1, 3, 5, 8, 10 and 14, as described in section 2.2.8.2. Proteoglycan and collagen release were measured in supernates as a measure of cartilage degradation and MS-275 chondroprotection. Total RNA was extracted from cartilage explants and reverse transcribed to cDNA, as described in section 2.2.12 and 2.2.6. *MMP1*, *MMP3*, *MMP13*, *ADAMTS4*, *ADAMTS5* and *TIMP1* expression were detected by qRT-PCR.

Cytokines significantly induced both proteoglycan and collagen release from cartilage explants. Cumulative cytokine-induced proteoglycan release was significantly increased compared to control at day 1 (*P=0.0022*) and remained significantly higher throughout the assay (Figure 3.7a). Maximum GAG release occurred between days 1 and 3, with release reaching a plateau after day 5. This supports the theory that the reduced sensitivity of proteoglycan release to HDAC inhibitors measured in the previous BNC assays was due to the rapid kinetics of proteoglycan release. Therefore, early harvest time-points, such as day 1 to day 3, are required to detect the repression of GAG release mediated by HDAC inhibitors. Cytokine-induced GAG release was significantly reduced by MS-275 at all time points apart from day 14. Cumulative cytokine-induced collagen release was also significant increased at day 1 compared to control (*P=0.0133*) and remained significantly higher throughout the assay (Figure 3.7b). Maximum

collagen release occurred between days 8 and 14. Cumulative induced collagen release was significantly reduced by MS-275 at all time points. The early release of proteoglycan and late release of collagen is consistent with previous studies (Milner et al, 2001; Milner et al, 2006; Young et al, 2005). MS-275 inhibition of both cytokine-induced collagen and proteoglycan release again demonstrates its chondroprotective properties.

MMP1 and *MMP13* expression was significantly increased by IL-1α and OSM when compared to controls. Cytokine-induced *MMP1* expression was significantly increased compared to control at day 1 (*P=0.058*), with significant induction also seen at day 5, 8 and 10 (*P=0.0053, P=0.0006* and *P=0.058* respectively). Cytokine-induced *MMP13* expression was seen at day 1 but did not reach statistical significance. However, I/O-induced *MMP13* expression compared to controls did reach statistical significance at days 5, 8, 10 and 14 (*P=0.0150, P=0.0005, P=0.0022* and *P=0.0002* respectively). The pattern of expression for both collagenases was similar, with the greatest expression observed at day 10, followed by a decline in expression at day 14 (Figure 3.8a and c). The early induction of collagenase expression, coupled with late collagen release, suggests that activation of the synthesised pro-collagenases plays a key regulatory role in cartilage degradation. This is consistent with the profile completed by Milner *et al*. (2006). However, this current profile detected slower kinetics of *MMP1* and *MMP13* induction compared to that seen in the profile conducted by Milner *et al*. (2006). Maximal collagenase expression was not reached until day 10 of this study but achieved at day 2 before reaching a plateau in the Milner profile. The reason for this is unknown.

Despite the contrasting results in the SW1353 and primary chondrocyte assays, MS-275 did decrease cytokine-induced *MMP1* and *MMP13* expression in the BNC assay (Figure 3.8a and c). This supports the theory that transcriptional regulation of *MMP1* and *MMP13* expression may differ in the SW1353 cell line compared to primary chondrocytes, either human or bovine. Interestingly, MS-275 in combination with cytokines initially induced both *MMP1* and *MMP13* expression at day 1 to a greater level than I/O alone, but this did not reach statistical significance. The reason for this is unknown and it would require further assays to determine if this is a true event or an experimental anomaly. However, MS-275 significantly reduced cytokine-induced *MMP1* expression at days 5, 8 and 10, and *MMP13* expression at days 5 and 10. MS-275 repression of key collagenases supports the theory that HDAC inhibitors mediate

chondroprotection through the inhibition of cytokine-induced metalloproteinase expression (Young et al, 2005).

Interestingly, at day 1, *MMP3* expression was rapidly and significantly induced by cytokines in combination with MS-275 (*P=0.0137*), more so than cytokines alone (Figure 3.8b). However, by day 3, I/O-induced expression was markedly reduced by MS-275, which continued until day 10. After the initial rapid cytokine induction of *MMP3* at day 3, there was a small decline in expression at day 5, followed by fairly consistent expression for the remainder of the assay. The rapid induction of *MMP3* between days 1 and day 3 is consistent with the previous BNC profile and chondrocyte monolayer assays (Barksby et al, 2006; Milner et al, 2006). Significant repression of cytokine-induced *MMP3* was achieved with MS-275 at day 5. However, despite MS-275 reducing I/O-induced *MMP3* expression between days 3 and 10, the combination of I/O and MS-275 caused a sudden induction of *MMP3* at day 14. The reason for this is unclear. Therefore, further assays are required to determine if this is a true event or an experimental anomaly.

ADAMTS4 expression, at day 1, was also induced to a greater level by cytokines in combination with MS-275 than cytokines alone (Figure 3.8d). However, from days 3 to 10 I/O-induced expression was markedly repressed by MS-275, with significant repression seen at days 8 and 10. Despite the significant inhibition of I/O-induced *ADAMTS4* expression at day 10, the combination of I/O and MS-275 again induced *ADAMTS4* expression to a greater level than cytokines alone at day 14. Cytokine-induced *ADAMTS4* expression was greatest at day 3, which correlated with the point of maximum GAG release, then declined during the remainder of the assay.

ADAMTS5 expression was significantly induced by IL-1α and OSM compared to control at all time points excluding day 3. MS-275 reduced cytokine-induced *ADAMTS5* at all time points, with significant repression seen at day 1 (Figure 3.8e). The level of I/O-induced *ADAMTS5* expression fluctuated throughout the assay, with two peaks of expression observed at days 3 and 8. The peak in expression observed at day 3 correlated with the point of maximal GAG release.

The rapid increase of *ADAMTS4* and *ADAMTS5* expression between days 0 and 3 is consistent with the profile conducted by Milner *et al*. (2006). However, the profile by Milner *et al*. (2006) showed that after the initial rapid increase in aggrecanase

expression, the expression of aggrecanases reached a plateau and remained at a similar level for the remainder of the assay. This was not seen in this study, with *ADAMTS4* expression exhibiting a steady decrease in expression after day 3 and *ADAMTS5* expression fluctuating throughout the assay. The reason for the different expression patterns of both aggrecanase genes between the profiles is not clear. The assay would have to be repeated to clarify this.

TIMP1 expression was rapidly induced with the combined treatment of cytokines and MS-275, but this was not statistically significant compared to control (Figure 3.8f). However, after this rapid induction, *TIMP1* expression steeply declined, almost back to basal level, and continued to decrease in I/O and MS275-treated explants until day 14. *TIMP1* expression was also induced at day 1 with cytokine treatment alone, but to a lesser degree than the combined treatment of I/O and MS-275. However, I/O induction of *TIMP1* was more sustained, with increased expression compared to control seen from days 1 to 8 and reaching significance at days 5 and 8 (*P=0.0069* and *P=0.0023*). However, I/O-induced expression rapidly decreased between days 8 and 10, returning to near basal levels at day 14. MS-275 significantly repressed I/O-induced *TIMP1* at days 5, 8 and 10. Both control and MS-275-treated samples showed gradual decrease in *TIMP1* expression during the assay. The induction of *TIMP1* expression in response to I/O treatment is consistent with Milner *et al*. (2006), where TIMP1 was the only member of the TIMP family which exhibited induction in response to cytokine treatment. However, after its initial induction, *TIMP1* expression remained at a fairly constant level for the remainder of the assay in the Milner profile. This contrasts with this current profile where I/O-induced expression decreased between day 8 and 10, returning to near basal levels at day 14.

The BNC profile also indicates that certain cytokine-induced genes may be more susceptible to MS-275 repression than others. For example, cytokine-induced *MMP1* expression was significantly repressed by MS-275 and remained low throughout the assay (Figure 3.8a), whereas MS-275 mediated-repression of *MMP13* continued to rise during the assay (Figure 3.8c). MS-275 inhibits HDAC1, HDAC2 and HDAC3, which may mean that genes more susceptible to MS-275 repression may be transcriptionally regulated by these HDACs to a greater extent than less susceptible genes. Further assays would be required to determine if this is true.

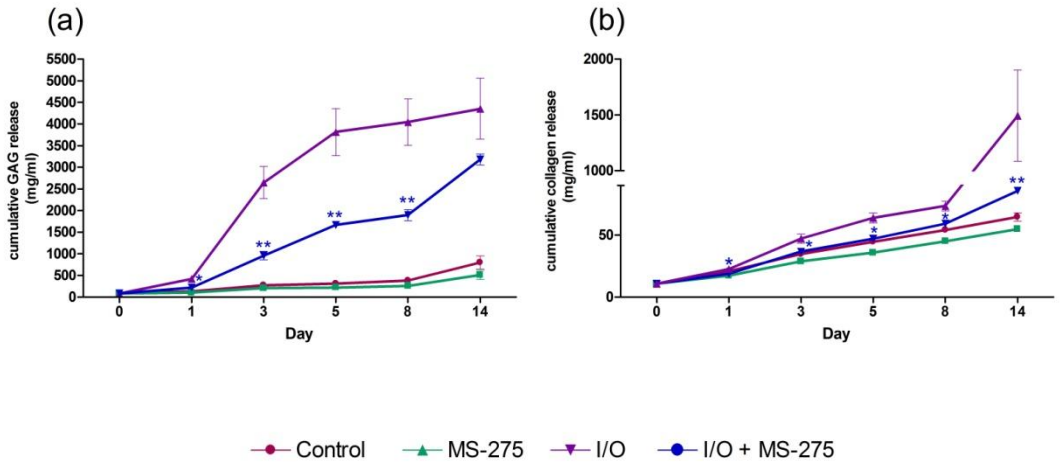

Figure 3.7. Cumulative GAG and collagen release during the BNC assay screen

Bovine nasal cartilage discs were cultured in the presence or absence of I/O (a combination of IL-1α (0.5ng/ml) and OSM (5ng/ml)) ± MS-275 (5μM) for 14 days. At days 3 and 7, medium was removed and the cartilage replenished with identical reagents. Cartilage and medium were harvested at days 0, 1, 3, 5, 8, 10 and 14. GAG and collagen release from explants into harvested supernates were measured via dimethylmethylene blue and hydroxyproline assays respectively. **(a)** Cumulative GAG release in response to I/O treatment alone and in combination with MS-275. **(b)** Cumulative collagen release in response to I/O treatment alone and in combination with MS-275. The assay was performed once using quadruplicate samples; means ± standard error are represented. **P*<0.05, ***P*<0.01, ****P*<0.001 representing the significant reduction of I/O-induced collagen and GAG release with the addition of MS-275.

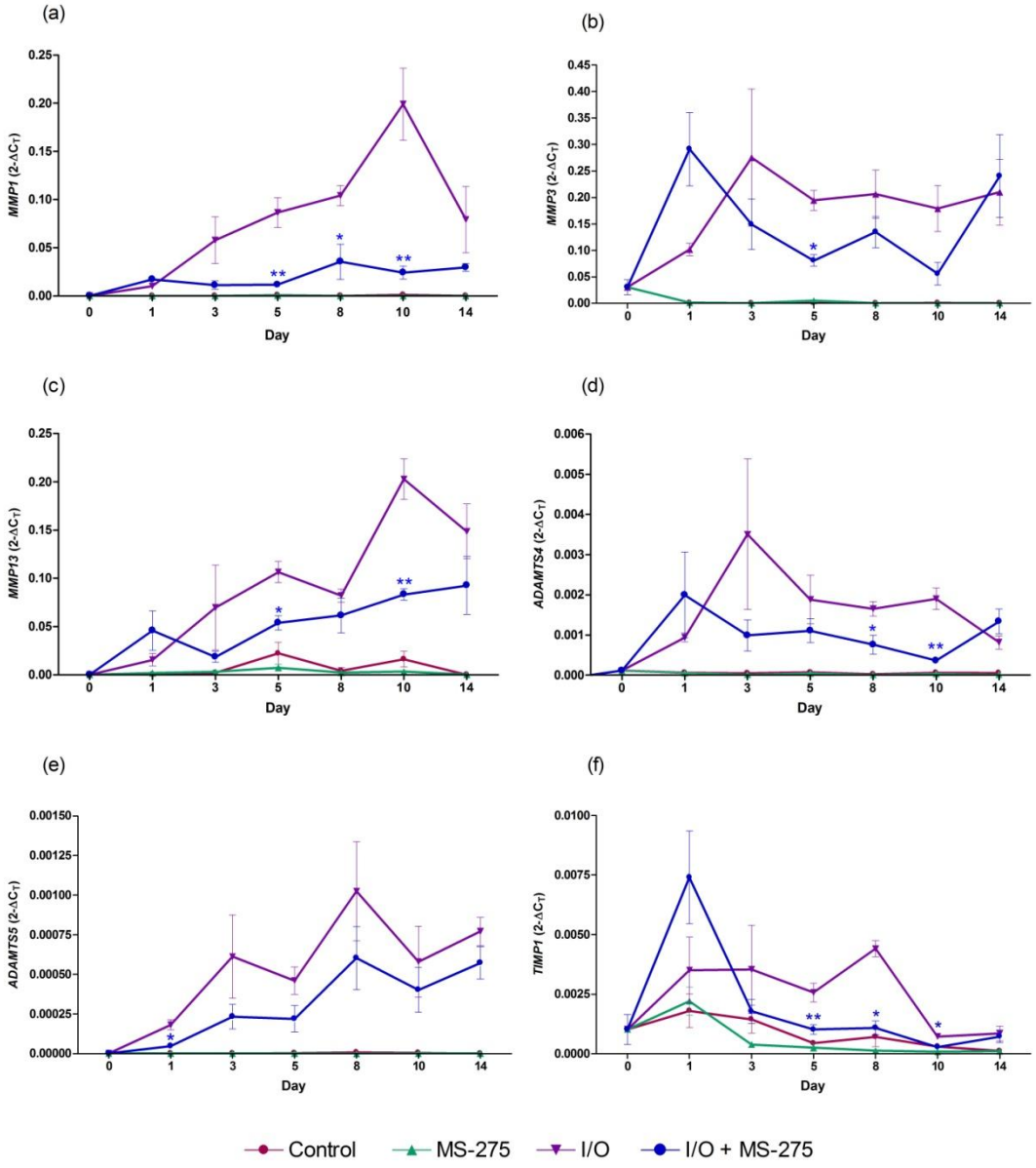

Figure 3.8. Profile of metalloproteinase and *TIMP1* expression in resorbing cartilage explants

Bovine nasal cartilage discs were cultured in the presence or absence of I/O (a combination of IL-1α (0.5ng/ml) and OSM (5ng/ml)) ± MS-275 (5μM) for 14 days. At days 3 and 7, medium was removed and the cartilage replenished with identical reagents. Cartilage and medium were harvested at days 0, 1, 3, 5, 8, 10 and 14. Total RNA was extracted from cartilage (as described in Materials and Methods), reverse transcribed to cDNA, and *MMP* and *TIMP* levels detected by real-time qRT-PCR. Each treatment was completed in quadruplicate; means ± standard errors are represented. **P*<0.05, ***P*<0.01, ****P*<0.001 representing the significant reduction of I/O-induced gene expression by MS-275 treatment.

3.2.6 Tubacin induces cellular α-tubulin acetylation levels

Tubacin has previously been shown to increase cellular α-tubulin acetylation levels via preventing HDAC6-mediated deacetylation (Haggarty et al, 2003). To determine if tubacin affects tubulin acetylation in chondrocytes, SW1353 cells were incubated with increasing concentrations of tubacin (1.25μM, 2.5μM, 5μM, 10μM and 20μM) and the level of acetylated α-tubulin assessed by immunoblotting with specific antibodies. SW1353 cells were also treated with TSA (100ng/ml), previously shown to induce α-tubulin acetylation, as a positive control. The assay was also repeated with niltubacin, an inactive analogue of tubacin, as a negative control (Haggarty et al, 2003). The level of acetylated α-tubulin was compared to total α-tubulin.

Consistent with previous studies, tubacin induced α-tubulin acetylation, thus supporting its role as a HDAC6 inhibitor (Figure 3.9). The level of acetylated α-tubulin increased in a concentration-dependent manner from 1.25μM to 5μM tubacin, but then appeared to decrease at the higher 10μM and 20μM concentrations. This contrasts with previously published data that indicates that tubacin increases acetylated α-tubulin in a concentration-dependent manner (Haggarty et al, 2003; Hideshima et al, 2005). Interestingly, the level of acetylation achieved with 5μM tubacin far exceeded that seen with TSA. This may indicate that tubacin is a more efficient inhibitor of HDAC6 activity than TSA. Niltubacin caused a slight induction of α-tubulin acetylation, but this was far less than that seen with TSA treatment. The level of α-tubulin acetylation remained unchanged in both assays.

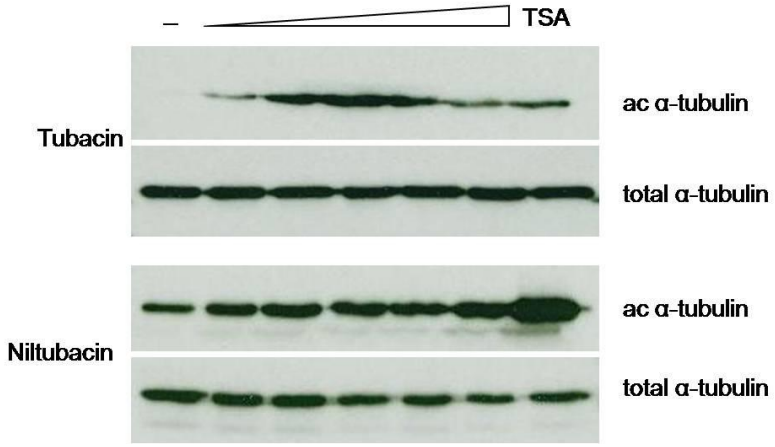

Figure 3.9. The effect of tubacin and niltubacin on α-tubulin acetylation levels in SW1353 cells

SW1353 cells were incubated with increasing concentrations of tubacin and inactive analogue niltubacin (1.25μM, 2.5μM, 5μM, 10μM and 20μM) for 6 hours. TSA (100ng/ml), a known inducer of α-tubulin acetylation, was added as a positive control. Total protein was extracted, resolved by SDS-PAGE, and the acetylation level of α-tubulin assessed by immunoblotting with specific antibodies. The level of α-tubulin acetylation was compared to total α-tubulin.

3.2.7 The effect of tubacin on cytokine-induced collagenase expression in the SW1353 cell line

Pan inhibitors TSA and NaBy, and the more selective inhibitors VPA and MS-275, have been shown to decrease cytokine-induced metalloproteinase expression, both in this study and in the previous study completed by Young *et al*. (2005). To determine whether specific HDAC6 inhibition could decrease cytokine-induced metalloproteinase expression, SW1353 cells were incubated with IL-1α and I/O, in the presence or absence of increasing concentrations of tubacin (1, 2.5, 5, 10 and 20μM). The expression of *MMP1* and *MMP13* were then determined by qRT-PCR. (*This assay was completed by Dr. Rose Davidson, University of East Anglia, UK*).

Both *MMP1* and *MMP13* expression were clearly induced by IL-1α and I/O (Figure 3.10a and b). Tubacin demonstrated a trend of concentration-dependent repression on both IL-1α- and I/O-induced *MMP13* expression, with IL-1α-induced expression significantly repressed by 20μM tubacin (Figure 3.10 b). Tubacin also demonstrated a trend of concentration-dependent repression of IL-1α-induced *MMP1* expression, with induced expression significantly repressed by 10μM tubacin (Figure 3.10 a). Tubacin also appeared to reduce I/O-induced *MMP1* in a concentration-dependent manner between the concentrations of 1 to 5μM, but with a lesser degree of repression observed with 10μM and 20μM tubacin. Therefore, tubacin did not repress cytokine-induced *MMP1* expression as efficiently as cytokine-induced *MMP13* expression. However, the repression of both cytokine-induced collagenases by tubacin indicates that the specific inhibition of HDAC6 activity may be sufficient to repress induced *MMP1* and *MMP13* expression in the SW1353 cell line. Further assays are required to confirm if tubacin can repress cytokine-induced *MMP1* and *MMP13* in primary chondrocytes.

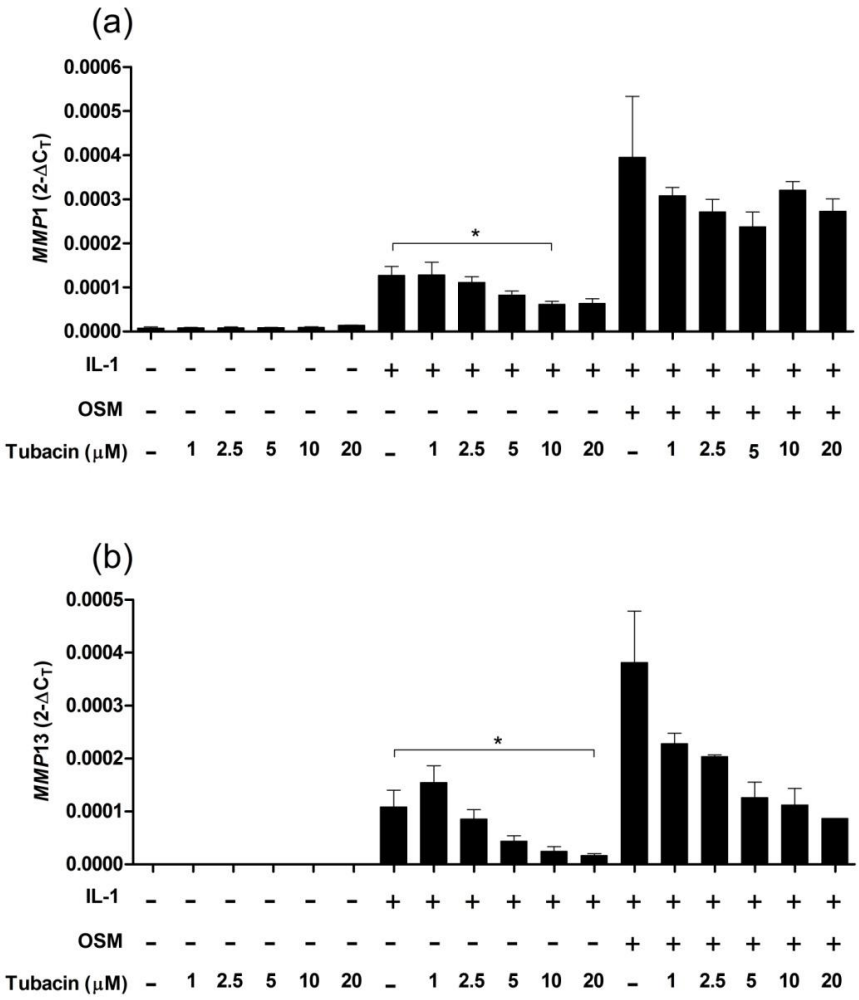

Figure 3.10. The effect of tubacin on cytokine-induced *MMP1* and *MMP13* expression in SW1353 cells

SW1353 cells were incubated with increasing concentrations of tubacin (1μM, 2.5μM, 5μM and 10μM) in combination with IL-1α (5ng/ml) or I/O (combination of IL-1α and OSM (10ng/ml)) for 6 hours. Total RNA was extracted with Cells-to-cDNA lysis buffer, reverse transcribed to cDNA and *MMP* expression determined via real-time qRT-PCR. **(a)** *MMP1* expression in response to cytokine and tubacin treatment. **(b)** *MMP13* expression in response to cytokine and tubacin treatment. The assay was completed once, using triplicate samples; means ± standard errors are represented. **P*<0.05.

3.2.8 Tubacin reduces cytokine-induced cartilage resorption

As tubacin exhibited the ability to repress cytokine-induced collagenase expression in the SW1353 cell line, we postulated that it may also prevent cytokine-induced cartilage degradation. In order to test this hypothesis, BNC explants were incubated with I/O (to stimulate cartilage degradation) in the presence or absence of tubacin/niltubacin (10μM). The level of proteoglycan and collagen release was defined as the percentage loss from the total content of cartilage explants at the start of the assay. Proteoglycan release is shown at day 3 and collagen release at day 14.

Maximal GAG release at day 3 was approximately 18%, with reduced release compared to previous assays likely accountable to the earlier harvest time point (Figure 3.11a). Cytokine-induced GAG release was significantly reduced to approximately 10% by tubacin treatment, with niltubacin exhibiting no significant effect. Maximal collagen release was approximately 30% (Figure 3.11b). Tubacin significantly reduced cytokine-induced collagen release to approximately 2%. Niltubacin also appeared to reduce cytokine-induced collagen release, but not significantly. Importantly, this assay indicates that inhibition of HDAC6 alone is capable of conferring a chondroprotective effect *in vitro*.

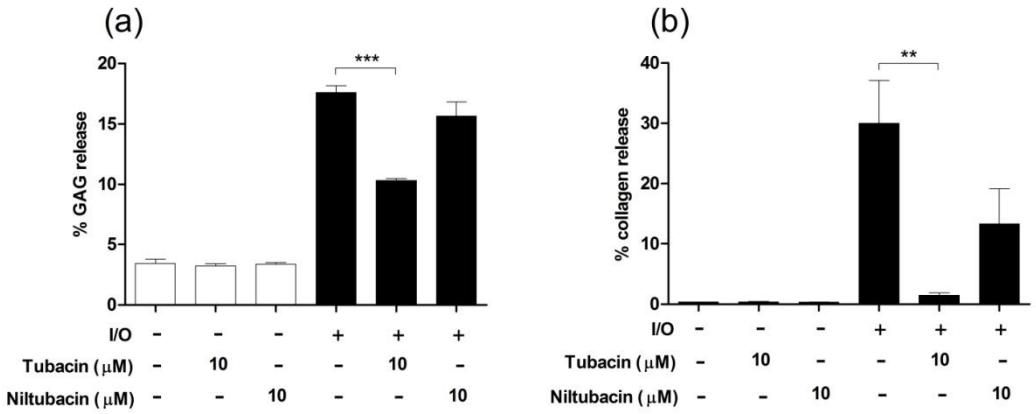

Figure 3.11. Tubacin prevents cytokine-induced cartilage resorption

Bovine nasal cartilage discs were cultured in the presence or absence of I/O (a combination of IL-1α (0.5ng/ml) and OSM (5ng/ml)) and tubacin or niltubacin (10μM). Supernates were harvested at days 3 and day 7, and fresh reagents replaced until day 14. Glycosaminoglycan (GAG) release is shown as at day 3 and was assayed using the dimethylmethylene blue method. Collagen release is shown as at day 14 and was measured using a hydroxyproline assay. **(a)** GAG release in response to I/O treatment alone and in combination with tubacin or niltubacin. **(b)** Collagen release in response to I/O treatment alone and in combination with tubacin or niltubacin. The assay was performed once using quadruplicate samples; means ± standard error are represented. **P*<0.05, ***P*<0.01, ****P*<0.001. GAG and collagen release are depicted as percentage release from the total in tissue at the start of the assay.

3.3 Discussion

HDAC inhibitors have been the subject of much research due to their potential use as cancer therapeutics, and the recent approval of vorinostat (Merck; trade name Zolinza) for the treatment of cutaneous T-cell lymphoma. Inhibitors have been found to induce the differentiation and apoptosis of transformed cells, which is accompanied by an up-regulation of repressed tumour suppressor gene expression. These effects are partially mediated by altering the acetylation status of chromatin and other non-histone proteins. However, the response to HDAC inhibitors seems to be dependent on cell type, the specific compound and experimental conditions (Balasubramanian et al, 2009).

Conceptually, HDAC inhibitors increase the acetylation status of chromatin and other non-histone proteins, resulting in increased gene transcription. However, microarray analysis has found that only 2-9% of the genome is regulated by HDAC inhibitors, with the expression of an equal number of genes suppressed as those activated (Glaser et al, 2003; LaBonte et al, 2009). An example of inhibitor-mediated gene repression is that of cytokine-induced metalloproteinase expression at the mRNA and protein level by broad spectrum inhibitors TSA and NaBy (Young et al, 2005). The data previously published by our laboratory also demonstrated that these compounds prevented cytokine-induced cartilage resorption in the BNC model. Young *et al*. (2005) noted that HDAC inhibitors do not directly inhibit collagenase activity, indicating that inhibitors likely alter metalloproteinase gene expression to mediate repression and induce their chondroprotective effect (Young et al, 2005).

The chondroprotective effect exhibited by HDAC inhibitors in the BNC assay indicates that they may have a potential use in the treatment of osteoarthritis. This is also supported by the reduced joint damage observed in inflammatory, and recently, osteoarthritic animal models as a result of HDAC inhibitor treatment (Chen et al, 2010; Chung et al, 2003; Keiichiro et al, 2004; Lin et al, 2007). The reduced joint damage in inflammatory animal models, mediated by inhibitors such as TSA and MS-275, was associated with reduced cytokine expression and increased expression of cell cycle regulators $p16^{INK4a}$ and $p21^{WAF/Cip1}$ (Chung et al, 2003; Keiichiro et al, 2004; Lin et al, 2007). However, most recently a rabbit model of OA has demonstrated that intra-articular injection of TSA reduced cartilage damage and suppressed the increased *MMP1*, *MMP3*, *MMP13* and IL-1 expression observed in the OA rabbit controls (Chen et al, 2010). This once again demonstrates that inhibitors partially mediate their

chondroprotective effect by the repression of cytokine-induced metalloproteinase expression, and importantly that they are capable of doing this in an *in vivo* setting.

Despite the abundance of data now demonstrating that these compounds are capable of repressing cytokine-induced metalloproteinase expression and conferring a chondroprotective effect, it is still unclear which histone deacetylases play a role in this process. The majority of arthritis-based research in regard to HDAC inhibitors has been conducted using 'pan' inhibitors such as TSA and NaBy, making it difficult to pinpoint if the inhibition of a specific HDAC or a group of HDACs mediates this chondroprotective effect. In order to determine which HDACs may be implicated, this current study selected inhibitors VPA, MS-275 and tubacin, which display variable degrees of selectivity towards members of the classical HDAC family, for use alongside the inhibitor TSA in both cell monolayer and BNC assays. The IC_{50} (median inhibitory concentration) value of each inhibitor is variable and dependent on cell type and HDAC isoform. TSA reportedly has an IC_{50} value of 50ng/ml (Furumai et al, 2001). VPA reportedly inhibits class I HDACs more efficiently than class II HDACs, with an IC_{50} value of 0.7mM-1mM for class I HDACs and >1mM for class II HDACs (HDAC4,5 and 7) (Gurvich et al, 2004). The inhibitory profile of VPA differs between publications, with HDAC6 inhibition detected in a study conducted by Gottlicher *et al*. (2001) (IC_{50} 2.4mM), which was not observed in a later publication by Gurvich *et al*. (2004). VPA also exhibits no inhibition towards HDAC10 (Gurvich et al, 2004). MS-275 is known as a class I selective inhibitor, preferentially inhibiting HDAC1 and HDAC2, with an IC_{50} value of 0.3µM-2.5µM, compared to HDAC3 with an IC_{50} value of 8µM. MS-275 does not inhibit HDAC8 (IC_{50} > 100µM) (Hu et al, 2003; Inoue et al, 2006). The IC_{50} value of tubacin-mediated HDAC6 inhibition has not been reported. However, the EC_{50} value (mean inhibitory concentration) for induced α-tubulin acetylation is reportedly 2.5µM (Haggarty et al, 2003), which reflects the level of HDAC6 inhibition. Inhibitor concentration ranges used in this current study were selected based on these reports.

The SW1353 chondrosarcoma cell line was used as a model to establish the effect of HDAC inhibitors on histone and α-tubulin acetylation. TSA, VPA and MS-275 induced concentration-dependent acetylation of both histone 3 and histone 4 in the SW1353 cell line. The induction of histone acetylation by all three compounds is consistent with previous *in vitro* and *in vivo* studies (Camphausen et al, 2004; Chung et al, 2003;

Gurvich et al, 2004; Hoshikawa et al, 1994; Hu et al, 2003; Saouaf et al, 2009). The effect of tubacin on histone acetylation was not tested. However, previous studies have indicated that tubacin has no effect on histone acetylation levels (Haggarty et al, 2003). This suggests that histones are not the primary substrate of HDAC6, which is also supported by HDAC6 knockout studies where no significant change in the level of histone acetylation was observed (Zhang et al, 2008; Zhang et al, 2003). This is not surprising as HDAC6 has been found to be primarily localised in the cytoplasm (Verdel et al, 2000). TSA and tubacin were the only inhibitors found to increase α-tubulin acetylation, confirming that they are the only inhibitors capable of repressing HDAC6 activity in the SW1353 cell line. TSA increased α-tubulin acetylation in a concentration-dependent manner, which is consistent with previous studies and its status as a broad spectrum inhibitor (Koeller et al, 2003). Tubacin did not increase α-tubulin acetylation in a concentration-dependent manner, with the largest increase of acetylation observed with 5μM followed by a reduction in acetylation at 10μM and 20μM. Previous studies have indicated that tubacin increases α-tubulin acetylation in a concentration-dependent manner (Haggarty et al, 2003; Hideshima et al, 2005). However, these studies were carried out in different cell lines (A549 and multiple myeloma human cell lines), which may indicate that tubacin's mode of action varies in the SW1353 cell line. VPA's inability to induce α-tubulin acetylation confirms that it does not inhibit HDAC6 activity, supporting the data of Gurvich *et al*. (2004). As expected, MS-275 did not induce tubulin acetylation which supports its status as a class I HDAC inhibitor.

The expression of *MMP1*, *MMP2*, *MMP3*, *MMP9*, *MMP10*, *MMP13*, *MMP28*, *ADAMTS4* and *ADAMTS5* were detected in the SW1353 cell line after incubation with cytokines and HDAC inhibitors. Of the genes detected, *MMP1*, *MMP3*, *MMP10* and *MMP13* were significantly induced by IL-1α and OSM, consistent with previous studies (Koshy et al, 2002; Rowan et al, 2003; Young et al, 2005). TSA significantly repressed all cytokine-induced genes in a concentration-dependent manner, consistent with data previously published by our laboratory and with the repression observed in an OA rabbit model (Chen et al, 2010; Young et al, 2005). VPA also successfully repressed all cytokine-induced genes. VPA decreased I/O-induced gene expression and IL-1α-induced *MMP3* and *MMP10* in a concentration-dependent manner. However, IL-1α-induced *MMP1* and *MMP13* expression was not reduced in a concentration-dependent manner, with a greater repression observed with 0.5mM than 1mM VPA. The reason for

this is unclear but could be related to the concentration-dependent class switch of inhibition from class I to both class I and II HDACs reported for VPA (Gurvich et al, 2004). VPA at 10mM achieved the greatest repression of all induced genes, reducing gene expression almost back to basal level. At this concentration it would be expected that both class I (HDAC1, 2 and 3) and class II HDACs (HDAC4, 5 and 7) would be repressed, suggesting that maximal repression of cytokine-induced genes by VPA is achieved with inhibition of members from both classes of classical HDACs in SW1353 cells. This study demonstrated that VPA does not inhibit HDAC6 in SW1353 cells, and it has previously been shown not to inhibit HDAC10 in 293T cells (Gurvich et al, 2004). This suggests that neither HDAC6 nor HDAC10 inhibition is essential to repress *MMP1*, *MMP3*, *MMP10* and *MMP13* expression in SW1353 cells. The inhibitory profiles published for VPA are yet to establish if the compound inhibits the activity of HDAC8, HDAC9 and HDAC11 (Gottlicher et al, 2001; Gurvich et al, 2004). Surprisingly, MS-275 did not repress cytokine-induced *MMP1*, *MMP10* and *MMP13* expression in the SW1353 cell line. This initially suggested that class I HDACs (HDAC1, 2 and 3) may not regulate collagenase or stromelysin-2 (*MMP10*) expression.

TSA, VPA and MS-275 all suppressed cytokine-induced *MMP3* expression in SW1353 cells, suggesting that HDAC inhibitors may mediate their chondroprotective effect through the regulation of this protease. Activation of pro-metalloproteinases, in particular pro-collagenases, is known to be a key regulatory step in ECM turnover and cartilage collagenolysis (Milner et al, 2001; Milner et al, 2006). MMP-3 is a known activator of all pro-collagenases (Knauper et al, 1996a; Knauper et al, 1993; Murphy et al, 1987). Therefore, inhibitor-mediated repression of *MMP3* expression could result in decreased MMP-3 protein and thus reduce subsequent activation of pro-collagenases.

TSA, VPA and MS-275 also reduced basal expression of *MMP2* in the SW1353 cell line. MMP-2 has wide substrate specificity against cartilage matrix constituents (including collagen) and is known as potent activator of pro-MMP-13 (Aimes & Quigley, 1995; Knauper et al, 1996b; Murphy et al, 2002). Increased *MMP2* has also been consistently detected in OA cartilage (Davidson et al, 2006; Kevorkian et al, 2004; Swingler et al, 2009). Therefore, the repression of *MMP2* expression demonstrates another mode by which inhibitors may mediate their chondroprotective effect.

TSA, VPA and MS-275 all induced basal *MMP28* expression in SW1353 cells. This is consistent with previous published data, where the inhibitors TSA, NaBy and VPA have been shown to induce *MMP28* expression in various cell lines (Swingler et al, 2010; Young et al, 2005). Data recently published by our laboratory shows that TSA induces the acetylation of transcription factor Sp1, which results in a Sp1 protein-complex binding to a promoter proximal GT-box causing increased *MMP28* expression. Consistent with previous data implicating HDAC1 in Sp1-mediated gene repression, luciferase assays also showed that siRNA knockdown of HDAC1 expression leads to increased *MMP28* promoter activity (Swingler et al, 2010). This demonstrates a direct link between HDAC1 and metalloproteinase expression. Significantly increased *MMP28* expression has consistently been detected in OA cartilage and synovium (Davidson et al, 2006; Kevorkian et al, 2004; Swingler et al, 2009). However, the role of *MMP28* in the context of OA is unclear, and its specific biological substrates remain unknown (Rodgers et al, 2009). The differential effects of HDAC inhibitors across the metalloproteinase family confirm that the compounds are not mediating responses through non-specific toxicity.

The effect of TSA, VPA and MS-275 on cytokine-induced *MMP13* expression was determined in primary articular chondrocytes. TSA and VPA significantly repressed I/O-induced *MMP13* expression, consistent with the repression observed in SW1353 cells. However, in contrast to the lack of repression observed in the SW1353 cell line, MS-275 significantly repressed I/O-induced *MMP13* expression in primary chondrocytes. This suggests that class I HDAC regulation (HDAC1, 2 and 3) of *MMP13* expression in the SW1353 cells varies from that within primary chondrocytes. Exploring the difference in HDAC regulation of *MMP13* expression between SW1353 cells and primary chondrocytes could further elucidate the role of HDACs in metalloproteinase regulation. The difference observed between the two cell types may be because SW1353 cells are derived from a chondrosarcoma, and HDACs are known to be aberrantly expressed or recruited to repressive complexes in various cancer types (Lucio-Eterovic et al, 2008; Wu et al, 2001). Previous screening of HDAC expression in the SW1353 cell line, by quantitative real-time PCR, detected the expression of all classical HDACs (data not shown).

Due to the repression of cytokine-induced *MMP13* expression in primary chondrocytes, we postulated that VPA and MS-275 could prevent cytokine-induced cartilage

degradation in the BNC model. TSA, VPA and MS-275 all significantly repressed cytokine-induced cartilage degradation. The concentration-dependent repression of both GAG and collagen release seen with TSA is consistent with the previous study conducted by Young *et al*. (2005). The concentration-dependent repression of both GAG and collagen release observed with MS-275 demonstrates that the inhibition of class I HDACs (not including HDAC8) alone is enough to confer a chondroprotective effect. Although VPA significantly repressed both collagen and GAG release, it was the least effective of the inhibitors tested. This may be because VPA does not target the HDACs required to repress the expression of cartilage degrading metalloproteinases or it may be that VPA is not as stable in culture as the other inhibitors. The need for an early harvest time-point to measure GAG release, such as day 3, is supported by the detection of maximal GAG release between days 1 and 3 of the BNC profile conducted in this thesis. Therefore, these assays need to be repeated with early harvest time-points to determine how efficient these compounds are at repressing cytokine-induced proteoglycan release. The chondroprotective effect of TSA, VPA and MS-275 are also consistent with the reduced cartilage damage observed in arthritis animal models after TSA, MS-275 and VPA treatment (Chen et al, 2010; Chung et al, 2003; Keiichiro et al, 2004; Lin et al, 2007; Saouaf et al, 2009).

The BNC model provides a useful assay system for studying chondrocytes encapsulated within their native environment and the mechanisms of cartilage degradation. Metalloproteinase and inhibitor expression has previously been profiled during the BNC assay (Milner et al, 2006). The profile of metalloproteinase expression conducted by this thesis identified the cytokine-induction of a number of metalloproteinase genes, and that activation of pro-collagenases is a key regulatory point in actively resorbing cartilage. This is consistent with the previous screen of metalloproteinase expression in resorbing bovine cartilage conducted by Milner *et al*. (2006).

The Milner profile indicated that ADAMTS-5 was the primary aggrecanase, and that MMP-1 and/or MMP-13 were the primary collagenases in the BNC model. In order to determine if HDAC inhibitor-mediated chondroprotection in the BNC model was due to repression of cytokine-induced metalloproteinase expression, and whether class I HDAC regulation of collagenases is different between SW1353 and primary chondrocyte cells, this thesis repeated the Milner profile in the presence of MS-275. Due to the importance of aggrecanases and collagenases in the previous BNC profile

and their known roles in cartilage ECM turnover, we chose to measure *MMP1*, *MMP13*, *ADAMTS4* and *ADAMTS5* expression, along with the known pro-collagenase activator *MMP3* and metalloproteinase endogenous inhibitor *TIMP*, by qRT-PCR. As expected, cytokines IL-1α and OSM synergistically induced proteoglycan and collagen release from explants. Cytokines also significantly induced the expression of all genes detected, consistent with the induction seen in the previous BNC profile and chondrocyte monolayer assays (Barksby et al, 2006; Koshy et al, 2002; Milner et al, 2006; Young et al, 2005). However, as stated previously, the kinetics of the induction of *MMP1* and *MMP13* was slower in this current profile than in that of Milner *et al*. (2006), with maximum expression reached at day 10 of this study as opposed to day 2 of the Milner profile. The expression patterns of *ADAMTS4* and *ADAMTS5* also varied between the two profiles. In the study completed by Milner *et al*. (2006), *ADAMTS4* and *ADAMTS5* expression increased rapidly between days 0 and 2 then reached a plateau. However, in the profile completed by this study, after the rapid cytokine-induction of aggrecanase expression between days 0 and 3, *ADAMTS4* expression steadily decreased and *ADAMTS5* expression fluctuated throughout the remainder of the assay. The reason for the different kinetics of collagenase gene induction and the expression patterns of both aggrecanase genes between the profiles is not clear. In order to clarify this, the assay would have to be repeated.

Proteoglycan release was maximal between days 1 and 5, which correlated with peaks in I/O-induced *ADAMTS4* and *ADAMTS5* expression observed at day 3. However, *ADAMTS5* I/O-induced expression also increased again at day 8. Maximal cytokine-induced collagen release occurred between days 8 and 14. The late release of collagen is consistent with previous BNC assays, with substantial collagen release rarely occurring before day 10 (Milner et al, 2001; Milner et al, 2006; Young et al, 2005). Maximal collagen release correlated with maximal I/O-induced *MMP1* and *MMP13* expression at day 10. However, cytokine-induced collagenase expression was seen as early as day 1, with no substantial increase in collagen release. This suggests that the activation of pro-collagenases is a key regulatory point in cartilage resorption. This is supported by the previous profile which detected pro-collagenases in the medium at day 5, but did not see active collagenases and collagenolysis until day 10 of culture (Milner et al, 2006). Both cytokine-induced proteoglycan and collagen release was significantly repressed by MS-

275. This again exhibits the chondroprotective property of MS-275, and that inhibition of HDAC1, 2 and 3 catalytic activity is sufficient to confer this effect.

MS-275 substantially repressed cytokine-induced collagenase and aggrecanase expression in bovine explants, achieving significant repression at various time points. This demonstrates that inhibitors likely prevent cytokine-induced cartilage degradation through the inhibition of metalloproteinase expression, particularly the collagenases and aggrecanases. MS-275 repression of cytokine-induced collagenase expression in the BNC model supports the repression of *MMP13* seen in monolayers of primary chondrocytes. This substantiates the theory that class I HDAC regulation of *MMP13* expression varies in the SW1353 cell line in comparison to primary chondrocytes. It also demonstrates that cytokine induction of collagenases and the repression of induced collagenases by MS-275 is the same in primary chondrocytes whether in monolayer or embedded within the ECM.

MMP3 expression was rapidly and robustly induced by cytokine treatment, with expression remaining consistently high compared to control during the BNC assay. MS-275 successfully inhibited cytokine-induced *MMP3* expression between days 3 and 10, consistent with the repression seen with all inhibitors in the SW1353 cell line. This suggests that inhibitors may block cartilage degradation through *MMP3* repression and prevention of subsequent pro-collagenase activation. It has previously been demonstrated that endogenous addition of MMP-3 to BNC cartilage can mediate pro-collagenase activation and induce collagenolysis (Milner et al, 2001).

Cytokine treatment also increased *TIMP1* expression, with significant induction compared to control seen at days 5 and 8. This is consistent with the previous BNC profile and with previous chondrocyte monolayer assays (Milner et al, 2006; Rowan et al, 2003). MS-275 significantly repressed induced *TIMP1* expression from days 5 to 10. Therefore, it is important to note that HDAC inhibitors can result in the reduced expression of endogenous metalloproteinase inhibitors. Overall, there was a gradual decrease in *TIMP1* observed during the assay, which may represent the anabolic to catabolic shift in gene expression thought to occur in the OA joint.

However, it is also important to note that at day 1 of the BNC assay, the cytokine induction of all genes, except *ADAMTS5*, was further potentiated when combined with MS-275. The reason for this is unclear, and contrasts with the inhibition of these genes

observed at 6 hours in SW1353 and primary chondrocyte monolayer experiments. The profile would have to be repeated to clarify the reason for these experimental anomalies.

Possibly the most interesting data was produced with HDAC6-specific inhibitor tubacin, which repressed cytokine-induced *MMP1* and *MMP13* expression in SW1353 cells (data provided by Dr. Rose Davidson, University of East Anglia, UK). Significant repression of IL-1α-induced *MMP1* expression was seen with 10μM tubacin, and *MMP13* with 20μM tubacin (although the level of significance was small). I/O-induced collagenase expression was not significantly repressed, but there was a clear concentration-dependent trend toward reduced expression of both genes. The data indicates that HDAC6 inhibition alone is capable of repressing cytokine-induced collagenase expression. Interestingly, the tubacin-mediated repression of cytokine-induced *MMP13* expression was more efficient than the repression of induced *MMP1* expression. This may suggest that HDAC6 plays a greater role in the regulation of *MMP13* expression than *MMP1* expression. The effect of this compound on cytokine-induced metalloproteinase expression is yet to be established in primary chondrocyte monolayer assays.

The repression of cytokine-induced *MMP1* and *MMP13* led us to postulate that tubacin may be capable of preventing cytokine-induced cartilage resorption. This was confirmed in the BNC assay, where tubacin significantly reduced cytokine-induced collagen and proteoglycan release. Both GAG and collagen release were significantly induced by cytokines compared to control, but did not reach the 80-100% level achieved in the previous BNC assays. GAG release was assayed at day 3, rather than the day 7 time-point used in previous assays, in order to increase the sensitivity of proteoglycan release to inhibitor treatment. Therefore, the reduced total percentage GAG release is likely accountable to the earlier harvest time-point. The reason for the reduced collagen release compared to previous assays is unclear, but collagen and GAG release are sometimes variable between different bovine nasal septa. Despite an overall reduction in GAG release, tubacin treatment still significantly reduced release from approximately 18% to 10%. Niltubacin, the inactive analogue of tubacin, had no inhibitory effect on cytokine-induced GAG release, demonstrating that tubacin is likely acting specifically. Cytokine-induced collagen release was reduced from 30% to 2% by tubacin treatment. Niltubacin also appeared to reduce collagen release but this did not reach statistical

significance. Therefore, this indicates that HDAC6 inhibition alone is capable of preventing cytokine-induced cartilage resorption.

Pro-inflammatory cytokine IL-1 is known to signal via nuclear factor κβ (NFκβ), resulting in metalloproteinase expression (Yan & Boyd, 2007). It has therefore been postulated that HDAC inhibitors may repress metalloproteinase expression by suppressing the NFκβ signalling pathway, but data surrounding this question are conflicting. For example, some previously published data and luciferase assays conducted in the laboratory of Dr. David Young (Newcastle University, UK) suggest that TSA potentiates signalling via this pathway, rather than repressing it (Ashburner et al, 2001; Chen et al, 2001; Young et al, 2005). Conversely, other data suggest that TSA and SAHA inhibitors can inhibit the DNA-binding ability of NFκβ in both A549 and human colon cell lines, resulting in gene repression (Imre et al, 2006; Yin et al, 2001). However, Chabane *et al*. (2008) demonstrated that TSA and BA did not affect the DNA-binding activity of NFκβ in IL-1-stimulated human chondrocytes (Chabane et al, 2008). In this instance, further research is required to elucidate the effect of HDAC inhibitors on NFκβ signalling. Conversely, IL-6 family cytokine OSM is known to signal through the JAK-STAT (Janus kinase-signal transducer and activator of transcription) pathway, which has been shown to induce metalloproteinase expression (Heinrich et al, 1998; Korzus et al, 1997). Catterall *et al*. (2001) demonstrated that STAT3 signalling indirectly mediates the ability of IL-1/OSM to induce *MMP1* gene expression in immortalised human chondrocyte cell line T/C28a4 cells (Catterall et al, 2001). Importantly, class I HDACs HDAC1, HDAC2 and HDAC3 have also been shown to play an essential role in STAT1-dependent transcription, and that HDAC inhibitors can therefore abrogate STAT1-induced gene expression (Klampfer et al, 2003; Klampfer et al, 2004). Therefore, HDAC inhibitors may also mediate their effects on metalloproteinase expression via the JAK/STAT pathway. It is also postulated that the anti-inflammatory properties of HDAC inhibitors and their ability to reduce cytokine expression may contribute to chondroprotection (Chen et al, 2010; Leoni et al, 2005). Therefore further studies are required to further elucidate the links between these cytokine-induced signalling pathways and HDAC inhibitor-mediated chondroprotection.

This study supports data previously published by our laboratory showing that the broad spectrum HDAC inhibitor TSA represses cytokine-induced metalloproteinase

expression in monolayer SW1353 and primary chondrocyte cells, as well as preventing cytokine-induced cartilage resorption in the BNC model. However, further to this it has demonstrated that HDAC inhibitors which block the catalytic activity of a specific class or member of the classical HDAC family are capable of repressing cytokine-induced metalloproteinase expression, both in monolayer cell assays and in the BNC assay. Interestingly, MS-275, which is class I specific (not including HDAC8), and HDAC6 specific tubacin demonstrated repression of induced metalloproteinase expression and exhibited a chondroprotective effect. This demonstrates that members of both the class I and class II HDAC family are involved in the regulation of metalloproteinase expression in cartilage, and subsequently in the regulation of cartilage homeostasis. VPA successfully inhibited both induced metalloproteinase expression and cartilage degradation, but a high concentration that potentially inhibited most members of the class I and II HDAC family was required to cause maximal inhibition. This suggests that VPA may not be the most effective inhibitor for potential OA therapy. However, VPA has previously been shown to be well tolerated in the treatment of human disorders such as epilepsy (Bialer & Yagen, 2007; Gottlicher et al, 2001; Nissinen & Pitkanen, 2007; Phiel et al, 2001), which may mean that the higher concentrations required for chondroprotection could also be well tolerated.

Due to the chondroprotective property of tubacin in the BNC model, the development of HDAC6 inhibitors for the treatment of OA looks particularly attractive. Furthermore, the therapeutic potential of a HDAC6 inhibitor is supported by the lack of major phenotype in the HDAC6 knockout mouse (Zhang et al, 2008). Zhang and colleagues demonstrated that HDAC6 is dispensable for normal development and that tubulin hyperacetylation, as a result of genetic HDAC6 inactivation or following treatment with HDAC inhibitors, has only minor effects on mice kept under standard laboratory conditions. This suggests that pharmacological inhibition of this enzyme may only have few side effects, but this was completed in a non-pathological setting. Interestingly, despite the lack of phenotype from HDAC6 deletion, the over-expression of HDAC6 has been linked with human X-linked chondrodysplasia (Simon et al, 2010). The over-expression of HDAC6 in these patients was attributed to an A to T SNP in the 3'UTR of HDAC6, which also lies in the seed sequence of microRNA-433 (hsa-miR-433). Simon *et al*. (2010) demonstrated that miR-433 down-regulates the expression of endogenous HDAC6 and that of an eGFP-reporter mRNA bearing the wild-type 3'UTR of HDAC6,

but that this effect is totally abolished when the reporter mRNA encodes the mutated HDAC6 3'UTR. Therefore, the mutation led to an accumulation of HDAC6 mRNA and protein in MG63 osteosarcoma cells, which mirrors the increased level of HDAC6 expression seen in the X-linked chondrodysplasia patients. It is thought that the increased level of HDAC6 expression contributes to the chondrodysplasia phenotype in humans through its interaction and inhibition of RUNX2 transcription factor, which is known to be essential for osteoblast differentiation (Simon et al, 2010). A mouse over expressing HDAC6 is yet to be described.

It has been shown recently that intra-articular injection of broad spectrum inhibitor TSA is capable of repressing induced metalloproteinase expression in the cartilage of an OA rabbit model (Chen et al, 2010). This importantly indicates that HDAC inhibitors are capable of repressing induced metalloproteinase expression within cartilage in an *in vivo* and pathological setting, further demonstrating the potential use of these compounds in the future treatment of OA. However, if a HDAC6 inhibitor was to be developed the broad-spectrum of HDAC6 substrates and its cellular roles must be taken into account. For example, HDAC6 is known to bind ubiquitinated, misfolded proteins and facilitate their accumulation into an aggresome (Kawaguchi et al, 2003). It has also established a role as 'stress sensor' through its induction of heat-shock proteins and contribution to the formation of cytoplasmic stress-granules (Boyault et al, 2007; Kovacs et al, 2005; Kwon et al, 2007). Therefore, HDAC6 inhibition in a pathological setting may lead to greater side-effects.

HDAC6 is a unique classical HDAC in that it has two catalytic HDAC domains, both of which are required for deacetylase activity, and a C-terminal zinc finger domain that binds ubiquitin (Seigneurin-Berny et al, 2001; Zhang et al, 2006; Zhang et al, 2003). It is also unique in that it has not been found in any known classical HDAC-containing repressive complexes, suggesting that it may be functionally distinct from other HDACs. It is interesting that its inhibition alone can mediate repression of cytokine-induced metalloproteinase expression and chondroprotection, since it is primarily localised to the cytoplasm. However, a fraction of HDAC6 has been shown to shuttle between the cytoplasm and nucleus in response to certain signalling pathways (Verdel et al, 2000). For example, a fraction of HDAC6 has been shown to translocate to the nucleus in response to proliferation arrest (Verdel et al, 2000). HDAC6 nuclear export is regulated by interaction between an N-terminally located nuclear export signal (NES1)

and CRM1/exportin1 proteins, with other uncharacterised mechanisms perhaps also contributing to this process (Kaffman & O'Shea, 1999; Verdel et al, 2000). It is also suggested that post-translational modifications of amino acids surrounding the NES1 motif of HDAC6, and/or interaction of yet unknown binding proteins to this region, might play a role in masking the NES1. This would therefore promote HDAC6 accumulation in the nucleus (Kaffman & O'Shea, 1999; Verdel et al, 2000). HDAC6 knockout in both embryonic stem cells and a murine model has indicated that α-tubulin is the main physiological substrate of HDAC6, with no significant change in histone acetylation levels observed (Zhang et al, 2008; Zhang et al, 2003). However, Zhang and colleagues have shown that purified HDAC6 can deacetylate histones *in vitro*, suggesting that HDAC6 may control gene transcription by deacetylating histones and potentially other nuclear proteins in some select cases (Zhang et al, 2006). Consistent with this, Zhang and colleagues stated that unpublished data from transient transfection assays identified that artificial recruitment of HDAC6 to promoter DNA repressed the transcription of reporter plasmids. This suggests that the presence of HDAC6 in the nucleus could impact on gene expression (Zhang et al, 2003). Whether the cellular localisation of HDAC6 impacts on its regulation of metalloproteinase expression is yet to be established, as is whether or not HDAC inhibitors or pro-inflammatory cytokines trigger the signalling pathways that influence its sub-cellular localisation. Therefore, the way in which HDAC6 mediates its chondroprotective effect will need to be the subject of further research.

In conclusion, this chapter shows that inhibition of class I HDACs (HDAC1, HDAC2 and HDAC3) by MS-275, and separately the inhibition of HDAC6 by tubacin, can repress cytokine-induced metalloproteinase expression and subsequently prevent cartilage degradation. Previously published data has also implicated specific HDACs in the transcriptional regulation of members of the matrix metalloproteinase family. For example, the knockdown of HDAC7 has been shown to repress both basal and IL-1-induced *MMP13* expression in SW1353 cells (Higashiyama et al, 2009). The next chapter aims to further clarify the specific roles of classical HDACs on the expression of *MMP13* in SW1353 and primary chondrocyte cells, using a siRNA approach.

Chapter IV: The role of histone deacetylases in cartilage gene regulation

Chapter IV

The role of histone deacetylases in cartilage gene regulation

4.1 Introduction

Previously published data demonstrate that broad spectrum HDAC inhibitors TSA and NaBy can decrease cytokine-induced metalloproteinase expression both in the SW1353 cell line and primary articular chondrocytes (Young et al, 2005). These compounds were also found to exhibit a chondroprotective effect against cytokine-induced cartilage resorption in the BNC assay. HDAC inhibitors have also been shown to reduce cartilage destruction in inflammatory arthritis mouse models, which is associated with reduced cytokine expression and increased expression of cell cycle regulators $p16^{INK4a}$ and $p21^{WAF/Cip1}$ (Chung et al, 2003; Keiichiro et al, 2004; Lin et al, 2007). Importantly, TSA has also been found to reduce cartilage degradation in an OA rabbit model, which was reported as partially mediated through the repression of induced IL-1α, *MMP1*, *MMP3* and *MMP13* expression (Chen et al, 2010).

In this thesis the repression of induced metalloproteinase expression by MS-275 and tubacin implicates both class I and II HDACs in the regulation of cytokine-induced metalloproteinase expression. Class I-specific inhibitor MS-275 decreased cytokine-induced metalloproteinase expression in primary articular chondrocytes and the BNC assay, whilst HDAC6-specific inhibitor tubacin decreased induced collagenase expression in the SW1353 cell line. Tubacin also significantly repressed cytokine-induced cartilage degradation in the BNC assay. This is thought to be mediated through the repression of cytokine-induced metalloproteinase expression via the inhibition of HDAC6 activity.

Members of the classical HDAC family have already been shown to have a direct effect on metalloproteinase gene expression. As previously described in chapter III, our laboratory has demonstrated that HDAC1 represses *MMP28* promoter activity through its interaction with the Sp1 transcription factor (Swingler et al, 2010). Interestingly, Chang *et al*. (2006) also detected a 6.5-fold increase in *MMP10* expression in the HDAC7 null mouse, with further experiments in human umbilical vein endothelial cells (HUVECs) indicating that HDAC7 inhibits MEF2 induction of *MMP10* expression. However, most significant to this thesis, Higashiyama *et al*. (2009) have recently

implicated HDAC7 in the regulation of *MMP13* expression in the SW1353 cell line, with the knockdown of HDAC7 in SW1353 cells resulting in decreased basal and IL-1α-induced *MMP13* expression. This study also profiled classical HDAC expression in OA versus normal knee cartilage by qRT-PCR and detected that HDAC7 was significantly increased in OA samples (Higashiyama et al, 2009). Higashiyama and colleagues concluded that elevated HDAC7 in human OA may contribute to cartilage degradation via promoting *MMP13* gene expression.

Profiles comparing metalloproteinase gene expression in OA cartilage and synovium to that of 'normal' tissue have consistently found *MMP13* to be significantly increased in OA tissue (Davidson et al, 2006; Kevorkian et al, 2004; Swingler et al, 2009). Cytokine-induced *MMP13* expression can also be significantly repressed by HDAC inhibitors, which has now been demonstrated *in vitro* in both cell and explant models (of this study), and *in vivo* in the OA rabbit model (Chen et al, 2010; Young et al, 2005). The repression of cytokine-induced *MMP13* by MS-275 and tubacin, observed in this study, suggests that class I HDACs (HDAC1, HDAC2 and HDAC3) and HDAC6 play a role in the regulation of *MMP13* expression. This project aimed to confirm the repression of *MMP13* expression in response to HDAC7 knockdown observed by Higashiyama *et al*. (2009), and to determine the role of all other classical HDAC members in both basal and IL-1α-induced *MMP13* expression. In order to do this, the expression of each classical HDAC was knocked down using siRNA technology in non-stimulated and IL-1α-stimulated SW1353 cells and primary human articular chondrocytes. The effect of this knockdown on *MMP13* expression was assessed by qRT-PCR. Understanding the role of classical HDACs in the regulation of OA-associated metalloproteinase genes, such as *MMP13*, could potentially enable the development of a specific HDAC inhibitor to modulate metalloproteinase expression, and subsequently prevent cartilage degradation. This project also aimed to profile the expression of classical HDACs in OA cartilage compared to normal cartilage, in order to confirm the aberrant expression of HDAC7 observed in OA cartilage by Higashiyama *et al*. (2009).

Aims

- Profile the expression of classical HDACs in cartilage from the femoral head of patients with fracture of the neck of femur (NOF) and patients with OA, using Taqman Low Density Array (TLDA).

- Optimise siRNA knockdown of classical HDACs in the SW1353 cell line at the mRNA and protein level.

- Complete siRNA knockdown at the mRNA level of each classical HDAC in non-stimulated and IL-1α-stimulated SW1353 and primary articular chondrocyte cells, and determine the effect of this knockdown on *MMP13* expression by qRT-PCR.

- Assess the effect of TSA treatment on classical HDAC expression in SW1353 cells.

4.2 Results

4.2.1 The profile of classical HDAC expression in OA versus normal neck of femur cartilage

Higashiyama and colleagues have previously profiled the expression of classical HDACs in cartilage obtained from the condyles and tibial plateaus of normal (n=6) (likely post-mortem) and OA (n=10) donor patients, by qRT-PCR. They identified that the expression of HDAC7 was significantly increased in OA cartilage when compared to normal cartilage. This finding was also confirmed by the immunostaining of cartilage sections with specific anti-HDAC7 antibodies, which identified increased HDAC7 positive cells in the middle and deep zone cartilage layers of OA sections when compared to normal (Higashiyama et al, 2009). The HDAC profile also showed decreased expression of HDAC4 and HDAC10 in OA cartilage, but this did not reach statistical significance (Higashiyama et al, 2009).

To confirm the increased expression of HDAC7 in OA cartilage reported by Higashiyama *et al*. (2009) and to assess the expression of other classical HDACs in the diseased tissue, the expression levels of all eleven HDACs (including two splice variants for HDAC9) were profiled in hip cartilage by Taqman Low Density Array (TLDA). Cartilage samples were obtained from patients undergoing total hip replacement due to OA of the hip (n=12) or a fracture to the neck of femur (NOF) (n=12). Cartilage from the fracture patients was phenotypically normal and will be referred to as such throughout. It should be noted that the OA cartilage in our study was from patients with end-stage disease, and gene expression patterns may be distinct from those occurring at disease initiation or early in disease progression. The cartilage samples were collected by Dr. Rose Davidson (Clark Laboratory, University of East Anglia) and the TLDA was completed in collaboration with the laboratory of Dr. David Young (Newcastle University, UK).

The profile (Figure 4.1) identified that the majority of HDAC genes have decreased expression in OA hip cartilage when compared to normal. In contrast to the study completed by Higashiyama *et al*. (2009), HDAC7 was one of the most significantly decreased genes in OA cartilage compared to the expression in normal cartilage (Figure 4.1). The expression of HDAC5 (* $P<0.05$), HDAC2, HDAC11 (** $P<0.01$), HDAC3 and HDAC8 (*** $P<0.001$) were also decreased in OA cartilage compared to normal.

Again, in contrast to the Higashiyama profile, HDAC10 expression was significantly increased in OA cartilage samples compared to normal. The expression of HDAC1, HDAC4, HDAC6 and HDAC9 (both variants) are not significantly altered in OA cartilage samples compared to normal (Figure 4.1). The lack of consistency between this profile and that conducted by Higashiyama *et al*. (2009) could be attributed to many factors. For example, the cartilage samples from this study were taken from the hip, whilst the samples used in the Higashiyama profile were obtained from the knee, which may contribute to altered gene expression. Also, the Higashiyama study does not state in what circumstance the normal tissue was obtained (although likely due to post-mortem), and thus could be another source of variability between the two profiles. The mean age of patients from which normal samples were taken in the Higashiyama study was also substantially younger (30.8 years) than mean age of the normal samples used in this current study (76.7 years), which could also contribute to the contrasting gene expression detected between the two profiles. It should be noted that the normal cartilage and OA cartilage samples were not age-matched in the Higashiyama study, with normal samples substantially younger than the OA samples (71.6 years) (Higashiyama et al, 2009). This could have potentially led to anomalies within the Higashiyama profile itself.

In conclusion, the current HDAC profile demonstrates that the majority of HDAC transcripts are decreased in OA hip cartilage compared to normal, suggesting that their altered expression may play a role in OA pathology. Due to the important role of HDACs in transcriptional regulation, it is possible that their altered expression in OA could contribute to, or be responsible for the aberrant expression of genes detected in diseased cartilage (Davidson et al, 2006; Kevorkian et al, 2004; Swingler et al, 2009). Therefore, further HDAC expression profiles will need to be conducted to confirm their altered expression in OA and to establish the consequences of this. A profile of HDAC expression in an animal OA model would likely be best for examining the kinetics of HDAC expression during disease development and progression.

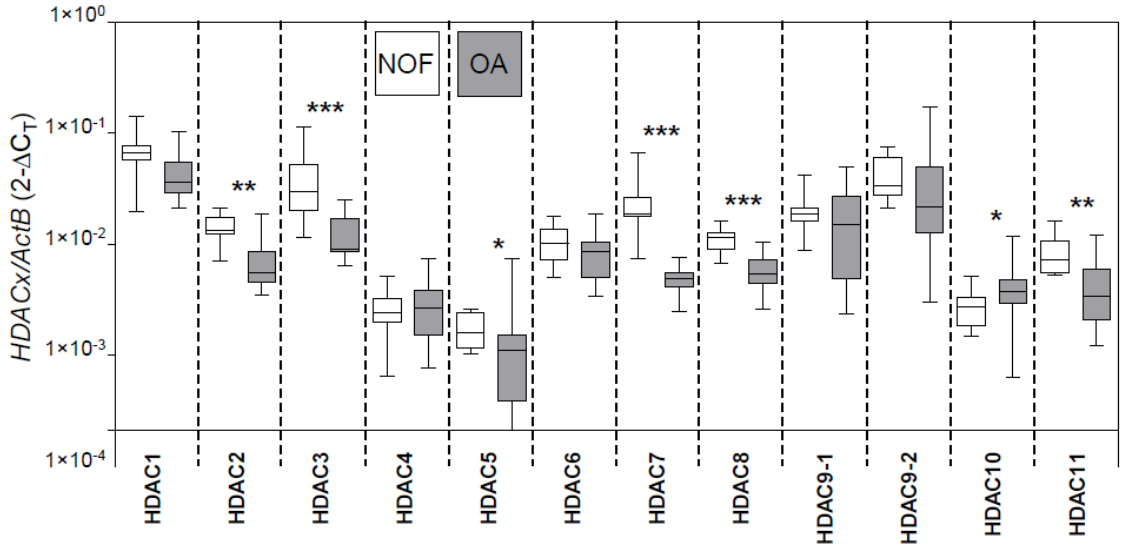

Figure 4.1. Profile of HDAC expression in OA cartilage compared to normal cartilage

Histone deacetylase expression was determined in RNA from the cartilage of neck of femur (NOF) fracture patients (open; n=12) and OA patients (grey; n=12). Gene expression was quantified as part of a Taqman Low Density Array (TLDA) using Applied Biosystems assays. Expression was normalised to the house-keeping gene ActB, whose expression showed the least variation amongst samples. Statistical differences were determined using a non-parametric Mann-Whitney U test where * represents $P<0.05$, ** $P<0.01$ and *** $P<0.001$. The expression of two splice variants of HDAC9 were determined. Data were kindly provided by Dr. David Young (Newcastle University, UK).

4.2.2 Optimising siRNA concentration and incubation time for effective HDAC mRNA knockdown

Assays to optimise siRNA knockdown of classical HDACs were undertaken in the SW1353 cell line. Cells were incubated with 100nM siRNA (of each individual HDAC siRNA pool) for 24 and 48 hours, followed by detection of HDAC expression by qRT-PCR in order to determine the time-point at which mRNA knockdown reached significance. It was established that significant mRNA knockdown could be achieved at 24 hours with 100nM siRNA, and that the majority of HDACs were optimally repressed at this time-point when compared to the levels of repression achieved at 48 hours (Figure 4.2a). Interestingly, overall HDAC expression was found to be reduced in control, non-target and HDAC siRNA samples at the 48 hour time point when compared to 24 hours of incubation. The reason for this remains unclear. It was decided that an incubation of 24 hours would be used for optimal knockdown at the mRNA level.

Cells were then incubated with 10nM, 25nM and 100nM siRNA (of each individual HDAC siRNA pool), followed by detection of HDAC expression by qRT-PCR in order to determine the optimal siRNA concentration for significant mRNA knockdown at 24 hours. It was determined that 25nM siRNA achieved significant mRNA knockdown at 24 hours, of a level similar to that of 100nM siRNA (Figure 4.2b). Therefore, the concentration of 25nM siRNA and an incubation period of 24 hours were chosen for future mRNA knockdown assays. The expression of HDAC2 and HDAC3 were also assessed after HDAC1 knockdown in order to determine if siRNA knockdown was specific. The expression of both HDACs was unaltered by HDAC1 knockdown, confirming that HDAC knockdown was specific (data not shown). This is particularly important in the case of HDAC2, due to its >80% homology with HDAC1.

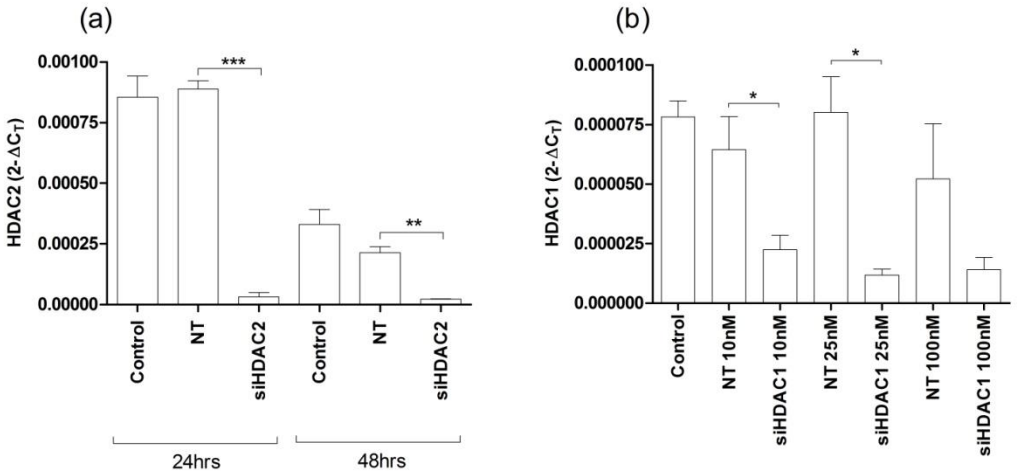

Figure 4.2. The optimisation of HDAC mRNA knockdown in the SW1353 cell line

In order to optimise siRNA incubation times for maximal HDAC mRNA knockdown, SW1353 cells were incubated with 100nM siRNA for each classical HDAC for 24 hours and 48 hours. Total RNA was extracted with Cells-to-cDNA lysis buffer, reverse transcribed to cDNA, and HDAC expression detected by real-time qRT-PCR. **(a)** An example of optimisation: HDAC2 knockdown after 24 hours and 48 hours of incubation with siRNA.

In order to optimise the concentration of siRNA for maximal HDAC mRNA knockdown, SW1353 cells were incubated with increasing concentrations of each HDAC siRNA (10nM, 25nM and 100nM) for 24 hours. Total RNA was extracted with Cells-to-cDNA lysis buffer, reverse transcribed to cDNA, and HDAC expression detected by real-time qRT-PCR. **(b)** An example of optimisation: HDAC1 knockdown after 24 hours of incubation with increasing concentrations of siRNA.

Assays were completed once, using triplicate samples; means ± standard errors are represented. **P*<0.05, ***P*<0.01, ****P*<0.001. *(C, control; NT, non-targeting siRNA; siHDACx, HDAC siRNA)*

4.2.3 Optimising non-targeting siRNA controls for mRNA knockdown assays

Non-targeting siRNA (negative siRNA) control reagents are designed to have no known targets within the cell line chosen to complete targeted siRNA knockdown. These reagents allow sequence-specific siRNA silencing to be distinguished from sequence-independent effects, such as toxicity resulting from transfection and hypersensitivity due to the introduction of double-stranded RNA. Thus non-targeting siRNA are essential to control for the effects of siRNA delivery. Initial knockdown assays in the SW1353 cell line indicated that some non-targeting siRNAs had significant effects on both basal and cytokine-induced *MMP13* expression. For example, the siGENOME Non-Targeting Pool 2 (Dharmacon, Thermo Scientific, Waltham, USA), which is comprised of four siGENOME non-targeting siRNAs identified to have minimal off-target signatures, was found to induce both basal and cytokine-induced *MMP13* expression in many knockdown assays completed in SW1353 cells. The induction of *MMP13* by this non-target control made it difficult to interpret knockdown data and was therefore unsuitable for this study. Silencer® Negative Control #1 siRNA (Ambion, Applied Biosystems, Warrington, UK) is a non-targeting siRNA designed to have no significant sequence similarity to human transcripts, but appeared to repress both basal and induced *MMP13* expression in SW1353 cells. This confirmed that this non-targeting siRNA was also not suitable for mRNA knockdown assays in this study, and further confirms that it is difficult to introduce siRNA into cells without having off-target effects. The non-targeting siRNA chosen for this study was AllStars Negative Control (Qiagen, West Sussex, UK) which displayed no significant effect on basal or cytokine-induced *MMP13* expression in the SW1353 cell line, allowing accurate comparison of gene-specific siRNA knockdown to negative control. However, the AllStars non-targeting siRNA did further potentiate IL-1α-induced *MMP13* expression in primary articular chondrocytes, which will be expanded upon later in this chapter.

4.2.4 Optimising siRNA concentration and incubation time for effective HDAC protein knockdown

To determine if siRNA knockdown of classical HDACs could be achieved at the protein level, SW1353 cells were incubated with 10nM, 25nM and 100nM siRNA targeted to HDAC1 or HDAC2 for 48 hours. After siRNA treatment the protein levels of HDAC1 and HDAC2 were assessed by immunoblot with specific antibodies and compared to GAPDH as a loading control. Immunoblots indicated that the knockdown of HDAC1 at the protein level, compared to untreated cells, could be achieved with all concentrations of HDAC1 siRNA tested (Figure 4.3a). Interestingly, 10nM siRNA was as effective at knocking down HDAC1 at the protein level as 25nM and 100nM siRNA. HDAC2 protein was also reduced by all HDAC2 siRNA concentrations compared to untreated cells (Figure 4.3b). The most significant repression of HDAC2 protein was achieved with 100nM siRNA. GAPDH expression remained unchanged by HDAC1 and HDAC2 siRNA treatment. This indicated that the pre-designed siGENOME *SMART*pool siRNAs used in this study are capable of repressing HDAC expression at the protein level, but this will also need to be confirmed for all other classical HDACs.

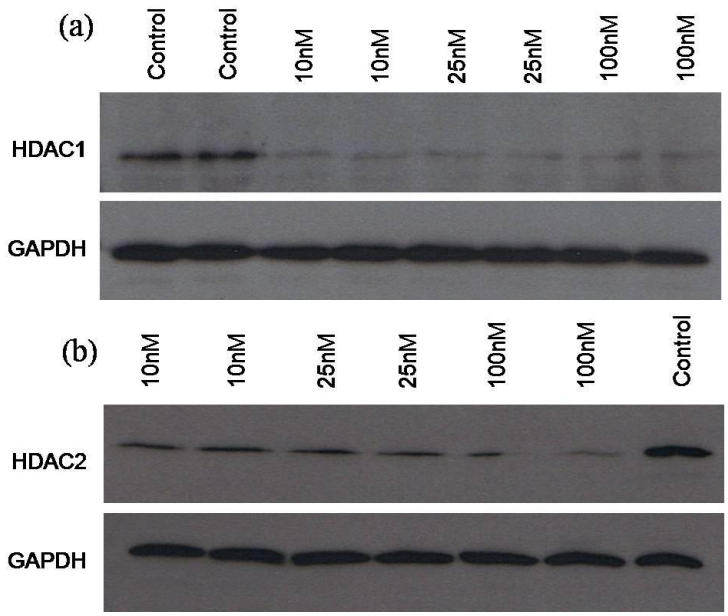

Figure 4.3. The optimisation of siRNA HDAC protein knockdown in the SW1353 cell line

SW1353 cells were incubated with increasing concentrations of HDAC1 or HDAC2 siRNA (10nM, 25nM and 100nM) for 48 hours. Total protein was extracted, resolved by SDS-PAGE, and the level of HDAC proteins assessed by immunoblotting with specific antibodies. The level of HDAC expression was compared to total GAPDH. **(a)** HDAC1 protein level after siRNA treatment. **(b)** HDAC2 protein level after siRNA treatment.

4.2.5 The effect of siRNA knockdown of classical HDACs on MMP13 expression in the SW1353 cell line

MMP-13 is thought to be the primary collagenase in OA. This is supported by its significantly increased expression in OA cartilage (Davidson et al, 2006; Kevorkian et al, 2004; Swingler et al, 2009), its over-expression leading to cartilage degradation similar to that of OA in mice (Neuhold et al, 2001) and by its inhibition preventing collagen release from human OA cartilage explants (Billinghurst et al, 1997). Understanding the transcriptional mechanisms involved in the regulation of this enzyme could potentially help elucidate its role in OA and lead to the development of possible OA therapeutics. This thesis has confirmed that TSA can significantly repress cytokine-induced *MMP13* expression in both SW1353 cells and primary articular chondrocytes, consistent with the study by Young *et al*. (2005). It has also shown that class I-specific (MS-275) and HDAC6-specific (tubacin) inhibitors are capable of repressing cytokine-induced *MMP13* expression. These findings indicate that both class I and class II HDACs play a role in the regulation of cytokine-induced *MMP13* expression. The involvement of Class II HDACs in the transcriptional regulation of *MMP13* expression is consistent with the study completed by Higashiyama *et al*. (2009), which reported that siRNA repression of HDAC7 mRNA significantly repressed *MMP13* expression in SW1353 cells. We therefore chose to establish the effect of siRNA knockdown of all members of the classical HDAC family on *MMP13* expression in the SW1353 cell line, and to later confirm these effects in primary articular chondrocytes.

SW1353 cells were incubated with 25nM non-targeting and HDAC siRNAs for 24 hours (as described in section 2.2.13), followed by serum starvation overnight. Cells were then incubated for a further 6 hours either in the presence or absence of IL-1α. The addition of IL-1α to siRNA treated cells enabled us to determine the role of HDACs in the regulation of basal and cytokine-induced *MMP13* expression. TSA (50ng/ml) was also added to non-siRNA-treated cells in the presence or absence of IL-1α as a positive control, due to its consistent repression of cytokine-induced *MMP13* expression. The addition of TSA also allowed us to compare the level of *MMP13* repression achieved through inhibition of all HDAC activity to that achieved by individual HDAC gene repression. Both HDAC and *MMP13* expression were determined by qRT-PCR. Mock transfections, where cells were treated with Dharmafect transfection regent and no

siRNA, were also included for all knockdown experiments to ensure that transfection reagent alone had no effect on gene expression.

Two knockdown experiments were completed in the SW1353 cell line, in which each classical HDAC was knocked down at the mRNA level and the subsequent effect on *MMP13* expression assessed. The first experiment was preliminary and completed with the siGENOME Non-Targeting Pool 2 (Dharmacon) as a negative control. This non-targeting siRNA was found to increase basal and cytokine-induced *MMP13* expression in some assays, making it impossible to confidently interpret the siRNA knockdown of HDAC4, HDAC5, HDAC6, HDAC7, HDAC8, HDAC9 and HDAC10 on *MMP13* expression. However, conclusions were successfully drawn from the knockdown of HDAC1, HDAC2, HDAC3 and HDAC11 (Appendix IV) of this preliminary study, which will be referred to in this chapter. The knockdown data shown in this chapter is therefore from the second complete SW1353 knockdown experiment, using the AllStars Negative Control non-targeting siRNA (Qiagen).

4.2.5.1 The effect of siRNA knockdown of class I HDACs on MMP13 expression in the SW1353 cell line

The expression of all class I HDACs were significantly repressed by siRNA treatment compared to non-targeting siRNA (Figure 4.4). Interestingly, it was also observed that HDAC3 expression appeared to be induced by TSA treatment (Figure 4.4c). This is consistent with a study previously completed by Hemmatazad *et al*. (2009) in which TSA induced HDAC3 expression in systemic sclerosis (SSc) skin fibroblasts at both the mRNA and protein level.

The knockdown of HDAC1 expression had no significant effect on basal *MMP13* expression when compared to the comparative non-targeting control. However, HDAC1 knockdown in IL-1α-stimulated cells led to a further potentiation of induced *MMP13* expression (Figure 4.4a). The potentiation of induced *MMP13* expression was also observed in preliminary experiments, but did not reach statistical significance (Appendix IV Figure 4a). This suggests that HDAC1 may repress cytokine-induced *MMP13* transcription in the SW1353 cell line. The transcriptional repression of MMP genes by HDAC1 is consistent with previous findings published by our laboratory, showing that HDAC1 represses *MMP28* promoter activity through its interaction with the Sp1 transcription factor (Swingler et al, 2010). However, to date, Sp1 has not been found to be involved the transcriptional regulation of *MMP13* expression.

The knockdown of HDAC2 expression significantly reduced basal and IL-1α-induced *MMP13* expression compared to comparative non-targeting siRNAs (Figure 4.4b). This effect was also observed in the preliminary experiment (Appendix IV Figure 4b), suggesting that HDAC2 plays a role in the induction of both basal and cytokine-induced *MMP13* expression (Figure 4.4b).

Knockdown of HDAC3 expression also resulted in the significant repression of basal and IL-1α-induced *MMP13* expression (Figure 4.4c). The repression of cytokine-induced *MMP13* expression in response to HDAC3 knockdown was also observed in the preliminary experiment, although no effect was observed on basal *MMP13* expression (Appendix IV Figure 4c). The consistent repression of cytokine-induced *MMP13* in response to HDAC3 knockdown suggests that HDAC3 plays a role in IL-1α induction of *MMP13*. However, the contrasting effect of HDAC3 knockdown on basal *MMP13* expression between the preliminary knockdown assay and this assay means

that further assays are required to determine the role of HDAC3 on *MMP13* transcription under normal conditions.

HDAC8 knockdown also resulted in significant inhibition of both basal and IL-1α-induced *MMP13* expression compared to non-target controls (Figure 4.4d), indicating that HDAC8 plays a role in the induction of *MMP13* expression. These data cannot be compared to the effect of HDAC8 knockdown in the preliminary experiment due to the siGENOME Non-Targeting siRNA inducing both basal and IL-1α-induced *MMP13* expression (data not shown).

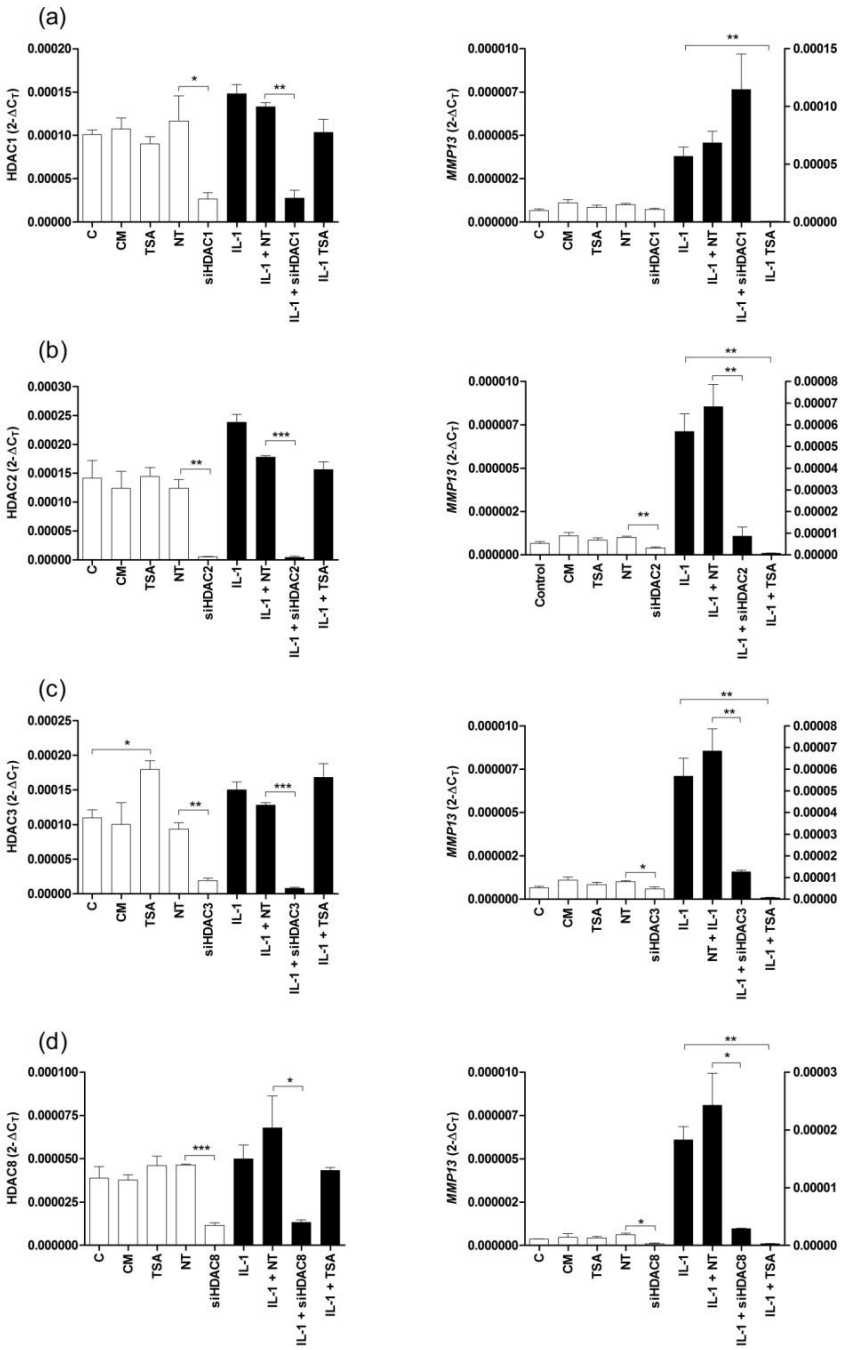

Figure 4.4. The effect of class I HDAC siRNA knockdown on *MMP13* expression in the SW1353 cell line.

SW1353 cells were incubated with 25nM siRNA for 24 hours in serum-containing medium. Cells were then serum-starved overnight, followed by IL-1α (5ng/ml) and/or TSA (50ng/ml) treatment (where appropriate) for 6 hours. Total RNA was extracted with Cells-to-cDNA lysis buffer, reverse transcribed to cDNA, and *MMP13* and HDAC expression detected by real-time qRT-PCR. **(a)** HDAC1 and *MMP13* expression after siRNA treatment. **(b)** HDAC2 and *MMP13* expression after siRNA treatment. **(c)** HDAC3 and *MMP13* expression after siRNA treatment. **(d)** HDAC8 and *MMP13* expression after siRNA treatment. Assays were completed twice, using triplicate samples. Data presented are representative of one assay; means ± standard errors are represented. **P*<0.05, ***P*<0.01, ****P*<0.001. For *MMP13* expression graphs, non-cytokine treated samples correspond to the left Y axis, and cytokine treated samples correspond to the right Y axis. *(C, control; CM, control-mock transfection; NT, non-targeting siRNA; siHDACx, HDAC siRNA)*

4.2.3.2 The effect of siRNA knockdown of class IIa HDACs on MMP13 expression in the SW1353 cell line

Significant siRNA knockdown of HDAC5 and HDAC9 expression was achieved in non-stimulated (cells treated with siRNA but not IL-1α) and IL-1α-stimulated SW1353 cells (Figure 4.5b and d). HDAC4 expression was significantly repressed in non-stimulated cells, but the repression in IL-1α treated cells did not reach statistical significance (Figure 4.5a). Significant HDAC7 knockdown was detected in IL-1α-treated cells but did not reach statistical significance in non-stimulated cells. Interestingly, it was also noted that HDAC4 expression was significantly increased in response to TSA treatment (Figure 4.5a).

Basal *MMP13* expression was significantly repressed in response to HDAC4, HDAC5 and HDAC7 knockdown (Figure 4.5a, b and c), suggesting that all three HDACs could potentially play a role in maintaining basal expression of *MMP13* in the SW1353 cell line. Interestingly, significant repression of basal *MMP13* was achieved in response to HDAC7 knockdown despite HDAC7 knockdown not reaching statistical significance in these cells (Figure 4.5c). This suggests that a small reduction in HDAC7 expression is capable of conferring repression of basal *MMP13* expression in SW1353 cells. Basal *MMP13* expression was not significantly reduced by HDAC9 knockdown, but there was however a trend to decreased expression in comparison to the non-targeting control (Figure 4.5d).

Cytokine-induced *MMP13* expression was significantly reduced in response to HDAC5, HDAC7 and HDAC9 siRNA knockdown (Figure 4.5b, c and d). Induced *MMP13* was also repressed by HDAC4 knockdown but did not reach statistical significance, which is likely to be due to inefficient knockdown of HDAC4 in these cells (Figure 4.5a). These data indicate that all class IIa HDACs play a role in the activation of basal and cytokine-induced *MMP13* expression in the SW1353 cell line.

The repression of *MMP13* expression in both non-stimulated and IL-1α-treated SW1353 cells by HDAC7 siRNA is consistent with the study completed by Higashiyama *et al.* (2009). Therefore, these data further suggest that HDAC7 plays a role in both basal and cytokine-induced *MMP13* expression. This current study also found that HDAC7 knockdown significantly repressed I/O- (IL-1α 5ng/ml and OSM 10ng/ml) induced

MMP13 expression in SW1353 cells, further confirming that HDAC7 plays a role in cytokine induction of *MMP13* expression (Appendix IV Figure 5a). In addition, HDAC7 knockdown was also found to correlate with the repression of IL-1α-induced *MMP1* expression, although no significant effect of HDAC7 knockdown was seen on basal *MMP1* expression (Appendix IV Figure 5b).

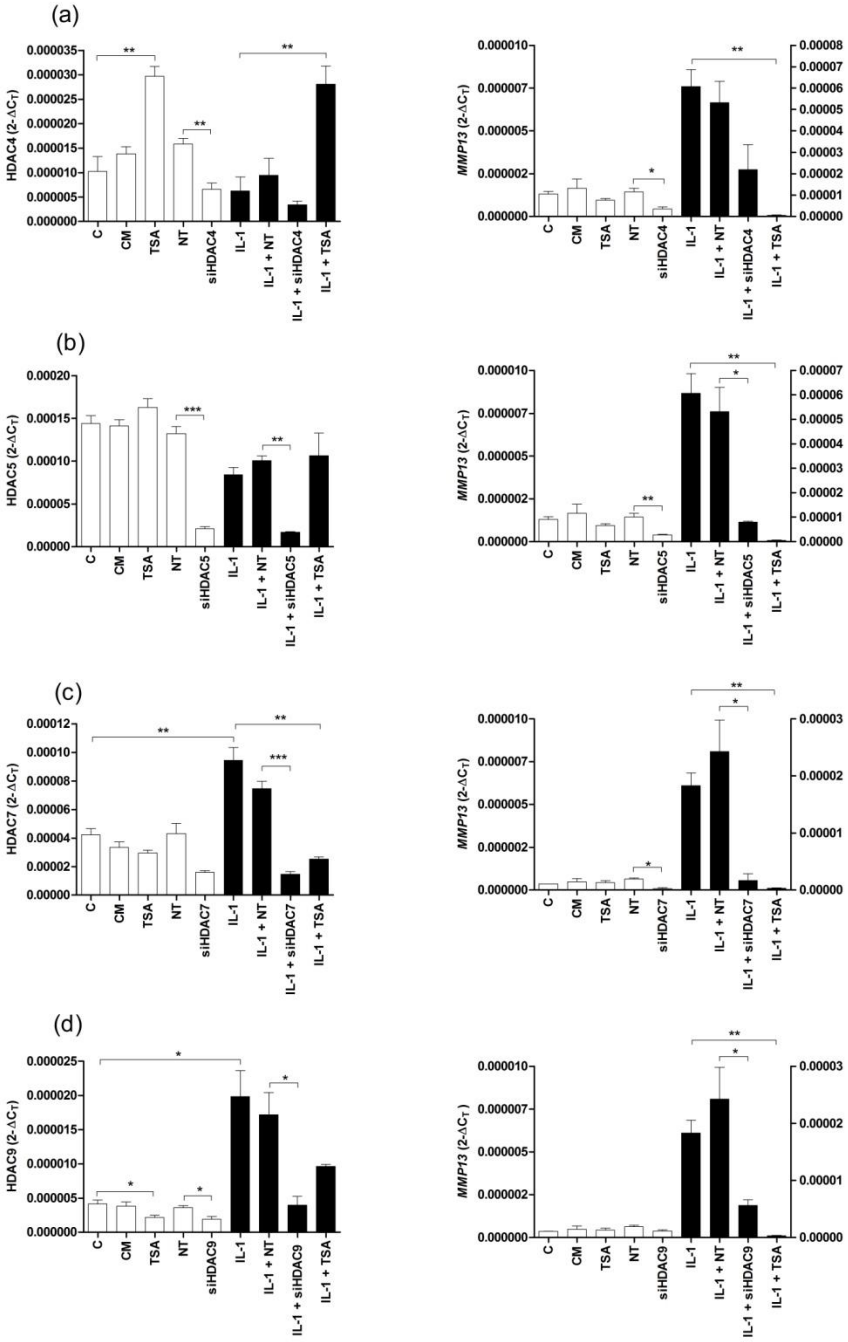

Figure 4.5. The effect of class IIa HDAC siRNA knockdown on *MMP13* expression in the SW1353 cell line

SW1353 cells were incubated with 25nM siRNA for 24 hours in serum-containing medium. Cells were then serum-starved overnight, followed by IL-1α (5ng/ml) and/or TSA (50ng/ml) treatment (where appropriate) for 6 hours. Total RNA was extracted with Cells-to-cDNA lysis buffer, reverse transcribed to cDNA, and *MMP13* and HDAC expression detected by real-time qRT-PCR. **(a)** HDAC4 and *MMP13* expression after siRNA treatment. **(b)** HDAC5 and *MMP13* expression after siRNA treatment. **(c)** HDAC7 and *MMP13* expression after siRNA treatment. **(d)** HDAC9 and *MMP13* expression after siRNA treatment. Assays were completed twice, using triplicate samples. Data presented are representative of one assay; means ± standard errors are represented. **P*<0.05, ***P*<0.01, ****P*<0.001. For *MMP13* expression graphs, non-cytokine treated samples correspond to the left Y axis, and cytokine treated samples correspond to the right Y axis. *(C, control; CM, control-mock transfection; NT, non-targeting siRNA; siHDACx, HDAC siRNA)*

4.2.3.3 The effect of siRNA knockdown of class IIb HDACs and HDAC11 on MMP13 expression in the SW1353 cell line

Significant siRNA knockdown of HDAC6 and HDAC11 expression was achieved in non-stimulated and IL-1α-stimulated cells compared to non-target controls (Figure 4.6a and c). However, siRNA treatment did not successfully repress HDAC10 expression and subsequently no effect was observed on the expression of *MMP13* (Figure 4.6b), meaning that HDAC10 knockdown will need to be repeated to establish its role in the transcriptional regulation of *MMP13* expression in SW1353 cells.

Basal and cytokine-induced *MMP13* expression was significantly reduced in response to HDAC6 knockdown (Figure 4.6a). The siRNA knockdown of HDAC6 expression also significantly repressed I/O-induced *MMP1* expression in SW1353 cells (Appendix IV Figure 6). This implicates HDAC6 in the induction of basal and cytokine-induced collagenase expression in SW1353 cells, which is also supported by the repression of cytokine-induced collagenase expression with tubacin treatment in the SW1353 cell line (See Figure 3.10).

Cytokine-induced *MMP13* expression was significantly repressed in response to HDAC11 knockdown, but no significant repression of basal *MMP13* expression was observed (Figure 4.6c). However, no significant effect was observed on either basal or cytokine-induced *MMP13* expression in response to HDAC11 knockdown in the preliminary experiment (Appendix IV Figure 7). Therefore further assays are required to establish the effect of HDAC11 knockdown on *MMP13* expression in SW1353 cells.

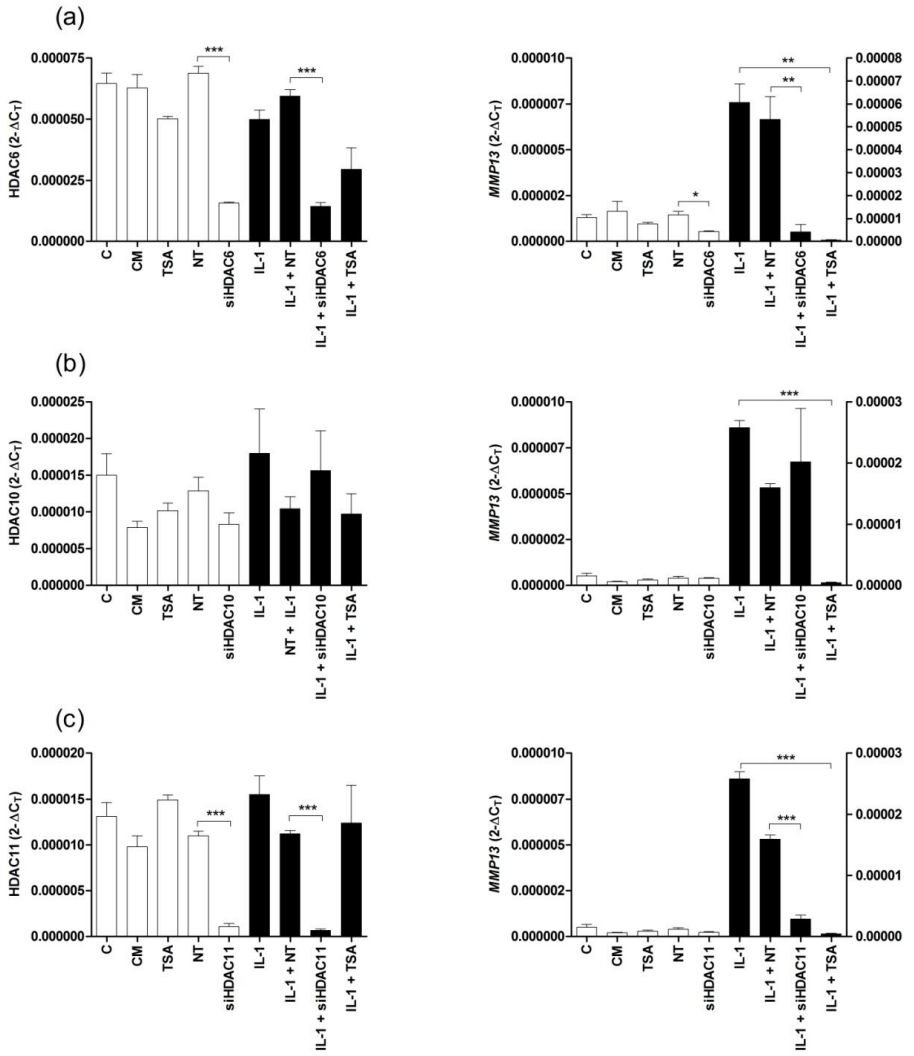

Figure 4.6. The effect of siRNA knockdown of class IIb HDACs and HDAC11 on *MMP13* expression in the SW1353 cell line

SW1353 cells were incubated with 25nM siRNA for 24 hours in serum-containing medium. Cells were then serum-starved overnight, followed by IL-1α (5ng/ml) and/or TSA (50ng/ml) treatment (where appropriate) for 6 hours. Total RNA was extracted with Cells-to-cDNA lysis buffer, reverse transcribed to cDNA, and *MMP13* and HDAC expression detected by real-time qRT-PCR. **(a)** HDAC6 and *MMP13* expression after siRNA treatment. **(b)** HDAC10 and *MMP13* expression after siRNA treatment. **(c)** HDAC11 and *MMP13* expression after siRNA treatment. Data presented are representative of one assay; means ± standard errors are represented. **P*<0.05, ***P*<0.01, ****P*<0.001. For *MMP13* expression graphs, non-cytokine treated samples correspond to the left Y axis, and cytokine-treated samples correspond to the right Y axis. *(C, control; CM, control-mock transfection; NT, non-targeting siRNA; siHDACx, HDAC siRNA)*

In conclusion, siRNA knockdown assays completed in the SW1353 cell line indicated that the repression of the majority of classical HDACs leads in turn to a repression of either basal or IL-1α-induced *MMP13* expression. This is clearly demonstrated when the data are presented as fold change of *MMP13* expression compared to comparative non-target controls, which is shown in Figure 4.7. Our original hypothesis was that specific HDACs would be involved in the regulation of *MMP13* expression, so the repression of *MMP13* in response to the specific knockdown of the majority of classical HDACs was not expected. HDAC1 was the only member of the classical HDAC family whose knockdown did not lead to *MMP13* repression, instead resulting in the further potentiation of IL-1α-induced expression (though basal expression was slightly reduced) (Figure 4.7). Interestingly the repression of IL-1α-induced *MMP13* exhibited after specific HDAC knockdown never reached the level of inhibition observed after TSA treatment, suggesting that more than one HDAC is involved in *MMP13* gene regulation in these cells.

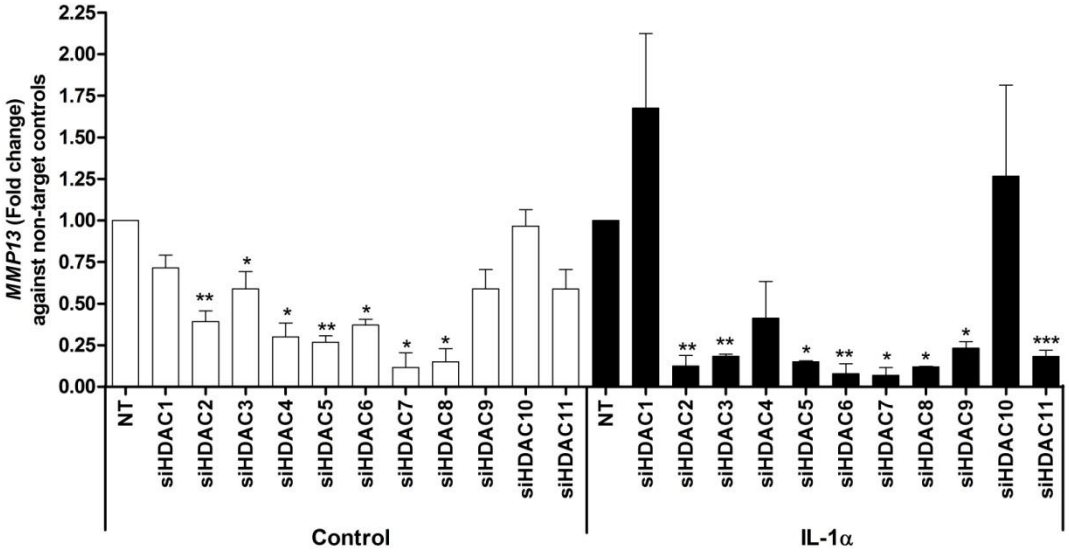

Figure 4.7. *MMP13* expression after siRNA knockdown of classical HDAC expression in SW1353 cells.

SW1353 cells were incubated with 25nM siRNA for 24 hours in serum-containing medium. Cells were then serum-starved overnight, followed by IL-1α (5ng/ml) treatment (where appropriate) for 6 hours. Total RNA was extracted with Cells-to-cDNA lysis buffer, reverse transcribed to cDNA, and *MMP13* expression detected by real-time qRT-PCR. Data presented is representative of the fold change in *MMP13* expression compared to non-targeting siRNA controls after HDAC knockdown. The data are representative of one experiment using triplicate samples; means ± standard errors are represented. **P*<0.05, ***P*<0.01, ****P*<0.001. *(NT, non-targeting siRNA; siHDACx, HDAC siRNA)*

4.2.4 The effect of siRNA knockdown of classical HDACs on MMP13 expression in primary articular chondrocytes

In order to further elucidate the role of classical HDACs in the transcriptional regulation of *MMP13*, siRNA knockdown experiments were repeated in primary articular chondrocytes. Two knockdown experiments were completed in primary cells, in which each classical HDAC was knocked down at the mRNA level and the effect on *MMP13* expression assessed by qRT-PCR. The data presented are representative of the second knockdown experiment, as HDAC knockdown was often not significant in the preliminary experiment.

The AllStars non-targeting siRNA appeared to potentiate cytokine induction of *MMP13* when compared to the induction of *MMP13* in cells treated with IL-1α alone. The AllStars non-targeting siRNA also altered basal *MMP13* expression in comparison to control non-transfected cells (Figure 4.8, 4.9 and 4.10). This effect was not observed in the preliminary knockdown experiment in primary articular chondrocytes, and due to time constraints, knockdown experiments could not be repeated a third time. This once again makes the effect of HDAC knockdown on cytokine-induced *MMP13* hard to interpret, with the repression of *MMP13* often significant when compared to the non-target control but not when compared to non-transfected controls. Therefore it is difficult to decide which control should be used for data analysis. The non-targeting control is the 'true' control as it involves introducing siRNA into the cell, but if this siRNA is then causing off-target effects it destroys its validity. This leaves the non-stimulated and the IL-1α-stimulated cells as comparative controls, but these cells have at no point been transfected with siRNA. In order to demonstrate the significant difference in the data depending on the control chosen, the fold change of *MMP13* expression has been calculated in comparison to both non-targeting siRNA controls and non-transfected controls (Figure 4.11a and b). The data have also been represented using the comparative C_T method ($2^{-\Delta CT}$) as used to analyse the SW1353 siRNA knockdown experiment.

4.2.4.1 The effect of siRNA knockdown of class I HDACs on MMP13 expression in primary articular chondrocytes

Significant siRNA knockdown of HDAC2 and HDAC3 expression was achieved in non-stimulated and IL-1α-stimulated cells compared to non-target controls (Figure 4.8b and c). HDAC1 expression was significantly knocked down in IL-1α-stimulated cells, but repression of basal expression did not reach statistical significance (Figure 4.8a). HDAC8 expression was repressed in both non-stimulated and IL-1α-treated cells, but did not reach statistical significance (Figure 4.8d).

The expression of both basal and cytokine-induced *MMP13* expression was increased in response to HDAC1 knockdown, but did not reach statistical significance compared to non-target control (Figure 4.8a). The correlation between HDAC1 knockdown and increased *MMP13* is also consistent with the induction of *MMP13* expression observed in SW1353 cells. This again supports the suggestion that HDAC1 represses the expression of *MMP13*.

The knockdown of HDAC2, HDAC3 and HDAC8 led to a repression in basal *MMP13* expression, but this did not reach statistical significance compared to non-target controls (Figure 4.8b, c and d). Therefore, this would suggest that HDAC2, HDAC3 and HDAC8 play a role in inducing the transcriptional expression of *MMP13* under normal conditions, which is also consistent with the data produced from the knockdown assays completed in the SW1353 cell line.

The effect of HDAC2, HDAC3 and HDAC8 knockdown on IL-1α-induced *MMP13* expression is harder to interpret due to the further potentiation of cytokine-induced *MMP13* expression by the non-targeting siRNA (Figure 4.8b, c and d). If the non-targeting siRNA is selected as the control, IL-1α-induced *MMP13* expression is significantly repressed by the knockdown of all three HDACs (Figure 4.8b, c and d). However, if non-transfected IL-1α-treated cells are used as the comparative control, HDAC2 knockdown has no significant impact on cytokine-induced *MMP13* expression (Figure 4.8b) and the repression observed in response to HDAC3 and HDAC8 knockdown does not reach statistical significance (Figure 4.8c and d). The potentiation of cytokine-induced *MMP13* expression by the non-targeting siRNA suggests that the non-transfected IL-1α control may be the most accurate comparative control. This would infer that HDAC2 does not play a role in the regulation of cytokine-induced

MMP13 expression in primary articular chondrocytes, but may do so in the maintenance of basal *MMP13* expression. It would also suggest that HDAC3 and HDAC8 knockdown causes a small repression of both basal and cytokine-induced *MMP13* expression, indicating that these enzymes may have a role in inducing *MMP13* transcription.

The contrasting results depending on the control selected are clearly seen when the data is presented as fold change of *MMP13* expression in relation to either non-target controls or non-transfected controls (Figure 4.11a and b). This means that when the change in *MMP13* expression (in response to specific HDAC knockdown) is consistent between the data sets normalised to both control types, it is more likely to reflect the true response to HDAC knockdown. For example, the increase of both basal and cytokine-induced *MMP13* expression in response to HDAC1 knockdown is seen when these data are normalised to both the non-target siRNA controls (Figure 4.11a) and non-transfected controls (Figure 4.11b). This strongly supports the theory that HDAC1 represses both basal and IL-1α-induced *MMP13* expression in primary chondrocytes. The repression of basal *MMP13* expression in response to HDAC2, HDAC3 and HDAC8 is also observed when the data are presented as fold change in comparison to both control types, with the level of repression dependent on the control selected (Figure 4.11a and b). This again supports the theory that HDAC2, HDAC3 and HDAC8 play a role in maintaining basal *MMP13* expression.

However, the effect of HDAC2 knockdown on the fold change of cytokine-induced *MMP13* expression varied depending on the control selected, with a potentiation of IL-1α-induced *MMP13* expression seen when compared to non-target control but no effect seen if compared to the non-transfected control (Figure 4.11a and b). The large potentiation of IL-1α-induced *MMP13* expression by the non-target siRNA suggests that the non-transfected IL-1α control is likely the most accurate of the controls.

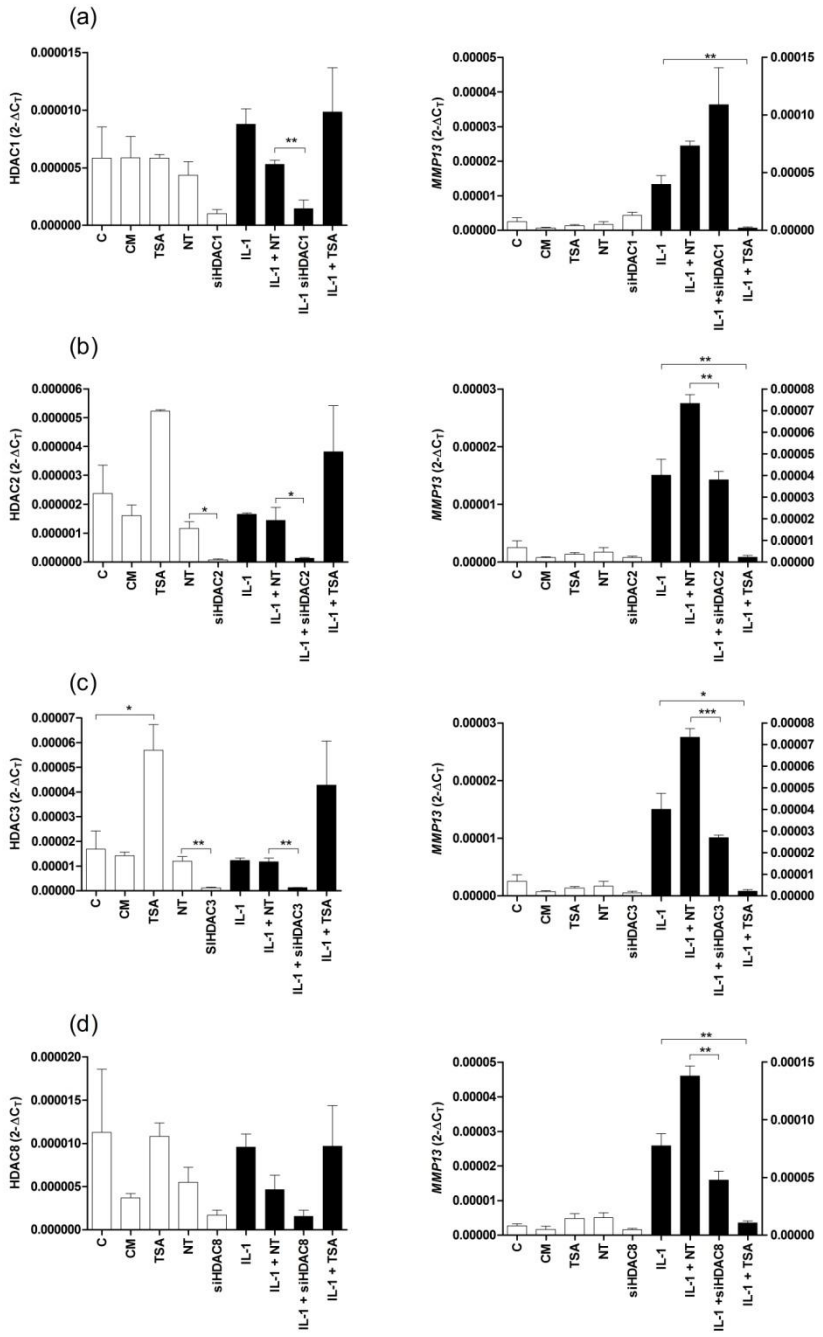

Figure 4.8. The effect of class I HDAC siRNA knockdown on *MMP13* expression in primary articular chondrocytes

Primary chondrocytes were incubated with 25nM siRNA for 24 hours in serum-containing medium. Cells were then serum-starved overnight, followed by IL-1α (5ng/ml) and/or TSA (50ng/ml) treatment (where appropriate) for 6 hours. Total RNA was extracted with Cells-to-cDNA lysis buffer, reverse transcribed to cDNA, and *MMP13* and HDAC expression detected by real-time qRT-PCR. **(a)** HDAC1 and *MMP13* expression after siRNA treatment. **(b)** HDAC2 and *MMP13* expression after siRNA treatment. **(c)** HDAC3 and *MMP13* expression after siRNA treatment. **(d)** HDAC8 and *MMP13* expression after siRNA treatment. Assays were completed twice, using triplicate samples. Data presented are representative of one experiment; means ± standard errors are represented. **P*<0.05, ***P*<0.01, ****P*<0.001. For *MMP13* expression graphs, non-cytokine treated samples correspond to the left Y axis, and cytokine-treated samples correspond to the right Y axis. *(C, control; CM, control-mock transfection; NT, non-targeting siRNA; siHDACx, HDAC siRNA)*

4.2.4.2 The effect of siRNA knockdown of class IIa HDACs on MMP13 expression in primary articular chondrocytes

Significant siRNA knockdown of HDAC5 and HDAC7 expression was achieved in both non-stimulated and IL-1α-stimulated cells (Figure 4.9b and c). HDAC4 expression was significantly knocked down in non-cytokine stimulated chondrocytes, but the repression in IL-1α-stimulated cells did not reach statistical significance (Figure 4.9a). HDAC9 expression was repressed in non-stimulated cells, but did not reach statistical significance (Figure 4.8d). HDAC9 knockdown in IL-1α-stimulated cells could not be calculated as HDAC9 expression was below the limits of detection by qRT-PCR. Interestingly, HDAC4 and HDAC5 expression were significantly increased by TSA treatment in primary chondrocytes (Figure 4.9a and b).

The knockdown of HDAC4 expression had no significant effect on basal *MMP13* expression when compared to non-target control (Figure 4.9a). Basal *MMP13* expression was increased in response to HDAC5 knockdown when compared to non-target, but did not reach statistical significance (Figure 4.9b). HDAC7 knockdown resulted in a repression of basal *MMP13* expression when compared to non-target control, but did not reach statistical significance (Figure 4.9c). Basal *MMP13* expression was slightly induced in response to HDAC9 knockdown compared to non-target control, but did not reach statistical significance (Figure 4.9d). However, the effect of class IIa HDAC knockdown on basal *MMP13* expression sometimes differs when compared to the non-transfected control. For example, HDAC4 knockdown had no effect on basal *MMP13* expression when compared to non-target siRNA control, but was repressed when compared to the non-transfected control. This can also be seen when the data are represented as fold change, with a 0.5 fold decrease in basal *MMP13* expression detected in response to HDAC4 knockdown when compared to non-transfected control, but no repression observed when compared to non-target control (Figure 4.11a and b). The effect of HDAC5 knockdown on basal *MMP13* expression is also different depending on the control selected, with no effect observed on basal *MMP13* expression compared to the non-transfected control, but a large induction seen when compared to the non-target siRNA control (Figure 4.11a and b). The small induction of basal *MMP13* expression in response to HDAC9 knockdown when compared to non-target control is also larger and statistically significant when compared

to the non-transfected control (Figure 4.11a and b). This again stresses the importance of selecting the correct comparative control for siRNA knockdown and indicates that further knockdown assays will have to be completed to clarify the effects of class IIa repression on *MMP13* expression. However, HDAC7 knockdown did not induce a significant change of basal *MMP13* expression when the data were normalised to both control types (Figure 4.11), suggesting that HDAC7 does not regulate the expression of *MMP13* under normal conditions in primary articular chondrocytes.

HDAC4 knockdown significantly repressed cytokine-induced *MMP13* expression when compared to the non-target siRNA, but resulted in a small potentiation of IL-1α-induced *MMP13* when compared to the non-transfected IL-1α control (Figure 4.9a). As stated previously, the non-transfected IL-1α control is likely to be the better control for establishing the effect of HDAC knockdown. Therefore these data suggest that HDAC4 inhibits cytokine induction of *MMP13* expression in primary chondrocytes.

Cytokine-induced *MMP13* expression was increased in comparison to both the non-target control and non-transfected IL-1α control in response to HDAC5 knockdown (Figure 4.9b). The knockdown of HDAC5 expression resulted in a 0.5-fold increase in *MMP13* expression when compared to non-target siRNA control, and a 2-fold increase in expression compared to the non-transfected IL-1α control (Figure 4.11a and b). Therefore, IL-1α-induced *MMP13* expression was increased in correlation to HDAC5 knockdown, suggesting that HDAC5 represses cytokine-induced *MMP13* expression in primary articular chondrocytes.

HDAC7 knockdown resulted in a significant repression of cytokine-induced *MMP13* if compared to the non-target siRNA, but had no significant effect on IL-1α-induced *MMP13* if compared to the non-transfected IL-1α control (Figure 4.9c). Therefore, with the non-transfected IL-1α sample as the control, HDAC7 appears to have no effect on cytokine-induced *MMP13* expression (Figure 4.11b). These data contrast with the induction of *MMP13* expression in response to HDAC7 knockdown in SW1353 cells, both in this study and in the study conducted by Higashiyama *et al*. (2009). This suggests that the regulation of *MMP13* expression via HDAC7 differs in the SW1353 cell line compared to primary chondrocytes. This is consistent with the inhibition of cytokine-induced *MMP13* expression by MS-275 in primary cells but not in SW1353

cells, which also indicates that HDAC regulation of *MMP13* transcription may vary between the two cell types.

It is unknown if HDAC9 was repressed in IL-1α-stimulated samples, thus the effect on cytokine-induced *MMP13* expression cannot be definitely determined. The possible effect of HDAC9 knockdown differs depending on the control selected, with a repression of cytokine-induced *MMP13* detected if compared to the non-target siRNA, but a small potentiation observed if compared to the non-transfected IL-1α control (this did not reach statistical significance) (Figure 4.9d). Therefore, with non-transfected IL-1α as the control, HDAC9 appears to slightly potentiate cytokine-induced *MMP13* expression (Figure 4.11b). This suggests that HDAC9 may play an inhibitory role in the induction of *MMP13* expression. However, due to the undetermined HDAC9 knockdown in these cells this cannot be certain.

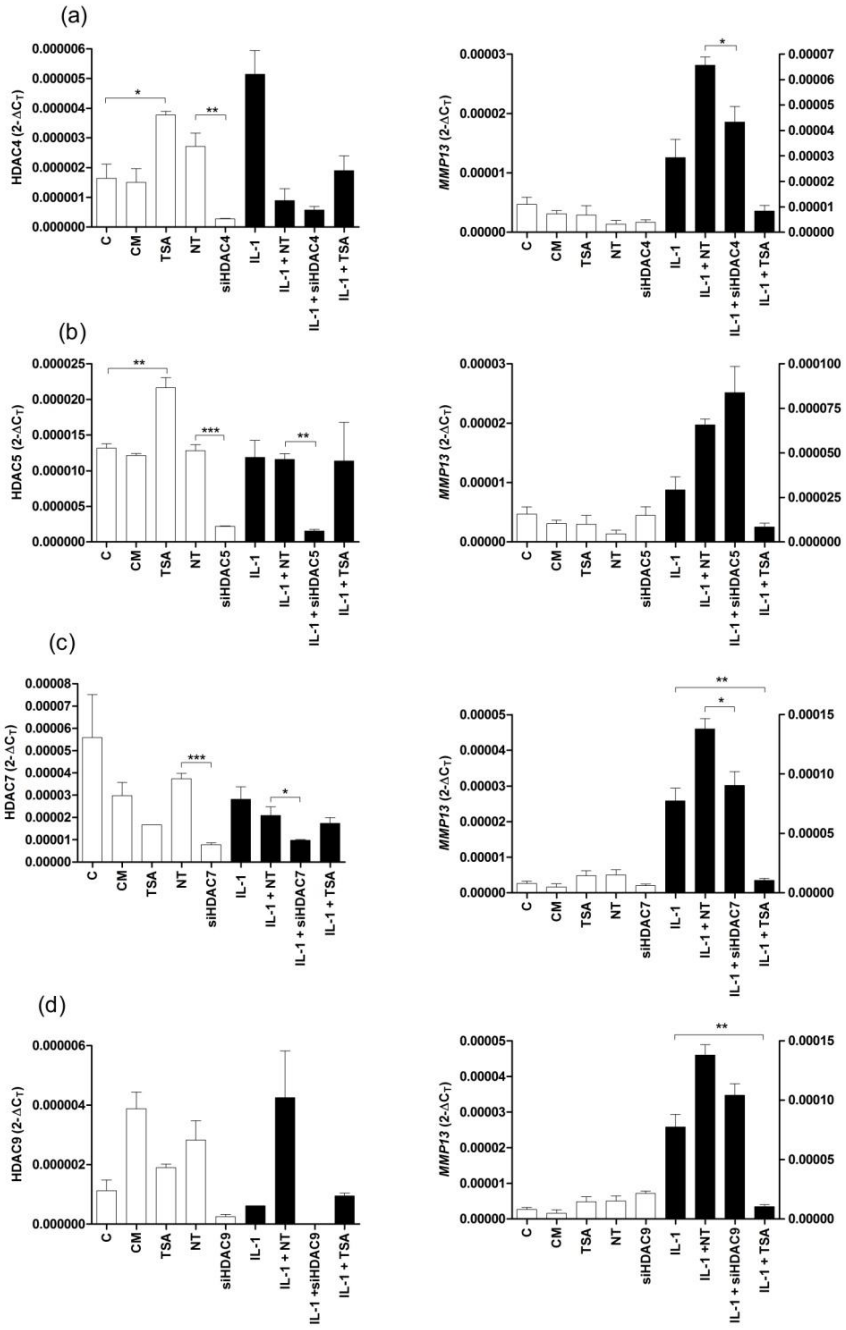

Figure 4.9. The effect of class IIa HDAC siRNA knockdown on *MMP13* expression in primary articular chondrocytes

Primary articular chondrocytes were incubated with 25nM siRNA for 24 hours in serum-containing medium. Cells were then serum-starved overnight, followed by IL-1α (5ng/ml) and/or TSA (50ng/ml) treatment (where appropriate) for 6 hours. Total RNA was extracted with Cells-to-cDNA lysis buffer, reverse transcribed to cDNA, and *MMP13* and HDAC expression detected by real-time qRT-PCR. **(a)** HDAC4 and *MMP13* expression after siRNA treatment. **(b)** HDAC5 and *MMP13* expression after siRNA treatment. **(c)** HDAC7 and *MMP13* expression after siRNA treatment. **(d)** HDAC9 and *MMP13* expression after siRNA treatment. Assays were completed twice, using triplicate samples. Data presented are representative of one assay; means ± standard errors are represented. **P*<0.05, ***P*<0.01, ****P*<0.001. For *MMP13* expression graphs, non-cytokine treated samples correspond to the left Y axis, and cytokine-treated samples correspond to the right Y axis. *(C, control; CM, control-mock transfection; NT, non-targeting siRNA; siHDACx, HDAC siRNA)*

4.2.4.1 The effect of siRNA knockdown of class IIb HDACs and HDAC11 on MMP13 expression in primary articular chondrocytes

HDAC6 expression was significantly repressed in IL-1α-stimulated cells, but the repression observed in non-stimulated cells did not reach statistical significance (Figure 4.10a). The knockdown of HDAC10 expression was statistically significant in both non-stimulated and IL-1α-treated cells (figure 4.10b). The statistical significance of HDAC11 knockdown could not be assessed as only one data point for each knockdown was observed (HDAC11 expression was below the limits of detection in the other samples) (figure 4.10c).

Basal *MMP13* expression was increased in response to HDAC6 knockdown when compared to non-target control, but no change was seen when compared to the non-transfected control (Figure 4.10a). This is also seen when the data are presented as fold-change (Figure 4.11a and b). Therefore, the effect of HDAC6 knockdown on basal *MMP13* expression is unclear and requires further investigation. HDAC10 and HDAC11 knockdown resulted in increased basal *MMP13* expression when compared to both the non-target and non-transfected IL-1α controls, with the induction of *MMP13* in correlation with HDAC11 knockdown reaching statistical significance (Figure 4.10b and c). This suggests that HDAC10 and HDAC11 may repress basal *MMP13* expression under normal conditions in primary articular chondrocytes.

Cytokine-induced *MMP13* expression was significantly increased in response to HDAC6 and HDAC11 knockdown compared to both the non-target and non-transfected IL-1α controls (Figure 4.10a and c). This was also seen when the data were expressed as the fold change of *MMP13* expression: HDAC6 knockdown resulted in a greater than 1-fold increase in *MMP13* expression when compared to the non-target siRNA control, and a greater than 3.5-fold increase when compared to the non-transfected IL-1α control (Figure 4.11a and b). HDAC11 knockdown resulted in a 1.5-fold increase in *MMP13* expression when compared to non-target siRNA control, and a greater than 1-fold increase in expression compared to the non-transfected IL-1α control (Figure 4.11a and b). The further induction of IL-1α-induced *MMP13* expression in response to HDAC6 and HDAC11 knockdown indicates that both enzymes may inhibit cytokine induction of *MMP13* in primary articular chondrocytes. The fact that HDAC6 appears to play an inhibitory role in the induction of *MMP13* is surprising since tubacin was previously

shown to repress cytokine induction of the collagenases in SW1353 cells and is chondroprotective in the BNC assay. The effect of tubacin on cytokine-induced *MMP13* expression is yet to be assessed in primary chondrocytes by qRT-PCR, which may again suggest that HDAC regulation of *MMP13* differs between the primary cells and the transformed cell line.

Cytokine-induced *MMP13* expression was also slightly increased by HDAC10 knockdown, but this did not reach statistical significance compared to non-target or non-transfected IL-1α control (Figure 4.9b).

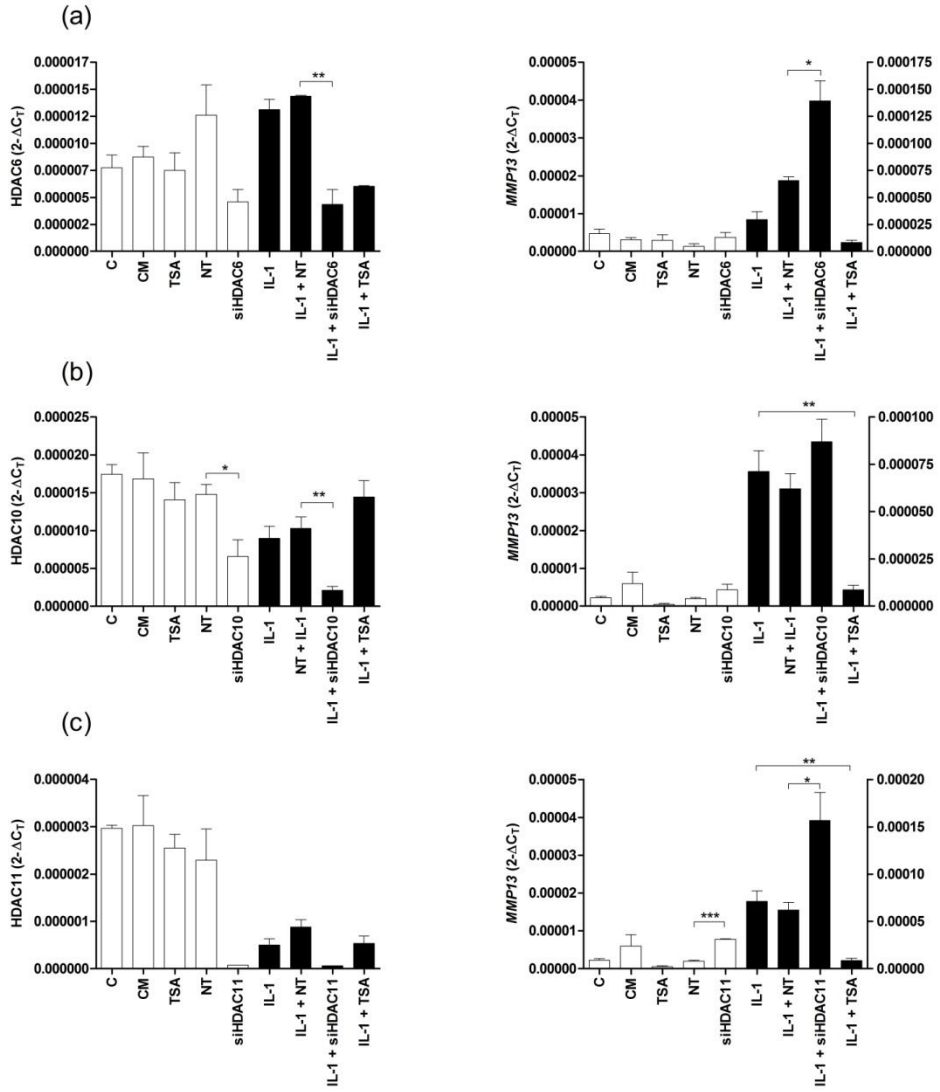

Figure 4.10. The effect of siRNA knockdown of class IIb HDACs and HDAC11 on *MMP13* expression in primary articular chondrocytes

Primary articular chondrocytes were incubated with 25nM siRNA for 24 hours in serum-containing medium. Cells were then serum-starved overnight, followed by IL-1α (5ng/ml) and/or TSA (50ng/ml) treatment (where appropriate) for 6 hours. Total RNA was extracted with Cells-to-cDNA lysis buffer, reverse transcribed to cDNA, and *MMP13* and HDAC expression detected by real-time qRT-PCR. **(a)** HDAC6 and *MMP13* expression after siRNA treatment. **(b)** HDAC10 and *MMP13* expression after siRNA treatment. **(c)** HDAC11 and *MMP13* expression after siRNA treatment. Assays were completed twice, using triplicate samples. Data presented are representative of one assay; means ± standard errors are represented. **P*<0.05, ***P*<0.01, ****P*<0.001. For *MMP13* expression graphs, non-cytokine treated samples correspond to the left Y axis, and cytokine-treated samples correspond to the right Y axis. *(C, control; CM, control-mock transfection; NT, non-targeting siRNA; siHDACx, HDAC siRNA)*

In conclusion, the knockdown data from primary chondrocytes is difficult to interpret due to the off-target effect of the AllStars non-target siRNA control. However, these data still identify possible roles for specific HDACs in *MMP13* regulation. For example, HDAC1 and HDAC11 knockdown caused clear induction of basal and cytokine-induced *MMP13*. This suggests that both enzymes repress both basal and IL-1α-induced *MMP13* expression in primary articular chondrocytes. HDAC5 and HDAC6 knockdown also resulted in the further potentiation of IL-1α-induced *MMP13* expression, suggesting that both enzymes inhibit cytokine induction of *MMP13* in primary articular chondrocytes. Conversely, HDAC3 and HDAC8 knockdown resulted in reduced basal and IL-1α-induced *MMP13* expression, indicating that both enzymes have an activatory role in the transcription of *MMP13*. The role of other HDACs in the transcriptional regulation of *MMP13* is less clear due to the off-target effects of the non-targeting control. This means that the knockdown assays need to be repeated to clarify the role of individual HDACs in the regulation of *MMP13* in primary chondrocyte cells. However, a non-targeting siRNA that consistently has no effect on *MMP13* expression will first have to be identified in order to validate future data.

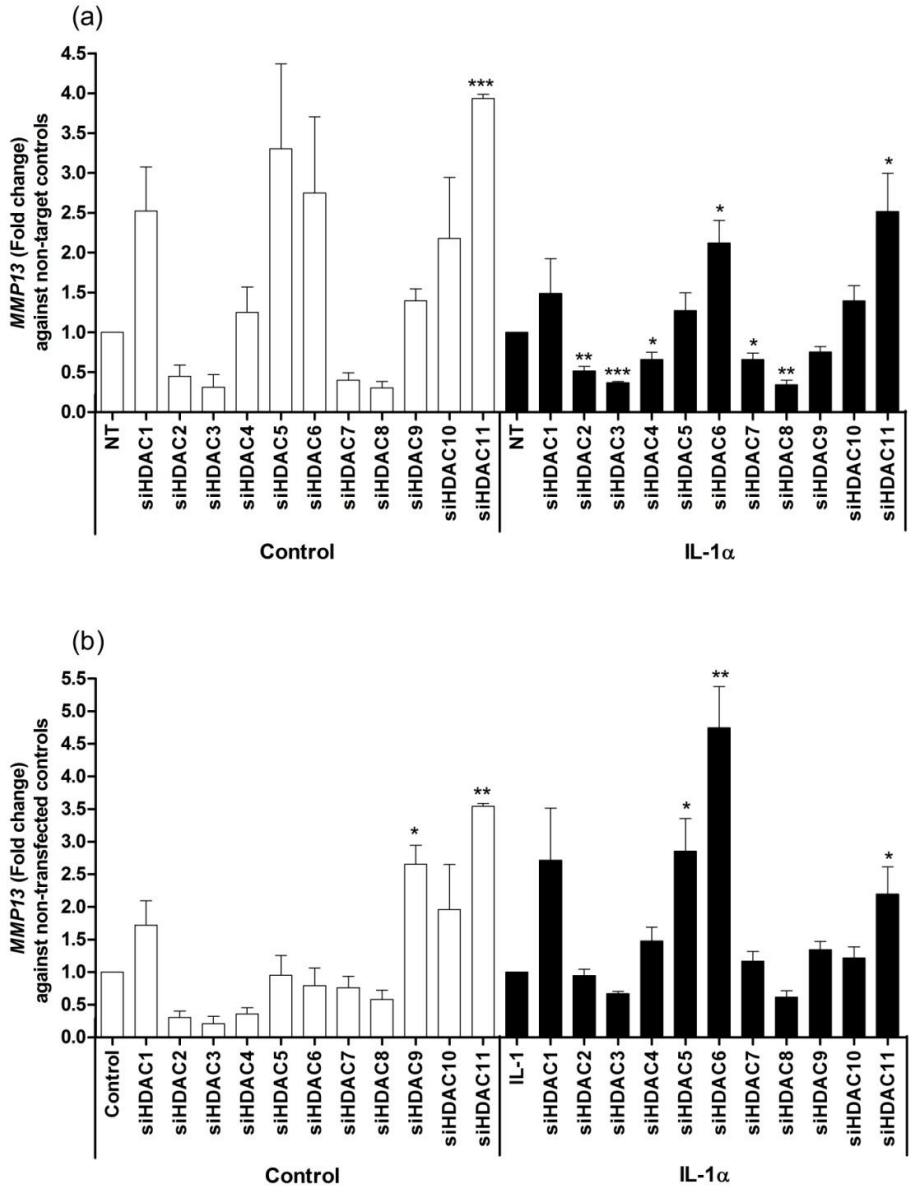

Figure 4.11 *MMP13* expression after siRNA knockdown of classical HDACs in primary articular chondrocyte cells.

Primary articular chondrocytes were incubated with 25nM siRNA for 24 hours in serum-containing medium. Cells were then serum-starved overnight, followed by IL-1α (5ng/ml) treatment (where appropriate) for 6 hours. Total RNA was extracted with Cells-to-cDNA lysis buffer, reverse transcribed to cDNA, and *MMP13* expression detected by real-time qRT-PCR. **(a)** Data presented are representative of the fold change of *MMP13* expression compared to non-targeting siRNA controls after HDAC knockdown. **(b)** Data presented are representative of the fold change of *MMP13* expression compared to control and IL-1α samples (which were not transfected with siRNA) after HDAC knockdown. The data are representative of one experiment using triplicate samples; means ± standard errors are represented. **P*<0.05, ***P*<0.01, ****P*<0.001. *(C, control; NT, non-targeting siRNA; siHDACx, HDAC siRNA)*

4.2.5 TSA alters HDAC3 and HDAC7 expression in SW1353 cells

It has previously been reported that broad spectrum inhibitors TSA and vorinostat (Merck; trade name Zolinza) can not only alter HDAC activity, but can also alter the transcriptional expression of specific HDACs in various cell lines (Dokmanovic et al, 2007; Hemmatazad et al, 2009). For example, TSA has been shown to directly suppress HDAC7 expression and increase HDAC3 expression in systemic sclerosis (SSc) skin fibroblasts at both the mRNA and protein level (Hemmatazad et al, 2009). Consistent with this, it was also noted in the HDAC siRNA knockdown assays undertaken in this thesis that TSA could alter HDAC expression in SW1353 and primary chondrocyte cells. This included the induced expression of HDAC3 and HDAC4 in the SW1353 cell line, and HDAC3, HDAC4 and HDAC5 in primary articular chondrocytes. In order to confirm if TSA could alter HDAC expression in the chondrocyte cell line in a concentration-dependent manner, SW1353 cells were incubated with increasing concentrations of TSA (5ng/ml, 25ng/ml, 50ng/ml and 100ng/ml) in the presence or absence of IL-1α or I/O (a combination of IL-1α (5ng/ml) and OSM (10ng/ml). The expression of HDAC1, HDAC2, HDAC3, HDAC4 and HDAC7 were then detected by qRT-PCR.

Consistent with the findings of Hemmatazad *et al*. (2009) in SSc skin fibroblasts, TSA induced HDAC3 expression (Figure 4.8a) and reduced HDAC7 expression (Figure 4.8b) in a concentration-dependent manner in the SW1353 cell line. The expression of HDAC1 and HDAC2 were unaltered by TSA treatment (data not shown). HDAC4 expression was significantly induced in response to 50ng/ml TSA (data not shown), which was consistent with the induction observed in the siRNA knockdown assays. However, the expression of HDAC4 was unaffected by all other TSA concentrations tested. HDAC expression remained unaltered in response to cytokine treatment, indicating that cytokines do not affect the transcriptional expression of HDACs. Therefore, these results demonstrate that TSA not only inhibits the catalytic activity of HDACs in the SW1353 cell line, but can also alter their expression at the mRNA level. It is yet to be confirmed if TSA can alter the expression of other HDACs in SW1353 cells and whether these changes in expression are seen at the protein level. It would also be interesting to confirm if more specific inhibitors such as MS-275 and tubacin can bring about changes in HDAC expression.

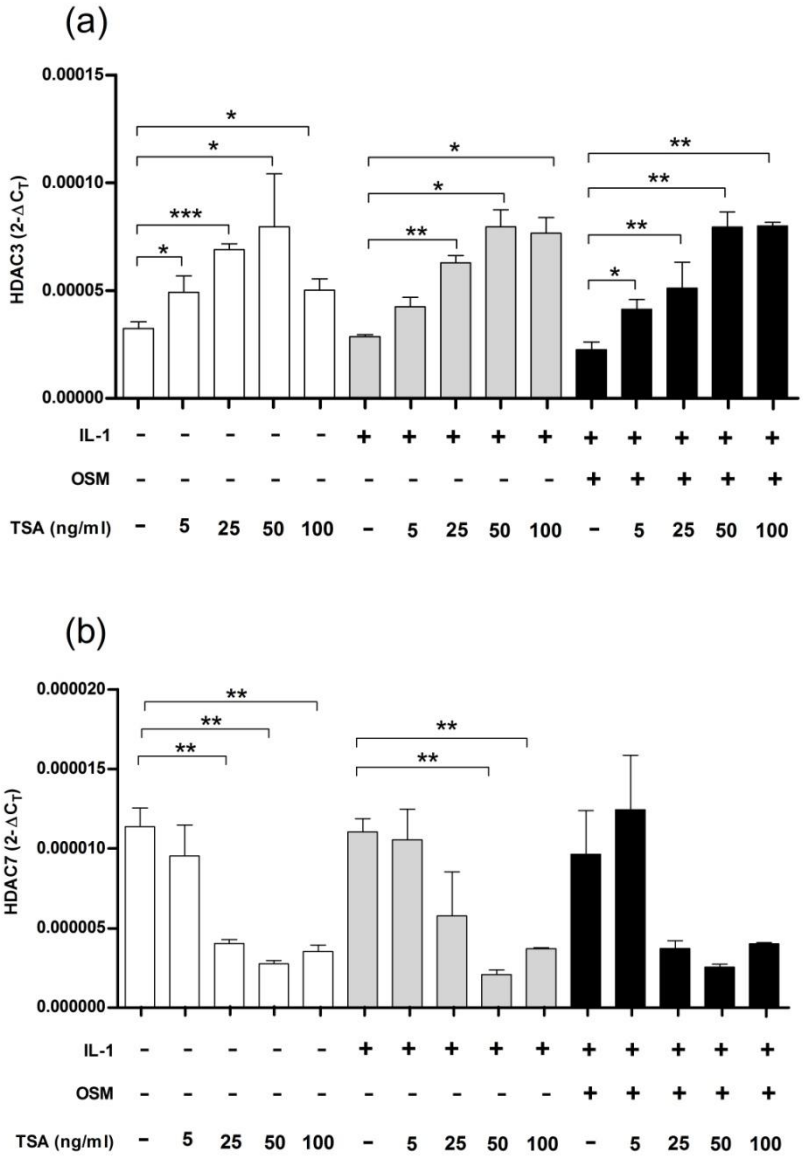

Figure 4.12. TSA alters HDAC3 and HDAC7 expression in the SW1353 cell line

SW1353 cells were incubated with increasing concentrations of TSA (5ng/ml, 25ng/ml, 50ng/ml and 100ng/ml) alone, and in the presence of IL-1α (5ng/ml) or I/O (combination of IL-1α and OSM (10ng/ml)) for 6 hours. Total RNA was extracted with Trizol, reverse transcribed to cDNA, and HDAC levels detected by real-time qRT-PCR. **(a)** HDAC3 expression after TSA treatment alone and in combination with cytokines. **(b)** HDAC7 expression after TSA treatment alone and in combination with cytokines. Assays were completed once using triplicate samples: means ± standard errors are represented. **P*<0.05, ***P*<0.01, ****P*<0.001.

4.3 Discussion

Broad spectrum and specific HDAC inhibitors have been shown to repress cytokine-induced metalloproteinase expression in cell monolayer assays, cartilage explant assays and in an OA rabbit model (Chen et al, 2010; Young et al, 2005). Importantly, HDAC inhibitors have also been shown to prevent *in vitro* and *in vivo* cartilage degradation, with their chondroprotective effect attributed to their ability to repress induced metalloproteinase expression (Chen et al, 2010; Young et al, 2005). The precise molecular pathways by which HDAC inhibitors mediate the repression of metalloproteinase expression are unknown. However, in this study it was hoped that by elucidating the individual roles of classical HDACs in the regulation of metalloproteinase expression that these pathways would become clearer.

The role of HDACs in OA cartilage was first explored by screening the expression of all classical HDACs in OA hip cartilage versus normal cartilage by TLDA array. This profile indicated that a majority of HDACs have significantly lower expression in OA cartilage including HDAC2, HDAC3, HDAC5, HDAC7, HDAC8 and HDAC11 compared to normal cartilage. HDAC10 was the only HDAC found to have significantly increased expression in OA cartilage. These results contrast with a previously published profile of HDAC expression in OA cartilage, which found that HDAC7 expression was significantly increased in OA cartilage and that HDAC4 and HDAC10 were substantially decreased (Higashiyama et al, 2009). As previously stated, the contrasting results between the two profiles could be due to a number of experimental variables, such as the joint from which cartilage samples were taken, the difference between the mean age of patients from which normal cartilage samples were taken, and possibly post-surgical processing of the tissue samples. For example, a previous metalloproteinase profile conducted by our laboratory found that *MMP1* expression was decreased in OA hip cartilage compared to NOF control cartilage, but increased in OA knee cartilage compared to post-mortem cartilage (Kevorkian et al, 2004). This is an example of how gene regulation may vary in cartilage derived from different joints, which may account for the contrasting HDAC expression detected by the two profiles. Also, chondrocytes derived from older patients have been found to have reduced metabolic activity, reduced proliferation and altered gene expression compared to chondrocytes derived from the cartilage of younger patients (Barbero et al, 2004; Dozin et al, 2002). Therefore, the large difference between the mean age of

normal cartilage donors used in the two studies could also contribute to the conflicting results. It should also be noted that the Higashiyama profile had not age-matched normal cartilage (30.8 years) and OA cartilage (71.6 years) samples, which may have led to anomalies within the Higashiyama study itself. Overall however, the HDAC profile of this study suggests that the hypothesis put forward by Higashiyama *et al*. (2009), stating that elevated HDAC7 in OA may contribute to cartilage degradation via promoting *MMP13* gene expression, is likely not true in the hip. Therefore, profiles with much larger sample numbers need to be completed to clarify the altered expression of HDACs in OA cartilage and to determine the potential consequences of this. It may also be better to profile HDAC expression in an OA animal model. This would enable HDAC expression to be profiled in response to OA development and progression.

As previously discussed, specific HDACs have already been implicated in the transcriptional regulation of members of the matrix metalloproteinase family; HDAC1 has been shown to repress the activity of the *MMP28* promoter (Swingler et al, 2010) and HDAC7 is postulated to induce *MMP13* expression (Higashiyama et al, 2009). Due to the significant role that MMP-13 is predicted to play in OA cartilage degradation, this project aimed to establish which classical HDACs play a role in the regulation of this enzyme and confirm the findings of Higashiyama *et al*. (2009). In order to do this siRNAs were used to knock down the expression of each classical HDAC at the mRNA level in non-stimulated and IL-1α-stimulated SW1353 cells and primary articular chondrocytes, with the effect of knockdown on *MMP13* expression assessed by qRT-PCR. We hypothesised that specific siRNA knockdown of each HDAC would potentially elucidate those that impact on *MMP13* expression, enabling selective inhibition of these enzymes in order to regulate *MMP13* expression. This proved not be a trivial undertaking, primarily due to the difficulty of finding a non-targeting siRNA that did not influence the expression of *MMP13*. Preliminary experiments in the SW1353 cell line showed that non-targeting siRNAs could significantly alter basal and IL-1α-induced *MMP13* expression, with siGENOME Non-Targeting Pool 2 (Dharmacon) causing induction of *MMP13* expression and Silencer® Negative Control #1 siRNA (Ambion) causing the repression of *MMP13*. The AllStars Negative Control (Qiagen) was finally found to have no effect on *MMP13* expression in the SW1353 cell line, so was used as the comparative control for the knockdown assays carried out in these cells. However, despite the AllStars Negative Control having no effect on *MMP13*

expression in SW1353 cells and the preliminary experiment conducted in primary articular chondrocytes, it was unfortunately found to alter both basal and cytokine-induced *MMP13* expression in the final experiment conducted in primary cells.

This study is not the first to see off-target effects with multiple non-targeting siRNAs, with a study conducted by Xu *et al*. (2007) reporting the induction of adipocyte differentiation (adipogenesis) in human foetal femur-derived mesenchymal stem cells (foetal MSCs) in response to commercially available non-targeting siRNA controls. Interestingly, one of the siRNA controls found to induce adipogenesis was the Silencer® Negative Control #1 siRNA, which was also found to induce off-target effects in this thesis (Xu et al, 2007). Off-target siRNA effects have be shown to be caused by either the presence of a cross-hybridizing region in mRNAs to the siRNA trigger (Jackson et al, 2003), translational silencing of unrelated transcripts by siRNA acting as microRNA (Birmingham et al, 2006), or inducing a non-specific interferon response (Marques & Williams, 2005). Microarray profiles have indicated that non-targeting siRNAs can alter the expression of a large number of genes that have limited sequence similarity to siRNA triggers (Jackson et al, 2003). A study conducted by Lin *et al*. (2005) also demonstrated that a 7-nucleotide motif of complementarity between a siRNA and an unintended gene is enough to result in degradation of the gene (Lin et al, 2005), thus supporting the view that partial sequence identity can elicit non-specific effects. These studies highlight the difficulty in finding a true control for RNA interference (RNAi) studies, and the need for continued research in the development of non-targeting siRNAs.

The siRNA assays completed in the SW1353 cell line indicated that the knockdown of nearly all classical HDACs correlates with a reduction of both basal and IL-1α-induced *MMP13* expression, with the exception of HDAC1 knockdown which resulted in the further potentiation of IL-1α-induced *MMP13* expression. This was surprising as we originally hypothesised that an individual HDAC or a specific group of HDACs would be shown to regulate *MMP13* expression in SW1353 cells. This hypothesis was partially based on the results from prior HDAC inhibitor assays, with specific inhibition of HDAC6 alone capable of repressing IL-1α-induced *MMP13* expression in the SW1353 cell line and conferring a chondroprotective effect in the BNC assay. Also, the individual knockdown of HDAC7 had previously been reported to repress both basal

and IL-1α-induced *MMP13* expression (Higashiyama et al, 2009), which indicated that specific HDACs may be involved in the transcriptional regulation of *MMP13*.

The repression of basal and IL-1α-induced collagenase expression detected in response to HDAC6 knockdown in the SW1353 cells is consistent with the repression of cytokine-induced *MMP13* expression caused by tubacin treatment in these cells. This suggests that HDAC6 plays a role in activating the transcription of *MMP13* in SW1353 cells, with the inhibition of its activity enough to confer repression of cytokine-induced collagenase expression. However, this contrasts with HDAC6 knockdown in primary articular chondrocytes, where HDAC6 knockdown resulted in the further potentiation of IL-1α-induced *MMP13* expression when compared to non-target and non-transfected controls. This indicates that HDAC6 inhibits cytokine induction of *MMP13* in primary articular chondrocytes, and that HDAC6 regulation of *MMP13* expression may differ in SW1353 cells compared to primary chondrocytes. The possible inhibitory role of HDAC6 on cytokine-induced *MMP13* expression in primary chondrocytes is surprising giving that tubacin represses cytokine-induced *MMP13* expression in the SW1353 cell line, and blocks cytokine-induced cartilage degradation in the BNC model. The effect of tubacin on cytokine-induced *MMP13* expression in primary chondrocytes is yet to be established. However, the repression of cytokine-induced cartilage degradation by tubacin would suggest that the compound must inhibit the expression of key cartilage-degrading metalloproteinases, such as *MMP13*. Thus further assays will have to be completed to confirm the effect of HDAC6 knockdown and inhibition on *MMP13* expression within primary cells.

The repression of basal and IL-1α-induced *MMP13* expression in response to HDAC7 knockdown in SW1353 cells is consistent with Higashiyama *et al*. (2009). This supports the hypothesis that HDAC7 may promote *MMP13* expression in the SW1353 cell line. Due to the problems faced in this current study in selecting a non-targeting siRNA that did not affect *MMP13* expression in SW1353 cells, it is interesting to note that the HDAC7 knockdown assays carried out in the Higashiyama study did not have a non-targeting siRNA control, and instead used non-transfected, non-stimulated and IL-1-treated cells as controls (Higashiyama et al, 2009).

HDAC1 was the only HDAC in which knockdown resulted in the further potentiation of IL-1α-induced *MMP13* expression in SW1353 cells. This indicates that HDAC1 is the

only classical HDAC to play an inhibitory role on IL-1α-induced *MMP13* expression in these cells. The knockdown of other class I HDACs (HDAC2, HDAC3 and HDAC8) resulted in the significant repression of both basal and IL-1α-induced *MMP13* expression. As stated previously, class I HDAC inhibitor (of HDAC1, HDAC2 and HDAC3) MS-275 surprisingly exhibited no repression of cytokine-induced *MMP13* expression in SW1353 cells, which is perhaps more surprising due to the potentially activatory role of HDAC2 and HDAC3 in activating transcription of *MMP13* in these cells. However, MS275 also inhibits HDAC1 activity which, due to the potential inhibition of cytokine-induced *MMP13* by this HDAC, may be enough to induce *MMP13* expression and counteract the repression achieved by HDAC2 and HDAC3 inhibition. However, further assays are required to confirm the effects of class I HDACs on *MMP13* expression in SW1353 cells, and to clarify further why class I inhibition is not enough to repress cytokine-induced *MMP13* in these cells.

It must also be remembered that the effect of siRNA HDAC knockdown on *MMP13* expression could potentially vary compared to the chemical inhibition of HDAC activity. This is because siRNA knockdown results in the loss of the HDAC protein and thus protein-protein interactions that may play a critical role in cellular functions such as transcriptional regulation. This is particularly important as HDACs commonly function in large transcriptionally repressive, multi-subunit protein complexes (Alland et al, 1997; Nagy et al, 1997). This means that deletion of an individual HDAC protein could potentially abolish the formation of these multi-subunit complexes, resulting in changes in transcription and cellular functions that would not occur by the inhibition of HDAC catalytic activity. This is why it is important to compare data from both HDAC knockdown and HDAC inhibition studies. Therefore this may account for any differences observed between HDAC inhibitor and HDAC knockdown assays in this study.

Although HDAC6 is unique in that it has not been found in any known classical HDAC-containing repressive complexes, it has been found to have other important non-deacetylase functions mediated by protein-protein interaction. For example, HDAC6 is known to bind poly-ubiquitinated proteins and dynein motors via its C-terminal zinc finger, thus recruiting misfolded proteins to dynein motors for transport to the aggresome (Kawaguchi et al, 2003). Therefore, the deletion of HDAC6 protein could essentially result in changes in cellular function that would not occur with HDAC6

inhibition alone. This may account for the previously discussed discrepancy between the knockdown of HDAC6 in primary articular chondrocytes and the tubacin inhibitor data.

In conclusion, the knockdown assays undertaken in the SW1353 cell line implicate all HDACs in the regulation of *MMP13* expression. Although the role of certain HDACs in the regulation of *MMP13* is supported by previous data, it still seems unusual for all classical HDACs to be implicated in the regulation of one gene, especially as mouse knockout assays have distinguished such specific roles for each enzyme in development and cellular function. Therefore, these assays need to be repeated to determine if this is true. It must also be remembered that the SW1353 cell line is a transformed one, with the over-expression or aberrant transcriptional recruitment of HDACs observed in many cancer types (Abbas & Gupta, 2008; Halkidou et al, 2004; Song et al, 2005; Wu et al, 2001). This means that HDAC regulation of *MMP13* expression in the SW1353 cell line may not truly reflect the role of HDACs in non-transformed cell types.

The knockdown assays undertaken in primary chondrocytes are difficult to interpret due to the off-target effects of the AllStars non-target siRNA on *MMP13* expression. However, as previously stated the data still identify possible roles for specific HDACs in *MMP13* regulation, with certain HDACs consistently altering *MMP13* expression when compared to both non-target siRNA controls and non-transfected controls: HDAC1 knockdown correlated with clear induction of basal and cytokine-induced *MMP13*, which was consistent with the HDAC1 knockdown assay in the SW1353 cell line. This strongly suggests that HDAC1 represses both basal and cytokine-induced *MMP13* expression in primary chondrocytes. HDAC1 has previously been shown to repress the expression of the *MMP28* promoter through its interaction with the Sp1 transcription factor (Swingler et al, 2010). Further assays will have to be completed to determine if HDAC1 mediates the repression of *MMP13* expression through the same pathway, but to date Sp1 has not been implicated in IL-1 signalling or *MMP13* expression. HDAC11 knockdown also correlated with the induction of basal and IL-1α-induced *MMP13* expression. This suggests that HDAC11 also represses both basal and IL-1α-induced *MMP13* expression in primary chondrocytes. HDAC5 knockdown resulted in the further potentiation of IL-1α-induced *MMP13* expression when compared to non-target and non-transfected controls. This indicates that HDAC5, like HDAC6, may inhibit cytokine induction of *MMP13* in primary articular chondrocytes.

HDAC10 knockdown resulted in an induction of basal *MMP13* when compared to both non-target and non-transfected controls, suggesting that HDAC10 induces the expression of *MMP13* under normal conditions. Conversely, both the siRNA knockdown of HDAC3 and HDAC8 expression resulted in reduced basal and IL-1α-induced *MMP13* expression when compared to all controls. This indicates that both enzymes have a role in activating the transcription of *MMP13*.

The role of other HDACs in the transcriptional regulation of *MMP13* within primary articular chondrocytes is less clear due to the off-target effects of the non-targeting control. This means that the effect of HDAC knockdown on *MMP13* expression differs when compared to either the non-targeting siRNA controls or non-transfected controls. If the non-transfected controls are selected as comparative controls HDAC2 knockdown represses basal *MMP13* expression but has no effect on IL-1α-induced expression: HDAC4 knockdown represses basal *MMP13* expression, but potentiates IL-1α-induced *MMP13* expression: HDAC5 knockdown, and separately HDAC6 knockdown, has no significant effect on basal *MMP13* expression: HDAC7 knockdown has no effect on basal or IL-1α-induced *MMP13* expression: HDAC9 knockdown induces basal and IL-1α-induced *MMP13* expression and HDAC10 knockdown has no effect on IL-1α-induced *MMP13* expression.

These data suggest that HDAC7 has no regulatory role on *MMP13* expression in primary articular chondrocytes, contrasting with the postulated role of HDAC7 in activating *MMP13* expression in SW1353 cells (Higashiyama et al, 2009). HDAC7 may therefore be an example of how HDAC regulation of *MMP13* expression differs in primary cells compared to the SW1353 cell line.

This means that further knockdown assays will have to be repeated to clarify the role of individual HDACs in the regulation of *MMP13* in SW1353 cells and primary articular chondrocyte cells. A non-target siRNA that consistently has no effect on *MMP13* expression will first need to be identified to confidently interpret future knockdown data.

The pre-designed siGENOME *SMART*pool siRNAs used in this study consist of four siRNAs which are targeted to different sequences within the same mRNA. These pooled siRNAs reportedly have less off-target effects, and are guaranteed to produce at least a 75% knockdown of target-gene expression. The reduced off-target effects of the pooled

siRNAs are reportedly due to the 'effective concentration' of the duplexes within the pool: at a total siRNA concentration of 100nM, the individual duplexes comprising the pool are at a much lower concentration of approximately 25nM. Thus the off-target activity of each duplex is reportedly reduced by a concentration-dependent mechanism. However, this essentially means you are introducing four different siRNAs into the cell, which conceptually increases the possibility of off-target effects. Recently, small quantities of each siRNA within the siGENOME *SMART*pools have become available for purchase, enabling the efficiency and off-target effects of each siRNA within the *SMART*pool to be determined. The efficiency and off-target effects of the individual siRNAs within SMARTpools used in this study are yet to be established due to time constraints.

The knockdown assays undertaken in the SW1353 cell line and primary chondrocytes indicated that TSA treatment could induce the expression of certain HDACs in both cell types. This included the induced expression of HDAC3 and HDAC4 in the SW1353 cell line, and HDAC3, HDAC4 and HDAC5 in primary chondrocytes. In order to explore this further, SW1353 cells were treated with increasing concentrations of TSA in the presence or absence of IL-1α and I/O, followed by the detection of HDAC1, HDAC2, HDAC3, HDAC4 and HDAC7 expression by qRT-PCR. These assays identified that TSA significantly induces HDAC3 expression, and significantly represses HDAC7 expression, in a concentration-dependent manner within the SW1353 cell line. These findings are consistent with a previous study completed by Hemmatazad *et al*. (2009) which demonstrated that TSA treatment causes almost complete repression of HDAC7 expression and induces the expression of HDAC3 in SSc skin fibroblasts at the mRNA and protein level. However, Hemmatazad detected decreased transcripts for nearly all other HDACs in response to TSA treatment (although not to such a significant degree as HDAC7), whilst the expression of other HDACs tested in this current study remained unchanged by TSA treatment. This could suggest that the impact of TSA on HDAC expression is cell-type dependent. Interestingly, broad spectrum inhibitors vorinostat and depsipeptide have also been shown to suppress the expression of HDAC7 at the mRNA and protein level in normal, immortalised and transformed cell lines (Dokmanovic et al, 2007).

Therefore, this demonstrates that broad spectrum HDAC inhibitors not only inhibit HDAC catalytic activity, but also regulate HDAC expression at the transcriptional level.

The importance of this finding is also yet to be established. For example, any induction of HDAC expression by a broad spectrum inhibitor, such as HDAC3 by TSA, is likely to have little impact on gene function due to any translated protein also being catalytically inhibited. It is yet to be established if more specific HDAC inhibitors modulate the expression of classical HDACs. However, Hemmatazad and colleagues postulate that the anti-fibrotic properties of TSA, observed in SSc skin fibroblasts, is mediated through its repression of HDAC7 expression (Hemmatazad et al, 2009; Huber et al, 2007). Also, Dokmanovic *et al*. (2007) observed that vorinostat caused the greatest suppression of HDAC7 expression in transformed cell lines sensitive to vorinostat-induced apoptosis, with little repression observed in normal and prostate cancer cells resistant to vorinostat-induced cell death. Therefore, it was postulated that HDAC7 may be a useful biomarker for predicting the response to vorinostat therapy. Indeed a repression in the transcription and subsequent translation of HDAC protein mediated by HDAC inhibitors could alter protein-protein interactions of co-repressor complexes, potentially resulting in changes in gene expression. This indicates that the regulation of HDAC expression, as well as the inhibition of HDAC catalytic activity, may play a role in the cellular effects induced by HDAC inhibitors.

In summary, this chapter has identified that the majority of classical HDACs are repressed at the mRNA level in OA hip cartilage, which contrasts with the previous profile of HDAC expression in OA cartilage completed by Higashiyama *et al*. (2009). This thesis has also confirmed that TSA can directly alter the expression of specific HDACs within the SW1353 cell line, indicating that broad spectrum inhibitors can regulate both the catalytic activity of HDACs and their transcriptional expression. This chapter has also identified the importance and difficulty in identifying a non-targeting siRNA control to enable confident interpretation of RNA interference data. The knockdown of classical HDAC expression within the SW1353 cell line identified that multiple HDACs may play a role in inducing the transcriptional expression of both basal and IL-1α-induced *MMP13* expression within these cells. Further assays are required to confirm this. The knockdown of classical HDAC expression in primary articular chondrocytes suggested specific roles for HDAC1, HDAC3, HDAC5, HDAC6, HDAC8, HDAC10 and HDAC11 in the transcriptional regulation of *MMP13* expression. However, due to the consistent off-target effects of the non-targeting siRNA, knockdown assays will need to be repeated to confirm these results.

Chapter V: General Discussion

Chapter V

General Discussion

5.1 General discussion

The characteristic cartilage destruction seen in the OA joint is mediated by proteases of the MMP and ADAMTS families. The role of these enzymes in cartilage destruction is supported by *in vitro* assays and *in vivo* arthritis models (Milner et al, 2001; Milner et al, 2006; Neuhold et al, 2001; Stanton et al, 2005). Previously published profiles of metalloproteinase expression in OA cartilage, conducted by our laboratory, have also detected aberrant expression of these enzymes in diseased cartilage versus normal cartilage (Davidson et al, 2006; Kevorkian et al, 2004; Swingler et al, 2009). The significant role that these proteases play in OA cartilage destruction is therefore well documented.

Metalloproteinase expression is primarily regulated at the level of transcription, which itself is influenced by changes in protein acetylation. This process is catalysed by enzymes from the histone acetyltransferase (HATs) and histone deacetylase (HDACs) families (Clark et al, 2007). Our laboratory has previously shown that broad spectrum HDAC inhibitors can repress cytokine-induced metalloproteinase expression in cell monolayer cultures and inhibit cytokine-induced cartilage resorption in the BNC assay (Young et al, 2005). The chondroprotective property of HDAC inhibitors has also been supported by the reduced joint damage observed in models of inflammatory arthritis, and most recently, models of osteoarthritis as a result of HDAC inhibitor treatment. Importantly, the reduced cartilage degradation measured in an OA rabbit model in response to TSA treatment was coupled with a repression of induced IL-1α, *MMP1*, *MMP3* and *MMP13* expression (Chen et al, 2010).

The molecular pathways by which HDAC inhibitors mediate repression of cytokine-induced metalloproteinase expression remain unclear. This study aimed to determine the profile of HDAC inhibition required in order to repress metalloproteinase expression, and to understand further the role of specific HDACs in basal and cytokine-induced metalloproteinase expression through the use of siRNA technology. This was designed

to give a more comprehensive understanding of the mechanisms by which HDAC inhibitors mediate their chondroprotective effect.

The SW1353 cell line represented a well characterised and reliable cell model in which to examine the effect of HDAC inhibitors on cellular acetylation levels and cytokine-induced metalloproteinase expression relevant to cartilage. TSA, VPA and MS-275 were found to increase histone acetylation in a concentration-dependent manner within SW1353 cells, indicating that all three compounds inhibit the catalytic activity of HDACs involved in the deacetylation of histones within these cells. TSA was the only compound found to increase α-tubulin acetylation, indicating that this was the only inhibitor to block HDAC6 activity. The lack of HDAC6 inhibition mediated by MS-275 was predicted due to its reported class I HDAC (HDAC1, HDAC2 and HDAC3) specificity (Hu et al, 2003; Inoue et al, 2006). However, previous reports on the ability of VPA to inhibit HDAC6 activity were conflicting, with an early study by Gottlicher *et al*. (2001) reporting inhibition, but a later study by Gurvich *et al*. (2004) detecting no inhibition. This current study confirms the data of Gurvich *et al*. (2004), showing that HDAC6 is not inhibited by VPA. In addition, tubacin treatment was found to increase α-tubulin acetylation in SW1353 cells, supporting its role as a HDAC6 specific inhibitor. Interestingly, the induction of α-tubulin acetylation by tubacin was not absolutely concentration-dependent in SW1353 cells, contrasting with the previously published data in A549 and multiple myeloma human cell lines (Haggarty et al, 2003; Hideshima et al, 2005). This may indicate that the efficiency of tubacin varies across cell lines or cell types.

TSA, VPA and MS-275 exhibited differential effects on cytokine-induced metalloproteinase expression within the SW1353 cell line and primary articular chondrocytes. Consistent with Young *et al*. (2005), TSA decreased the expression of all the cytokine-induced genes detected in SW1353 cells in a concentration-dependent manner, as well as decreasing I/O-induced *MMP13* expression in primary articular chondrocytes.

VPA also decreased the expression of all the cytokine-induced genes detected in SW1353 cells, as well as I/O-induced *MMP13* expression in primary chondrocytes. Gurvich *et al*. (2004) reported that VPA does not inhibit HDAC6 (supported by this current study) or HDAC10 activity (Gurvich et al, 2004). This indicates that neither

HDAC6 nor HDAC10 inhibition is essential for the repression of cytokine-induced *MMP1*, *MMP3*, *MMP10* and *MMP13* expression in SW1353 cells, nor the repression of cytokine-induced *MMP13* expression in primary chondrocytes. Interestingly, VPA decreased I/O-induced *MMP1* and *MMP13* expression in SW1353 cells in a concentration-dependent manner, but a greater repression of IL-1α-induced collagenase expression was observed using 0.5mM than with 1mM VPA. We postulate that this may be a result of VPAs reported concentration-dependent class switch of inhibition from class I to both class I and II HDACs, which reportedly occurs at concentrations greater than 1mM (Gurvich et al, 2004). Despite the VPA data indicating that HDAC6 inhibition is not essential to repress I/O-induced *MMP13* expression in SW1353 and primary chondrocyte cells, the inhibition of HDAC6 alone by tubacin decreased IL-1α and I/O-induced *MMP1* and *MMP13* expression in SW1353 cells. This study therefore shows that HDAC6 inhibition alone is capable of conferring repression of cytokine-induced collagenase expression in SW1353 cells. Consistent with this, tubacin also significantly reduced cytokine-induced collagen and GAG release from bovine cartilage explants. This suggests that this compound must inhibit the expression of key cartilage degrading enzymes from primary chondrocytes when embedded within the cartilage matrix.

MS-275 was not as effective at repressing cytokine-induced metalloproteinase expression in SW1353 cells as TSA and VPA, with no concentration-dependent repression of cytokine-induced *MMP1*, *MMP10* or *MMP13* expression detected in response to MS-275 treatment. However, MS-275 did decrease cytokine-induced *MMP3* expression. Therefore TSA, VPA and MS-275 all inhibited cytokine-induced *MMP3* expression in the SW1353 cell line, suggesting that HDAC inhibitors may partially mediate their chondroprotective effect through the repression of *MMP3* expression. It is possible that the repression of cytokine-induced *MMP3* expression could result in decreased MMP-3 protein, thus reducing the activation of pro-collagenases and subsequent cartilage resorption. MS-275 decreased I/O-induced *MMP13* expression in a concentration-dependent manner in primary human articular chondrocytes, despite exhibiting no repression on I/O-induced *MMP13* expression in SW1353 cells. Importantly, this demonstrates that class I HDAC (HDAC1, HDAC2 and HDAC3) inhibition is enough to repress cytokine-induced *MMP13* expression in primary chondrocytes. This also suggests that the transcriptional regulation of *MMP13*

by class I HDACs (HDAC1, HDAC2 and HDAC3) differs in SW1353 cells compared to primary articular chondrocytes. Understanding this difference could potentially further elucidate the role of class I HDACs in the transcriptional regulation of *MMP13* expression.

The efficiency of TSA- and VPA-mediated repression of I/O-induced *MMP13* expression differed between the SW1353 cell line and primary chondrocyte cells. TSA significantly decreased I/O-induced *MMP13* expression at 25ng/ml in SW1353 cells, but a much higher concentration of 100ng/ml was required to achieve significant repression in primary chondrocytes. In contrast, 5mM VPA was required to achieve significant repression of I/O-induced *MMP13* expression in SW1353 cells, but a much lower concentration of 0.5mM significantly repressed expression in primary articular chondrocytes. This again suggests that HDAC regulation of *MMP13* expression may differ between SW1353 cells and primary chondrocytes. In addition to this, VPA at 0.5mM reportedly only inhibits class I HDACs (whether VPA inhibits HDAC8 activity is yet to be established). This further supports the theory that class I HDAC inhibition is sufficient to repress cytokine-induced *MMP13* expression in primary chondrocytes, but is not enough to repress expression in SW1353 cells. Therefore, at this stage class I HDAC inhibition (HDAC1, HDAC2 and HDAC3), or separately HDAC6 inhibition, was found to be sufficient to repress cytokine-induced *MMP* expression.

TSA, VPA and MS-275 were all found to significantly reduce cytokine-induced cartilage degradation in the BNC assay. This is consistent with the previously reported *in vivo* chondroprotection exhibited by these compounds in animal models of inflammatory arthritis, and TSA in the OA rabbit model (Chen et al, 2010; Chung et al, 2003; Keiichiro et al, 2004; Lin et al, 2007; Saouaf et al, 2009). This current study found that the chondroprotective property of MS-275 correlated with its ability to decrease cytokine-induced *MMP1*, *MMP3*, *MMP13*, *ADAMTS4* and *ADAMTS5* expression in the cytokine treated bovine cartilage explants. This confirms that MS-275 can repress I/O-induced *MMP13* expression in primary chondrocytes, whether in monolayer or embedded within the cartilage matrix. Importantly, this also indicates that class I HDAC inhibition is enough to decrease cytokine-induction of key OA-associated metalloproteinase genes of chondrocytes embedded in the cartilage matrix. Consistent with this, the recently published OA rabbit model demonstrated that TSA treatment

reduced the increased expression of *MMP1*, *MMP3* and *MMP13* expression detected in the cartilage of OA rabbit controls (Chen et al, 2010). However, this is the first study to identify that class I HDAC inhibition alone is sufficient to repress cytokine-induced metalloproteinase expression in cartilage. The effect of MS-275 on cytokine-induced metalloproteinase gene expression *in vivo* is yet to be tested.

The BNC assays of this study demonstrated that cytokine-induced proteoglycan release exhibits less sensitivity to HDAC inhibitor treatment than induced collagen release. This was found to be a result of the rapid kinetics of proteoglycan loss. This study therefore demonstrates that early harvest time points, such as day 3 of the BNC assay, are required to detect accurately the effect of HDAC inhibitor treatment on cytokine-induced GAG release.

The profile of cytokine-induced metalloproteinase expression during the BNC assay identified the significant induction of *MMP1*, *MMP3*, *MMP13*, *ADAMTS4*, *ADAMTS5* and *TIMP1* expression in cartilage explants, in response to I/O treatment. Cytokine induction of these genes is consistent with the previous profile of metalloproteinase expression in the BNC assay, conducted by Milner *et al*. (2006). I/O-induced *MMP1* and *MMP13* expression was detected as early as day 1 of this study. The early induction of collagenase genes, coupled with the late collagen release detected at day 10 of this current profile, suggests that activation of the synthesised pro-collagenases may be the key regulatory factor in cartilage degradation. This is consistent with the profile completed by Milner *et al*. (2006). However, our current profile detected slower kinetics of *MMP1* and *MMP13* induction compared to that detected in the Milner *et al*. (2006) profile, with maximal collagenase expression not being reached until day 10 of this study, but achieved at day 2 of the Milner profile. Therefore this current profile may demonstrate that a threshold of MMP-13 is required for collagen degradation, rather than its actual activation providing a regulatory step in cartilage degradation. The expression patterns of *ADAMTS4* and *ADAMTS5* also varied between the two profiles. In the study completed by Milner *et al*. (2006), *ADAMTS4* and *ADAMTS5* expression increased rapidly between days 0 and 2 then reached a plateau. However, after the rapid cytokine-induction of aggrecanase expression detected in this study between days 0 and 3, *ADAMTS4* expression steadily decreased and *ADAMTS5* expression fluctuated throughout the remainder of the assay. This current profile also found that I/O-induced

TIMP1 expression decreased between days 8 and 10, returning to near basal levels at day 14. However, Milner et al. (2006) found that after the initial induction of *TIMP1* expression, that its expression remained at a fairly constant level for the remainder of the assay. Therefore, *TIMP1* expression decreased most significantly at day 10 of this study, which correlated with the point of maximal I/O-induced *MMP1* and *MMP13* expression. This suggests that collagen degradation occurs when the expression level of catabolic enzymes, such as MMP-1 and MMP-13, exceeds that of the protease inhibitors, such as TIMP-1. This is consistent with the anabolic to catabolic shift in gene expression which is generally thought to occur in the OA joint.

The reason for the differing kinetics of collagenase gene induction and expression patterns of aggrecanase genes and *TIMP1* between this current profile and that of Milner *et al*. (2006) is not clear. However, the differences may be attributed to the variability of age or breed of animal used between both studies. The assay would have to be repeated to clarify this.

The profile of classical HDAC expression in OA cartilage versus normal cartilage indicated that a majority of HDACs have significantly lower expression in OA cartilage compared to normal, including HDAC2, HDAC3, HDAC5, HDAC7, HDAC8 and HDAC11. HDAC10 was the only HDAC found to have significantly increased expression in OA cartilage. These results contrasted with a previously published profile by Higashiyama *et al*. (2009), which found that HDAC7 expression was significantly increased in OA cartilage and that HDAC4 and HDAC10 were substantially decreased. As previously stated, the contrasting results between the two profiles could be due to a number of experimental variables between the studies. However, the HDAC profile of this study does suggest that the hypothesis of Higashiyama *et al*. (2009), stating that elevated HDAC7 in OA may contribute to cartilage degradation via promoting *MMP13* gene expression, is questionable. In order to understand the role of HDAC expression in OA onset and progression it may be best to profile HDAC expression in an OA animal model. This is because large cohorts of patients may be required to identify a correlation between HDAC expression and OA through gene profiling. Also, available human OA tissue is predominantly at ‘end stage’, and therefore does not allow the study of HDAC expression during the onset and progression of the disease.

A number of single nucleotide polymorphisms (SNPs) have been identified in the classical HDAC family, which are all listed on the international HapMap project website (www.hapmap.org). The HapMap project is a catalogue of genetic sequences of different individuals, enabling the identification of chromosomal regions where genetic variations are shared. However, despite the identification of SNPs in all members of the HDAC family, very few have been found to have clinical association. As previously discussed, a SNP in the 3'UTR of HDAC6 has been associated with the onset of X-linked chondrodysplasia. The HDAC6 3'UTR variant suppressed hsa-miR-433-mediated post-transcriptional regulation resulting in the over expression of HDAC6. It is postulated that the increased level of HDAC6 expression contributes to the chondrodysplasia phenotype through its interaction and inhibition of RUNX2 transcription factor, which is known to be essential for chondrocyte hypertrophy (Simon et al, 2010). Therefore, it would be of great interest to determine if any SNPs in the HDAC family are associated with OA onset through the genetic profiling of OA patients.

We hypothesised that specific siRNA knockdown of each individual HDAC would potentially elucidate those that impact on *MMP13* expression, enabling selective inhibition of these enzymes in order to regulate *MMP13* expression. However, the siRNA experiments completed in the SW1353 cell line indicated that the individual knockdown of nearly all classical HDACs leads to a reduction of basal and/or IL-1α-induced *MMP13* expression. The original hypothesis was partially based upon HDAC inhibitor assays showing that class I HDAC (HDAC1, HDAC2 and HDAC3) inhibition, and separately HDAC6 inhibition, was capable of repressing IL-1α-induced *MMP13* expression in cell monolayer assays and conferring a chondroprotective effect in the BNC assay. It was also based on the study of Higashiyama *et al*. (2009), which reported that the individual knockdown of HDAC7 repressed both basal and IL-1α-induced *MMP13* expression in SW1353 cells. The siRNA knockdown data in primary chondrocytes was difficult to interpret due to the off-target effects of the non-targeting siRNA on *MMP13* expression, although conclusions could be drawn from these assays by using the non-transfected controls. The knockdown assays completed in primary cells identified a more select group of HDACs to be involved in the regulation of *MMP13* expression than that seen in SW1353 cells.

HDAC1 was the only classical HDAC in which repression resulted in the further potentiation of IL-1α-induced *MMP13* expression in SW1353 cells, suggesting that HDAC1 represses cytokine induction of *MMP13* expression in SW1353 cells. Consistent with this, HDAC1 knockdown was also found to increase both basal and cytokine-induced *MMP13* expression in primary articular chondrocytes, indicating that HDAC1 also represses *MMP13* expression in primary cells. HDAC1 has previously been shown to repress the expression of the *MMP28* promoter through its interaction with the Sp1 transcription factor (Swingler 2009). However, further assays are required to determine the mechanisms by which HDAC1 may repress *MMP13* expression. Indeed, if HDAC1 is found to repress *MMP13* expression in primary chondrocytes, this would contrast with the repression of I/O-induced *MMP13* expression achieved by class I HDAC inhibition with MS-275 in these cells.

Consistent with tubacin's repression of cytokine-induced *MMP13* expression in SW1353 cells, HDAC6 knockdown resulted in decreased basal and IL-1α-induced *MMP13* expression in these cells. However, HDAC6 knockdown resulted in the further potentiation of IL-1α-induced *MMP13* expression in primary chondrocytes, suggesting HDAC6 may repress cytokine induction of *MMP13* expression in primary cells. The effect of tubacin on cytokine-induced *MMP13* expression is yet to be established in primary cells, but is required to help clarify the role of HDAC6 in the regulation of *MMP13* expression in these cells. However, as previously stated, the chondroprotective property of tubacin suggests that the compound must inhibit the expression of key cartilage degrading metalloproteinases, such as MMP-13. It must also be remembered that siRNA knockdown results in the complete loss of HDAC protein, thus abolishing not only enzymatic activity but also protein-protein interactions that are required for HDACs to form multi-subunit protein complexes and fulfil their scaffold protein functions. This means that the effect of HDAC inhibition can potentially vary compared to the effect of HDAC knockdown. This may be the cause of the discrepancy between the effect of HDAC6 knockdown and HDAC6 inhibition detected in this study. Thus further assays will have to be undertaken to confirm the effect of HDAC6 knockdown and inhibition on *MMP13* expression within primary cells.

The implication of all classical HDACs in the regulation of *MMP13* expression in SW1353 cells seems unusual. This is because it seems unlikely for all HDACs to be

implicated in the regulation of one gene, especially as mouse knockout assays have distinguished such specific roles for each enzyme in development and cellular function. However, the repression of basal and IL-1α-induced *MMP13* expression in response to HDAC7 knockdown in SW1353 cells, detected in this study, is consistent with the Higashiyama (2009) study. This therefore supports the hypothesis that HDAC7 may promote *MMP13* expression in the SW1353 cell line. In contrast HDAC7 knockdown was found to have no effect on basal or IL-1α-induced *MMP13* expression in primary articular chondrocytes. These data suggest that HDAC7 has no regulatory role on *MMP13* expression in primary articular chondrocytes, contrasting with the hypothesis of Higashiyama *et al*. (2007) that increased HDAC7 expression in OA cartilage may contribute to increased MMP-13 expression, resulting in cartilage degradation. The effect of HDAC7 knockdown on *MMP13* expression in primary chondrocytes was not reported in the Higashiyama study. However, primary articular chondrocytes and cartilage derived from the HDAC7 null mouse could be used to further explore the role of HDAC7 in the transcriptional regulation of *MMP13* expression. For example, if HDAC7 does increase *MMP13* expression, HDAC7 null chondrocytes would be postulated to exhibit a lower level of *MMP13* expression in response to cytokine treatment than wild type chondrocytes. Therefore, HDAC7 null cartilage may also be expected to exhibit a lower level of degradation in response to cytokine treatment than cartilage derived from wild type mice alone. Indeed, the use of HDAC null chondrocytes and cartilage could be used to further explore the role of all HDACs in regards to the transcriptional regulation of *MMP* expression.

It must also be remembered that the SW1353 cell line is a transformed one, with the over-expression or aberrant transcriptional recruitment of HDACs observed in many cancer types (Abbas & Gupta, 2008; Halkidou et al, 2004; Song et al, 2005; Wu et al, 2001). This may account for the implication of all HDACs in the regulation of *MMP13* expression detected in SW1353 cells by the knockdown assays of this study. Therefore, HDAC regulation of *MMP13* expression in the SW1353 cell line may not truly reflect the role of HDACs in non-transformed cell types. However, the non-specific effect of HDAC knockdown on *MMP13* expression within the SW1353 cells is most likely due to a problem in the siRNA technique used, rather than the SW1353 cells being a transformed cell line. Further assays are required to determine if this is true.

HDAC knockdown in primary chondrocytes identified that HDAC11 knockdown correlates with the induction of basal and IL-1α-induced *MMP13* expression, suggesting that HDAC11, like HDAC1, represses both basal and IL-1α-induced *MMP13* expression in primary chondrocytes. HDAC5 knockdown resulted in the further potentiation of IL-1α-induced *MMP13* expression when compared to non-target and non-transfected controls. This indicates that HDAC5, like HDAC6, may inhibit cytokine induction of *MMP13* in primary articular chondrocytes. HDAC10 knockdown resulted in an induction of basal *MMP13* expression, suggesting that HDAC10 induces the expression of *MMP13* under normal conditions. Conversely, the siRNA knockdown of HDAC3 and HDAC8 expression both resulted in reduced basal and IL-1α-induced *MMP13* expression, indicating that both enzymes have a role in activating the transcription of *MMP13*. The role of other HDACs in the transcriptional regulation of *MMP13* expression within these cells was less clear due to the off-target effects of the non-targeting control. However, the data did suggest that HDAC2 had no regulatory role in IL-1-induced *MMP13* expression. This means that the knockdown of HDAC3 (indicating that it activates *MMP13* expression) is the only knockdown assay to agree with the MS-275 data in primary chondrocytes, which showed that class I (HDAC1, HDAC2 and HDAC3) inhibition can repress I/O-induced *MMP13* expression. Overall, the knockdown assays in primary chondrocytes highlight the need to identify a non-targeting siRNA that does not influence the expression of *MMP13*, and the need to repeat these assays to clarify the conclusions drawn from the knockdown assays of this study.

This study used pre-designed siGENOME *SMART*pool siRNAs for HDAC knockdown. The siGENOME *SMART*pools consist of four siRNAs which are targeted to different sequences within the same mRNA. These *SMART*pools reportedly have reduced off-target effects due to the 'effective concentration' of the duplexes within the pool: at a total siRNA concentration of 100nM, the individual duplexes comprising the pool are at a much lower concentration, approximately 25nM. Thus the off-target activity of each duplex is reportedly reduced by a concentration-dependent mechanism. However, as stated previously this essentially means four different siRNAs are being introduced into the cell, which conceptually increases the possibility of off-target effects. The efficiency and off-target effects of each of the siRNAs within the *SMART*pools used by this study are yet to be determined. Recently, small quantities of each of the siRNAs within the

siGENOME *SMART*pools have become available to purchase, enabling the efficiency and off-target effects of each siRNA within the *SMART*pool to be determined. This would need to be completed by this study to ensure that the HDAC siRNA *SMART*pools are not producing off-target effects. It would also be interesting to compare the efficiency of HDAC knockdown, and the subsequent effect on *MMP13* expression, produced by the single siRNAs compared to their use in siRNA *SMART*pools.

This study also identified that TSA significantly induces HDAC3 expression and significantly represses HDAC7 expression within the SW1353 cell line, in a concentration-dependent manner. These findings are consistent with Hemmatazad *et al*. (2009), which demonstrated that TSA treatment causes almost complete repression of HDAC7 expression and induces the expression of HDAC3 in systemic sclerosis (SSc) skin fibroblasts. However, Hemmatazad *et al*. (2009) detected decreased transcripts for nearly all other HDACs in response to TSA treatment (although not to such a significant degree as HDAC7), where as this study detected no change in HDAC1 or HDAC2 expression in response to TSA treatment within SW1353 cells. This suggests that the impact of TSA on HDAC expression is dependent on cell type.

Interestingly, broad spectrum inhibitors vorinostat and depsipeptide have also been shown to suppress the expression of HDAC7 at the mRNA and protein level in normal, immortalised and transformed cell lines (Dokmanovic et al, 2007). This demonstrates that broad spectrum HDAC inhibitors not only inhibit HDAC catalytic activity, but also regulate HDAC expression at the transcriptional level. This study is the first to report this effect in SW1353 cells. The importance of this finding is also yet to be established as any induction of HDAC expression by a broad spectrum inhibitor, such as HDAC3 by TSA, is likely to have little impact on gene function due to any translated protein also being catalytically inhibited. However, as previously stated, HDACs are found in multi-subunit protein complexes (Alland et al, 1997; Nagy et al, 1997), as well as having other scaffold protein functions (Kawaguchi et al, 2003). Therefore, any significant change in expression, such as the large repression of HDAC7, caused by inhibitor treatment could potentially affect the non-deacetylase-related functions of HDACs. This means that HDAC inhibitors, through their regulation of HDAC expression, could potentially confer the same effect as HDAC siRNA knockdown on metalloproteinase expression. It is yet to be established if more specific HDAC

inhibitors modulate the expression of classical HDACs. However, Hemmatazad and colleagues postulate that the anti-fibrotic properties of TSA, observed in SSc skin fibroblasts, is mediated through its repression of HDAC7 expression (Hemmatazad et al, 2009; Huber et al, 2007). Also, Dokmanovic *et al*. (2007) observed that vorinostat caused the greatest suppression of HDAC7 expression in transformed cell lines sensitive to vorinostat-induced apoptosis, with little repression observed in normal and prostate cancer cells resistant to vorinostat-induced cell death. Therefore further assays are required to establish the importance of this finding.

5.2 Summary of Main Findings

The HDAC inhibitor assays of this study indicate that HDAC regulation of OA-associated metalloproteinases, such as *MMP13*, may differ between the SW1353 cell line and primary chondrocytes. For example, class I HDAC (HDAC1, HDAC2 and HDAC3) inhibition by MS-275 is sufficient to repress cytokine-induced *MMP1* and *MMP13* expression in primary cells, whether in monolayer or cartilage explant, but is not enough to decrease expression in the SW1353 cell line. This may question the validity of SW1353 cells as a model of primary chondrocytes. The validity of SW1353 cells as a model of primary chondrocytes has previously been questioned by Gebauer *et al*. (2005) due to a microarray of 312 chondrocyte relevant genes detecting little similarity between IL-1β-induced gene expression in the SW1353 cell line compared to primary chondrocytes. However, the study did state that the pattern of IL-1β-induced MMP expression, including *MMP1*, *MMP3* and *MMP13*, mirrored that or primary cells, thus supporting their use for studying the transcription regulation of metalloproteinase genes (Gebauer et al, 2005).

This thesis also revealed that inhibition of class I HDACs (HDAC1, HDAC2 and HDAC3), and separately the inhibition of HDAC6, can repress cytokine-induced cartilage degradation. The lack of phenotype in the HDAC6 null mouse suggests that specific HDAC6 inhibition may have minimal side-effects, although further research would be required to determine this. Therefore the possible use of HDAC6 specific inhibitors may provide a possible therapeutic strategy in the treatment of arthritides. This study also identified that many HDACs have decreased expression in end-stage OA cartilage compared to normal, and identified the need to profile HDAC expression in the cartilage of an OA animal model to truly understand the role of HDAC expression

in OA onset and progression. The siRNA knockdown assays of this study indicate that knockdown of nearly all classical HDACs leads to a reduction of basal and/or IL-1α-induced *MMP13* expression in SW1353 cells, whilst a more select group of HDACs were identified to regulate *MMP13* expression in primary chondrocytes. However, the knockdown assays of this study will need to be repeated with non-targeting siRNA controls which have no effect on *MMP13* expression in order to validate the conclusions drawn from the knockdown assays of this study.

In conclusion, class I HDACs and HDAC6 were found to play an important role in metalloproteinase expression, with their inhibition enough to repress the expression of cartilage degrading enzymes. Therefore, the role of these enzymes in OA and the regulation of metalloproteinase expression will be the focus of future research.

Future Directions

Future work would include determining the effect of tubacin on cytokine-induced metalloproteinase expression in primary chondrocytes, in monolayer and in cartilage explants. Tubacin's repression of cytokine-induced *MMP1* and *MMP13* expression in SW1353 cells, and its chondroprotective effect in the BNC assay, indicates that HDAC6 plays a significant role in the transcription regulation of cytokine-induced MMPs. Therefore, further elucidating the effect of tubacin on metalloproteinase expression in primary cells is essential to further understand how it mediates its chondroprotective effect. Further confirming tubacin's chondroprotective effect *in vitro* would also be required before the compound could be tested *in vivo* in a pathological setting. In order to determine the potential of using tubacin in the treatment of OA, the compound would need to be tested in an OA animal model, such as the well characterised DMM (destabilisation of the medial meniscus) model. The effect of DMM in the HDAC6 null mouse would also enable the effect of complete HDAC6 ablation on induced *MMP* expression in an OA setting. This would therefore be the aim of future research.

Due to the chondroprotection and repression of cytokine-induced *MMP* expression exhibited by MS-275, it would be of interest to determine if MS-275 can reduce induced *MMP* expression and protect against cartilage destruction in an OA animal model. Previous studies have shown that MS-275 can reduce cartilage damage in inflammatory arthritis models (Lin et al, 2007) where its use was well tolerated. However, its effect *in*

vivo on metalloproteinase expression and in an OA setting is yet to be established. The possible use of MS-275 for future OA treatment is doubtful due to the side-effects reported in clinical trials for its possible use in cancer treatment (Gore et al, 2008). Therefore, the aim of testing MS-275 in an OA animal model would be to further understand the role of class I HDACs on metalloproteinase expression in an OA setting. This could perhaps help in the development of a more specific inhibitor.

The siRNA knockdown experiments completed in this study emphasise the need for non-targeting siRNAs which do not have off-target effects in order to validate RNA interference data. Therefore, the identification of a non-targeting siRNA that does not produce off-target effects is essential for the validation of future knockdown data. The individual siRNAs within the HDAC *SMART*pool would also be tested to assure that they produce no off-target effects, and are efficient at HDAC knockdown. The use of individual siRNAs may be best for future knockdown assays, thus further assays comparing *SMART*pool siRNAs to individual siRNAs would be required. Once a non-targeting siRNA has been identified and the efficiency of HDAC knockdown assessed, the HDAC knockdown assays in SW1353 cells and primary chondrocytes will have to be repeated in order to confirm the findings of this study.

Future work would also focus on determining if class I HDACs (HDAC1, HDAC2 and HDAC3) and HDAC6 are directly recruited to the MMP-13 promoter, or whether they affect its expression indirectly via signalling pathways. This could be determined through chromatin immunoprecipitation (ChIP) assays (including ChIP-on-chip technology), as well as HDAC overexpression and knockdown assays.

Appendices

Appendix I: The effect of HDAC inhibitors on cytokine-induced *MMP* expression in SW1353 cells

Appendix I

The effect of TSA on cytokine-induced *MMP* expression in SW1353 cells

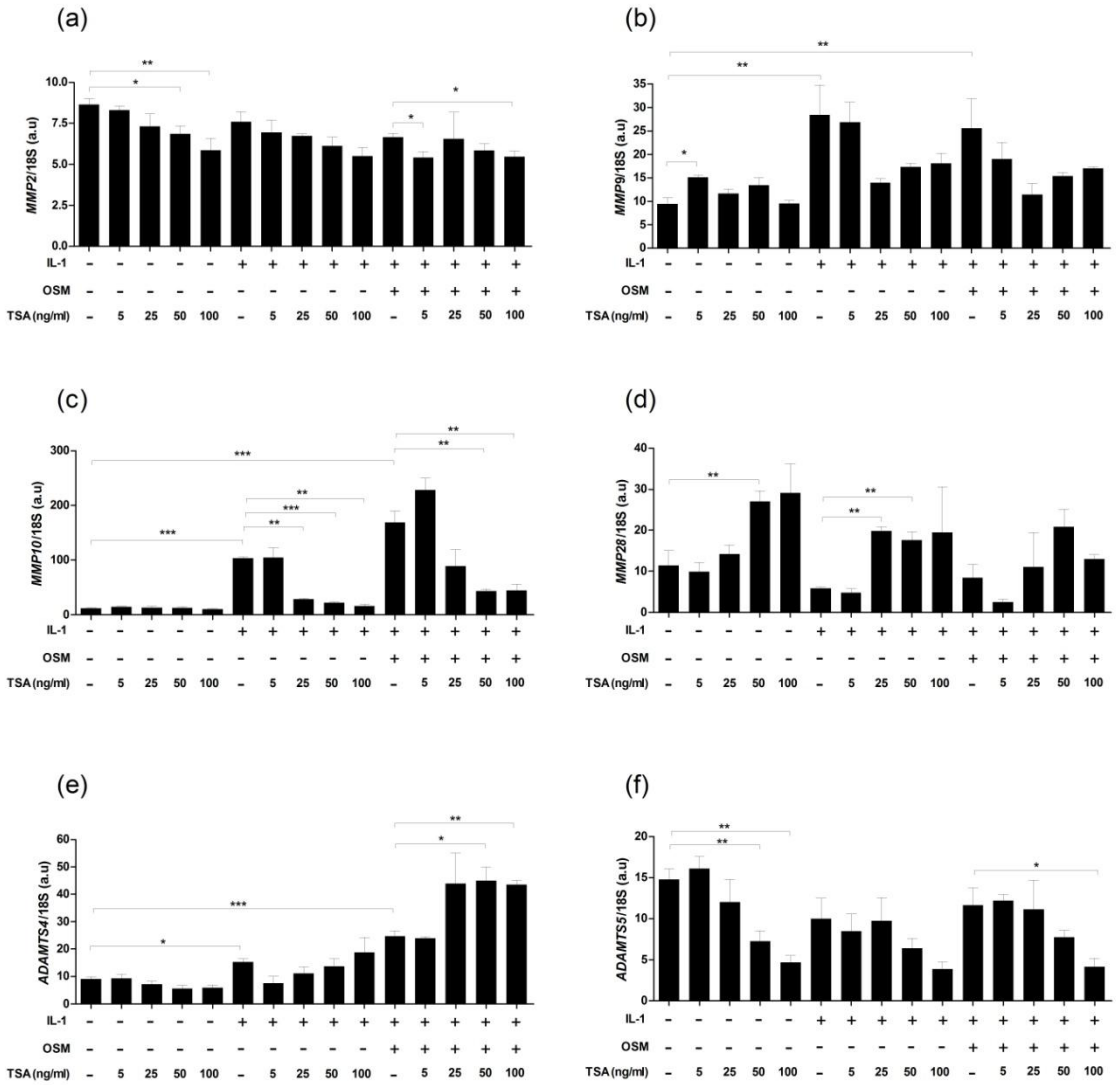

Appendix Figure 1. The effect of Trichostatin A on cytokine- induced *MMP* expression in SW1353 cells

SW1353 cells were incubated with increasing concentrations of TSA (5ng/ml, 25ng/ml, 50ng/ml and 100ng/ml) in combination with IL-1α (5ng/ml) or I/O (combination of IL-1α and OSM (10ng/ml)) for 6 hours. Total RNA was extracted with Trizol, reverse transcribed to cDNA, and *MMP* levels detected by real-time qRT-PCR **(a)** *MMP2* **(b)** *MMP9* **(c)** *MMP10* **(d)** *MMP28* **(e)** *ADAMTS4* **(f)** *ADAMTS5*. Assays were completed once, using triplicate samples; means ± standard errors are represented. **P*<0.05, ***P*<0.01, ****P*<0.001.

The effect of VPA on cytokine-induced *MMP* expression in SW1353 cells

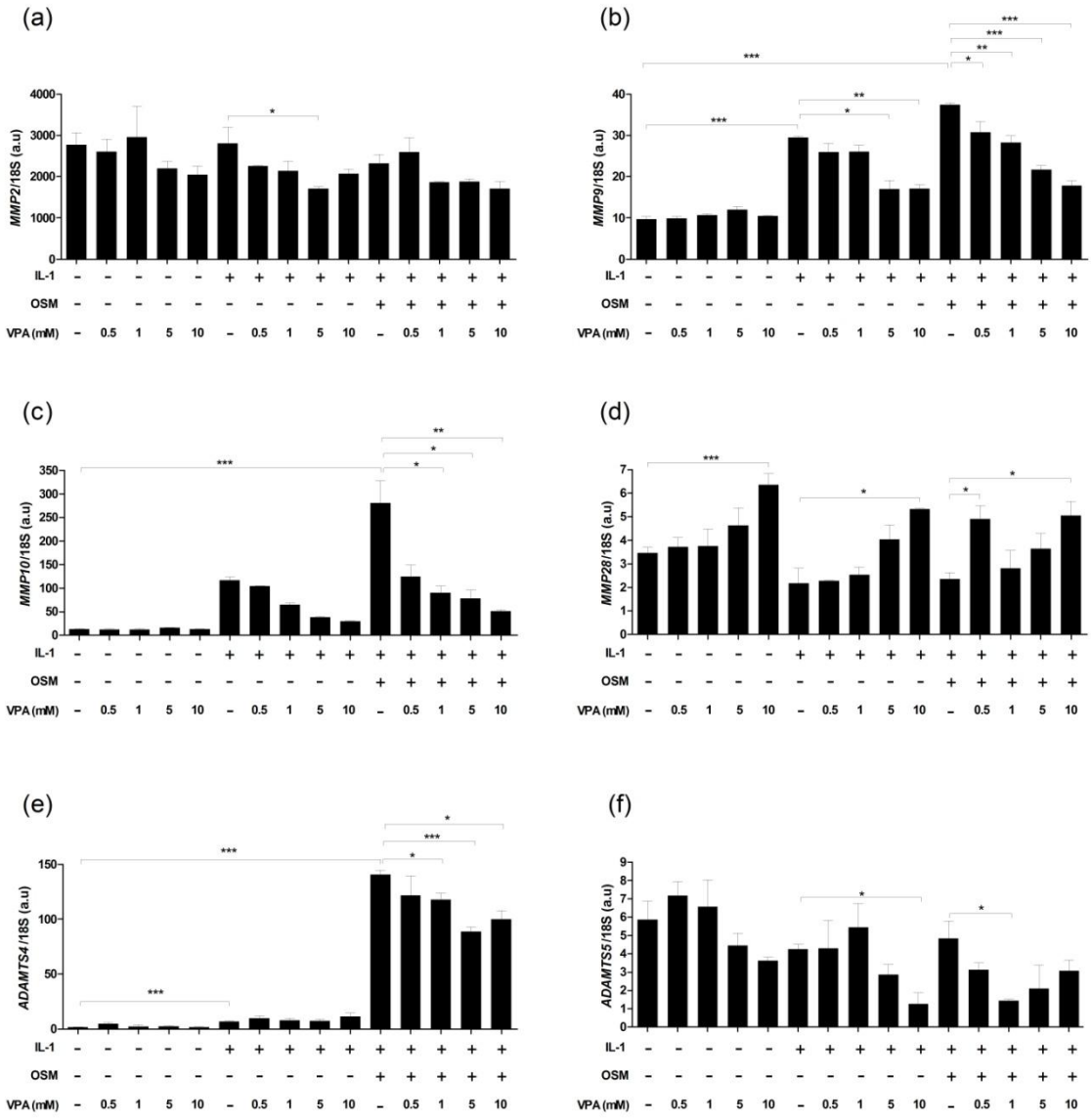

Appendix Figure 2. The effect of VPA on cytokine-induced *MMP* expression

SW1353 cells were incubated with increasing concentrations of VPA (0.5mM, 1mM, 5mM and 10mM) in combination with IL-1 (5ng/ml) or I/O (combination of IL-1 and OSM (10ng/ml)) for 6 hours. Total RNA was extracted with Trizol, reverse transcribed to cDNA, and *MMP* levels detected by real-time qRT-PCR **(a)** *MMP2* **(b)** *MMP9* **(c)** *MMP10* **(d)** *MMP28* **(e)** *ADAMTS4* **(f)** *ADAMTS5*. Assays were completed once, using triplicate samples; means ± standard errors are represented. **P*<0.05, ***P*<0.01, ****P*<0.001.

The effect of MS-275 on cytokine-induced *MMP* expression in SW1353 cells

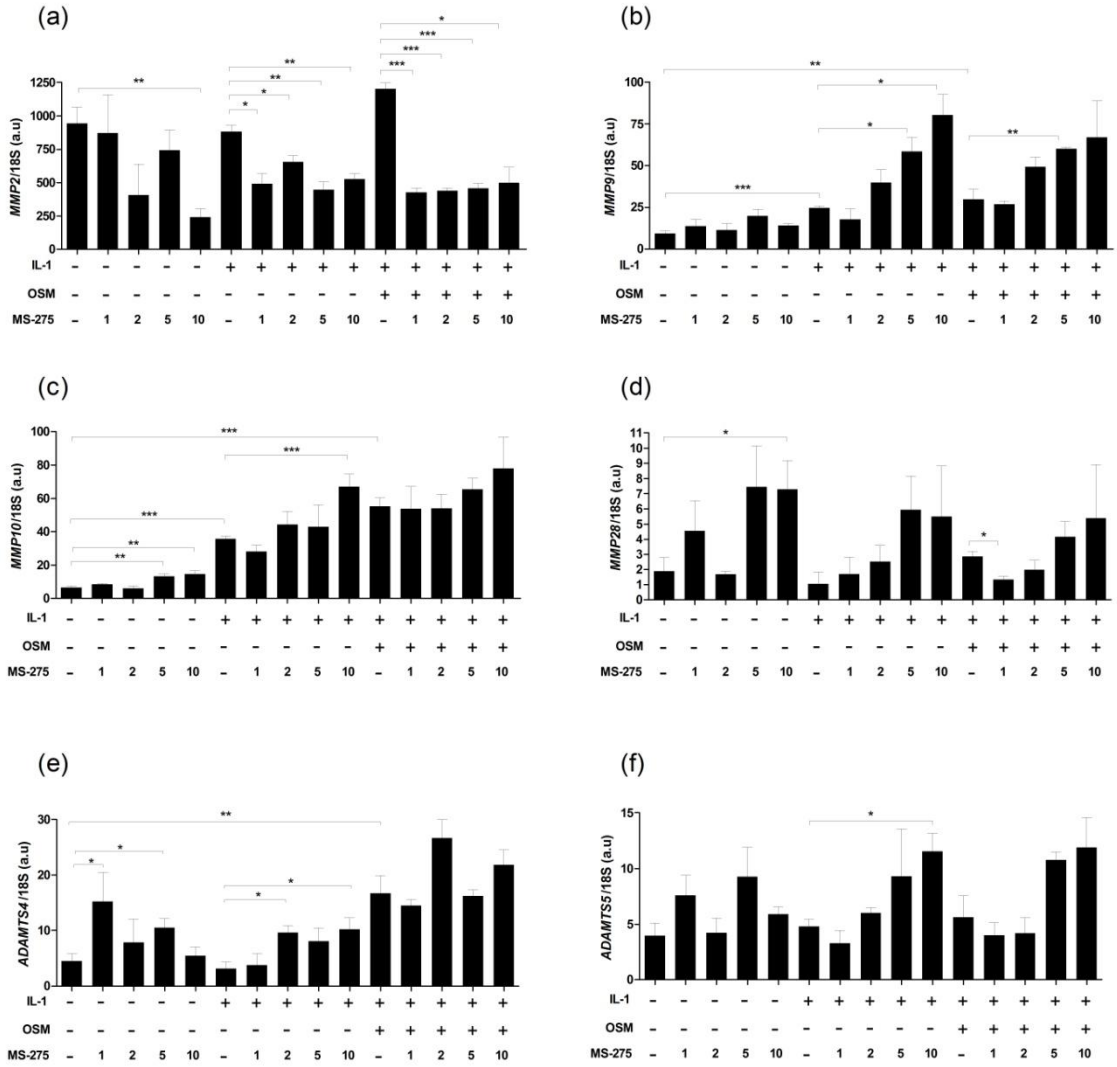

Appendix Figure 3. The effect of MS-275 on cytokine-induced *MMP* expression

SW1353 cells were incubated with increasing concentrations of MS-275 (1µM, 2µM, 5µM and 10µM) in combination with IL-1 (5ng/ml) or I/O (combination of IL-1 and OSM (10ng/ml)) for 6 hours. Total RNA was extracted with Trizol, reverse transcribed to cDNA, and *MMP* levels detected by real-time qRT-PCR **(a)** *MMP2* **(b)** *MMP9* **(c)** *MMP10* **(d)** *MMP28* **(e)** *ADAMTS4* **(f)** *ADAMTS5*. Assays were completed once, using triplicate samples; means ± standard errors are represented. **P*<0.05, ***P*<0.01, ****P*<0.001.

Appendix II: Primer Sequences

Appendix II

Primer Sequences

Gene	Primer/Probe	Sequence (5'-3')
MMP-1	Forward Primer:	AAGATGAAAGGTGGACCAACAATT
	Reverse Primer:	CCAAGAGAATGGCCGAGTTC
	Probe:	FAM-CAGAGAGTACAACTTACATCGTGTTGCGGCTC-TAMRA
MMP-2	Forward Primer:	AACTACGATGACGACCGCAAGT
	Reverse Primer:	AGGTGTAAATGGGTGCCATCA
	Probe:	FAM-CTTCTGCCCTGACCAAGGGTACAGCC-TAMRA
MMP-3	Forward Primer:	TTCCGCCTGTCTCAAGATGATAT
	Reverse Primer:	AAAGGACAAAGCAGGATCACAGTT
	Probe:	FAM-TCAGTCCCTCTATGGACCTCCCCCTGAC-TAMRA
MMP-9	Forward Primer:	AGGCGCTCATGTACCCTATGTAC
	Reverse Primer:	GCCGTGGCTCAGGTTCA
	Probe:	FAM-CATCCGGCACCTCTATGGTCCTCG
MMP-10	Forward Primer:	GGACCTGGGCTTTATGGAGATAT
	Reverse Primer:	CCCAGGGAGTGGCCAAGT
	Probe:	FAM- CATCAGGCACCAATTTATTCCTCGTTGCT-TAMRA
MMP-13	Forward Primer:	AAATTATGGAGGAGATGCCCATT
	Reverse Primer:	TCCTTGGAGTGGTCAAGACCTAA
	Probe:	FAM-CTACAACTTGTTTCTTGTTGCTGCGCATGA-TAMRA
MMP-28	Forward Primer:	TTTGAGACCTGGGACTCCTACAG
	Reverse Primer:	CCCAGAAATGGCTCCCTTTA
	Probe:	FAM- ACTCTTCCTTCGATGCCATCACTGTAGACAG-TAMRA
ADAMTS4	Forward primer:	CAAGGTCCCATGTGCAACGT
	Reverse primer:	CATCTGCCACCACCAGTGTCT
	Probe:	FAM-CCGAAGAGCCAAGCGCTTTGCTTC-TAMRA
ADAMTS5	Forward primer:	TGTCCTGCCAGCGGATGT
	Reverse primer:	ACGGAATTACTGTACGGCCTACA
	Probe:	FAM-TTCTCCAAAGGTGACCGATGGCACTG-TAMRA

Table 1. Primer probe sequences for human metalloproteinases detected in this study.

Appendix II

Gene	Universal Probe	Primers	Primer Sequence (5'-3')
HDAC1	58	Left primer: Right primer:	CAGCGATGACTACATTAAATTCTTG AGTCCTCACCAACGTTGAATC
HDAC2	72	Left primer: Right primer:	CAGATCGTGTAATGACGGTATCA CCTTTTCCAGCACCAATATCC
HDAC3	89	Left primer: Right primer:	TCTGGGCTGTGATCGATTG CTTGACATATTCAACGCATTCC
HDAC4	24	Left primer: Right primer:	GTGGTAGAACTGGTCTTCAAGG GACCACAGCAAAGCCATTC
HDAC5	3	Left primer: Right primer:	AAGGTCCTtCATCGTGGACTG GCACAGAGGGGTCATTGTAGA
HDAC6	58	Left primer: Right primer:	AGTTCACCTTCGACCAGGAC GCCAGAACCTACCCTGCTC
HDAC7	71	Left primer: Right primer:	CCATGGGGGATCCTGAGT GAGAACTCTCGGGCGATG
HDAC8	52	Left primer: Right primer:	GGCAGTTGGCAACACTCAT GTCAAGTATGTCCAGCATCGAG
HDAC9	84	Left primer: Right primer:	TCTTGGAGAAGCAGAAGCAATA GCTTCAGTTGTTCAATAGATTTCG
HDAC10	42	Left primer: Right primer:	TGGGAAGCTCCTGTACCTCTT GGCTGGAGTGGCTGCTATAC
HDAC11	80	Left primer: Right primer:	ATCACGCTCGCCATCAAGt GGCATCAAGATCAATGATGGTA

Table 2. Primer sequences for all human classical histone deacetylases and corresponding universal probes.

Appendix II

Gene	Primer	Primer sequence (5'-3')
MMP1	Left Primer:	GATGCCGCTGTTTCTGAGGA
	Right Primer:	GACTGAGCGACTAACACGACACAT
MMP3	Left Primer:	TTAGAGAACATGGGGACTTTTTG
	Right Primer:	CGGGTTCGGGAGGCACAG
MMP13	Left Primer:	CCCTCTGGTCTGTTGGCTCAC
	Right Primer:	CTGGCGTTTTGGGATGTTTAGA
ADAMTS4	Left Primer:	GCGCCCGCTTCATCACTG
	Right Primer:	TTGCCGGGGAAGGTCACG
ADAMTS5	Left Primer:	AAGCTGCCGGCCGTGGAAGGAA
	Right Primer:	TGGGTTATTGCAGTGGCGGTAGG
TIMP1	Left Primer:	TGGGCACCTGCACATCACC
	Right Primer:	CATCTGGGCCCGCAAGGACTG

Table 3. Bovine primer sequences for metalloproteinases and TIMP1 detected in this study.

Appendix III: Transfection Reagents and siRNA Sequences

Appendix III

Transfection reagents and siRNA sequences

Non-targeting siRNAs

siGENOME Non-Targeting siRNA Pool #2: (Dharmacon of Thermo Scientific, Waltham, USA)

Order number: D-001206-14-05

Silencer® Negative Control #1 siRNA: (Ambion, Warrington, UK)

Order number: AM4611

AllStar Negative Control: (Qiagen, West Sussex, UK)

Order number: 1027780

Thermo SCIENTIFIC siRNA Reagents

DharmaFECT1 Transfection Reagent: catalogue Item T-2001-02

5X siRNA Buffer Dharmacon: B-002000-UB-100

siGENOME SMARTpool M-003493-02-0005, Human HDAC1

siGENOME SMARTpool siRNA D-003493-01, HDAC1

Target sequence: CUAAUGAGCUUCCAUACAA

siGENOME SMARTpool siRNA D-003493-02, HDAC1

Target sequence: GAAAGUCUGUUACUACUAC

siGENOME SMARTpool siRNA D-003493-04, HDAC1

Target sequence: GGACAUCGCUGUGAAUUGG

siGENOME SMARTpool siRNA D-003493-09, HDAC1

Target sequence: CCGGUCAUGUCCAAAGUAA

siGENOME SMARTpool M-003495-02-0005, Human HDAC2

siGENOME SMARTpool siRNA D-003495-01, HDAC2

Target sequence: CCAAUGAGUUGCCAUAUAA

siGENOME SMARTpool siRNA D-003495-04, HDAC2

Target Sequence: GCAAAGAAAGCUAGAAUUG

siGENOME SMARTpool siRNA D-003495-05, HDAC2

Target sequence: CGGUAUCAUUCCAUAAAUA

siGENOME SMARTpool siRNA D-003495-18, HDAC2

Target sequence: CCAUAAAGCCACUGCCGAA

siGENOME SMARTpool M-003883, Human HDAC3

siGENOME SMARTpool siRNA D-003496-01, HDAC3

Target sequence: GGAAAGCGAUGUGGAGAUU

siGENOME SMARTpool siRNA D-003496-02, HDAC3

Target sequence: AAAGCGAUGUGGAGAUUUA

siGENOME SMARTpool siRNA D-003496-03, HDAC3

Target sequence: GCAUUGAUGACCAGAGUUA

siGENOME SMARTpool siRNA D-003496-04, HDAC3

Target sequence: GGAAUGCGUUGAAUAUGUC

siGENOME SMARTpool M-003883, Human HDAC3

siGENOME SMARTpool siRNA D-003497-01, HDAC4

Target sequence: CGACAGGCCUCGUGUAUGA

siGENOME SMARTpool siRNA D-003497-02, HDAC4

Target sequence: AAAUUACGGUCCAGGCUAA

siGENOME SMARTpool siRNA D-003497-06, HDAC4

Target sequence: GAGUGUCGACCUCCUAUAA

siGENOME SMARTpool siRNA D-003497-19, HDAC4

Target sequence: GUAAAUAAAGACUGCGUUA

siGENOME SMARTpool M-005474, Human HDAC5

siGENOME SMARTpool siRNA D-003498-05, HDAC5

Target sequence: GUUAUUAGCACCUUUAAGA

siGENOME SMARTpool siRNA D-003498-06, HDAC5

Target sequence: AAAGUGCGUUCAAGGCUAA

siGENOME SMARTpool siRNA D-003498-07, HDAC5

Target sequence: CAGCAGAGCACCCUCAUUG

siGENOME SMARTpool siRNA D-003498-07, HDAC5

Target sequence: GAAUUCCUCUUGUCGAAGU

siGENOME SMARTpool M-006044, Human HDAC6

siGENOME SMARTpool siRNA D-003499-01, HDAC6

Target sequence: GCACCGAGCUGAUCCAAAC

siGENOME SMARTpool siRNA D-003499-02, HDAC6

Target sequence: GAUGAGCAGUUAAAUGAAU

siGENOME SMARTpool siRNA D-003499-03, HDAC6

Target sequence: GCAGUUAAAUGAAUUCCAU

siGENOME SMARTpool siRNA D-003499-04, HDAC6

Target sequence: GGUGUUGGAUGAGCAGUUA

siGENOME SMARTpool M-001098416, Human HDAC7A

siGENOME SMARTpool siRNA D-009330-02, HDAC7A

Target sequence: GGAAGAACCUAUGAAUCUC

siGENOME SMARTpool siRNA D-009330-04, HDAC7A

Target sequence: GAAGCUAGCGGAGGUGAUU

siGENOME SMARTpool siRNA D-009330-05, HDAC7A

Target sequence: GACAAGAGCAAGCGAAGUG

siGENOME SMARTpool siRNA D-009330-06, HDAC7A

Target sequence: AGAAUCCACUGCUCCGAAA

siGENOME SMARTpool M-001098416, Human HDAC8

siGENOME SMARTpool siRNA D-003500-01, HDAC8

Target sequence: GCUGGGAGCUGACACAAUA

siGENOME SMARTpool siRNA D-003500-02, HDAC8

Target sequence: GGAAUUGGCAAGUGUCUUA

siGENOME SMARTpool siRNA D-003500-03, HDAC8

Target sequence: GCAAGUGUCUUAAGUACAU

siGENOME SMARTpool siRNA D-003500-06, HDAC8

Target sequence: GACGGAAAUUUGAGCGUAU

siGENOME SMARTpool M-0058177, Human HDAC9

siGENOME SMARTpool siRNA D-005241-07, HDAC9

Target sequence: GAACAAAUGCGACAGCAAA

siGENOME SMARTpool siRNA D-005241-09, HDAC9

Target sequence: ACAGAAUCCUCAGUCAGUA

siGENOME SMARTpool siRNA D-005241-10, HDAC9

Target sequence: CAACGCAUUCUAAUUCAUG

siGENOME SMARTpool siRNA D-005241-11, HDAC9

Target sequence: CAUCUCACCUUUAGACCUA

siGENOME SMARTpool M-032018, Human HDAC10

siGENOME SMARTpool siRNA D-004072-01, HDAC10

Target sequence: GGACCGCGCUUGUGUACCA

siGENOME SMARTpool siRNA D-004072-02, HDAC10

Target sequence: CCACUGGCCUUUGAGUUUG

siGENOME SMARTpool siRNA D-004072-03, HDAC10

Target sequence: CUCCAGACCUCGCCCAUGA

siGENOME SMARTpool siRNA D-004072-04, HDAC10

Target sequence: GGUGAACAGUGGUAUAGCA

Appendix III

siGENOME SMARTpool NM-032018, Human HDAC11

siGENOME SMARTpool siRNA D-004258-01, HDAC11

Target sequence: GCACAGAGGAUGAUGAGUA

siGENOME SMARTpool siRNA D-004258-02, HDAC11

Target sequence: CAUCAUUGCUGACUCCAUA

siGENOME SMARTpool siRNA D-004258-03, HDAC11

Target sequence: GCAAAGUGAUCAAUUUCCU

siGENOME SMARTpool siRNA D-004258-04, HDAC11

Target sequence: CACACGAGGCGCUAUCUUA

Appendix IV: The effect of HDAC knockdown on *MMP13* expression in the SW1353 cell line: Data from Preliminary Experiments

Appendix IV

The effect of HDAC knockdown on *MMP13* expression in the SW1353 cell line: Data from the preliminary experiments

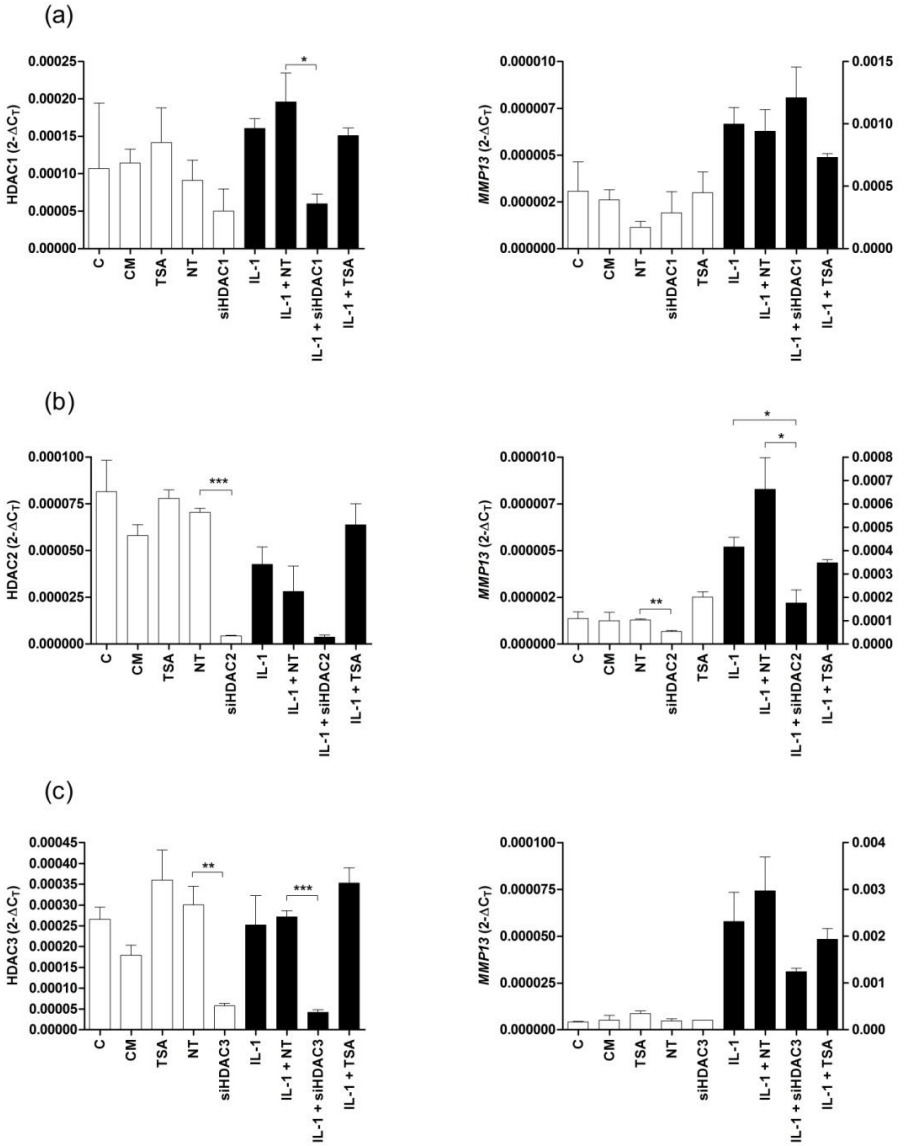

Figure 4. The effect of HDAC1, HDAC2 or HDAC3 siRNA knockdown on *MMP13* expression in the SW1353 cell line

SW1353 cells were incubated with 25nM siRNA for 24 hours in serum-containing medium. Cells were then serum-starved overnight, followed by IL-1α (5ng/ml) and/or TSA (50ng/ml) treatment (where appropriate) for 6 hours. Total RNA was extracted with Cells-to-cDNA lysis buffer, reverse transcribed to cDNA, and *MMP13* and HDAC expression detected by real-time qRT-PCR. **(a)** HDAC1 and *MMP13* expression after siRNA treatment. **(b)** HDAC2 and *MMP13* expression after siRNA treatment. **(c)** HDAC3 and *MMP13* expression after siRNA treatment. Data presented is representative of one assay; means ± standard errors are represented. **P*<0.05, ***P*<0.01, ****P*<0.001. For *MMP13* expression graphs, non-cytokine treated samples correspond to the left Y axis, and cytokine treated samples correspond to the right Y axis.

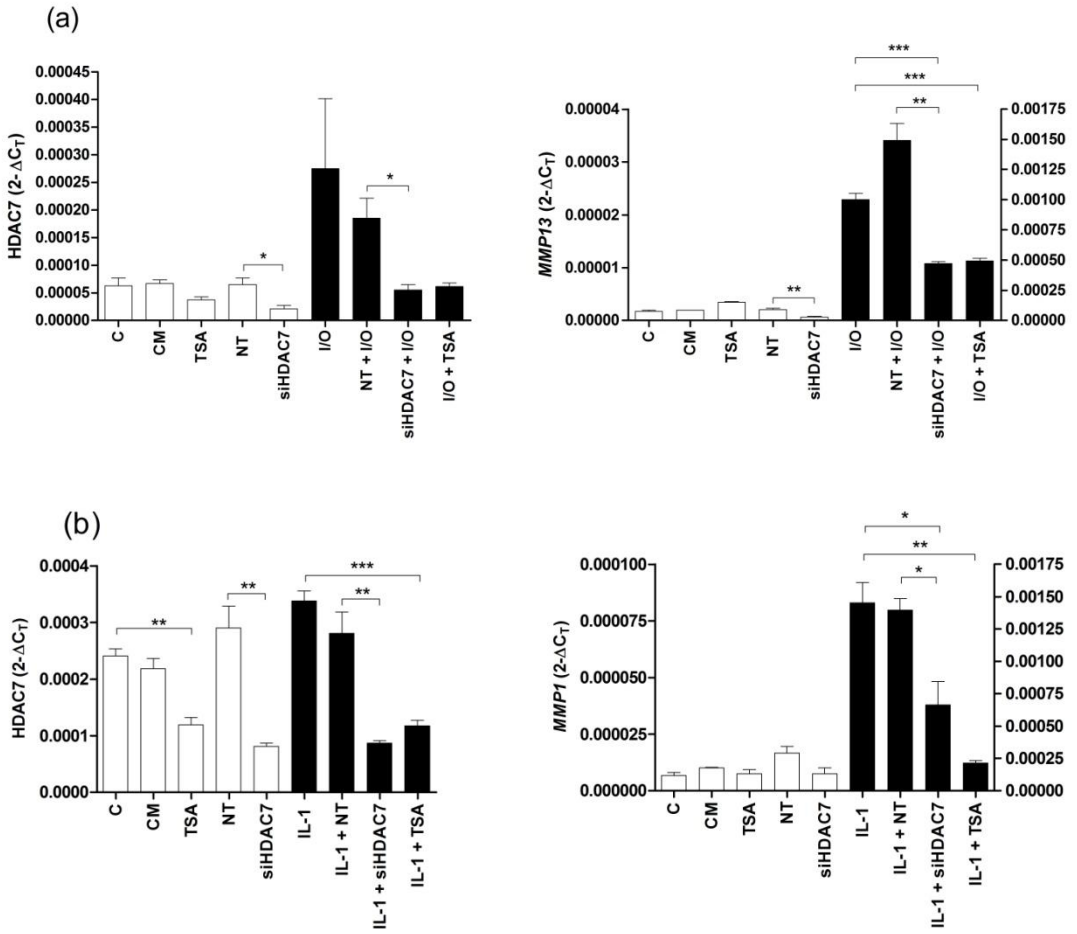

Figure 5. The effect of HDAC7 knockdown on *MMP1* and *MMP13* expression in the SW1353 cell line

SW1353 cells were incubated with 25nM siRNA for 24 hours in serum-containing medium. Cells were then serum-starved overnight, followed by IL-1α (5ng/ml) or I/O (a combination of IL-1α and OSM (10ng/ml)), and/or TSA (50ng/ml) treatment (where appropriate) for 6 hours. Total RNA was extracted with Cells-to-cDNA lysis buffer, reverse transcribed to cDNA, and *MMP13* and HDAC expression detected by real-time qRT-PCR. **(a)** HDAC7 and *MMP13* expression after siRNA treatment. Data presented is representative of one assay; means ± standard errors are represented. **(b)** HDAC7 and *MMP1* expression after siRNA treatment. **P*<0.05, ***P*<0.01, ****P*<0.001. Data presented is representative of one assay; means ± standard errors are represented. For the metalloproteinase expression graph, non-cytokine treated samples correspond to the left Y axis, and cytokine treated samples correspond to the right Y axis.

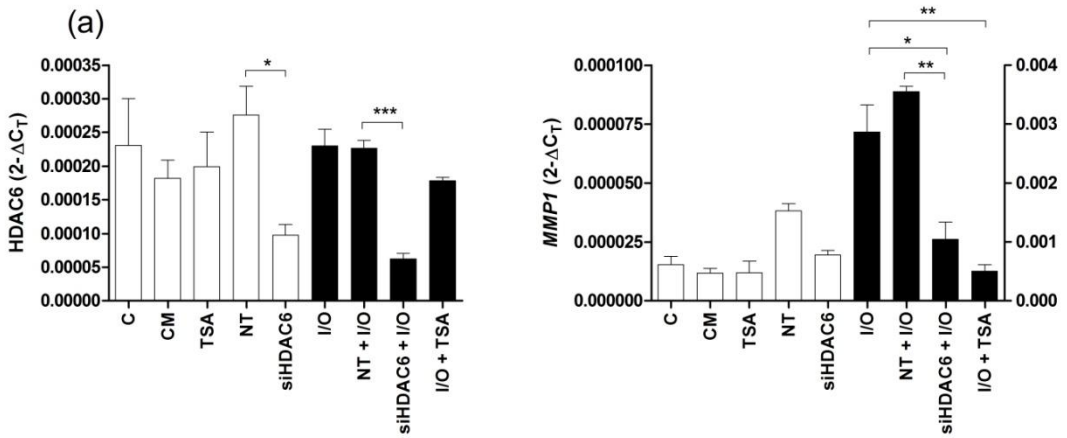

Figure 6. The effect of HDAC6 siRNA knockdown on *MMP1* expression in the SW1353 cell line

SW1353 cells were incubated with 25nM HDAC6 siRNA for 24 hours in serum-containing medium. Cells were then serum-starved overnight, followed by I/O (a combination of IL-1α (5ng/ml) and OSM (10ng/ml)) and/or TSA (50ng/ml) treatment (where appropriate) for 6 hours. Total RNA was extracted with Cells-to-cDNA lysis buffer, reverse transcribed to cDNA, and *MMP1* and HDAC expression detected by real-time qRT-PCR. **(a)** HDAC6 and *MMP1* expression after siRNA treatment. Data presented is representative of one assay; means ± standard errors are represented. **P*<0.05, ***P*<0.01, ****P*<0.001. For the *MMP11* expression graph, non-cytokine treated samples correspond to the left Y axis, and cytokine treated samples correspond to the right Y axis.

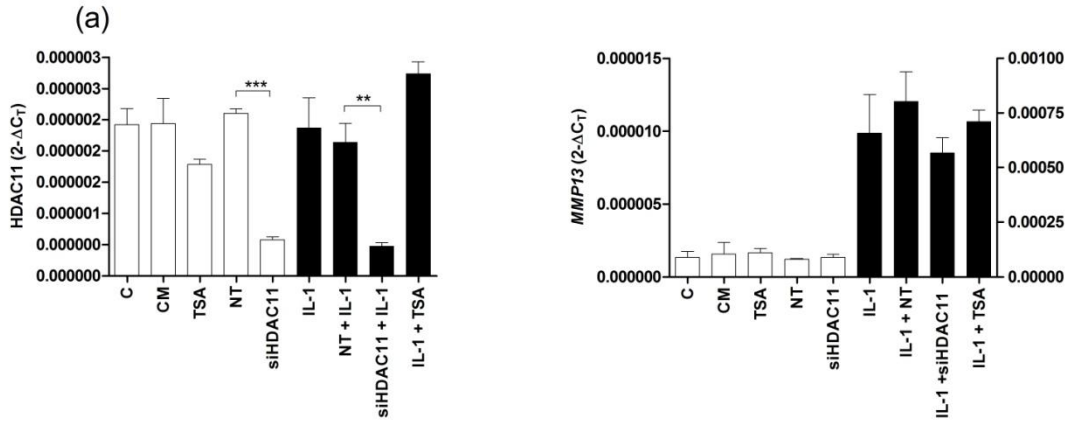

Figure 7. The effect of HDAC11 siRNA knockdown on *MMP13* expression in the SW1353 cell line

SW1353 cells were incubated with 25nM HDAC11 siRNA for 24 hours in serum-containing medium. Cells were then serum-starved overnight, followed by IL-1α (5ng/ml) and/or TSA (50ng/ml) treatment (where appropriate) for 6 hours. Total RNA was extracted with Cells-to-cDNA lysis buffer, reverse transcribed to cDNA, and *MMP1*, *MMP13* and HDAC expression detected by real-time qRT-PCR. **(a)** HDAC11 and *MMP13* expression after siRNA treatment. Data presented is representative of one assay; means ± standard errors are represented. **P*<0.05, ***P*<0.01, ****P*<0.001. For *MMP13* expression graphs, non-cytokine treated samples correspond to the left Y axis, and cytokine treated samples correspond to the right Y axis.

Appendix V: Reagents and Suppliers

Appendix V

Reagents and Suppliers

Reagent	Supplier	Product Code
1,9- Dimethyl-Methylene Blue	Sigma-Aldrich	341088
20x LumGlo Reagent and 20x Peroxide	Cell Signaling	7003
30% Acrylamide/Bis solution	Bio-Rad laboratories	161-0157
4-(Dimethylamino)benzaldehyde	Sigma-Aldrich	D2004
ABgene® PCR Plates	Thermo Scientific	AB-0600
Analytical grade RNase-free water	Fisher Scientific	W/0100/21
BCA™ Protein Assay Kit	Pierce Proteomics	23227
Bromophenol blue	Sigma-Aldrich	B-8026
Cell lysis buffer Cells-to-cDNA II	Ambion	AM8723
Chloramine T-hydrate	Sigma-Aldrich	C9887
Chondroitin 4-sulphate	Sigma-Aldrich	27042
D-Cysteine hydrochloride monohydrate	Sigma-Aldrich	C8005
Dimethyl Sulfoxide (DMSO)	Fisher Scientific	D/4121/PB08
D-MEM High Glucose	GIBCO Invitrogen	42430-025
D-MEM Low Glucose	GIBCO Invitrogen	21885-025
DNase I	Ambion	AM2222
DNase I recombinant RNase-free	Roche	04716728001
dNTP Mix (100mM total)	Bioline	BIO-39028
dNTP Mix (10mM total)	Bioline	BIO-39044
Dulbecco's Phosphate Buffered Saline (D-PBS)	Invitrogen	14190-086
Extra thick filter paper	Bio-Rad laboratories	1703960
Gentamicin	Fisher Scientific	VX15710049
Heat inactivated fetal calf serum	BioSera	51830-500
Immobilon-P polyvinylidene diflouride (PVDF)	Millipore	IPVH00010
Interleukin-1	R&D Systems	200-LA-002
Kodak BioMax maximum sensitivity film	Sigma-Aldrich	Z363030-50EA
L-Glutamine	Gibco Invitrogen	25030
Magic Marker™ XP Western Standard	Invitrogen	LC56202
MicroAmp™ 8 Cap Strip	Applied Biosystems	N801-0535
MicroAmp™ Fast Optical 96-well reaction plate	Applied Biosystems	4346906
MicroAmp™ Optical 96-well reaction plate	Applied Biosystems	N801-0560
MicroAmp™ Optical Adhesive Film	Applied Biosystems	4311971
M-MLV Reverse Transcriptase	Invitrogen	28025-021
MS-275	ALEXIS Biochemicals	270-378-M005
Nystatin	Fisher-Scientific	15340-029
Oncostatin M	R&D Systems	295-OM-010
Papain	Sigma-Aldrich	76218
$Pd(N)_6$ Random hexamers	GE Healthcare	27-2166-01
Penicillin-Streptomycin	GIBCO Invitrogen	15140-148
Perchloric Acid 70%	Fisher Scientific	P/1280/PB15
Pheno-Chloroform-Isoamyl 25:24:1	Sigma Aldrich	2069
Ponceaus Solution	Sigma	7170
Precision Plus Protein™ Dual Color Standards	Bio-Rad laboratories	161-0374
Random Primers	Invitrogen	48190-011
RNA*later*	Ambion	AM 7020
RNasin® Ribonuclease Inhibitor	Promega	N2115
Sodium Acetate	Fisher Scientific	S/2120/53

Sodium Dodecyl Sulphate (SDS)	Melford	B2008
SuperScript® II Reverse Transcriptase	Invitrogen	18064-014
SYBR® Green PCR Master Mix	Applied Biosystems	4309155
Tetramethylethylenediamine (TEMED)	Bio-Rad Laboratories	161-0800
Trans-Hydroxy-L-proline	Sigma-Aldrich	H5534
Tris Base Ultra Pure	Sigma Aldrich	B2005
Tris-sodium citrate	Fisher Scientific	S/3320/53
TRIzol® Reagent	Invitrogen	15596-018
Trypsin-EDTA (0.25% EDTA)	GIBCO Invitrogen	T4049
Tween-20	Sigma-Aldrich	P7949
Valproic Acid	Calbiochem	676380

Table 4. A list of reagents, including the suppliers and product codes, used in this study

References

References

Abbas A, Gupta S (2008) The role of histone deacetylases in prostate cancer. *Epigenetics* **3**(6)**:** 300-309

Acharya MR, Sparreboom A, Venitz J, Figg WD (2005) Rational Development of Histone Deacetylase Inhibitors as Anticancer Agents: A Review. *Mol Pharmacol* **68**(4)**:** 917-932

Aimes RT, Quigley JP (1995) Matrix metalloproteinase-2 is an interstitial collagenase. Inhibitor-free enzyme catalyzes the cleavage of collagen fibrils and soluble native type I collagen generating the specific 3/4- and 1/4-length fragments. *J Biol Chem* **270**(11)**:** 5872-5876

Alland L, Muhle R, Hou H, Jr., Potes J, Chin L, Schreiber-Agus N, DePinho RA (1997) Role for N-CoR and histone deacetylase in Sin3-mediated transcriptional repression. *Nature* **387**(6628)**:** 49-55

Almonte-Becerril M, Navarro-Garcia F, Gonzalez-Robles A, Vega-Lopez MA, Lavalle C, Kouri JB (2010) Cell death of chondrocytes is a combination between apoptosis and autophagy during the pathogenesis of Osteoarthritis within an experimental model. *Apoptosis* **15**(5)**:** 631-638

Amour A, Slocombe PM, Webster A, Butler M, Knight CG, Smith BJ, Stephens PE, Shelley C, Hutton M, Knauper V, Docherty AJ, Murphy G (1998) TNF-alpha converting enzyme (TACE) is inhibited by TIMP-3. *FEBS Lett* **435**(1)**:** 39-44

Archer CW, Rooney P, Wolpert L (1982) Cell shape and cartilage differentiation of early chick limb bud cells in culture. *Cell Differentiation* **11**(4)**:** 245-251

Arden N, Nevitt MC (2006) Osteoarthritis: epidemiology. *Best Pract Res Clin Rheumatol* **20**(1)**:** 3-25

Arnold MA, Kim Y, Czubryt MP, Phan D, McAnally J, Qi X, Shelton JM, Richardson JA, Bassel-Duby R, Olson EN (2007) MEF2C transcription factor controls chondrocyte hypertrophy and bone development. *Dev Cell* **12**(3)**:** 377-389

Ashburner BP, Westerheide SD, Baldwin AS, Jr. (2001) The p65 (RelA) subunit of NF-kappaB interacts with the histone deacetylase (HDAC) corepressors HDAC1 and HDAC2 to negatively regulate gene expression. *Mol Cell Biol* **21**(20)**:** 7065-7077

Balasubramanian S, Verner E, Buggy JJ (2009) Isoform-specific histone deacetylase inhibitors: the next step? *Cancer Lett* **280**(2)**:** 211-221

Bannuru RR, Natov NS, Obadan IE, Price LL, Schmid CH, McAlindon TE (2009) Therapeutic trajectory of hyaluronic acid versus corticosteroids in the treatment of knee osteoarthritis: a systematic review and meta-analysis. *Arthritis Rheum* **61**(12)**:** 1704-1711

References

Barbero A, Grogan S, Schafer D, Heberer M, Mainil-Varlet P, Martin I (2004) Age related changes in human articular chondrocyte yield, proliferation and post-expansion chondrogenic capacity. *Osteoarthritis Cartilage* **12**(6)**:** 476-484

Barksby HE, Hui W, Wappler I, Peters HH, Milner JM, Richards CD, Cawston TE, Rowan AD (2006) Interleukin-1 in combination with oncostatin M up-regulates multiple genes in chondrocytes: implications for cartilage destruction and repair. *Arthritis Rheum* **54**(2)**:** 540-550

Benito MJ, Veale DJ, FitzGerald O, van den Berg WB, Bresnihan B (2005) Synovial tissue inflammation in early and late osteoarthritis. *Ann Rheum Dis* **64**(9)**:** 1263-1267

Berg WBvd, Miossec P (2004) *Cytokines and joint injury*, Basel: Birkhäuser.

Bhaskara S, Chyla BJ, Amann JM, Knutson SK, Cortez D, Sun Z-W, Hiebert SW (2008) Deletion of Histone Deacetylase 3 Reveals Critical Roles in S Phase Progression and DNA Damage Control. *Molecular Cell* **30**(1)**:** 61-72

Bialer M, Yagen B (2007) Valproic Acid: second generation. *Neurotherapeutics* **4**(1)**:** 130-137

Bieliauskas AV, Weerasinghe SV, Pflum MK (2007) Structural requirements of HDAC inhibitors: SAHA analogs functionalized adjacent to the hydroxamic acid. *Bioorg Med Chem Lett* **17**(8)**:** 2216-2219

Billinghurst RC, Dahlberg L, Ionescu M, Reiner A, Bourne R, Rorabeck C, Mitchell P, Hambor J, Diekmann O, Tschesche H, Chen J, Van Wart H, Poole AR (1997) Enhanced cleavage of type II collagen by collagenases in osteoarthritic articular cartilage. *J Clin Invest* **99**(7)**:** 1534-1545

Birmingham A, Anderson EM, Reynolds A, Ilsley-Tyree D, Leake D, Fedorov Y, Baskerville S, Maksimova E, Robinson K, Karpilow J, Marshall WS, Khvorova A (2006) 3' UTR seed matches, but not overall identity, are associated with RNAi off-targets. *Nat Methods* **3**(3)**:** 199-204

Bitton R (2009) The economic burden of osteoarthritis. *Am J Manag Care* **15**(8 Suppl)**:** S230-235

Bjerling P, Silverstein RA, Thon G, Caudy A, Grewal S, Ekwall K (2002) Functional divergence between histone deacetylases in fission yeast by distinct cellular localization and in vivo specificity. *Mol Cell Biol* **22**(7)**:** 2170-2181

Bode W (1995) A helping hand for collagenases: the haemopexin-like domain. *Structure* **3**(6)**:** 527-530

Bode W, Gomis-Ruth FX, Stockler W (1993) Astacins, serralysins, snake venom and matrix metalloproteinases exhibit identical zinc-binding environments (HEXXHXXGXXH and Met-turn) and topologies and should be grouped into a common family, the 'metzincins'. *FEBS Lett* **331**(1-2)**:** 134-140

References

Bondeson J, Wainwright SD, Lauder S, Amos N, Hughes CE (2006) The role of synovial macrophages and macrophage-produced cytokines in driving aggrecanases, matrix metalloproteinases, and other destructive and inflammatory responses in osteoarthritis. *Arthritis Res Ther* **8**(6)**:** R187

Boyault C, Zhang Y, Fritah S, Caron C, Gilquin B, Kwon SH, Garrido C, Yao TP, Vourc'h C, Matthias P, Khochbin S (2007) HDAC6 controls major cell response pathways to cytotoxic accumulation of protein aggregates. *Genes Dev* **21**(17)**:** 2172-2181

Brentano F, Kyburz D, Schorr O, Gay R, Gay S (2005) The role of Toll-like receptor signalling in the pathogenesis of arthritis. *Cell Immunol* **233**(2)**:** 90-96

Brew K, Dinakarpandian D, Nagase H (2000) Tissue inhibitors of metalloproteinases: evolution, structure and function. *Biochim Biophys Acta* **1477**(1-2)**:** 267-283

Calich AL, Domiciano DS, Fuller R (2010) Osteoarthritis: can anti-cytokine therapy play a role in treatment? *Clin Rheumatol* **29**(5)**:** 451-455

Camphausen K, Scott T, Sproull M, Tofilon PJ (2004) Enhancement of xenograft tumor radiosensitivity by the histone deacetylase inhibitor MS-275 and correlation with histone hyperacetylation. *Clin Cancer Res* **10**(18 Pt 1)**:** 6066-6071

Canty EG, Kadler KE (2005) Procollagen trafficking, processing and fibrillogenesis. *J Cell Sci* **118**(Pt 7)**:** 1341-1353

Canty EG, Lu Y, Meadows RS, Shaw MK, Holmes DF, Kadler KE (2004) Coalignment of plasma membrane channels and protrusions (fibripositors) specifies the parallelism of tendon. *J Cell Biol* **165**(4)**:** 553-563

Cao J, Hymowitz M, Conner C, Bahou WF, Zucker S (2000) The propeptide domain of membrane type 1-matrix metalloproteinase acts as an intramolecular chaperone when expressed in trans with the mature sequence in COS-1 cells. *J Biol Chem* **275**(38)**:** 29648-29653

Carey N, La Thangue NB (2006) Histone deacetylase inhibitors: gathering pace. *Curr Opin Pharmacol* **6**(4)**:** 369-375

Caron JP, Fernandes JC, Martel-Pelletier J, Tardif G, Mineau F, Geng C, Pelletier JP (1996) Chondroprotective effect of intraarticular injections of interleukin-1 receptor antagonist in experimental osteoarthritis. Suppression of collagenase-1 expression. *Arthritis Rheum* **39**(9)**:** 1535-1544

Catterall JB, Carrere S, Koshy PJ, Degnan BA, Shingleton WD, Brinckerhoff CE, Rutter J, Cawston TE, Rowan AD (2001) Synergistic induction of matrix metalloproteinase 1 by interleukin-1alpha and oncostatin M in human chondrocytes involves signal transducer and activator of transcription and activator protein 1 transcription factors via a novel mechanism. *Arthritis Rheum* **44**(10)**:** 2296-2310

Cauwe B, Steen PE, Opdenakker G (2007) The biochemical, biological, and pathological kaleidoscope of cell surface substrates processed by matrix metalloproteinases. *Crit Rev Biochem Mol Biol* **42**(3)**:** 113-185

Cawston TE, Curry VA, Summers CA, Clark IM, Riley GP, Life PF, Spaull JR, Goldring MB, Koshy PJ, Rowan AD, Shingleton WD (1998) The role of oncostatin M in animal and human connective tissue collagen turnover and its localization within the rheumatoid joint. *Arthritis Rheum* **41**(10)**:** 1760-1771

Chabane N, Zayed N, Afif H, Mfuna-Endam L, Benderdour M, Boileau C, Martel-Pelletier J, Pelletier JP, Duval N, Fahmi H (2008) Histone deacetylase inhibitors suppress interleukin-1beta-induced nitric oxide and prostaglandin E2 production in human chondrocytes. *Osteoarthritis Cartilage* **16**(10)**:** 1267-1274

Chang S, McKinsey TA, Zhang CL, Richardson JA, Hill JA, Olson EN (2004) Histone deacetylases 5 and 9 govern responsiveness of the heart to a subset of stress signals and play redundant roles in heart development. *Mol Cell Biol* **24**(19)**:** 8467-8476

Chang S, Young BD, Li S, Qi X, Richardson JA, Olson EN (2006) Histone deacetylase 7 maintains vascular integrity by repressing matrix metalloproteinase 10. *Cell* **126**(2)**:** 321-334

Chapman K, Takahashi A, Meulenbelt I, Watson C, Rodriguez-Lopez J, Egli R, Tsezou A, Malizos KN, Kloppenburg M, Shi D, Southam L, van der Breggen R, Donn R, Qin J, Doherty M, Slagboom PE, Wallis G, Kamatani N, Jiang Q, Gonzalez A, Loughlin J, Ikegawa S (2008) A meta-analysis of European and Asian cohorts reveals a global role of a functional SNP in the 5' UTR of GDF5 with osteoarthritis susceptibility. *Hum Mol Genet* **17**(10)**:** 1497-1504

Chen L, Fischle W, Verdin E, Greene WC (2001) Duration of nuclear NF-kappaB action regulated by reversible acetylation. *Science* **293**(5535)**:** 1653-1657

Chen WP, Bao JP, Hu PF, Feng J, Wu LD (2010) Alleviation of osteoarthritis by Trichostatin A, a histone deacetylase inhibitor, in experimental osteoarthritis. *Mol Biol Rep*

Cheung KS, Hashimoto K, Yamada N, Roach HI (2009) Expression of ADAMTS-4 by chondrocytes in the surface zone of human osteoarthritic cartilage is regulated by epigenetic DNA de-methylation. *Rheumatol Int* **29**(5)**:** 525-534

Chitnavis J, Sinsheimer JS, Clipsham K, Loughlin J, Sykes B, Burge PD, Carr AJ (1997) Genetic influences in end-stage osteoarthritis. Sibling risks of hip and knee replacement for idiopathic osteoarthritis. *J Bone Joint Surg Br* **79**(4)**:** 660-664

Chung YL, Lee MY, Wang AJ, Yao LF (2003) A therapeutic strategy uses histone deacetylase inhibitors to modulate the expression of genes involved in the pathogenesis of rheumatoid arthritis. *Mol Ther* **8**(5)**:** 707-717

Cicuttini FM, Baker JR, Spector TD (1996) The association of obesity with osteoarthritis of the hand and knee in women: a twin study. *J Rheumatol* **23**(7)**:** 1221-1226

Clark IM, Swingler TE, Young DA (2007) Acetylation in the regulation of metalloproteinase and tissue inhibitor of metalloproteinases gene expression. *Front Biosci* **12:** 528-535

Clouet J, Vinatier C, Merceron C, Pot-vaucel M, Maugars Y, Weiss P, Grimandi G, Guicheux J (2009) From osteoarthritis treatments to future regenerative therapies for cartilage. *Drug Discov Today* **14**(19-20)**:** 913-925

Colige A, Li SW, Sieron AL, Nusgens BV, Prockop DJ, Lapiere CM (1997) cDNA cloning and expression of bovine procollagen I N-proteinase: a new member of the superfamily of zinc-metalloproteinases with binding sites for cells and other matrix components. *Proc Natl Acad Sci U S A* **94**(6)**:** 2374-2379

Colige A, Vandenberghe I, Thiry M, Lambert CA, Van Beeumen J, Li SW, Prockop DJ, Lapiere CM, Nusgens BV (2002) Cloning and characterization of ADAMTS-14, a novel ADAMTS displaying high homology with ADAMTS-2 and ADAMTS-3. *J Biol Chem* **277**(8)**:** 5756-5766

Cruickshanks HA, Tufarelli C (2009) Isolation of cancer-specific chimeric transcripts induced by hypomethylation of the LINE-1 antisense promoter. *Genomics* **94**(6)**:** 397-406

Dai J, Ikegawa S (2010) Recent advances in association studies of osteoarthritis susceptibility genes. *J Hum Genet* **55**(2)**:** 77-80

Davidson RK, Waters JG, Kevorkian L, Darrah C, Cooper A, Donell ST, Clark IM (2006) Expression profiling of metalloproteinases and their inhibitors in synovium and cartilage. *Arthritis Res Ther* **8**(4)**:** R124

Davie JR, Spencer VA (1999) Control of histone modifications. *J Cell Biochem* **Suppl 32-33:** 141-148

Dayer JM, Bresnihan B (2002) Targeting interleukin-1 in the treatment of rheumatoid arthritis. *Arthritis Rheum* **46**(3)**:** 574-578

de Ruijter AJ, van Gennip AH, Caron HN, Kemp S, van Kuilenburg AB (2003) Histone deacetylases (HDACs): characterization of the classical HDAC family. *Biochem J* **370**(Pt 3)**:** 737-749

Derfoul A, Miyoshi AD, Freeman DE, Tuan RS (2007) Glucosamine promotes chondrogenic phenotype in both chondrocytes and mesenchymal stem cells and inhibits MMP-13 expression and matrix degradation. *Osteoarthritis Cartilage* **15**(6)**:** 646-655

Dobosy JR, Selker EU (2001) Emerging connections between DNA methylation and histone acetylation. *Cell Mol Life Sci* **58**(5-6)**:** 721-727

Dobrovic A, Simpfendorfer D (1997) Methylation of the BRCA1 gene in sporadic breast cancer. *Cancer Res* **57**(16)**:** 3347-3350

Doherty M (2000) Genetics of hand osteoarthritis. *Osteoarthritis Cartilage* **8 Suppl A:** S8-10

Dokmanovic M, Perez G, Xu W, Ngo L, Clarke C, Parmigiani RB, Marks PA (2007) Histone deacetylase inhibitors selectively suppress expression of HDAC7. *Mol Cancer Ther* **6**(9)**:** 2525-2534

Dozin B, Malpeli M, Camardella L, Cancedda R, Pietrangelo A (2002) Response of young, aged and osteoarthritic human articular chondrocytes to inflammatory cytokines: molecular and cellular aspects. *Matrix Biol* **21**(5)**:** 449-459

Drummond DC, Noble CO, Kirpotin DB, Guo Z, Scott GK, Benz CC (2005) Clinical development of histone deacetylase inhibitors as anticancer agents. *Annu Rev Pharmacol Toxicol* **45:** 495-528

Dudhia J (2005) Aggrecan, aging and assembly in articular cartilage. *Cell Mol Life Sci* **62**(19-20)**:** 2241-2256

Duvic M, Olsen EA, Breneman D, Pacheco TR, Parker S, Vonderheid EC, Abuav R, Ricker JL, Rizvi S, Chen C, Boileau K, Gunchenko A, Sanz-Rodriguez C, Geskin LJ (2009) Evaluation of the long-term tolerability and clinical benefit of vorinostat in patients with advanced cutaneous T-cell lymphoma. *Clin Lymphoma Myeloma* **9**(6)**:** 412-416

Engel J, Prockop DJ (1991) The zipper-like folding of collagen triple helices and the effects of mutations that disrupt the zipper. *Annu Rev Biophys Biophys Chem* **20:** 137-152

Esteller M (2007) Cancer epigenomics: DNA methylomes and histone-modification maps. *Nat Rev Genet* **8**(4)**:** 286-298

Evangelou E, Chapman K, Meulenbelt I, Karassa FB, Loughlin J, Carr A, Doherty M, Doherty S, Gomez-Reino JJ, Gonzalez A, Halldorsson BV, Hauksson VB, Hofman A, Hart DJ, Ikegawa S, Ingvarsson T, Jiang Q, Jonsdottir I, Jonsson H, Kerkhof HJ, Kloppenburg M, Lane NE, Li J, Lories RJ, van Meurs JB, Nakki A, Nevitt MC, Rodriguez-Lopez J, Shi D, Slagboom PE, Stefansson K, Tsezou A, Wallis GA, Watson CM, Spector TD, Uitterlinden AG, Valdes AM, Ioannidis JP (2009) Large-scale analysis of association between GDF5 and FRZB variants and osteoarthritis of the hip, knee, and hand. *Arthritis Rheum* **60**(6)**:** 1710-1721

Felson DT, Anderson JJ, Naimark A, Walker AM, Meenan RF (1988) Obesity and knee osteoarthritis. The Framingham Study. *Ann Intern Med* **109**(1)**:** 18-24

Felson DT, Zhang Y, Hannan MT, Kiel DP, Wilson P, Anderson JJ (1993) The Effect of Postmenopausal Estrogen Therapy on Bone Density in Elderly Women. *N Engl J Med* **329**(16)**:** 1141-1146

References

Fernandes J, Tardif G, Martel-Pelletier J, Lascau-Coman V, Dupuis M, Moldovan F, Sheppard M, Krishnan BR, Pelletier JP (1999) In vivo transfer of interleukin-1 receptor antagonist gene in osteoarthritic rabbit knee joints: prevention of osteoarthritis progression. *Am J Pathol* **154**(4)**:** 1159-1169

Fernandes RJ, Hirohata S, Engle JM, Colige A, Cohn DH, Eyre DR, Apte SS (2001) Procollagen II amino propeptide processing by ADAMTS-3. Insights on dermatosparaxis. *J Biol Chem* **276**(34)**:** 31502-31509

Fernandez-Catalan C, Bode W, Huber R, Turk D, Calvete JJ, Lichte A, Tschesche H, Maskos K (1998) Crystal structure of the complex formed by the membrane type 1-matrix metalloproteinase with the tissue inhibitor of metalloproteinases-2, the soluble progelatinase A receptor. *EMBO J* **17**(17)**:** 5238-5248

Finnin MS, Donigian JR, Cohen A, Richon VM, Rifkind RA, Marks PA, Breslow R, Pavletich NP (1999) Structures of a histone deacetylase homologue bound to the TSA and SAHA inhibitors. *Nature* **401**(6749)**:** 188-193

Fischle W, Dequiedt F, Hendzel MJ, Guenther MG, Lazar MA, Voelter W, Verdin E (2002) Enzymatic Activity Associated with Class II HDACs Is Dependent on a Multiprotein Complex Containing HDAC3 and SMRT/N-CoR. *Molecular Cell* **9**(1)**:** 45

Francis-West PH, Abdelfattah A, Chen P, Allen C, Parish J, Ladher R, Allen S, MacPherson S, Luyten FP, Archer CW (1999) Mechanisms of GDF-5 action during skeletal development. *Development* **126**(6)**:** 1305-1315

Franses RE, McWilliams DF, Mapp PI, Walsh DA (2009) Osteochondral angiogenesis and increased protease inhibitor expression in OA. *Osteoarthritis Cartilage*

Fukui N, McAlinden A, Zhu Y, Crouch E, Broekelmann TJ, Mecham RP, Sandell LJ (2002) Processing of type II procollagen amino propeptide by matrix metalloproteinases. *J Biol Chem* **277**(3)**:** 2193-2201

Furumai R, Komatsu Y, Nishino N, Khochbin S, Yoshida M, Horinouchi S (2001) Potent histone deacetylase inhibitors built from trichostatin A and cyclic tetrapeptide antibiotics including trapoxin. *Proc Natl Acad Sci U S A* **98**(1)**:** 87-92

Gao L, Cueto MA, Asselbergs F, Atadja P (2002) Cloning and functional characterization of HDAC11, a novel member of the human histone deacetylase family. *J Biol Chem* **277**(28)**:** 25748-25755

Gebauer M, Saas J, Sohler F, Haag J, Söder S, Pieper M, Bartnik E, Beninga J, Zimmer R, Aigner T (2005) Comparison of the chondrosarcoma cell line SW1353 with primary human adult articular chondrocytes with regard to their gene expression profile and reactivity to IL-1[beta]. *Osteoarthritis and Cartilage* **13**(8)**:** 697-708

Gendron C, Kashiwagi M, Lim NH, Enghild JJ, Thogersen IB, Hughes C, Caterson B, Nagase H (2007) Proteolytic activities of human ADAMTS-5: comparative studies with ADAMTS-4. *J Biol Chem* **282**(25)**:** 18294-18306

Glant TT, Mikecz K, Roughley PJ, Buzas E, Poole AR (1986) Age-related changes in protein-related epitopes of human articular-cartilage proteoglycans. *Biochem J* **236**(1)**:** 71-75

Glaser KB, Staver MJ, Waring JF, Stender J, Ulrich RG, Davidsen SK (2003) Gene expression profiling of multiple histone deacetylase (HDAC) inhibitors: defining a common gene set produced by HDAC inhibition in T24 and MDA carcinoma cell lines. *Mol Cancer Ther* **2**(2)**:** 151-163

Glasson SS, Askew R, Sheppard B, Carito B, Blanchet T, Ma HL, Flannery CR, Peluso D, Kanki K, Yang Z, Majumdar MK, Morris EA (2005) Deletion of active ADAMTS5 prevents cartilage degradation in a murine model of osteoarthritis. *Nature* **434**(7033)**:** 644-648

Glasson SS, Askew R, Sheppard B, Carito BA, Blanchet T, Ma HL, Flannery CR, Kanki K, Wang E, Peluso D, Yang Z, Majumdar MK, Morris EA (2004) Characterization of and osteoarthritis susceptibility in ADAMTS-4-knockout mice. *Arthritis Rheum* **50**(8)**:** 2547-2558

Goldring MB (1999) The role of cytokines as inflammatory mediators in osteoarthritis: lessons from animal models. *Connect Tissue Res* **40**(1)**:** 1-11

Goldring MB (2000) The role of the chondrocyte in osteoarthritis. *Arthritis Rheum* **43**(9)**:** 1916-1926

Goldring MB, Goldring SR (2007) Osteoarthritis. *J Cell Physiol* **213**(3)**:** 626-634

Goldring MB, Tsuchimochi K, Ijiri K (2006) The control of chondrogenesis. *J Cell Biochem* **97**(1)**:** 33-44

Gomis-Ruth FX, Maskos K, Betz M, Bergner A, Huber R, Suzuki K, Yoshida N, Nagase H, Brew K, Bourenkov GP, Bartunik H, Bode W (1997) Mechanism of inhibition of the human matrix metalloproteinase stromelysin-1 by TIMP-1. *Nature* **389**(6646)**:** 77-81

Gore L, Rothenberg ML, O'Bryant CL, Schultz MK, Sandler AB, Coffin D, McCoy C, Schott A, Scholz C, Eckhardt SG (2008) A phase I and pharmacokinetic study of the oral histone deacetylase inhibitor, MS-275, in patients with refractory solid tumors and lymphomas. *Clin Cancer Res* **14**(14)**:** 4517-4525

Gottlicher M, Minucci S, Zhu P, Kramer OH, Schimpf A, Giavara S, Sleeman JP, Lo Coco F, Nervi C, Pelicci PG, Heinzel T (2001) Valproic acid defines a novel class of HDAC inhibitors inducing differentiation of transformed cells. *EMBO J* **20**(24)**:** 6969-6978

Greene J, Wang M, Liu YE, Raymond LA, Rosen C, Shi YE (1996) Molecular Cloning and Characterization of Human Tissue Inhibitor of Metalloproteinase 4. *J Biol Chem* **271**(48)**:** 30375-30380

Gregoretti IV, Lee YM, Goodson HV (2004) Molecular evolution of the histone deacetylase family: functional implications of phylogenetic analysis. *J Mol Biol* **338**(1)**:** 17-31

Grunstein M (1997) Histone acetylation in chromatin structure and transcription. *Nature* **389**(6649)**:** 349-352

Guilak F, Fermor B, Keefe FJ, Kraus VB, Olson SA, Pisetsky DS, Setton LA, Weinberg JB (2004) The role of biomechanics and inflammation in cartilage injury and repair. *Clin Orthop Relat Res*(423)**:** 17-26

Gurvich N, Tsygankova OM, Meinkoth JL, Klein PS (2004) Histone deacetylase is a target of valproic acid-mediated cellular differentiation. *Cancer Res* **64**(3)**:** 1079-1086

Haberland M, Mokalled MH, Montgomery RL, Olson EN (2009) Epigenetic control of skull morphogenesis by histone deacetylase 8. *Genes Dev* **23**(14)**:** 1625-1630

Haggarty SJ, Koeller KM, Wong JC, Grozinger CM, Schreiber SL (2003) Domain-selective small-molecule inhibitor of histone deacetylase 6 (HDAC6)-mediated tubulin deacetylation. *Proc Natl Acad Sci U S A* **100**(8)**:** 4389-4394

Halkidou K, Gaughan L, Cook S, Leung HY, Neal DE, Robson CN (2004) Upregulation and nuclear recruitment of HDAC1 in hormone refractory prostate cancer. *Prostate* **59**(2)**:** 177-189

Hardingham TE, Muir H (1974) Hyaluronic acid in cartilage and proteoglycan aggregation. *Biochem J* **139**(3)**:** 565-581

Hashimoto K, Oreffo RO, Gibson MB, Goldring MB, Roach HI (2009) DNA demethylation at specific CpG sites in the IL1B promoter in response to inflammatory cytokines in human articular chondrocytes. *Arthritis Rheum* **60**(11)**:** 3303-3313

Heinrich PC, Behrmann I, Muller-Newen G, Schaper F, Graeve L (1998) Interleukin-6-type cytokine signalling through the gp130/Jak/STAT pathway. *Biochem J* **334 (Pt 2):** 297-314

Hellio Le Graverand-Gastineau MP (2009) OA clinical trials: current targets and trials for OA. Choosing molecular targets: what have we learned and where we are headed? *Osteoarthritis and Cartilage* **17**(11)**:** 1393-1401

Hemmatazad H, Rodrigues HM, Maurer B, Brentano F, Pileckyte M, Distler JH, Gay RE, Michel BA, Gay S, Huber LC, Distler O, Jungel A (2009) Histone deacetylase 7, a potential target for the antifibrotic treatment of systemic sclerosis. *Arthritis Rheum* **60**(5)**:** 1519-1529

Henderson B, Revell PA, Edwards JC (1988) Synovial lining cell hyperplasia in rheumatoid arthritis: dogma and fact. *Ann Rheum Dis* **47**(4)**:** 348-349

Hess-Stumpp H, Bracker TU, Henderson D, Politz O (2007) MS-275, a potent orally available inhibitor of histone deacetylases--the development of an anticancer agent. *Int J Biochem Cell Biol* **39**(7-8)**:** 1388-1405

Hideshima T, Bradner JE, Wong J, Chauhan D, Richardson P, Schreiber SL, Anderson KC (2005) Small-molecule inhibition of proteasome and aggresome function induces synergistic antitumor activity in multiple myeloma. *Proc Natl Acad Sci U S A* **102**(24)**:** 8567-8572

Higashiyama R, Miyaki S, Yamashita S, Yoshitaka T, Lindman G, Ito Y, Sasho T, Takahashi K, Lotz M, Asahara H (2009) Correlation between MMP-13 and HDAC7 expression in human knee osteoarthritis. *Mod Rheumatol*

Holmes DF, Graham HK, Kadler KE (1998) Collagen fibrils forming in developing tendon show an early and abrupt limitation in diameter at the growing tips. *J Mol Biol* **283**(5)**:** 1049-1058

Hong S, Derfoul A, Pereira-Mouries L, Hall DJ (2009) A novel domain in histone deacetylase 1 and 2 mediates repression of cartilage-specific genes in human chondrocytes. *FASEB J* **23**(10)**:** 3539-3552

Hoshikawa Y, Kwon HJ, Yoshida M, Horinouchi S, Beppu T (1994) Trichostatin A induces morphological changes and gelsolin expression by inhibiting histone deacetylase in human carcinoma cell lines. *Exp Cell Res* **214**(1)**:** 189-197

Hu E, Dul E, Sung CM, Chen Z, Kirkpatrick R, Zhang GF, Johanson K, Liu R, Lago A, Hofmann G, Macarron R, de los Frailes M, Perez P, Krawiec J, Winkler J, Jaye M (2003) Identification of novel isoform-selective inhibitors within class I histone deacetylases. *J Pharmacol Exp Ther* **307**(2)**:** 720-728

Huber LC, Distler JH, Moritz F, Hemmatazad H, Hauser T, Michel BA, Gay RE, Matucci-Cerinic M, Gay S, Distler O, Jungel A (2007) Trichostatin A prevents the accumulation of extracellular matrix in a mouse model of bleomycin-induced skin fibrosis. *Arthritis Rheum* **56**(8)**:** 2755-2764

Hulmes DJ (2002) Building collagen molecules, fibrils, and suprafibrillar structures. *J Struct Biol* **137**(1-2)**:** 2-10

Humphrey GW, Wang Y, Russanova VR, Hirai T, Qin J, Nakatani Y, Howard BH (2001) Stable histone deacetylase complexes distinguished by the presence of SANT domain proteins CoREST/kiaa0071 and Mta-L1. *J Biol Chem* **276**(9)**:** 6817-6824

Hunziker EB, Kapfinger E, Geiss J (2007) The structural architecture of adult mammalian articular cartilage evolves by a synchronized process of tissue resorption and neoformation during postnatal development. *Osteoarthritis Cartilage* **15**(4)**:** 403-413

Imre G, Gekeler V, Leja A, Beckers T, Boehm M (2006) Histone deacetylase inhibitors suppress the inducibility of nuclear factor-kappaB by tumor necrosis factor-alpha receptor-1 down-regulation. *Cancer Res* **66**(10)**:** 5409-5418

Inoue S, Mai A, Dyer MJ, Cohen GM (2006) Inhibition of histone deacetylase class I but not class II is critical for the sensitization of leukemic cells to tumor necrosis factor-related apoptosis-inducing ligand-induced apoptosis. *Cancer Res* **66**(13)**:** 6785-6792

Jackson AL, Bartz SR, Schelter J, Kobayashi SV, Burchard J, Mao M, Li B, Cavet G, Linsley PS (2003) Expression profiling reveals off-target gene regulation by RNAi. *Nat Biotech* **21**(6)**:** 635-637

Kadler KE, Holmes DF, Graham H, Starborg T (2000) Tip-mediated fusion involving unipolar collagen fibrils accounts for rapid fibril elongation, the occurrence of fibrillar branched networks in skin and the paucity of collagen fibril ends in vertebrates. *Matrix Biol* **19**(4)**:** 359-365

Kadler KE, Holmes DF, Trotter JA, Chapman JA (1996) Collagen fibril formation. *Biochem J* **316 (Pt 1):** 1-11

Kaffman A, O'Shea EK (1999) Regulation of nuclear localization: a key to a door. *Annu Rev Cell Dev Biol* **15:** 291-339

Kao HY, Lee CH, Komarov A, Han CC, Evans RM (2002) Isolation and characterization of mammalian HDAC10, a novel histone deacetylase. *J Biol Chem* **277**(1)**:** 187-193

Karouzakis E, Gay RE, Gay S, Neidhart M (2009) Epigenetic control in rheumatoid arthritis synovial fibroblasts. *Nat Rev Rheumatol* **5**(5)**:** 266-272

Karsenty G, Wagner EF (2002) Reaching a genetic and molecular understanding of skeletal development. *Dev Cell* **2**(4)**:** 389-406

Kashiwagi M, Tortorella M, Nagase H, Brew K (2001) TIMP-3 is a potent inhibitor of aggrecanase 1 (ADAM-TS4) and aggrecanase 2 (ADAM-TS5). *J Biol Chem* **276**(16)**:** 12501-12504

Kawaguchi Y, Kovacs JJ, McLaurin A, Vance JM, Ito A, Yao TP (2003) The deacetylase HDAC6 regulates aggresome formation and cell viability in response to misfolded protein stress. *Cell* **115**(6)**:** 727-738

Keffer J, Probert L, Cazlaris H, Georgopoulos S, Kaslaris E, Kioussis D, Kollias G (1991) Transgenic mice expressing human tumour necrosis factor: a predictive genetic model of arthritis. *Embo J* **10**(13)**:** 4025-4031

Keiichiro N, Takamitsu K, Shin-ichi M, Zheng-Nan S, Takayuki F, Hideyuki D, Aki Y, Jiro Y, Masahiro Y, Yoshihumi N, Hajime I, Hiroshi A (2004) Histone deacetylase inhibitor suppression of autoantibody-mediated arthritis in mice via regulation of p16 expression. *Arthritis & Rheumatism* **50**(10)**:** 3365-3376

Kellgren JH, Lawrence JS (1957) Radiological assessment of osteo-arthrosis. *Ann Rheum Dis* **16**(4)**:** 494-502

Kevorkian L, Young DA, Darrah C, Donell ST, Shepstone L, Porter S, Brockbank SM, Edwards DR, Parker AE, Clark IM (2004) Expression profiling of metalloproteinases and their inhibitors in cartilage. *Arthritis Rheum* **50**(1)**:** 131-141

Klampfer L, Huang J, Sasazuki T, Shirasawa S, Augenlicht L (2003) Inhibition of interferon gamma signaling by the short chain fatty acid butyrate. *Mol Cancer Res* **1**(11)**:** 855-862

Klampfer L, Huang J, Swaby LA, Augenlicht L (2004) Requirement of histone deacetylase activity for signaling by STAT1. *J Biol Chem* **279**(29)**:** 30358-30368

Knauper V, Lopez-Otin C, Smith B, Knight G, Murphy G (1996a) Biochemical characterization of human collagenase-3. *J Biol Chem* **271**(3)**:** 1544-1550

Knauper V, Wilhelm SM, Seperack PK, DeClerck YA, Langley KE, Osthues A, Tschesche H (1993) Direct activation of human neutrophil procollagenase by recombinant stromelysin. *Biochem J* **295 (Pt 2):** 581-586

Knauper V, Will H, Lopez-Otin C, Smith B, Atkinson SJ, Stanton H, Hembry RM, Murphy G (1996b) Cellular mechanisms for human procollagenase-3 (MMP-13) activation. Evidence that MT1-MMP (MMP-14) and gelatinase a (MMP-2) are able to generate active enzyme. *J Biol Chem* **271**(29)**:** 17124-17131

Knutson SK, Chyla BJ, Amann JM, Bhaskara S, Huppert SS, Hiebert SW (2008) Liver-specific deletion of histone deacetylase 3 disrupts metabolic transcriptional networks. *EMBO J* **27**(7)**:** 1017-1028

Koeller KM, Haggarty SJ, Perkins BD, Leykin I, Wong JC, Kao MC, Schreiber SL (2003) Chemical genetic modifier screens: small molecule trichostatin suppressors as probes of intracellular histone and tubulin acetylation. *Chem Biol* **10**(5)**:** 397-410

Korzus E, Nagase H, Rydell R, Travis J (1997) The mitogen-activated protein kinase and JAK-STAT signaling pathways are required for an oncostatin M-responsive element-mediated activation of matrix metalloproteinase 1 gene expression. *J Biol Chem* **272**(2)**:** 1188-1196

Koshy PJ, Lundy CJ, Rowan AD, Porter S, Edwards DR, Hogan A, Clark IM, Cawston TE (2002) The modulation of matrix metalloproteinase and ADAM gene expression in human chondrocytes by interleukin-1 and oncostatin M: a time-course study using real-time quantitative reverse transcription-polymerase chain reaction. *Arthritis Rheum* **46**(4)**:** 961-967

Kovacs JJ, Murphy PJ, Gaillard S, Zhao X, Wu JT, Nicchitta CV, Yoshida M, Toft DO, Pratt WB, Yao TP (2005) HDAC6 regulates Hsp90 acetylation and chaperone-dependent activation of glucocorticoid receptor. *Mol Cell* **18**(5)**:** 601-607

Krasnokutsky S, Samuels J, Abramson SB (2007) Osteoarthritis in 2007. *Bull NYU Hosp Jt Dis* **65**(3)**:** 222-228

Kristensen LS, Nielsen HM, Hansen LL (2009) Epigenetics and cancer treatment. *Eur J Pharmacol* **625**(1-3)**:** 131-142

Kuettner KE (1992) Biochemistry of articular cartilage in health and disease. *Clinical Biochemistry* **25**(3)**:** 155-163

Kumar P, Oka M, Toguchida J, Kobayashi M, Uchida E, Nakamura T, Tanaka K (2001) Role of uppermost superficial surface layer of articular cartilage in the lubrication mechanism of joints. *J Anat* **199**(Pt 3)**:** 241-250

Kurdistani SK, Tavazoie S, Grunstein M (2004) Mapping global histone acetylation patterns to gene expression. *Cell* **117**(6)**:** 721-733

Kwon S, Zhang Y, Matthias P (2007) The deacetylase HDAC6 is a novel critical component of stress granules involved in the stress response. *Genes Dev* **21**(24)**:** 3381-3394

LaBonte M, Wilson P, Fazzone W, Groshen S, Lenz H-J, Ladner R (2009) DNA microarray profiling of genes differentially regulated by the histone deacetylase inhibitors vorinostat and LBH589 in colon cancer cell lines. *BMC Medical Genomics* **2**(1)**:** 67

Lagger G, O'Carroll D, Rembold M, Khier H, Tischler J, Weitzer G, Schuettengruber B, Hauser C, Brunmeir R, Jenuwein T, Seiser C (2002) Essential function of histone deacetylase 1 in proliferation control and CDK inhibitor repression. *EMBO J* **21**(11)**:** 2672-2681

Laherty CD, Yang WM, Sun JM, Davie JR, Seto E, Eisenman RN (1997) Histone deacetylases associated with the mSin3 corepressor mediate mad transcriptional repression. *Cell* **89**(3)**:** 349-356

Lamande SR, Bateman JF (1999) Procollagen folding and assembly: the role of endoplasmic reticulum enzymes and molecular chaperones. *Semin Cell Dev Biol* **10**(5)**:** 455-464

Lee H, Rezai-Zadeh N, Seto E (2004) Negative regulation of histone deacetylase 8 activity by cyclic AMP-dependent protein kinase A. *Mol Cell Biol* **24**(2)**:** 765-773

Lees JF, Tasab M, Bulleid NJ (1997) Identification of the molecular recognition sequence which determines the type-specific assembly of procollagen. *EMBO J* **16**(5)**:** 908-916

Leoni F, Fossati G, Lewis EC, Lee JK, Porro G, Pagani P, Modena D, Moras ML, Pozzi P, Reznikov LL, Siegmund B, Fantuzzi G, Dinarello CA, Mascagni P (2005) The histone deacetylase inhibitor ITF2357 reduces production of pro-inflammatory cytokines in vitro and systemic inflammation in vivo. *Mol Med* **11**(1-12)**:** 1-15

Li SW, Sieron AL, Fertala A, Hojima Y, Arnold WV, Prockop DJ (1996) The C-proteinase that processes procollagens to fibrillar collagens is identical to the protein

previously identified as bone morphogenic protein-1. *Proc Natl Acad Sci U S A* **93**(10)**:** 5127-5130

Li Y, Meng G, Huang L, Guo QN (2009) Hypomethylation of the P3 promoter is associated with up-regulation of IGF2 expression in human osteosarcoma. *Hum Pathol* **40**(10)**:** 1441-1447

Lin HS, Hu CY, Chan HY, Liew YY, Huang HP, Lepescheux L, Bastianelli E, Baron R, Rawadi G, Clement-Lacroix P (2007) Anti-rheumatic activities of histone deacetylase (HDAC) inhibitors in vivo in collagen-induced arthritis in rodents. *Br J Pharmacol* **150**(7)**:** 862-872

Lin X, Ruan X, Anderson MG, McDowell JA, Kroeger PE, Fesik SW, Shen Y (2005) siRNA-mediated off-target gene silencing triggered by a 7 nt complementation. *Nucleic Acids Res* **33**(14)**:** 4527-4535

Little CB, Meeker CT, Golub SB, Lawlor KE, Farmer PJ, Smith SM, Fosang AJ (2007) Blocking aggrecanase cleavage in the aggrecan interglobular domain abrogates cartilage erosion and promotes cartilage repair. *J Clin Invest* **117**(6)**:** 1627-1636

Loulakis P, Shrikhande A, Davis G, Maniglia CA (1992) N-terminal sequence of proteoglycan fragments isolated from medium of interleukin-1-treated articular-cartilage cultures. Putative site(s) of enzymic cleavage. *Biochem J* **284 (Pt 2):** 589-593

Lucio-Eterovic AK, Cortez MA, Valera ET, Motta FJ, Queiroz RG, Machado HR, Carlotti CG, Jr., Neder L, Scrideli CA, Tone LG (2008) Differential expression of 12 histone deacetylase (HDAC) genes in astrocytomas and normal brain tissue: class II and IV are hypoexpressed in glioblastomas. *BMC Cancer* **8:** 243

Luger K, Mader AW, Richmond RK, Sargent DF, Richmond TJ (1997) Crystal structure of the nucleosome core particle at 2.8 A resolution. *Nature* **389**(6648)**:** 251-260

MacGregor AJ, Antoniades L, Matson M, Andrew T, Spector TD (2000) The genetic contribution to radiographic hip osteoarthritis in women: results of a classic twin study. *Arthritis Rheum* **43**(11)**:** 2410-2416

Magnano MD, Chakravarty EF, Broudy C, Chung L, Kelman A, Hillygus J, Genovese MC (2007) A pilot study of tumor necrosis factor inhibition in erosive/inflammatory osteoarthritis of the hands. *The Journal of Rheumatology* **34**(6)**:** 1323-1327

Marmorstein R (2001) Structure of histone deacetylases: insights into substrate recognition and catalysis. *Structure* **9**(12)**:** 1127-1133

Maroudas A, Bayliss MT, Uchitel-Kaushansky N, Schneiderman R, Gilav E (1998) Aggrecan turnover in human articular cartilage: use of aspartic acid racemization as a marker of molecular age. *Arch Biochem Biophys* **350**(1)**:** 61-71

Marques JT, Williams BR (2005) Activation of the mammalian immune system by siRNAs. *Nat Biotechnol* **23**(11)**:** 1399-1405

McKinsey TA, Zhang CL, Lu J, Olson EN (2000) Signal-dependent nuclear export of a histone deacetylase regulates muscle differentiation. *Nature* **408**(6808)**:** 106-111

Meachim G (1963) The effect of scarification on articular cartilage in the rabbit. *J Bone Joint Surg Br* **45-B**(1)**:** 150-161

Messier SP, Gutekunst DJ, Davis C, DeVita P (2005) Weight loss reduces knee-joint loads in overweight and obese older adults with knee osteoarthritis. *Arthritis Rheum* **52**(7)**:** 2026-2032

Millward-Sadler SJ, Salter DM (2004) Integrin-dependent signal cascades in chondrocyte mechanotransduction. *Ann Biomed Eng* **32**(3)**:** 435-446

Milner JM, Elliott SF, Cawston TE (2001) Activation of procollagenases is a key control point in cartilage collagen degradation: interaction of serine and metalloproteinase pathways. *Arthritis Rheum* **44**(9)**:** 2084-2096

Milner JM, Rowan AD, Cawston TE, Young DA (2006) Metalloproteinase and inhibitor expression profiling of resorbing cartilage reveals pro-collagenase activation as a critical step for collagenolysis. *Arthritis Res Ther* **8**(5)**:** R142

Miska EA, Karlsson C, Langley E, Nielsen SJ, Pines J, Kouzarides T (1999) HDAC4 deacetylase associates with and represses the MEF2 transcription factor. *EMBO J* **18**(18)**:** 5099-5107

Miyamoto Y, Mabuchi A, Shi D, Kubo T, Takatori Y, Saito S, Fujioka M, Sudo A, Uchida A, Yamamoto S, Ozaki K, Takigawa M, Tanaka T, Nakamura Y, Jiang Q, Ikegawa S (2007) A functional polymorphism in the 5[prime] UTR of GDF5 is associated with susceptibility to osteoarthritis. *Nat Genet* **39**(4)**:** 529-533

Montgomery RL, Davis CA, Potthoff MJ, Haberland M, Fielitz J, Qi X, Hill JA, Richardson JA, Olson EN (2007) Histone deacetylases 1 and 2 redundantly regulate cardiac morphogenesis, growth, and contractility. *Genes Dev* **21**(14)**:** 1790-1802

Montgomery RL, Hsieh J, Barbosa AC, Richardson JA, Olson EN (2009) Histone deacetylases 1 and 2 control the progression of neural precursors to neurons during brain development. *Proc Natl Acad Sci U S A* **106**(19)**:** 7876-7881

Montgomery RL, Potthoff MJ, Haberland M, Qi X, Matsuzaki S, Humphries KM, Richardson JA, Bassel-Duby R, Olson EN (2008) Maintenance of cardiac energy metabolism by histone deacetylase 3 in mice. *J Clin Invest* **118**(11)**:** 3588-3597

Moreland LW (2009) Cytokines as targets for anti-inflammatory agents. *Ann N Y Acad Sci* **1182:** 88-96

Morgan TG, Rowan AD, Dickinson SC, Jones D, Hollander AP, Deehan D, Cawston TE (2006) Human nasal cartilage responds to oncostatin M in combination with interleukin 1 or tumour necrosis factor alpha by the release of collagen fragments via collagenases. *Ann Rheum Dis* **65**(2)**:** 184-190

Morgelin M, Paulsson M, Hardingham TE, Heinegard D, Engel J (1988) Cartilage proteoglycans. Assembly with hyaluronate and link protein as studied by electron microscopy. *Biochem J* **253**(1)**:** 175-185

Murphy G, Cockett MI, Stephens PE, Smith BJ, Docherty AJ (1987) Stromelysin is an activator of procollagenase. A study with natural and recombinant enzymes. *Biochem J* **248**(1)**:** 265-268

Murphy G, Knauper V, Atkinson S, Butler G, English W, Hutton M, Stracke J, Clark I (2002) Matrix metalloproteinases in arthritic disease. *Arthritis Res* **4 Suppl 3:** S39-49

Nagase H, Woessner JF, Jr. (1999) Matrix metalloproteinases. *J Biol Chem* **274**(31)**:** 21491-21494

Nagy L, Kao HY, Chakravarti D, Lin RJ, Hassig CA, Ayer DE, Schreiber SL, Evans RM (1997) Nuclear receptor repression mediated by a complex containing SMRT, mSin3A, and histone deacetylase. *Cell* **89**(3)**:** 373-380

Najm WI, Reinsch S, Hoehler F, Tobis JS, Harvey PW (2004) S-adenosyl methionine (SAMe) versus celecoxib for the treatment of osteoarthritis symptoms: a double-blind cross-over trial. [ISRCTN36233495]. *BMC Musculoskelet Disord* **5:** 6

Nakayama M, Wada M, Harada T, Nagayama J, Kusaba H, Ohshima K, Kozuru M, Komatsu H, Ueda R, Kuwano M (1998) Hypomethylation status of CpG sites at the promoter region and overexpression of the human MDR1 gene in acute myeloid leukemias. *Blood* **92**(11)**:** 4296-4307

Nau H, Hauck RS, Ehlers K (1991) Valproic acid-induced neural tube defects in mouse and human: aspects of chirality, alternative drug development, pharmacokinetics and possible mechanisms. *Pharmacol Toxicol* **69**(5)**:** 310-321

Neuhold LA, Killar L, Zhao W, Sung ML, Warner L, Kulik J, Turner J, Wu W, Billinghurst C, Meijers T, Poole AR, Babij P, DeGennaro LJ (2001) Postnatal expression in hyaline cartilage of constitutively active human collagenase-3 (MMP-13) induces osteoarthritis in mice. *J Clin Invest* **107**(1)**:** 35-44

Nissinen J, Pitkanen A (2007) Effect of antiepileptic drugs on spontaneous seizures in epileptic rats. *Epilepsy Res* **73**(2)**:** 181-191

Nuttall RK, Pennington CJ, Taplin J, Wheal A, Yong VW, Forsyth PA, Edwards DR (2003) Elevated membrane-type matrix metalloproteinases in gliomas revealed by profiling proteases and inhibitors in human cancer cells. *Mol Cancer Res* **1**(5)**:** 333-345

Oliveria SA, Felson DT, Cirillo PA, Reed JI, Walker AM (1999) Body weight, body mass index, and incident symptomatic osteoarthritis of the hand, hip, and knee. *Epidemiology* **10**(2)**:** 161-166

Pelletier JP, Martel-Pelletier J, Abramson SB (2001) Osteoarthritis, an inflammatory disease: potential implication for the selection of new therapeutic targets. *Arthritis Rheum* **44**(6)**:** 1237-1247

Pelletier JP, Mineau F, Ranger P, Tardif G, Martel-Pelletier J (1996) The increased synthesis of inducible nitric oxide inhibits IL-1ra synthesis by human articular chondrocytes: possible role in osteoarthritic cartilage degradation. *Osteoarthritis Cartilage* **4**(1)**:** 77-84

Phiel CJ, Zhang F, Huang EY, Guenther MG, Lazar MA, Klein PS (2001) Histone deacetylase is a direct target of valproic acid, a potent anticonvulsant, mood stabilizer, and teratogen. *J Biol Chem* **276**(39)**:** 36734-36741

Piccard H, Van den Steen PE, Opdenakker G (2007) Hemopexin domains as multifunctional liganding modules in matrix metalloproteinases and other proteins. *J Leukoc Biol* **81**(4)**:** 870-892

Pischon N, Darbois LM, Palamakumbura AH, Kessler E, Trackman PC (2004) Regulation of collagen deposition and lysyl oxidase by tumor necrosis factor-alpha in osteoblasts. *J Biol Chem* **279**(29)**:** 30060-30065

Pollard TC, Gwilym SE, Carr AJ (2008) The assessment of early osteoarthritis. *J Bone Joint Surg Br* **90**(4)**:** 411-421

Porter S, Clark IM, Kevorkian L, Edwards DR (2005) The ADAMTS metalloproteinases. *Biochem J* **386**(Pt 1)**:** 15-27

Presle N, Pottie P, Dumond H, Guillaume C, Lapicque F, Pallu S, Mainard D, Netter P, Terlain B (2006) Differential distribution of adipokines between serum and synovial fluid in patients with osteoarthritis. Contribution of joint tissues to their articular production. *Osteoarthritis Cartilage* **14**(7)**:** 690-695

Pulai JI, Del Carlo M, Jr., Loeser RF (2002) The alpha5beta1 integrin provides matrix survival signals for normal and osteoarthritic human articular chondrocytes in vitro. *Arthritis Rheum* **46**(6)**:** 1528-1535

Raffetto JD, Khalil RA (2008) Matrix metalloproteinases and their inhibitors in vascular remodeling and vascular disease. *Biochem Pharmacol* **75**(2)**:** 346-359

Richette P, Corvol M, Bardin T (2003) Estrogens, cartilage, and osteoarthritis. *Joint Bone Spine* **70**(4)**:** 257-262

Richmond RS, Carlson CS, Register TC, Shanker G, Loeser RF (2000) Functional estrogen receptors in adult articular cartilage: estrogen replacement therapy increases chondrocyte synthesis of proteoglycans and insulin-like growth factor binding protein 2. *Arthritis Rheum* **43**(9)**:** 2081-2090

Roach HI, Aigner T (2007) DNA methylation in osteoarthritic chondrocytes: a new molecular target. *Osteoarthritis Cartilage* **15**(2)**:** 128-137

Roach HI, Yamada N, Cheung KS, Tilley S, Clarke NM, Oreffo RO, Kokubun S, Bronner F (2005) Association between the abnormal expression of matrix-degrading enzymes by human osteoarthritic chondrocytes and demethylation of specific CpG sites in the promoter regions. *Arthritis Rheum* **52**(10)**:** 3110-3124

Rodgers UR, Kevorkian L, Surridge AK, Waters JG, Swingler TE, Culley K, Illman S, Lohi J, Parker AE, Clark IM (2009) Expression and function of matrix metalloproteinase (MMP)-28. *Matrix Biol* **28**(5)**:** 263-272

Rogerson FM, Stanton H, East CJ, Golub SB, Tutolo L, Farmer PJ, Fosang AJ (2008) Evidence of a novel aggrecan-degrading activity in cartilage: Studies of mice deficient in both ADAMTS-4 and ADAMTS-5. *Arthritis Rheum* **58**(6)**:** 1664-1673

Rolauffs B, Williams JM, Grodzinsky AJ, Kuettner KE, Cole AA (2008) Distinct horizontal patterns in the spatial organization of superficial zone chondrocytes of human joints. *J Struct Biol* **162**(2)**:** 335-344

Roughley PJ (2001) Articular cartilage and changes in arthritis: noncollagenous proteins and proteoglycans in the extracellular matrix of cartilage. *Arthritis Res* **3**(6)**:** 342-347

Roughley PJ, Barnett J, Zuo F, Mort JS (2003) Variations in aggrecan structure modulate its susceptibility to aggrecanases. *Biochem J* **375**(Pt 1)**:** 183-189

Rowan AD, Hui W, Cawston TE, Richards CD (2003) Adenoviral gene transfer of interleukin-1 in combination with oncostatin M induces significant joint damage in a murine model. *Am J Pathol* **162**(6)**:** 1975-1984

Sakao K, Takahashi KA, Arai Y, Saito M, Honjo K, Hiraoka N, Asada H, Shin-Ya M, Imanishi J, Mazda O, Kubo T (2009) Osteoblasts derived from osteophytes produce interleukin-6, interleukin-8, and matrix metalloproteinase-13 in osteoarthritis. *J Bone Miner Metab* **27**(4)**:** 412-423

Sandy JD, Neame PJ, Boynton RE, Flannery CR (1991) Catabolism of aggrecan in cartilage explants. Identification of a major cleavage site within the interglobular domain. *Journal of Biological Chemistry* **266**(14)**:** 8683-8685

Saouaf SJ, Li B, Zhang G, Shen Y, Furuuchi N, Hancock WW, Greene MI (2009) Deacetylase inhibition increases regulatory T cell function and decreases incidence and severity of collagen-induced arthritis. *Exp Mol Pathol* **87**(2)**:** 99-104

Sauerland K, Raiss RX, Steinmeyer J (2003) Proteoglycan metabolism and viability of articular cartilage explants as modulated by the frequency of intermittent loading. *Osteoarthritis Cartilage* **11**(5)**:** 343-350

Schumacher BL, Block JA, Schmid TM, Aydelotte MB, Kuettner KE (1994) A novel proteoglycan synthesized and secreted by chondrocytes of the superficial zone of articular cartilage. *Arch Biochem Biophys* **311**(1)**:** 144-152

Seigneurin-Berny D, Verdel A, Curtet S, Lemercier C, Garin J, Rousseaux S, Khochbin S (2001) Identification of components of the murine histone deacetylase 6 complex:

link between acetylation and ubiquitination signaling pathways. *Mol Cell Biol* **21**(23)**:** 8035-8044

Shah MH, Binkley P, Chan K, Xiao J, Arbogast D, Collamore M, Farra Y, Young D, Grever M (2006) Cardiotoxicity of histone deacetylase inhibitor depsipeptide in patients with metastatic neuroendocrine tumors. *Clin Cancer Res* **12**(13)**:** 3997-4003

Siegel RC, Pinnell SR, Martin GR (1970) Cross-linking of collagen and elastin. Properties of lysyl oxidase. *Biochemistry* **9**(23)**:** 4486-4492

Simon D, Laloo B, Barillot M, Barnetche T, Blanchard C, Rooryck C, Marche M, Burgelin I, Coupry I, Chassaing N, Gilbert-Dussardier B, Lacombe D, Grosset C, Arveiler B (2010) A mutation in the 3'-UTR of the HDAC6 gene abolishing the post-transcriptional regulation mediated by hsa-miR-433 is linked to a new form of dominant X-linked chondrodysplasia. *Hum Mol Genet* **19**(10)**:** 2015-2027

Sniekers YH, Weinans H, Bierma-Zeinstra SM, van Leeuwen JP, van Osch GJ (2008) Animal models for osteoarthritis: the effect of ovariectomy and estrogen treatment - a systematic approach. *Osteoarthritis Cartilage* **16**(5)**:** 533-541

Song J, Noh JH, Lee JH, Eun JW, Ahn YM, Kim SY, Lee SH, Park WS, Yoo NJ, Lee JY, Nam SW (2005) Increased expression of histone deacetylase 2 is found in human gastric cancer. *APMIS* **113**(4)**:** 264-268

Spector TD, MacGregor AJ (2004) Risk factors for osteoarthritis: genetics. *Osteoarthritis Cartilage* **12 Suppl A:** S39-44

Stanton H, Rogerson FM, East CJ, Golub SB, Lawlor KE, Meeker CT, Little CB, Last K, Farmer PJ, Campbell IK, Fourie AM, Fosang AJ (2005) ADAMTS5 is the major aggrecanase in mouse cartilage in vivo and in vitro. *Nature* **434**(7033)**:** 648-652

Striethol S, Maurer B, Peters MA, Pap T, Gay S (2008) Epigenetic modifications in rheumatoid arthritis. *Arthritis Res Ther* **10**(5)**:** 219

Suri S, Gill SE, Massena de Camin S, McWilliams DF, Wilson D, Walsh DA (2007) Neurovascular invasion at the osteochondral junction and in osteophytes in osteoarthritis. *Annals of the Rheumatic Diseases* **66**(11)**:** 1423-1428

Swingler TE, Kevorkian L, Culley KL, Illman SA, Young DA, Parker AE, Lohi J, Clark IM. (2010) MMP28 gene expression is regulated by Sp1 transcription factor acetylation. *Biochem J*, Vol. 427, pp. 391-400.

Swingler TE, Waters JG, Davidson RK, Pennington CJ, Puente XS, Darrah C, Cooper A, Donell ST, Guile GR, Wang W, Clark IM (2009) Degradome expression profiling in human articular cartilage. *Arthritis Res Ther* **11**(3)**:** R96

Takami N, Osawa K, Miura Y, Komai K, Taniguchi M, Shiraishi M, Sato K, Iguchi T, Shiozawa K, Hashiramoto A, Shiozawa S (2006) Hypermethylated promoter region of DR3, the death receptor 3 gene, in rheumatoid arthritis synovial cells. *Arthritis Rheum* **54**(3)**:** 779-787

Takeda S, Bonnamy JP, Owen MJ, Ducy P, Karsenty G (2001) Continuous expression of Cbfa1 in nonhypertrophic chondrocytes uncovers its ability to induce hypertrophic chondrocyte differentiation and partially rescues Cbfa1-deficient mice. *Genes Dev* **15**(4)**:** 467-481

Termeer C, Benedix F, Sleeman J, Fieber C, Voith U, Ahrens T, Miyake K, Freudenberg M, Galanos C, Simon JC (2002) Oligosaccharides of Hyaluronan activate dendritic cells via toll-like receptor 4. *J Exp Med* **195**(1)**:** 99-111

Tong JK, Hassig CA, Schnitzler GR, Kingston RE, Schreiber SL (1998) Chromatin deacetylation by an ATP-dependent nucleosome remodelling complex. *Nature* **395**(6705)**:** 917-921

Tortorella MD, Burn TC, Pratta MA, Abbaszade I, Hollis JM, Liu R, Rosenfeld SA, Copeland RA (1999) Purification and cloning of aggrecanase-1: a member of the ADAMTS family of proteins. *Science* **284**(5420)**:** 1664-1666

Trivedi CM, Luo Y, Yin Z, Zhang M, Zhu W, Wang T, Floss T, Goettlicher M, Noppinger PR, Wurst W, Ferrari VA, Abrams CS, Gruber PJ, Epstein JA (2007) Hdac2 regulates the cardiac hypertrophic response by modulating Gsk3[beta] activity. *Nat Med* **13**(3)**:** 324-331

Tuuttila A, Morgunova E, Bergmann U, Lindqvist Y, Maskos K, Fernandez-Catalan C, Bode W, Tryggvason K, Schneider G (1998) Three-dimensional Structure of Human Tissue Inhibitor of Metalloproteinases-2 at 2.1 A Resolution. *Journal of Molecular Biology* **284:** 1133-1140

Ueta C, Iwamoto M, Kanatani N, Yoshida C, Liu Y, Enomoto-Iwamoto M, Ohmori T, Enomoto H, Nakata K, Takada K, Kurisu K, Komori T (2001) Skeletal malformations caused by overexpression of Cbfa1 or its dominant negative form in chondrocytes. *J Cell Biol* **153**(1)**:** 87-100

Ungerstedt JS, Sowa Y, Xu WS, Shao Y, Dokmanovic M, Perez G, Ngo L, Holmgren A, Jiang X, Marks PA (2005) Role of thioredoxin in the response of normal and transformed cells to histone deacetylase inhibitors. *Proc Natl Acad Sci U S A* **102**(3)**:** 673-678

Ushiyama T, Inoue K, Nishioka J (1995) Expression of estrogen receptor related protein (p29) and estradiol binding in human arthritic synovium. *J Rheumatol* **22**(3)**:** 421-426

Uzel MI, Scott IC, Babakhanlou-Chase H, Palamakumbura AH, Pappano WN, Hong HH, Greenspan DS, Trackman PC (2001) Multiple bone morphogenetic protein 1-related mammalian metalloproteinases process pro-lysyl oxidase at the correct physiological site and control lysyl oxidase activation in mouse embryo fibroblast cultures. *J Biol Chem* **276**(25)**:** 22537-22543

Valdes AM, Loughlin J, Oene MV, Chapman K, Surdulescu GL, Doherty M, Spector TD (2007) Sex and ethnic differences in the association of ASPN, CALM1, COL2A1,

COMP, and FRZB with genetic susceptibility to osteoarthritis of the knee. *Arthritis Rheum* **56**(1)**:** 137-146

Van Wart HE, Birkedal-Hansen H (1990) The cysteine switch: a principle of regulation of metalloproteinase activity with potential applicability to the entire matrix metalloproteinase gene family. *Proc Natl Acad Sci U S A* **87**(14)**:** 5578-5582

Vannini A, Volpari C, Filocamo G, Casavola EC, Brunetti M, Renzoni D, Chakravarty P, Paolini C, De Francesco R, Gallinari P, Steinkuhler C, Di Marco S (2004) Crystal structure of a eukaryotic zinc-dependent histone deacetylase, human HDAC8, complexed with a hydroxamic acid inhibitor. *Proc Natl Acad Sci U S A* **101**(42)**:** 15064-15069

Vega RB, Matsuda K, Oh J, Barbosa AC, Yang X, Meadows E, McAnally J, Pomajzl C, Shelton JM, Richardson JA, Karsenty G, Olson EN (2004) Histone deacetylase 4 controls chondrocyte hypertrophy during skeletogenesis. *Cell* **119**(4)**:** 555-566

Verdel A, Curtet S, Brocard MP, Rousseaux S, Lemercier C, Yoshida M, Khochbin S (2000) Active maintenance of mHDA2/mHDAC6 histone-deacetylase in the cytoplasm. *Curr Biol* **10**(12)**:** 747-749

Verdin E, Dequiedt F, Kasler HG (2003) Class II histone deacetylases: versatile regulators. *Trends Genet* **19**(5)**:** 286-293

Verzijl N, DeGroot J, Thorpe SR, Bank RA, Shaw JN, Lyons TJ, Bijlsma JW, Lafeber FP, Baynes JW, TeKoppele JM (2000) Effect of collagen turnover on the accumulation of advanced glycation end products. *J Biol Chem* **275**(50)**:** 39027-39031

Waltregny D, De Leval L, Glenisson W, Ly Tran S, North BJ, Bellahcene A, Weidle U, Verdin E, Castronovo V (2004) Expression of histone deacetylase 8, a class I histone deacetylase, is restricted to cells showing smooth muscle differentiation in normal human tissues. *Am J Pathol* **165**(2)**:** 553-564

Wu WS, Vallian S, Seto E, Yang WM, Edmondson D, Roth S, Chang KS (2001) The growth suppressor PML represses transcription by functionally and physically interacting with histone deacetylases. *Mol Cell Biol* **21**(7)**:** 2259-2268

Xu Y, Mirmalek-Sani SH, Lin F, Zhang J, Oreffo RO (2007) Adipocyte differentiation induced using nonspecific siRNA controls in cultured human mesenchymal stem cells. *RNA* **13**(8)**:** 1179-1183

Yan C, Boyd DD (2007) Regulation of matrix metalloproteinase gene expression. *J Cell Physiol* **211**(1)**:** 19-26

Yang WM, Tsai SC, Wen YD, Fejer G, Seto E (2002) Functional domains of histone deacetylase-3. *J Biol Chem* **277**(11)**:** 9447-9454

Yin L, Laevsky G, Giardina C (2001) Butyrate suppression of colonocyte NF-kappa B activation and cellular proteasome activity. *J Biol Chem* **276**(48)**:** 44641-44646

Young DA, Lakey RL, Pennington CJ, Jones D, Kevorkian L, Edwards DR, Cawston TE, Clark IM (2005) Histone deacetylase inhibitors modulate metalloproteinase gene expression in chondrocytes and block cartilage resorption. *Arthritis Res Ther* **7**(3)**:** R503-512

Zhang CL, McKinsey TA, Chang S, Antos CL, Hill JA, Olson EN (2002) Class II histone deacetylases act as signal-responsive repressors of cardiac hypertrophy. *Cell* **110**(4)**:** 479-488

Zhang Y, Gilquin B, Khochbin S, Matthias P (2006) Two catalytic domains are required for protein deacetylation. *J Biol Chem* **281**(5)**:** 2401-2404

Zhang Y, Kwon S, Yamaguchi T, Cubizolles F, Rousseaux S, Kneissel M, Cao C, Li N, Cheng HL, Chua K, Lombard D, Mizeracki A, Matthias G, Alt FW, Khochbin S, Matthias P (2008) Mice lacking histone deacetylase 6 have hyperacetylated tubulin but are viable and develop normally. *Mol Cell Biol* **28**(5)**:** 1688-1701

Zhang Y, Li N, Caron C, Matthias G, Hess D, Khochbin S, Matthias P (2003) HDAC-6 interacts with and deacetylates tubulin and microtubules in vivo. *Embo J* **22**(5)**:** 1168-1179

Zucker S, Drews M, Conner C, Foda HD, DeClerck YA, Langley KE, Bahou WF, Docherty AJ, Cao J (1998) Tissue inhibitor of metalloproteinase-2 (TIMP-2) binds to the catalytic domain of the cell surface receptor, membrane type 1-matrix metalloproteinase 1 (MT1-MMP). *J Biol Chem* **273**(2)**:** 1216-1222

Zwerina J, Redlich K, Polzer K, Joosten L, Kronke G, Distler J, Hess A, Pundt N, Pap T, Hoffmann O, Gasser J, Scheinecker C, Smolen JS, van den Berg W, Schett G (2007) TNF-induced structural joint damage is mediated by IL-1. *Proc Natl Acad Sci U S A* **104**(28)**:** 11742-11747